

Spring 2010

Development of a geopolymer-based cementitious coating for the rehabilitation of buried concrete infrastructure

Carlos Montes
Louisiana Tech University

Follow this and additional works at: <https://digitalcommons.latech.edu/dissertations>



Part of the [Civil Engineering Commons](#)

Recommended Citation

Montes, Carlos, "" (2010). *Dissertation*. 405.
<https://digitalcommons.latech.edu/dissertations/405>

This Dissertation is brought to you for free and open access by the Graduate School at Louisiana Tech Digital Commons. It has been accepted for inclusion in Doctoral Dissertations by an authorized administrator of Louisiana Tech Digital Commons. For more information, please contact digitalcommons@latech.edu.

**DEVELOPMENT OF A GEOPOLYMER-BASED
CEMENTITIOUS COATING FOR THE
REHABILITATION OF BURIED
CONCRETE INFRASTRUCTURE**

by

Carlos Montes, B.S., M.S.

A Dissertation Presented in Partial Fulfillment
of the Requirement for the Degree
Doctor of Philosophy

COLLEGE OF ENGINEERING AND SCIENCE
LOUISIANA TECH UNIVERSITY

May 2010

UMI Number: 3459547

All rights reserved

INFORMATION TO ALL USERS

The quality of this reproduction is dependent upon the quality of the copy submitted.

In the unlikely event that the author did not send a complete manuscript and there are missing pages, these will be noted. Also, if material had to be removed, a note will indicate the deletion.



UMI 3459547

Copyright 2011 by ProQuest LLC.

All rights reserved. This edition of the work is protected against unauthorized copying under Title 17, United States Code.



ProQuest LLC
789 East Eisenhower Parkway
P.O. Box 1346
Ann Arbor, MI 48106-1346

LOUISIANA TECH UNIVERSITY

THE GRADUATE SCHOOL


March-25-2010

Date

We hereby recommend that the dissertation prepared under our supervision
by Carlos Montes Montoya

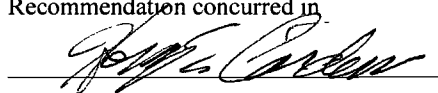
entitled "Development of a Geopolymer Based Cementitious Coating for the
Rehabilitation of Buried Concrete Infrastructure"

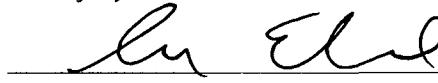
be accepted in partial fulfillment of the requirements for the Degree of
Ph.D. in Engineering


Supervisor of Dissertation Research


Head of Department

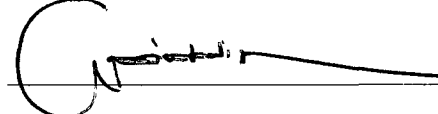
Department

Recommendation concurred in






Advisory Committee




Approved:

Director of Graduate Studies

Approved.

Dean of the Graduate School


Dean of the College

DEDICATION

To

*God, for His love and inspiration,
Mom, for her love, patience, and prayers,
Dad, who sent his blessings from Heaven to complete this work*

ABSTRACT

The current research project was devoted to the incorporation of geopolymers as a new material for Trenchless projects, taking advantage of their properties in a field in which they had not been used before, providing a substantial help to municipalities to meet their rehabilitation needs. Trenchless Technologies are a family of methods, materials and equipment capable of being used for the installation of new or replacement or rehabilitation of existing underground infrastructure with minimal disruption to surface traffic, business, and other activities.

The dissertation research work described herein is divided into six primary objectives: (1) the evaluation of geopolymer as a suitable candidate material for the rehabilitation of aging buried concrete infrastructure; (2) the study of the main parameters behind the process of geopolymerization; (3) the development of a geopolymer-based rehabilitation method with enhanced workability by means of a surface-active agent; (4) the evaluation of copper-substituted geopolymer with possible biocide properties; (5) testing and field validation of the resulting material; and (6) the study of its commercialization potential.

Materials of a new generation are needed to suit the growing rehabilitation needs of buried concrete infrastructure. Many municipalities currently undergo difficult material selection processes; based on the best match between low cost and high quality. An optimal solution is not easy to achieve since ordinary Portland cement (OPC)

provides low cost and good workability, but, in many cases, does not provide extended durability; on the other hand epoxies and other organic polymers often resist biogenic corrosion well, yet are many times not within the budget of municipalities.

Geopolymers are cementitious materials of a new generation. Their outstanding properties are the object of growing research all over the world, especially in France, Australia and the USA. However, regardless of their excellent mechanical strength and corrosion resistance properties, geopolymers are often seen by the construction industry as materials with poor workability and unsuitable for big scale projects. This perception and other drawbacks are addressed in the present work.

The dissertation begins with the identification and study of the main variables controlling the geopolymerization process and their influence on the final material properties. A selection of materials is then conducted and the design of an appropriate formulation is achieved. The next step was to solve the problem of turning geopolymers into a friendly material for contractors. As spray coatings are a very common and convenient method for the application of cementitious materials, this process was especially emphasized throughout the dissertation. Several additives and mixing methods were experimented with during this research project to help on this objective.

Having produced a sprayable geopolymer admixture, work was then conducted to evaluate the final properties of the resulting material and a comparison with products currently used by the industry. The encapsulation of copper with the intention of a future evaluation as a biogenic agent embedded in geopolymer was also considered. Important conclusions are made in this regard. An evaluation of the commercialization potential of this material is further discussed.

APPROVAL FOR SCHOLARLY DISSEMINATION

The author grants to the Prescott Memorial Library of Louisiana Tech University the right to reproduce, by appropriate methods, upon request, any or all portions of this Dissertation. It is understood that "proper request" consists of the agreement, on the part of the requesting party, that said reproduction is for his personal use and that subsequent reproduction will not occur without written approval of the author of this Dissertation. Further, any portions of the Dissertation used in books, papers, and other works must be appropriately referenced to this Dissertation.

Finally, the author of this Dissertation reserves the right to publish freely, in the literature, at any time, any or all portions of this Dissertation.

Author Carlos Montes
Date 05/06/2010

TABLE OF CONTENTS

DEDICATION	iii
ABSTRACT	iv
LIST OF TABLES	xii
LIST OF FIGURES	xiv
ACKNOWLEDGMENTS	xvii
CHAPTER 1 INTRODUCTION	1
1.1 Background	1
1.2 Objective	4
1.3 Organization of the Dissertation	4
1.4 Key Contributions	6
CHAPTER 2 LITERATURE REVIEW	8
2.1 Pipelines: Statement of the Problem	8
2.1.1 Background	8
2.1.2 Some Types of Pipe Damage and Deterioration	9
2.1.2.1 Leakiness	9
2.1.2.2 Mechanical Wear	9
2.1.2.3 Corrosion	11
2.1.3 Mechanism of Corrosion	13
2.1.3.1 Inorganic Chemical Corrosion	14
2.1.3.2 Bacterial Induced Corrosion	15
2.1.4 Currently Used Rehabilitation Methods	17
2.2 Coatings for the Rehabilitation of Pipes	18
2.2.1 Basic Concepts	18
2.2.2 Desirable Characteristics of a Coating	20
2.2.3 Actual Materials Used for Coatings	21
2.2.3.1 Portland Cement Mortars	21
2.2.3.2 Polymer Cement Concrete	24
2.2.3.3 Reaction Resin Cements or Polymer Concrete	28
2.2.3.3.1 Some Types of Resins for Polymer Concrete	29
2.2.4 Surface Preparation	31
2.2.5 Coating Techniques	34
2.2.5.1 Guniting	34
2.2.5.2 Spray Lining	34
2.2.5.3 Curing	36
2.2.6 Quality Tests Conducted on Coatings	36
2.2.6.1 Corrosion Resistance	37
2.2.6.2 External Water Pressure Loading	38
2.2.6.3 Abrasion Resistance	38

2.2.6.4 Bond Tensile Strength Test.....	38
2.2.6.5 Wetting and Drying.....	39
2.2.6.6 Freezing and Thawing.....	39
2.3 Geopolymer Cements.....	39
2.3.1 Basics	39
2.3.2 Raw Materials	40
2.3.2.1 Metakaolin	40
2.3.2.2 Fly Ash.....	40
2.3.2.3 Other Materials	42
2.3.3 Chemistry	42
2.3.4 Characterization	45
2.3.5 Curing	46
2.3.6 Properties	46
2.3.7 Ecological Advantages.....	49
2.3.8 Uses.....	50
2.3.9 Metal Encapsulation.....	51
2.3.10 Related Patents.....	52
2.4 Surfactant Theory.....	52
2.4.1 Surface Tension	52
2.4.2 Surfactants.....	54
2.4.3 Air Entraining Agents	55
2.4.4 The Effect of Air Entrainment in Concrete.....	57
2.4.5 Superplasticizers	60
2.5 Bactericide Coatings	63
2.6 General Conclusions	64
CHAPTER 3 STUDY OF THE MAIN PARAMETERS OF	
GEOPOLYMERIZATION	67
3.1 Introduction.....	67
3.2 Production of a Geopolymer Sample at Louisiana Tech Laboratory	68
3.2.1 Formulation.....	68
3.2.2 Raw Materials	68
3.2.2.1 Metakaolin	68
3.2.2.2 Alkaline Solution	70
3.2.3 Procedure	70
3.2.4 Results.....	71
3.2.5 Observations	72
3.3 First Preliminary Design of Experiments	72
3.3.1 Objectives	72
3.3.2 Design of Experiments.....	73
3.3.3 Materials	73
3.3.4 Methodology	75
3.3.5 Results and Discussion	75
3.3.6 Conclusions.....	78
3.4 Second Design of Experiments.....	79
3.4.1 Objective	79
3.4.2 Design of Experiments.....	79

3.4.3	Materials	80
3.4.4	Methodology	81
3.4.5	Results and Discussion	81
3.4.6	Conclusions.....	85
3.5	General Conclusions	85
CHAPTER 4 CORROSION RESISTANCE OF GEOPOLYMER COMPARED TO PORTLAND CEMENT		87
4.1	Introduction.....	87
4.2	Materials	87
4.3	Mix Design.....	88
4.4	Methodology	89
4.5	Results and Observations.....	91
4.5.1	Change in Mass.....	91
4.5.2	Remaining Compressive Strength.....	94
4.5.3	Visual Appearance	98
4.6	Discussion.....	101
4.6.1	Mass Loss.....	101
4.6.2	Remaining Compressive Strength.....	102
4.7	Conclusions.....	102
CHAPTER 5 OPTIMIZATION OF THE ACTIVATOR SOLUTION.....		103
5.1	Introduction.....	103
5.2	Design of Experiments.....	103
5.3	Materials	104
5.4	Methodology	106
5.5	Results and Discussion	107
5.5.1	Compressive Strength	107
5.5.2	Remaining Compressive Strength.....	110
5.5.3	Mass Loss.....	112
5.5.4	Flow	114
5.6	Decision Support Table.....	116
5.7	Conclusions.....	118
CHAPTER 6 DEVELOPMENT OF A SPRAYABLE GEOPOLYMER MORTAR....		121
6.1	Introduction.....	121
6.2	Preliminary Tests of the Mortar as Coating.....	122
6.2.1	First Coating Test.....	122
6.2.2	Second Coating Test	123
6.2.3	Third Coating Test	123
6.2.4	Use of Superplasticizer	124
6.3	Design of Experiments.....	124
6.3.1	Effect of NaOH Concentration and Sil/Hyd Ratio on Viscosity	124
6.3.2	Materials and Equipment	125
6.3.3	Procedure	125
6.3.4	Results.....	126
6.3.4.1	Viscosity Curves	126
6.3.4.2	DOE MINITAB Results	129

6.3.5	Conclusions.....	131
6.4	Preliminary Spraying Tests.....	131
6.4.1	Initial Spray Test using Portland Cement	131
6.4.2	Achieving Sprayability using Surfactants.....	133
6.4.2.1	Initial Tests.....	133
6.4.2.2	Compressive Strength Evaluation/ Curing Regimes/Reformulation	134
6.4.2.3	Spraying of a Concrete Wall.....	138
6.4.2.4	Change of the Order of Mixing the Surfactant	138
6.5	Surfactant Addition Testing Program	139
6.5.1	Design of Experiments.....	139
6.5.2	Materials and Formulation.....	139
6.5.3	Procedure	140
6.5.4	Results and Discussion	140
6.5.4.1	Compressive Strength	140
6.5.4.2	Flow	142
6.5.4.3	Viscosity	144
6.5.4.4	Surface Tension	147
6.6	Field Tests.....	149
6.6.1	Field Test with DNA Construction.....	149
6.6.2	Second Field Test (with Spraybuddy).....	151
6.6.3	Third Field Test (Second with Spraybuddy).....	152
6.6.4	Conclusions.....	153
6.7	Proposed Final Formulation.....	154
6.8	General Conclusions	154
CHAPTER 7 QUALITY TESTS, COPPER ADDITION AND COMMERCIAL OPPORTUNITIES		156
7.1	Background.....	156
7.2	Quality Testing.....	157
7.2.1	Mechanical Strength	157
7.2.1.1	Compressive Strength	158
7.2.1.2	Flexural Strength.....	158
7.2.1.3	Tensile Strength	159
7.2.1.4	Young's Modulus and Poisson Ratio.....	160
7.2.2	Corrosion Resistance	161
7.2.3	Absorption, Voids and Air Content	162
7.2.4	Length Change in a Sulfate Solution	164
7.2.5	Abrasion Resistance.....	165
7.2.6	Bond Strength (Adhesion)	166
7.2.7	Viscosity and Flow	167
7.2.8	Pot Life (Setting Time).....	168
7.2.9	XRD Phase Identification Analysis	169
7.2.10	Summary (Product Specification Table).....	169
7.3	Copper Addition Testing Program.....	170
7.3.1	Design of Experiments.....	170
7.3.2	Materials	171

7.3.3 Procedure	171
7.3.4 Results.....	172
7.3.4.1 Compressive Strength	172
7.3.4.2 Flow	173
7.3.4.3 XRD	175
7.3.5 TEM/EDS Evaluations.....	176
7.4 Commercialization Potential.....	180
7.5 General Conclusions	180
CHAPTER 8 SUMMARY, CONCLUSIONS AND RECOMMENDATIONS	183
8.1 Summary	183
8.2 Conclusions.....	185
8.3 Recommendations.....	187
APPENDIX A EXPERIMENTAL DETAILS FOR CHAPTER 3.....	189
A.1 Particle Size Distribution of Metakaolin.....	190
A.2 Particle Size Distribution of Class F Fly Ash	192
A.3 Weight Proportions for Section 3.3.4.....	193
A.4 Results for Section 3.3.4	194
A.5 Compressive Strength Results for Section 3.3.4.....	196
A.6 Compressive Strength Results for Section 3.4.2.....	197
APPENDIX B EXPERIMENTAL DETAILS FOR THE CORROSION TESTS	198
B.1 Weight Proportions for Section 4.3.....	199
B.2 Preparation of Sulfuric Acid Solutions	200
B.3 Mass Loss Results	201
B.4 Remaining Compressive Strength Results	202
APPENDIX C SOFTWARE OUTPUT AND EXPERIMENTAL RESULTS FOR CHAPTER 5	203
C.1 MINITAB Experimental Setup	204
C.2 MINITAB Output for Compressive Strength.....	205
C.3 R Output for Compressive Strength	206
C.4 MINITAB Output for Remaining Compressive Strength	207
C.5 R Output for Remaining Compressive Strength	208
C.6 MINITAB Output for Mass Loss.....	209
C.7 R Output for Remaining Mass Loss.....	210
C.8 Minitab Output For Flow	211
C.9 ROutput For Flow	212
C.10 Weights For Section 5.4	213
C.11 Compressive Strength Results.....	214
C.12 Remaining Compressive Strength, Mass Loss And Flow Results	215
APPENDIX D SOFTWARE OUTPUT AND EXPERIMENTAL RESULTS FOR CHAPTER 6	217
D.1 Weights for Section 6.3.1.....	218
D.2 Viscosity Results for 6.3.4	219
D.3 ANOVA Table from MINITAB	220
D.4 MINITAB Input And Outputs For Section 6.5.4	221
D.5 ANOVA Tables from MINITAB.....	223
D.6 MINITAB Input and Outputs for Section 6.5.4.4	225

D.7 ANOVA Table for Surfactant Addition.....	226
APPENDIX E EXPERIMENTAL RESULTS FOR CHAPTER 7	227
E.1 Young's Modulus and Poisson Ratio	228
E.2 Data for Length Change in a Sulfate Solution.....	229
APPENDIX F XRD CURVES FOR TABLE 7.9.....	230
F.1 XRD Pattern for Class F Fly Ash	231
F.2 XRD Pattern for Class F Fly Ash Geopolymer	232
APPENDIX G XRD REPORTS FOR GEOPOLYMER WITH ADDITION OF COPPER.....	233
G.1 XRD Pattern for the Sample With 10% Added Cu_2SO_4	234
G.2 XRD Pattern for the Sample With 50% Added Cu_2SO_4	235
G.3 XRD Pattern for the Sample With 10% Added $\text{Cu}_2(\text{NO}_3)\cdot 3\text{H}_2\text{O}$	236
G.4 XRD Pattern for the Sample With 50% Added $\text{Cu}_2(\text{NO}_3)\cdot 3\text{H}_2\text{O}$	237
APPENDIX H PLANET EUREKA REPORT	238
REFERENCES	244

LIST OF TABLES

Table 2.1	Main hydration reactions of Portland cement.....	23
Table 2.2	Recommended thicknesses for lining operations.....	35
Table 3.1	Important variables in geopolymerization	67
Table 3.2	Formulation for the first geopolymer experiment at Louisiana Tech.	68
Table 3.3	Chemical composition of the metakaolin sample used for this test.....	69
Table 3.4	Chemical composition of the metakaolin used for the literature reference paper.....	69
Table 3.5	Compressive strength of sample geopolymer specimens.	72
Table 3.6	Research variables for the first preliminary design of experiments.	73
Table 3.7	Chemical composition of the fly ash.	74
Table 3.8	Phase composition of the fly ash.	74
Table 3.9	Chemical composition of the sodium silicate utilized.	75
Table 3.10	Research variables for the first preliminary design of experiments.	79
Table 3.11	Design of experiments obtained using MINITAB.....	80
Table 3.12	Oxide composition of the fly ashes used in this study.....	81
Table 3.13	Results of the TAGUCHI design of experiments obtained with MINITAB. .	82
Table 4.1	Chemical composition of metakaolin, fly ash and OPC utilized in study.	88
Table 4.2	Mix designs for fly ash, metakaolin and OPC based mortars.....	89
Table 4.3	Seven-day compressive strength of mortar specimens.	94
Table 5.1	Chemical composition of fly ash utilized in this study.....	105
Table 5.2	Mineralogical composition of fly ash utilized in this study.....	105
Table 5.3	Characteristics of sodium silicates utilized in this study	106
Table 5.4	Coding for research variables in R	109
Table 5.5	Decision Support Table for the Design of Experiments results.....	117
Table 6.1	Design of experiments to evaluate viscosity.....	125
Table 6.2	Preliminary spraying tests.....	134
Table 6.3	Effect of water, surfactant and curing regime on sprayable geopolymer mortar.....	135
Table 6.4	Results from the repetition of the successful mix design under higher temperature conditions.....	136
Table 6.5	Supplementary spraying tests performed.....	137
Table 6.6	Research variables for the surfactant design of experiments.....	139
Table 6.7	Final proposed mix design.....	154
Table 7.1	Compressive strength results for the proposed geopolymer mix.....	158
Table 7.2	Flexural strength of geopolymer mix with and without the addition of fibers.	159
Table 7.3	Tensile strength results for geopolymer mix.	160
Table 7.4	Remaining compressive strength and mass loss of final geopolymer mix. .	161

Table 7.5	Mass of specimens required for ASTM C-642.....	162
Table 7.6	Values calculated using standard ASTM C-642.....	163
Table 7.7	Length change (%) of coating formulation bars in a solution of NaSO ₄	164
Table 7.8	Test results for the geopolymer coating formulation and OPC.	166
Table 7.9	XRD Phase analysis of the geopolymer coating and Class F Fly Ash	169
Table 7.10	Specification sheet for the geopolymer coating.....	170
Table 7.11	Design of experiments for copper addition.....	171
Table 7.12	XRD Phase content evaluation	175

LIST OF FIGURES

Fig. 2.1	Types of polymers used for PCC.....	24
Fig. 2.2	Mechanism of formation of polymer-cement co-matrix.	26
Fig. 2.3	A proposed chemical reaction between the polymer, cement matrix and aggregate.	27
Fig. 2.4	Unsaturated polyester (left) and styrol (right).	30
Fig. 2.5	An example of an epoxy reaction.	31
Fig. 2.6	Sialate net of a geopolymer.	43
Fig. 2.7	A proposed geopolymerization reaction.	44
Fig. 2.8	The three types of geopolymer.	44
Fig. 2.9	Proposed structural model for K-Polysialate-siloxo geopolymer.....	45
Fig. 2.10	Molecules of surfactants compared to molecules of superplasticizers.....	61
Fig. 2.11	Top: Surfactant molecule and formation of air bubbles (a, b). Bottom: Superplasticizer molecule	62
Fig. 2.12	Comparison of the action of surfactant molecules (top) and superplasticizer molecules (bottom) on cement particles.	63
Fig. 3.1	Particle size distribution of the metakaolin used for the test.	70
Fig. 3.2	Mixing of activator solution and metakaolin to produce geopolymer cement. .	71
Fig. 3.3	Casting of geopolymer specimen (<i>left</i>), Geopolymer specimens obtained at room (<i>left</i>) and 75°C (<i>right</i>).	71
Fig. 3.4	Particle size distribution of the fly ash used in this study.	74
Fig. 3.5	Effect of the type of silicate.....	76
Fig. 3.6	Effect of AS/FA ratio	76
Fig. 3.7	Effect of Sil/Hyd ratio	77
Fig. 3.8	Effect of temperature	78
Fig. 3.9	Main Effects Plot from the Taguchi Design of Experiments.	83
Fig. 4.1	Mass loss vs. immersion time for class C fly ash-based geopolymer mortar....	91
Fig. 4.2	Mass loss vs. immersion time for metakaolin based geopolymer mortar.	92
Fig. 4.3	Mass loss vs. immersion time for OPC mortar specimens.	92
Fig. 4.4	Mass loss vs. immersion time for class F, class C and metakaolin geopolymer and OPC mortar specimens.....	93
Fig. 4.5	Remaining compressive strength vs. immersion time for class C fly ash-based geopolymer mortar specimens.....	95
Fig. 4.6	Remaining compressive strength vs. immersion time for metakaolin-based geopolymer mortar specimens	95
Fig. 4.7	Remaining compressive strength vs. immersion time for OPC mortar specimens versus time.....	96

Fig. 4.8	Remaining compressive strength of class F geopolymer after 8 weeks compared to class C fly ash and metakaolin geopolymer and Portland cement (pH=0.6).	97
Fig. 4.9	Remaining compressive strengths of fly ash and metakaolin geopolymer and Portland cement	98
Fig. 4.10	Visual appearance of fly ash geopolymer (left) and metakaolin geopolymer (right) after 8 weeks of exposure.	99
Fig. 4.11	Visual appearance of OPC-silica fume specimens after 8 weeks of exposure.	99
Fig. 4.12	Visual appearance of Class F fly ash geopolymer after 8 weeks of exposure.	100
Fig. 5.1	Particle size distribution of fly ash utilized in this study	106
Fig. 5.2	Main effects plot for compressive strength	108
Fig. 5.3	Interaction plot for compressive strength	109
Fig. 5.4	Main effects plot for remaining compressive strength.	110
Fig. 5.5	Interaction plot for remaining compressive strength	111
Fig. 5.6	Main effects plot for mass loss	113
Fig. 5.7	Interaction plot for mass loss	114
Fig. 5.8	Main effects plot for flow	115
Fig. 5.9	Interaction plot for flow	115
Fig. 6.1	First coating test using a 12" diameter concrete pipe.	122
Fig. 6.2	Third coating test using the reformulated N-10-1.5 mix design.	124
Fig. 6.3	Time vs Viscosity curves for geopolymer pastes made with a sil/hyd ratio of 1.	127
Fig. 6.4	Time vs Viscosity curves for geopolymer pastes made with a silicate/hydroxide ratio of 1.5.	128
Fig. 6.5	Time vs Viscosity curves for geopolymer pastes made with a silicate/hydroxide ratio of 1.5.	129
Fig. 6.6	Main effects plot for viscosity.	130
Fig. 6.7	Interaction plot for viscosity.	130
Fig. 6.8	Tyrolessa mortar sprayer.	132
Fig. 6.9	Spraying geopolymer over wood board.	132
Fig. 6.10	Spraying over a concrete wall.	138
Fig. 6.11	Main effects plot for Compressive Strength.	141
Fig. 6.12	Interaction plot for Compressive Strength.	142
Fig. 6.13	Main effects plot for Flow.	143
Fig. 6.14	Interaction plot for Flow.	143
Fig. 6.15	Main effects plot for Viscosity.	144
Fig. 6.16	Interaction plots for viscosity.	145
Fig. 6.17	Viscosity Curves for samples with a 0.25% of surfactant (left) and 0.75% of surfactant (right).	146
Fig. 6.18	Viscosity Curves for samples with a 1.25% of surfactant (left) and 1.75% of surfactant (right).	146
Fig. 6.19	Viscosity Curves for samples with a concentration of 10%, 20% and 30%.	147
Fig. 6.20	Main Effects Plot for Surface Tension.	148
Fig. 6.21	Interaction Plot for Surface Tension.	148
Fig. 6.22	Forms of droplets from the surface tension meter.	149
Fig. 6.23	Mixing and spraying with first field test.	150

Fig. 6.24 Spraying and finishing with DNA.....	151
Fig. 6.25 A finished section of the manhole coated with the mix design.....	151
Fig. 6.26 Spraying with Spraybuddy.....	152
Fig. 6.27 Second spraying test with Spraybuddy.....	153
Fig. 7.1 Tensile strength tests on geopolymer mix.....	160
Fig. 7.2 Remaining Compressive Strength from Class F Fly Ash Geopolymer, OPC and the Coating Formulation after 8 weeks of immersion in a H ₂ SO ₄ solution of pH = 0.6.....	162
Fig. 7.3 Viscosity vs time graph for 30 minutes.....	168
Fig. 7.4 Yield stress after several rest periods.....	168
Fig. 7.5 Main effects plot for compressive strength.....	172
Fig. 7.6 Interaction plot for compressive strength.....	173
Fig. 7.7 Main effects plot for Flow.....	174
Fig. 7.8 Interaction plot for Flow.....	175
Fig. 7.9 EDS analysis of geopolymer particles.....	178

ACKNOWLEDGMENTS

I would like to greatly thank my advisor, Dr. Erez Allouche, for his wonderful support and guidance throughout my time as a graduate student. His supervision went many times beyond professional work, and he inspired me tremendously to pursue both research and personal goals. I always felt completely supported and encouraged during my time as a graduate student. I would also like to thank Dr. Ray Sterling for believing in my contributions to the department and for his strong support and vote of confidence in my work.

I would like to thank also Dr. Henry Cardenas, Dr. Jay Wang, Dr. Sven Eklund and Dr. Nazimuddin Wasiuddin for their input and guidance as members of my graduate advisory committee. I would further and very specially like to thank Nathan Pettit and Chris Morgan for their committed support to help me complete the technical parts of my thesis work. The present project would have never been completed without their help.

Very importantly, I would like to thank my family: my mom, my brothers and sisters and nephews and nieces for their kind love and support throughout my stay in Louisiana. Last but not least, I would like to thank the friends I have met during my stay at Louisiana Tech. These special thanks are directed to Cristian Pasluosta, Juan M. Fontana, John Matthews, Ivan Diaz, Saiprasad Vaidya, Sandi Perry, Eric Steward, Eric Slusser and Cheng Wang and additionally my friends from overseas, Jaime Carnero, Summer Mancillas, Alejandro Garcia, Sixto Marquez and very specially Stephen Eastment for all their support for the completion of this work and for making me happy with their friendship.

CHAPTER 1

INTRODUCTION

1.1 Background

The problem of the deterioration of concrete sewer pipes and manholes is an increasing concern for civil engineers across North America and the world. Many of these structures, installed during the decade of the 1960's, have reached or are reaching the end of their service life and are compromising the potable water and wastewater conveyance systems. The EPA estimated losses associated with the degradation of concrete sewer pipes and wastewater treatment facilities by sulfuric acid attack to be as high as \$10 billion [1].

Sewer pipelines constitute some of the most important components among the sanitary installations of cities. They are generally old structures, built with an expected service life of 50 years. However, when they deteriorate, generally by biological corrosion or abrasion by water or sewage streams, their replacement by means of the traditional open-cut methods is complicated because traffic disruption and restoration of pavement and soils is necessary. That is the reason why the use of trenchless technologies for replacement and rehabilitation is important to help keep public works efficient, besides making them long-lasting and economical. It is important to assure that the materials used for the rehabilitation of these utilities are the most durable in every way: being corrosion and wear resistant; withstanding the normal loads and stresses of a sewer

pipe; and having a strong bond to concrete so that long term functionality may be guaranteed. Among the most common methods for pipe rehabilitation are gunite lining and spray lining, but other methods are also used.

Coating materials used with these methods are of various kinds; for example; cementitious, epoxies and other polymers. Cementitious coatings are preferred because they increase the pH of the pipe and because of their good workability. Epoxies generally provide higher corrosion resistance, yet these materials have a number of disadvantages that make them unsuitable for certain applications. Portland cement for example, is known to deteriorate rapidly under acidic environments. Epoxies, on the other hand, are often expensive and out of the budget of many municipalities. However, there is potential for a relatively new material –geopolymer- discovered in the early 1970's as a good replacement candidate for both Portland cement and epoxies for pipe rehabilitation.

Geopolymers are inorganic alumino-silicate polymers synthesized with the aid of temperature. They are used in replacement of Portland cement for a growing number of applications, and their properties, like mechanical strength and corrosion resistance, are generally superior to those of Portland cement. However, and in spite of their good properties, there are still a variety of reasons of why geopolymers are not widely used. One of them is their poor workability; geopolymers are known for their short setting times and high viscosities. There have been many efforts to overcome these disadvantages, from the selection of raw materials to the formulation of the activator solution, but still, a more complete solution is needed.

Among the many additives used in the concrete industry, surfactants have been used commonly as air-entrainers to increase durability to concretes under freeze-thaw

conditions. Surfactants create a set of small, stable and unconnected air spheres within the mass of the concrete, increasing its resistance to attacks like freeze and thaw. They also have an observable good effect on concrete and mortar workability. Their use in geopolymers, has been little researched, if not completely ignored.

Furthermore, the main mechanism to lower the pH values of sewers is biologically generated sulfide. Sulfate reducing bacteria reduce inorganic sulfate ions present in the sewage to sulfide ions, which react immediately with dissolved hydrogen in the wastewater to form dissolved hydrogen sulfide, which then is oxidized into sulfuric acid by aerobic bacteria that reside on the inner surface of the pipe wall above the water level. The sulfuric acid attacks the hardened cement paste by dissolution and expansion which causes the deterioration of the pipe and sometimes cracking and complete collapse.

To attack the problem of biogenic corrosion, some researchers have proposed the use of copper oxide as a bactericide. Copper oxide embedded in epoxy has been used successfully to prevent the growth of H₂S producing bacteria. Coincidentally, geopolymers have been used to encapsulate heavy metals with the purpose of immobilization of toxic wastes. These metals include not only copper, but lead and arsenic as well. Both of these areas of research offer an interesting scenario for geopolymers to be used both as a protective coating and as a biogenic agent.

1.2 Objective

The main objective of this dissertation is to design and develop a geopolymer-based mortar coating for the rehabilitation and protection of concrete sewer pipes and manholes against sulfuric acid corrosion.

This objective was divided into several specific objectives:

- To evaluate geopolymer as a suitable candidate material for the rehabilitation of buried infrastructure.
- To study the different parameters of geopolymerization and to design an optimal mix design for the geopolymer mortar in terms of strength and corrosion resistance.
- To study surfactants as workability agents for geopolymers and to characterize the resulting formulation in rheological and surface tension terms.
- To study copper addition to create a copper-substituted geopolymer with possible biocide properties.
- To perform field and quality tests for the resulting invention.
- To explore the commercialization potential of the new geopolymer-based product.

1.3 Organization of the Dissertation

The dissertation is divided into eight chapters: (1) Introduction; (2) Literature Review; (3) Study of the Main Parameters of Geopolymerization; (4) Compressive Strength and Corrosion Resistance of Geopolymers compared to Portland Cement; (5) Optimization of the Activator Solution; (6) Development of a Sprayable Geopolymer

Mortar; (7) Quality Tests, Copper Addition and Commercial Opportunities; and (8) Summary, Conclusions and Recommendations.

Chapter 1 consists of a general introduction of the problem, along with a description of the existing geopolymer technology and the objectives of the dissertation.

Chapter 2 discusses the fields of knowledge related to this contribution, starting from the rehabilitation problem faced in North America and the details of the corrosion mechanisms by sulfuric acid. Then, the chapter proceeds to state the basics of geopolymers chemistry, setting mechanism, uses, advantages and problems. It also describes the existing knowledge on surfactant theory on what is relevant to cements and concretes, ending with a description of a copper incorporated coating for biogenic protection.

Chapter 3 is related to the study of the main parameters of geopolymerization addressed to the understanding the role of geopolymerization fundamental variables, such as raw material, activator solution parameters and curing programs.

Chapter 4 relates a comparative study of compressive strength and corrosion resistance between geopolymers and Portland cement. The study was conducted by means of an eight week testing program based on the exposure of different geopolymer formulations and Portland cement to sulfuric acid solutions of pH values similar to those commonly found in sewers and manholes.

Chapter 5 addresses the testing program developed to develop an optimal activator solution to suit the properties needed for the geopolymer-based coating. Important conclusions regarding the main parameters of the activator solutions are made.

Chapter 6 studies the rheological and surface tension properties of geopolymer with the addition of surfactants. The properties of geopolymer under the action of different surfactants of different concentrations were characterized. Field tests were also conducted and included in this chapter.

Chapter 7 examines the different quality tests conducted on the sprayable grout formulation. These tests complete the characterization needed to offer a specification sheet on the product. The chapter covers all the tests commonly conducted to cementitious coatings to be used in the field of rehabilitation. It also describes the incorporation of copper and encapsulation in geopolymers. Characterization under Scanning Electronic Microscopy (SEM) is presented, and a final recommendation is made based on experimental results. Additionally, a scenario of the commercial opportunities for this product is presented.

Chapter 8 presents the main conclusions and suggests future research directions.

1.4 Key Contributions

The main contributions of the work in this dissertation are described in detail below:

1. The development of a novel product for rehabilitation of concrete sewers and manholes. This product is a novel alternative to solve the many problems that municipalities face to conduct work on their sanitary systems. After being sufficiently tested in an industrial level, the geopolymer coating can become a commercial product with potential economic success.
2. The study of geopolymers from an engineering perspective, rather than a pure chemical or materials science perspective. Although there has been much

research about the main mechanisms behind geopolymerization, not many efforts have been conducted to try and incorporate geopolymers as products and solutions for the construction industry.

3. The study of geopolymer plastic behavior under different alkaline solutions and with different levels of surfactants. Important conclusions are drawn upon these behaviours.
4. The study of an alternative product with possible bactericide properties to solve the corrosion problem of sewers from the root. The role of geopolymer as an encapsulating agent of heavy metals (copper) is also studied.
5. The creation of a product with offers a licensing commercial opportunity to Louisiana Tech.

CHAPTER 2

LITERATURE REVIEW

2.1 Pipelines: Statement of the Problem

2.1.1 Background

Corrosion and deterioration of concrete pipes is a main concern associated with wastewater conveyance and treatment facilities around the world. The EPA [1] estimated losses associated with the degradation of concrete sewer pipes and wastewater treatment facilities by sulfuric acid attack in North America to be as high as \$10 billion. The problem has grown worse in recent years especially in industrialized areas in the southern part of the USA where a large number of sewer lines are scheduled to be replaced over the next five years.

Hydrogen Sulfide (H_2S) can be generated by sewage with slow streams. When present in the atmosphere of the sewer, this acid gas can be converted into the corrosive sulfuric acid and seriously damage concrete structures [2]. The process is carried away by biological means. Certain sulfate-reducing bacteria can split oxygen from the sulfate ion, which is left in the form S^{2-} , and then immediately reacts with water to form a mixture of H_2S and HS^- [3].

H_2S is then chemically converted to H_2SO_4 at the crown of the concrete sewer pipes. Parker [4] conducted studies on *Thiobacillus Thiooxidans*, the bacteria that is responsible for the generation of sulfuric acid in sewers. Several genus of the

Thiooxidans bacteria to produce sulfuric acid have been identified: *T thiparus*, *T thiooxidans*, *T neapolitanus*, *T intermedius* and *T novellas* [5]. All these bacteria contribute in the process of decreasing the pH of the pipe down to the production of sulfuric acid.

The EPA [1] conducted a survey on areas with sulfuric acid corrosion problems. Out of the 89 cities responding to this survey, 36% reported sewer collapses due to this problem. The study pointed out 16 states with severe corrosion problems on their sewers, including Louisiana.

For all these cities the development of new materials and technologies for the rehabilitation of existing and the construction of new facilities is an area of significant interest to many owners of wastewater collection and treatment systems.

2.1.2 Some Types of Pipe Damage and Deterioration

2.1.2.1 Leakiness

Leakiness is defined as water entering or leaving the pipe. It usually occurs in pipe joints, pipe walling, and connection to pipes and manholes.

Among the possible causes of damage creating leakiness are wrong material selection, material aging and a damage event like a localized corrosion or collapse. The non-adherence between the coating and the host material is also a cause of this problem. In order to prevent leakiness, it is necessary to take into account internal or external stresses that may cause changes to the material during utilization [6].

2.1.2.2 Mechanical Wear

Mechanical wear takes place in the wetted section of the pipe. It is a measure of the fine material removed by the action of a water or sewage stream in the inside of the

pipe. Mechanical wear increases the roughness of the pipe and can lead to its destruction by promoting corrosion and causing reduction of wall thickness [7].

Wear can also be defined as damage to a solid surface caused by the removal or displacement of material by the mechanical action of a contacting solid, liquid or gas. Gradual deterioration is often implied, and the effects are, for the most part, surface-related phenomena, but these restrictions should not be rigorously applied when analyzing wear problems or failures.

Surfaces are not completely flat at the microscopic level. At high magnification, even the best polished surface will show ridges and valleys, asperities and depressions. At these points, the contact pressure may be close to the hardness of the softer material; plastic deformation takes place on a very local scale. When sliding begins, these junctions have to be broken by the friction force, and this mechanism provides the adhesive component of the friction. Some asperities may plow across the surface of the mating material and the resulting plastic deformation or elastic hysteresis contributes to the friction force [8].

Fluids with particles, or slurry erosion, are the progressive loss of material from a solid surface by the action of a mixture of solid particles in a liquid in motion with respect to the solid surface. Slurry is by definition a physical mixture of solid particles and a liquid (usually water) of such a consistency that it can be pumped. The particles are in suspension in a liquid, and most pumpable slurries contain at least 10% solids [9].

Scouring wear is the wear caused by various materials carried along by the water, such as sand, gravel, solid metals, and textiles. Some variables related with this kind of stress include piping materials; pipe diameter; stressing or expansion condition of the

pipe; density of water-solid mixture; composition of water-solid mixture; type, size, form, ductility of solid particles; angle of attack between solid particles and pipe walling; velocity of flow; type of flow (laminar/turbulent); temperature of water-solids admixture; and the chemistry of sewage.

The possible consequences of damage are the removal of the piping (or coating) material from the surface; increased roughness and reduction in hydraulic effectiveness. Other effects are the reduction of wall thickness with the consequent reduction of bearing strength and water tightness, and very importantly, the reduction of corrosion protection [7].

The combined effects of wear and corrosion can result in total material losses that are much greater than the additive effects of each process taken alone, which indicates a synergism between the two processes. Although corrosion can often occur in the absence of mechanical wear, the opposite is rarely true. Corrosion accompanies the wear process to some extent in most environments. Corrosion and wear processes involve many mechanisms, the combined actions of which lead to the mutual reinforcement of their effectiveness [8].

2.1.2.3 Corrosion

Corrosion is the reaction of a material with its environment, which causes a measurable change in the material (corrosion manifestation) and can lead to the impairment of the function of a component or a complete system (corrosion damage) [10]. Field experience has demonstrated that sulfate attack usually manifests itself in the form of loss of adhesion and strength [11]. Usually the corroding medium is a liquid substance, but gases and even solids can also act as corroding media. In some instances,

the corrodent is a bulk fluid; in others, it is a film (a biofilm, for example), droplets, or a substance adsorbed on or absorbed in another substance [12].

In the field of sewage installations, corrosion is understood as all the reactions to non-metallic and metallic construction and other materials with their environment which, due to chemical, electro-chemical and microbiological processes, lead to an impairment of the construction or other material. It cannot be excluded that such damage, which is designated as corrosion, is caused by a combined stressing due to chemical, microbiological and mechanical actions [7]. Corrosion can also happen without the aid of mechanical stress.

The extent of corrosion manifestation depends primarily on aggressiveness of corrosion medium and available materials and the temperature and concentration of corrosion medium [7]. At the atomic level, the resistance of concrete to an aggressive sulfate environment is dependent upon the permeability of the concrete and the composition of the hydrated cement paste. Once sulfate ions ingress into the concrete, the form of sulfate attack, and therefore the effects of the attack, depend upon the amounts of monosulfate hydrate, calcium aluminate hydrate, unhydrated tricalcium aluminate and calcium hydroxide in the cement paste.

The two forms of sulfate attack that are known to exist are the following:

- Reaction with monosulfate hydrate, calcium aluminate hydrate, and/or unhydrated tricalcium aluminate to produce ettringite; and
- Reaction with calcium hydroxide to produce gypsum, which results in a decrease in pore solution alkalinity.

Expansion may occur during sulfate attack due to the formation of ettringite and gypsum. In addition, the loss of calcium hydroxide through the production of gypsum can decrease the pore solution alkalinity, resulting in decalcification and loss of calcium-silicate hydrate, the primary strength-giving component of the cement paste. External sulfate attack on concrete may lead to cracking, spalling, increased permeability and strength loss. Sulfate damage to concrete typically starts at the surface exposed to the sulfate environment and sulfate-containing salt that form on the concrete surface. Alternating wetting and drying increases the severity of sulfate attack [12].

The materials that are normally subject to corrosion are cement bound materials (concrete, asbestos cement, fiber cement, mortar) and metallic materials (steel, cast iron). Vitrified clay pipes and sewage tiles are resistant to corrosion, except for hydrofluoric acid. Plastic materials are resistant under certain environments, and they can corrode with a specific corrosion agent and the aid of additional mechanical and thermal stressing. Unalloyed or low alloyed metallic materials must receive internal and external corrosion protection in the form of galvanizing and/or plastomer coating.

A more extended description of the corrosion mechanism is given in the next section.

2.1.3 Mechanism of Corrosion

Internal corrosion in pipes usually occurs due to bad practices of manufacture as in not following guidelines; formation of aggressive sewage due to the influx of various substances; and biogenic acid corrosion (microbiological processes).

2.1.3.1 Inorganic Chemical Corrosion

Internal corrosion is caused by aggressive substances that are already in the sewage or form by means of chemical processes. Generally, among the characteristics of these sewages are suitable concentrations of corrosive substances, low pH values, low flow velocities, long flow periods, high temperatures, and bacterial influences, among others. Aggressive cleaning of the sewers can destroy protective layers [13].

Corrosion by an acid can result in the formation of a salt, which slows the reaction because the salt formation on the surface is then attacked [14].

It was reported that concrete pipes are attacked chemically when subjected to the action of acids with pH values of 6.5 or less over long periods of time [15]. Under anaerobic conditions, the acidity in municipal and industrial sewers could reach pH values of 3 or 2, and in some extreme cases 0.5 [16], thus greatly reducing the useful service life of these structures.

Materials that cause concrete deterioration can be divided into two groups: a) materials that dissolve the hardened cement paste (dissolving attack); and b) materials that cause a volume change in the concrete mass (expansion attack). Generally, agents causing the first type of corrosion are acids or strong bases that react with the aluminates and ferrites in the hardened concrete to form soluble salts and Ca(OH)_2 , which are easily leached out of the concrete matrix. This attack can be recognized visually by the appearance of an eroded surface. The second attack is commonly caused by expansive phases produced by a reaction between sulfates present in the sewage and aluminate-hydrates and calcium hydroxides present in the cement paste. The crystallization of such phases leads to expansion of the hardened concrete, and consequently to cracking,

spalling and delamination of the concrete mass. Ettringite is a common crystal product of this type of attack [17]. Possible consequences of a corrosion attack include: a) leakiness; b) reduction in wall thickness and thus reduction in load bearing capacity (and possible formation of cracks, deformation and/or collapse); and, c) increase in the roughness and subsequent reduction of the pipe's hydraulic effectiveness [7].

Susceptibility to chemical attack is an inherent characteristic of hardened Portland cement paste. Additives introduced in attempts to enhance Portland cement corrosion resistance include, among others, silica fume, fly ash and blast furnace slag. These additives react with Ca(OH)_2 present in the cement pastes to produce C-S-H, and were shown to enhance the resistance of hardened cement paste in environments with pH values above 4.5 [15].

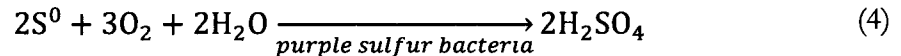
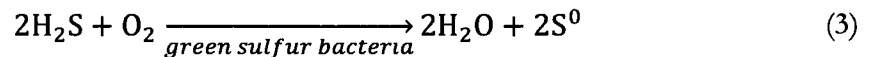
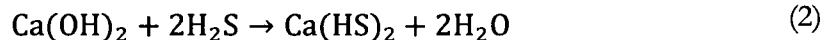
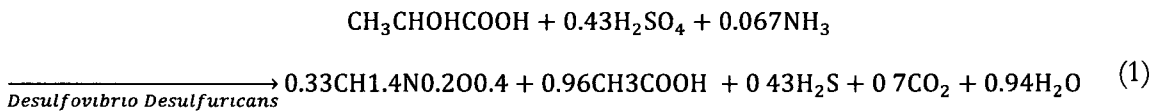
2.1.3.2 Bacterial Induced Corrosion

This process of bacterial induced corrosion is usually called Biogenic Sulfuric Acid corrosion (BSC). While aggressive sewage affects only the “wet” area of a pipe, bacteriological agents affect the “gas space” above the water level. There are different forms of BSC: the endogenous form (the cause of BSC lies within the sewer system), which is itself divided in two forms: autogenous (sulfides developed from organic and inorganic sulfur mixes in wall slime of sewer and deposits) and allogenous (sulfides develop due to disadvantageous operating conditions in other places of the sewer system); and the exogenous form, in which sulfides can be introduced directly with commercial and industrial effluent.

Proteins contained in the deposit are reduced by means of microbial processes under anaerobic or aerobic conditions to volatile sulfuric combinations, mainly H_2S . In

addition, sulfates can be reduced to hydrogen sulfide by means of bacterial metabolism under anaerobic conditions (desulphurication) [14].

Sulfate-reducing bacteria (SRB) from the genera *Desulfovibrio* are the cause of anaerobic corrosion. SRB that exist in a slime layer convert the naturally occurring sulfates in the wastewater into H₂S. (Eq. 1). Hydrogen sulfide can directly attack concrete sewer pipe by reacting with calcium hydroxide to form calcium bisulfide (Eq. 2) Portion of the hydrogen sulfide escapes to the concrete substrate above the water line from the sewer atmosphere and react with oxygen to form elemental sulfur. Elemental sulfur is a substrate to many *Thiobacilli* specie which metabolize it into sulfuric acid. Moreover, H₂S can react with water vapour to produce a mild acidic condition which condenses on the substrate surface above the water line. This process lowers the pH to levels favorable for the growth of *Thiobacilli* bacteria. *Thiobacilli* bacteria are acidophilic and grow at pH 2-3. Hydrogen sulfide can also be oxidized aerobically by green sulfur bacteria and purple sulfur bacteria to sulfuric acid through several steps (Eq. 3 and 4).



The main parameters of this process are temperature, flow time and depositing. Good conditions for the development of bacteriological attack are very long flow distances, sewers not fully utilized and very minimum ventilations. With an ideal temperature, a concentration of up to 23% is possible. The degree of attack can be

divided into weak, medium and strong, according to the following criteria: pH value in condensate water droplets at the sewer walling; sulfide concentration in the free cross section of the sewer; available quantity of *thiobacilli* [14].

Low pH values in concrete sewer pipes are usually produced by biologically-generated sulfide. This process takes place in two stages. Sulfate reducing bacteria reduce inorganic sulfate ions present in the sewage to sulfide ions, which react immediately with dissolved hydrogen in the wastewater to form dissolved hydrogen sulfide. This hydrogen sulfide is released to the atmosphere due to turbulence in the waste stream and condenses near the crown of the pipe above the waterline. In the second stage, the hydrogen sulfide is oxidized into sulfuric acid by aerobic bacteria that reside on the inner surface of the pipe wall above the water level. One species of bacteria, *Thiobacillus Thiooxidans*, is known to grow well in the laboratory in environments with pH as low as 0.5. The sulfuric acid attacks the hardened cement paste by dissolution and expansion. The H^+ ion acts as a dissolving agent while the SO_4^{2-} ion produces expansion when reacting with the above mentioned concrete phases [18].

2.1.4 Currently Used Rehabilitation Methods

Measures adopted to deal with sulfuric acid are generally directed at limiting the formation of hydrogen sulfide by means of sulfur content elimination. The introduction of bactericides to the waste stream has also been attempted, but their use was found to be impractical due to the large quantities needed and the potential damage to biologically-based processes at the treatment plant. Other mitigation methods such as chlorination, injection of compressed air and the addition of lime were attempted with limited success.

The use of certain types of aggregates also helps preventing corrosion of the cement matrix [19].

Another family of mitigation methods focuses on protection of the concrete wall via the introduction of a thin layer of chemically resistant material on the inner surface of the concrete pipe. Materials used to coat concrete pipes include polyurethane, polyurea, epoxy, mortar epoxy, high alumina cement and asphalt. Shortcomings associated with coating systems include difficulties in ensuring an adequate bond between the spray-on coating and the host pipe substrate, as well as the formation of pinholes that allow sulfuric acid and/or the bacteria to penetrate the coating and destroy the bond between the coating and the inner wall of the host pipe or chamber. Yet another coating system consists of thermoplastic panels (e.g., polyvinylchloride) that are connected to the concrete wall mechanically (i.e., T-lock). Used extensively in the 1960s and 1970s, such systems were found to be prone to sulfuric acid penetrating the thermoplastic liner at the seam lines and corroding the concrete behind the liner [20, 21].

2.2 Coatings for the Rehabilitation of Pipes

2.2.1 Basic Concepts

Coating is a generic term for one or more layers of interconnected coating materials on a base with which they are connected through adhesion.

Coating processes, as used in sewers, serve the purpose of replacing or improving the resistance against physical, biological, chemical and/or biochemical attacks from inside, for hindering a renewed build-up for incrustation, for re-establishing and/or increasing the static bearing strength as well as leak tightness [22].

It is important to understand that the protection offered by a coating is effective until the coating is penetrated by a pit, pore, crack or by damage or wear. When corrosion products start to form between the base material and the coating, they will lift off the coating and allow further corrosion. However, even though the smoothness and continuity of a coating is desirable, in the practice, it is most times not feasible.

There are four basic methods of application: in-situ concrete lining, displacement process, gunite lining and spray lining. As these last two are the most relevant with the present work, they will be discussed further in this chapter.

The main area of application for coatings within the scope of rehabilitation are sewers of cement bound materials (concrete and reinforced concrete) since other materials (plastics, vitrified clay) present disadvantageous conditions for the adhesion of coating materials [22].

An important differentiating feature of the coating process is its thickness. There are four principal subdivisions: waterproofing, sealing, film-forming and coating with mortar [22].

From those, only mortar coatings are appropriate for rehabilitation. The thinnest values for this process are 5 mm for resin, 10 mm for plastic modified mortar and 20 mm for cement bound mortar. The respective thickness of layer depends on the aims being pursued as well as the type of damage. For corrosion, 5 mm is usually enough. For bearing relationship, static requirements would determine thickness.

2.2.2 Desirable Characteristics of a Coating

These are the characteristics that a good sewer coating material should have [23]:

- Consistence in accordance to the spray or gunite method used for application.
- Good wetting of the concrete pipe surface.
- Good adhesion and good internal bonding.
- General insensibility to variations in the surface condition and to the influence of weather.
- Low shrinkage and swelling.
- Low thermal expansion coefficient.
- Insensitivity to induced stresses such as shrinkage, formation of cracks, changes of moisture and temperature.
- Insensitivity to wetting and drying cycles.
- No disadvantageous electrochemical behavior that can cause corrosion to the reinforcement steel.
- Leak tightness towards flowing water, low capillary water take up.
- Porosity to water vapor.
- High degree of resistance to diffusion of chemically reactive or aggressive gases and ions.
- Chemical resistance to substances contained in the sewage and especially to biogenic sulfuric acid corrosion and physiologically safe.
- Resistance to alkali influences from the concrete.
- High resistance to wear.
- Fast hardening times.

When selecting an appropriate coating, a sequence of decisions needs to be made to cover several fundamental points. The first is the need to be clear about the service conditions. This clarity is the key to material selection. The second decision is the choice of application process for the material. This decision involves the question of compatibility with the coating material; that is, not all materials can be applied by all processes. A further question of compatibility arises between both material and process with the substrate, for example, whether distortion from high-temperature processes can be tolerated [8].

2.2.3 Actual Materials Used for Coatings

2.2.3.1 Portland Cement Mortars

Type V Portland cement is regularly used (when Portland cement is used for sewage and water pipeline coatings) because of its sulfate-attack resistance properties. This cement has a very low C_3A composition which accounts for its high sulfate resistance. The maximum content of C_3A allowed is five-percent for type V Portland cement. This type is used in concrete that has a tendency to be exposed to alkali soil and ground water sulfates. Another limitation is that the $C_4AF + 2 \cdot C_3A$ composition cannot exceed twenty percent. This type of cement is essential in the construction of canal linings, culverts, and siphons because of their contact with ground waters containing sulfates. It is required because sulfates cause serious deterioration and swelling to the other types of Portland cement. The serious deterioration will eventually cause the concrete to fail. Type V Portland cement is a very uncommon type used in everyday construction but is routinely used in harsh marine environments [24].

The reason of why Type V Portland Cement is resistant to sulfate attack is directly related to its hydration mechanism. Table 2.1 shows the four main reactions during Portland cement hydration.

The first two reactions give C-S-H as the main product, which is the compound directly related to the strength properties of hardened cement/concrete. The fourth reaction rarely happens due to the small amount of gypsum commonly added to Portland cement (4-6%) and C_4AF mostly remains as an un-hydrated compound (situation which may always be a source of problems as it will be described later). The third reaction is the main responsible of the low resistance to sulfates of most Portland cements.

Since only a small amount of gypsum is added to the admixture, in most cases, the early-formed ettringite ($C_6A\hat{S}_3H_{32}$) reverts to a low-sulfate form often referred to as "monosulfoaluminate" ($C_4A\hat{S}H_{12}$). However, this compound is unstable and will react to form ettringite when a new source of sulfate is present [25]. For sewers, this source may appear due to the exposure of the concrete to sulphuric acid in residual waters or because of the presence of the bacteria *Desulfovibrio Desulfuricans* which produces sulphuric acid under septic conditions [18].

Table 2.1 Main hydration reactions of Portland cement.

ALITE REACTION (MAIN)	$2C_3S + 6H \rightarrow C_3S_2H_3 + 3CH$
BELITE REACTION (LONG TERM)	$2C_2S + 6H \rightarrow C_3S_2H_3 + CH$
CALCIUM ALUMINATE REACTION	$C_3A + 3C\hat{S}H_2 + 26H \rightarrow C_6A\hat{S}_3H_{32}$, which in the absence of gypsum reverts to: $2C_3A + C_6A\hat{S}_3H_{32} + 4H \rightarrow 3C_4A\hat{S}H_{12}$
CALCIUM FERROALUMINATE REACTION	$C_4AF + 3C\hat{S}H_2 + 21H \rightarrow C_6(A,F)\hat{S}_3H_{32} + (A,F)H_3$ which in the absence of gypsum reverts to: $C_4AF + C_6(A,F)\hat{S}_3H_{32} + 7H \rightarrow 3C_4(A,F)\hat{S}H_{12} + (A,F)H_3$

For Type I-III Portland cements, important amounts of monosulfoaluminate present in the hydrated mixture will lead to delayed ettringite formation, and thereby, cracking if the concrete is exposed to a late source of sulfates. In the case of Type V Portland Cement, since the amount of C_3A is low enough to guarantee that a large amount of monosulfoaluminate will not be produced by the reverse reaction of ettringite due to lack of an early source of sulfates, the risk of cracking due to delayed ettringite formation is importantly reduced, although not 100% eliminated.

Among the advantages of Portland cements are the following:

- Most economical coating.
- Type V resistant to sulfate attack because of its low C_3A content.
- Good adhesion to concrete surfaces.
- Low viscosity, easy to be applied by gunite or spray lining processes.
- Low thermal expansion coefficient.
- Physiologically safe.

Some of its disadvantages are:

- It is not 100% inert to sulfate attack. Usually degrades with time.
- Tendency to the propagation of cracks.
- High permeability allowing the diffusion of reactive or aggressive chemical species.
- Long setting times.
- Low resistance to wear and abrasion.
- Low resistance to alkali-aggregate attack.

2.2.3.2 Polymer Cement Concrete

Polymer-modified mortar and concrete are prepared by mixing either a polymer or monomer in a dispersed, powdery, or liquid form with fresh cement mortar and concrete mixtures, and subsequently curing, and if necessary, the monomer contained in the mortar or concrete is polymerized in situ [26].

The polymers and monomers used as cement modifiers are shown in Fig. 2.1.

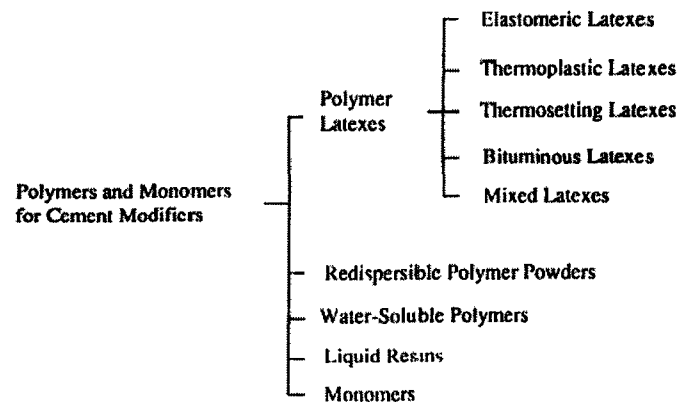


Fig. 2.1 Types of polymers used for PCC [26].

With the addition of resin additives, there are created two-binder medium systems: the cement paste matrix and the plastics system mixed with it. With the use of stable synthetic resin emulsions and droplet sizes in the nanometer region, the hardening resin fills the fine interstices of the coating hydrate crystals and forms an “organic reinforcement” in the cement paste there.

The mechanical properties of the plastic used only have a small influence on the properties of the hardened plastics-modified mortar. However, the geometric-mechanical bonding into the cement paste matrix and the adhesive bonding to the aggregate grains is of decisive importance [22].

It should be specially noted that increasing the amount of polymer over a determinate value will decrease the compressive resistance about 1 N/mm^2 per 1% of the additive. Furthermore, the formation of foam must be prevented, for it would cause an excessive amount of pores and therefore, increase the concrete's permeability.

Polymer modification of cement mortar and concrete is governed by both cement hydration and polymer film formation processes in their binder phase. The cement hydration process generally precedes the polymer formation process. In due course, a co-matrix phase is formed by both cement hydration and polymer film formation processes.

The mechanism for the formation of the polymer-cement co-matrix is shown in Fig. 2.2. As it can be seen, in the first stage immediately after mixing, cement and polymer particles, as well as the aggregates, stand together without any interaction (a), then, as soon as cement particles start to hydrate, a layer of polymer particles deposit partially over the hydrated cement particle (b). In the third stage, a mixture of cement gel and cement unhydrated particles are enveloped with a layer of polymer particles (c), and

in the final stage, the pores and interstitial spaces inside the hydrated cement matrix are filled by a polymer layer, which provides a bond between cement hydrates and aggregates (d) [26].

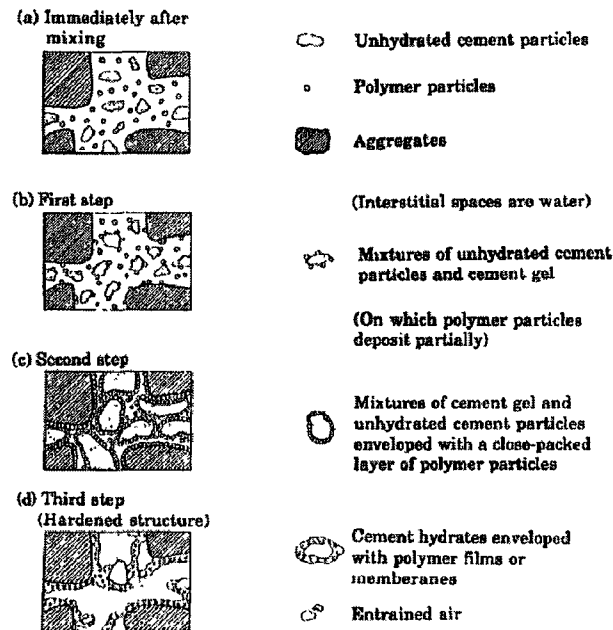


Fig. 2.2 Mechanism of formation of polymer-cement co-matrix [26].

In Fig. 2.3., a proposed chemical reaction between a polyester, the cement matrix and an aggregate is proposed. After hydrolysis, an atom of oxygen of the polymer layer is able to react with the Ca^{2+} ions present in the interstitial solution in the pores of the cement matrix, and these ions are able to react with another atom bonded to another cement matrix surface or with oxygen from an aggregate.

The sealing effect due to the polymer films or membranes formed in the structure also provides a considerable increase in waterproofness or watertightness, resistance to chloride ion penetration, moisture transmission, carbonation and oxygen diffusion,

chemical resistance and freeze-thaw durability. Such an effect is promoted with increasing polymer-cement ratio.

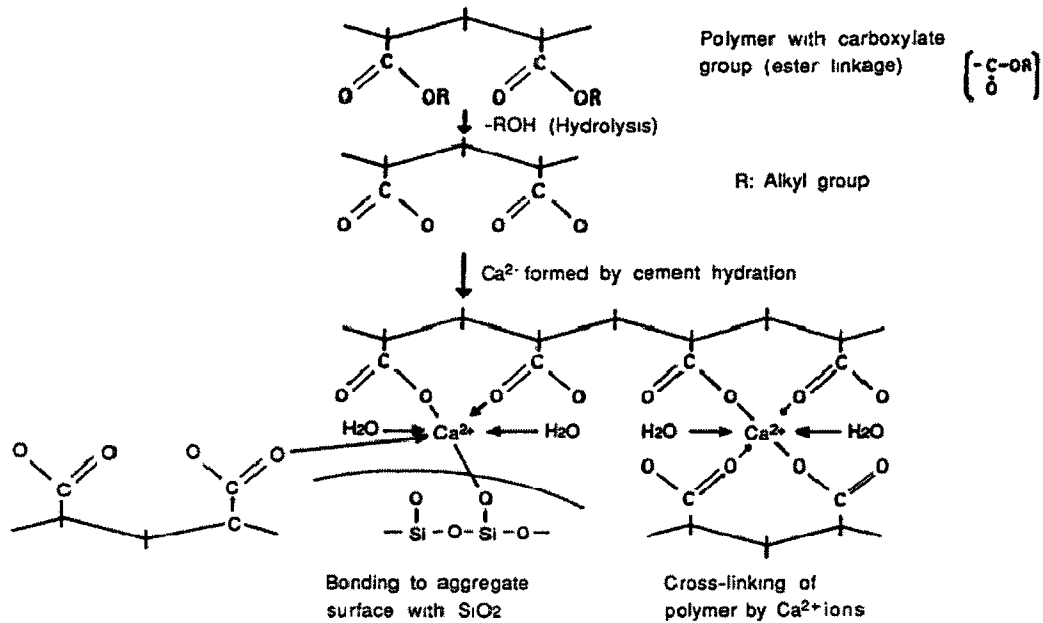


Fig. 2.3 A proposed chemical reaction between the polymer, cement matrix and aggregate [26].

Advantages of Polymer Concrete:

- Decreased permeability, significantly lowering the diffusion of reactive or aggressive species.
- Increased adhesion to concrete surfaces.
- Higher resistance to wear and water flows.
- Higher corrosion resistance.

Disadvantages of polymer concrete:

- High cost of polymeric additives.
- Difficulty to control the composite's expansion coefficient.

2.2.3.3 Reaction Resin Cements or Polymer Concrete

If a mortar contains no cement and if the whole binding medium consists of a synthetic resin mixture capable of reaction at the usual construction temperatures, then one talks of a reaction resin mortar, or of a Polymer Concrete (PC). Most reaction resins are based on unsaturated polyesters, epoxy resins and “cold hardening” methacryl resins.

These cements usually lack of capillary pore cavities; therefore, their durability in weathering and other operational conditions is excellent. What can be critical with certain types of resins is the durability of the bond to old concrete with its long-term moisturing, which are the typical conditions found in sewers.

Reaction resin coatings are generally mixed from at least two components. The hardening occurs by means of chemical reaction immediately after the mixing of the two components. The speed of the reaction is a temperature-dependent quantity and decisively influences the hardening behavior.

Because of the stresses that build up, consideration must be given to the different thermal coefficients of expansion of the piping material and the coating. If the coefficients of linear expansion of resin and pipe differ, then there will be disadvantageous effects on the adhesion or the bonding. The coefficients of the reaction resin can be markedly reduced by means of aggregates and very fine filler materials, which will achieve similar values to that of the cement concrete.

The adhesion mechanisms between mineral and polymer substances are still very incompletely researched. In general, however, it can be said that very good adhesion strength can be achieved when the old concrete surface is clean and dry and the best

possible wetting occurs. Experience has also shown that the drier the pipe is during working, the better the adhesion will be [22].

Some of the advantages of polymer concrete are:

- Porosity almost null, disabling the diffusion of reactive species to the concrete.
- High resistance to wear and water flows.
- Higher corrosion resistance than PCC.
- May contain bactericide agents.

Disadvantages of polymer concrete:

- High cost of polymeric resins.
- Sometimes the reactions may be hazardous for health or environmentally dangerous.
- Adhesion may be poor under certain conditions.
- Thermal expansion differences are considerable.

2.2.3.3.1 Some Types of Resins for Polymer Concrete

The first kind are Unsaturated Polyester resins (UP). By UP resins there is understood the solvents of unsaturated polyester in a polymerizable fluid monomer (e.g. styrol) (Fig. 2.4). The hardening reaction is a co- and mixed- polymerization (among others) that requires the formation of a radical for completion. The radicals are contributed mainly by the organic peroxides (hardener) whose effecting mechanism is triggered by heat ($>80^{\circ}\text{C}$) or, for cold hardening, by the addition of an accelerator.

Care should be taken when handling these resins because the main components are easily flammable, peroxide is caustic, styrol water vapors are damaging to health and certain mixtures of hardeners and accelerators are explosive. [22].

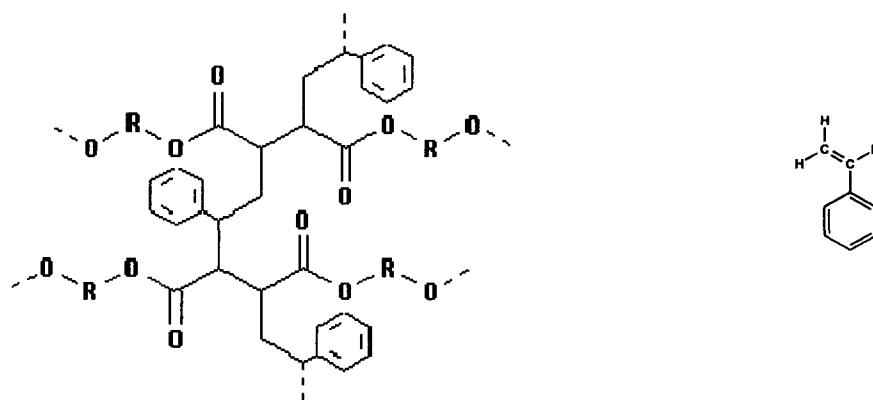


Fig. 2.4 Unsaturated polyester (left) [22] and styrol (right).

Epoxy resins are the second kind. Only two basic types of epoxy resins are used in structural work as standard resins, Bisphenol-A and Bisphenol-F as well as mixtures of the two. Common hardening systems in structural work are cyclo-aliphatic amines, aliphatic polyamines and polyaminoamines (polyamine).

As with all chemical reactions, EP is also dependent on temperatures for its speed of hardening. Epoxy resins are characterized by high strength, good adhesion and chemical resistance. Epoxy resin coatings are resistant to mechanical influences. [22].

Fig. 2.5 shows an example of the reaction of an epoxy resin.

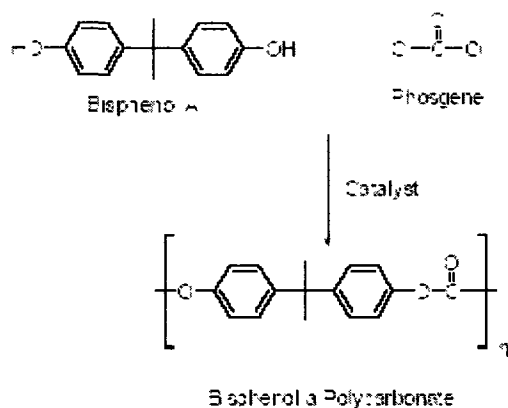


Fig. 2.5 An example of an epoxy reaction [22].

The last example are Polyurethane Resins (PR). Polyurethane is the generic term for plastic materials ranging from hard to elastic that are manufactured out of poly-alcohols and poly-isocyanates. The hardening reaction is a poly-addition. Two components are required in this reaction that must be available in an exact mixture relationship.

Polyurethanes are characterized by their suitability for a large range of applications. It is possible, to a much larger extent than with other reaction resins, to adjust certain properties according to requirements, (e.g., expansion, resistance to wear, resistance to chemicals and to solvents). The resistance to chemicals generally rises with increasing hardness of the coating.

With single-component materials in concrete construction, the reaction takes place with the water vapor available in the air or with the water vapor available in the pores system of the concrete [22].

2.2.4 Surface Preparation

In order to be coated, the surface must be able to absorb stresses from the shrinkage of coating materials and inherent stresses in the coating system caused by

temperature and moisture changes. These inherent stresses comprehend radial and normal shearing stresses.

After the right material has been selected, one must be sure that the concrete pipe for a coating must be [22]:

- free of loose and soft parts and easily removed layers,
- free of cracks parallel to the surface,
- free of fines,
- a roughness suitable for coating materials,
- free of foreign materials (specially deposits of rats),
- a surface must be eroded to the aggregate.

If concrete shows chemical attack damage, further investigations must be made. If there is corrosion of reinforcement, carbonization and chloride contents must be determined.

Among the methods for erosion of surfaces are the following: washing (also with chemicals), acidifying, brushing (manual and mechanical), caulking (chiseling, hammering), bush hammering, grinding, milling, sand blasting, steel shot spraying, moist spraying, steam jets, high pressure water jets (most commonly used), high pressure water-sand jets, scarfing, scarfing and milling and scarfing and sandblasting.

Before the lining process is started, the pipe section must be thoroughly cleaned and inspected. The importance of proper surface preparation to the durability of any coating system cannot be overemphasized. Without proper surface preparation, the finest coating applied with the greatest of skill, will fall short of its maximum performance or

may even fail miserably. A coating can perform its function only so long as it remains intact and firmly bonded to the substrate.

An adequately prepared surface not only provides a good anchor for the coating, but also ensures a surface free of corrosion products and contaminants that might shorten the life of the film by spreading along the coating/substrate interface and destroying adhesion or by actually breaking through the coating.

The principle surface contaminants that adversely affect the performance of the coatings include oils, greases, dirt, rust, mill scale, water and salts (which may be the product of previous corrosion) such as chlorides and sulfides. These contaminants must be removed from the surface before paint is applied.

Selection of the cleaning process is governed by the soil or contaminant to be removed, the degree of cleanliness required, the type of coating to be applied, and the size, shape, material and end use of the part. In addition, the speed with which the process runs will affect the cleaning characteristics.

Methods of cleaning can be classified as:

- Mechanical cleaning including power brushing, grinding and abrasive blasting.
- Chemical cleaning including emulsion cleaning, solvent cleaning, vapor degreasing, alkaline cleaning, acid cleaning, pickling and steam cleaning.

To meet rigid requirements for surface cleanness, mechanical and chemical cleaning methods can be used in conjunction [11].

2.2.5 Coating Techniques

2.2.5.1 Gunite

Gunite is a concrete that is conveyed in a close pressure-resistant hose or pipe to the site and is there applied by means of spraying and then consolidated. Shuttering and vibration are not necessary. This process is usually a man-entering process, and spray lining is applied when the diameter is too small to fulfill this requirement.

Depending on the type of starting mixture, gunite can be dry or wet. In the dry process, the premix consisting in cement, aggregates and admixtures is added in a dry state to the conveying pipe and then added with water at the spray jet. In the wet process, the premix consisting of cement, aggregate, additional water and additives is fed in a wet state to the conveying pipe and conveyed in either a thin or thick flow.

At the start of the process, gunite has a lot of rebound material that can in no case be used again as a part of the starting mixture. The expertise of the operator is critical in this process, since most of the steps are carried out by hand [22].

2.2.5.2 Spray Lining

The pipe must be dry before it can be lined; usually a set of rubber disks are pulled through the pipe several times to ensure that any remaining encrustation and water are removed. A lining machine, which size depends on the pipe diameter, applies a 1:1 sand mortar mix. Table 2.2 contains recommended pipe lengths and optimum lining thicknesses for lining operations.

Table 2.2 Recommended thicknesses for lining operations.

Pipe diameter (mm)	Recommended pipe length (m)	Recommended lining thickness (mm)
75-150	85-120	5
150-450	165	5-6
450-600	180	9-10
>600	550 max.	9-10

Immediately after the lining machine is withdrawn from the pipe section, the curing period begins. The pipe ends are capped to prevent air circulation which can lead to rapid drying and the subsequent cracking of the lining. Several important procedures must be followed during this period, which usually lasts 24-48 hours for normal Portland cement mortars. First, the lining thickness must be inspected to verify that it is in the acceptable range for the pipe diameter. A thickness gauge is inserted inside each end of the pipe section and thicknesses are determined at 300 mm intervals as far in as can be reliably measured. At each interval, lining thickness measurements should be made at the 3, 6, 9 and 12 positions. A second task that must be performed during the curing period is the inspection of all appurtenances to ensure that they are in working order. Valves, especially ball valves, should be checked to ensure that they still operate through their full range of travel (note that it is not a good idea to line through valves, especially ball valves). When necessary, laterals and service connections that are <50 mm in diameter should be cleared by backflushing with water or by injecting compressed air. A third task is prevention of rapid curing of pipe that may be exposed to direct sunlight, which is usually accomplished by steady spraying with water during daylight hours.

Several steps must also be followed during the reconnection process. First, any appurtenances that were cleaned and hand-lined must be inspected, approved and reconnected. Second, the newly lined pipe must be conditioned before the service can be

restored. In the conditioning process, the main is flushed to lower the pH, which can reach 10 or higher. It is then fully charged with chlorinated water and allowed to stand for periods that range from 15 min to 24 hours. Next, the main is discharged and dechlorinated and then recharged with system water. Bacteriological samples must be taken to ensure that water quality standards are met [27].

2.2.5.3 Curing

Curing is an advantage for the intended application, since steam and hot water curing are standard methods already used for long time by the pipe industry [49].

2.2.6 Quality Tests Conducted on Coatings

Many tests exist for the establishing the reliability of the protective coatings, and they can be subdivided in the following groups [28]:

- Field tests
- Simulated service tests
- Laboratory (accelerated) tests

Field tests produce the most reliable performance data because all the variables and phenomena that occur during real operation of the pipelines are present. However, it is always desirable to have control over a few of the most important variables that are known to affect a determinate process, and that is where simulated service tests (isolation of a few variables) and laboratory tests (isolation of one or two variables) are useful. It is important to know that in most cases the interaction between one or several variables for a process may be an important variable itself [29].

Specific requirements for the coating of sewers are detailed in Sections 2.2.6.1 through 2.2.6.2 [22, 29]:

2.2.6.1 Corrosion Resistance

For this test, prisms of coating material are prepared, and when fully hardened, they are stored under aggressive media: nitric acid, hydrochloric acid, sulfuric acid, or ammonium sulfate for up to 70 or 128 days. Then, samples are weighed and measured, and differences are determined. Five percent weight loss is maximum allowed and 2% should be acceptable [22].

As an alternative to mass loss, changes in cement paste strength after periods of sulfate exposure relative to the strength after seven days hydration can also be used to indicate the sulfate resistance of a determinate cement sample [12]. In this “accelerated test,” cubic cement samples are exposed to a source of sulfates, while maintaining the pH and sulfate concentration constant, and compressive strength tests are made before and after the test.

Another option of measuring sulfate resistance are the ASTM tests C452 and C1012 which are based on expansion. Much of the criticism for these tests centers on the specimen size, curing, form of sulfate exposure, duration of test and assessment of sulfate resistance by expansion measurements. The reason for this criticism is that the deterioration most often reported in the field is not caused by ettringite formation; rather, it is due to the decomposition of CH and C-S-H to gypsum by sulfate ions, and conversion of these products to aragonite (presumably due to carbonation). Neither of the currently accepted ASTM test methods predicts this form of damage. Because both ASTM C452 and C1012 use mortar bar expansion as a measure of sulfate resistance; only the ettringite form of sulfate attack is considered. On the other hand, when measuring loss of strength, both, ettringite formation and gypsum formation are taken into account.

ASTM C452 and C1012 may be used after the accelerated test to determine if the mode of failure was ettringite formation.

The above test is used for direct sulfuric acid attack, and it is not suitable for sulfuric acid coming from a biological source. To prepare a biogenic corrosion test, a corresponding sewer atmosphere is created in an acclimatized water noxious gas cupboard. Gaseous H₂S settles on the concrete surface and provides substrate for *thiobacillus*, a bacteria which is injected. The strength of attack depends on the number of bacteria present. Loss of substance is then measured.

2.2.6.2 External Water Pressure Loading

Amount of water pressure, duration of pressure can be varied. For resistance to immersion in water, a previously soaked concrete plate is coated to a thickness of 20 mm with the reaction resin mortar and immersed in water. After 28 and 90 days, the tensile adhesive strength of the coating on the plate is determined. The decay of the tensile adhesive strength must not be more than 20%.

2.2.6.3 Abrasion Resistance

This test is done with the use of coated half-pipes of channels that are built into the test stand and then tilted to about 22.5° backwards and forward to the horizontal over an eccentric shaft. In the channel it is placed a defined mixture of water and various aggregates through which the mechanical attack takes place.

2.2.6.4 Bond Tensile Strength Test

Adhesive strength is the tensile force active at right angles to a test surface that is required to separate a coating from the pipe.

2.2.6.5 Wetting and Drying

The test setup consists of a stainless container for storing water, a high velocity fan for drying, electronic switches to control wet and dry cycles and a mechanism to maintain the water temperature. The samples must be stored without touching each other. The cycles were of two hours of soaking and three hours of drying, with an additional filling and draining period of one hour to give a total cycle time of six hours. Four wet-dry cycles must be completed per day. The water is not recirculated, and hence any chemicals bleached from the samples will not affect the water quality for the subsequent cycles.

2.2.6.6 Freezing and Thawing

If the system is expected to undergo freezing and thawing processes in the field, it is recommended to perform the test according to ASTM C666, whether the tests are conducted in air or in water.

2.3 Geopolymer Cements

2.3.1 Basics

Geopolymers are cementitious materials of a new generation discovered by J. Davidovits in the decade of the late 1970's. Geopolymers are inorganic alumino-silicate polymers that come from the chemical reaction under highly alkaline conditions between an active pozzolanic material (such as fly ash or metakaolin) and an activator solution based in a molar mixture of sodium hydroxide and an alkaline silicate (e.g., sodium or potassium silicate). Geopolymers are usually referred to as inorganic alumino-silicates [30]. The term "polysialate" was also suggested by Davidovits for the chemical designation of geopolymers based on silico-aluminate [31, 32, 33, 34].

2.3.2 Raw Materials

2.3.2.1 Metakaolin

The term “metakaolin” designates different calcined kaolinite species, some reactive and some non-reactive. At about 100-200 degrees C, clay minerals lose most of their adsorbed water. The temperature at which kaolinite loses water by dehydroxilation is in the range of 500-800 degrees C. This thermal activation of a mineral is also referred to as calcining. Beyond the temperature of dehydroxilation, kaolinite retains two-dimensional order in the crystal structure, and the product is termed “metakaolin”. The key in producing metakaolin for use as a supplementary cementing material or pozzolan is to achieve as near to complete dehydroxilation as possible without over-heating. Successful processing results in a disordered, amorphous state, which is highly pozzolanic. Thermal exposure beyond a defined point will result in sintering and the formation of mullite, which is dead burnt and not reactive. In other words, kaolinite, to be optimally altered to a metakaolin state, requires that it is thoroughly roasted but not burnt [35].

Before 1978, there were two species of metakaolin calcined, one at 550 C and the other at 925 C, but both metakaolins reacted weakly. However, the metakaolin manufactured in Europe in 1974 at 750 C proved to have excellent reactivity for geopolymerization [36].

2.3.2.2 Fly Ash

The term “fly ash” is used to describe any of the fine particulate material precipitated from the stock gases of industrial furnaces burning solid fuels [37]. Fly ash generated in large quantities in coal-based thermal power plants is a potential raw

material for geopolymers due to the presence of silica and alumina bearing phases as major constituents.

Fly ash was initially used in Portland cement concrete, not only as a pozzolan and to enhance rheological properties, but also for the reduction of the alkaline-aggregate reaction.

Combustion residues do not require thermal pretreatment. The future could be that electricity utilities can produce energy and low-CO₂ cement in the same plant. The coal in suspension is burnt instantaneously at around 1500 C. The remaining matter present in the coal (essentially constituted of silica, alumina and iron oxide), melts while in suspension, and then on rapid cooling as it is carried out by the fluid gases, solidifies into fine spherical particles.

As a general rule, fly ash is extracted by means of electrostatic precipitators. Generally, fly ash is divided into two categories: low calcium fly ash (Class F) and high-calcium fly ash (Class C).

The fly ash spheres are made of amorphous and crystalline elements, mostly mullite, hematite, magnetite, quartz and unburned carbon residue.

It appears that the reactivity of the fly ash depends upon the nature and proportion of the glass phase present, which in turn, for a given type and source of coal, is generally determined by the operating temperatures within the boiler.

The average composition of coal fly ash in terms of Si:Al ratio may be appropriate for the synthesis of poly(sialate), Si:Al = 1 and poly(sialate-siloxo), Si:Al = 2. Fly ashes can also be classified by their glass content (57-73%) low, (>90% high) and

intermediate (77-90%). High glass content favors geopolymerization and high content of anhydrite, hematite or magnetite slows down the reaction.

2.3.2.3 Other Materials

Other materials, including synthetic precursors, have been used to produce geopolymers [38, 39], but their use is still not widespread.

Geopolymer cements can also be made from natural sources of pozzolanic materials such as lava or blast furnace slag. Blast furnace slag is a mixture of poorly crystalline phases of calcium, aluminum and silicon oxides. Slag is generated by high temperature as a liquid in the blast furnace during iron production. In the context of geopolymers, the key networking cations are Al^{3+} and Si^{4+} ; with divalent Ca^{2+} and Mg^{2+} atoms acting as modifiers of the net together with the alkalis [40]. Slags from particular blast furnaces are relatively consistent on their chemical properties; however, like fly ashes, blast furnace slags do vary between furnaces and locations. Shi [41] contributed significantly to the understanding of the reactivity of different slags, but much remains to be discovered respecting the networks they form after hardening [42].

2.3.3 Chemistry

The polymerization process is carried out by putting the pozzolanic material in contact with the alkaline activator solution which gives as a result, the presence of polymeric chains. These polymeric chains can be hypothetically considered as a result of a polycondensation of ortho-sialate ions. Since the exact reaction mechanism has not been fully determined yet, it is usually assumed that the synthesis is carried out by the means of oligomers, (a polymer that consists of two, three, or four monomers, (e.g.,

dimers, trimmers) which provide the unitary structures of the tridimensional macromolecular net (Fig. 2.6).

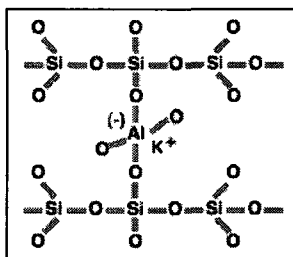


Fig. 2.6 Sialate net of a geopolymer.

Geopolymers that are based on aluminosilicates are called polysialates. This term is an abbreviation of poly-(silico-oxo-aluminate) or $(-\text{Si-O-Al-O-})_n$ (being n the degree of polymerization). The sialate net consists of SiO_4 and AlO_4 tetrahedra linked together by shared oxygen atoms. Inside the cavities of the net, positive ions (Na^+ , K^+ , Li^+ , Ca^{++} , Ba^{++} , NH_4^+ , H_3O^+) should be present to balance the negative charge of Al^{3+} so that Al can be linked to 4 oxygens, like Si. The empirical formula for polysialates is the following:

$$M_n(-(\text{SiO}_2)_z-\text{AlO}_2)_n w\text{H}_2\text{O}, \quad (5)$$

where M is any of the above mentioned cat ions, n is the degree of polymerization, z , which can be 1, 2 or 3, determines the type of resulting geopolymer, that means if $z = 1$, the net will be of the polysialate type. If $z = 2$, then the net will be a poly(sialate-siloxo) and if $z = 3$, the net will be a poly(sialate-disiloxo), and w is the number of water molecules associated, as it is shown in Fig. 2.7 and 2.8.

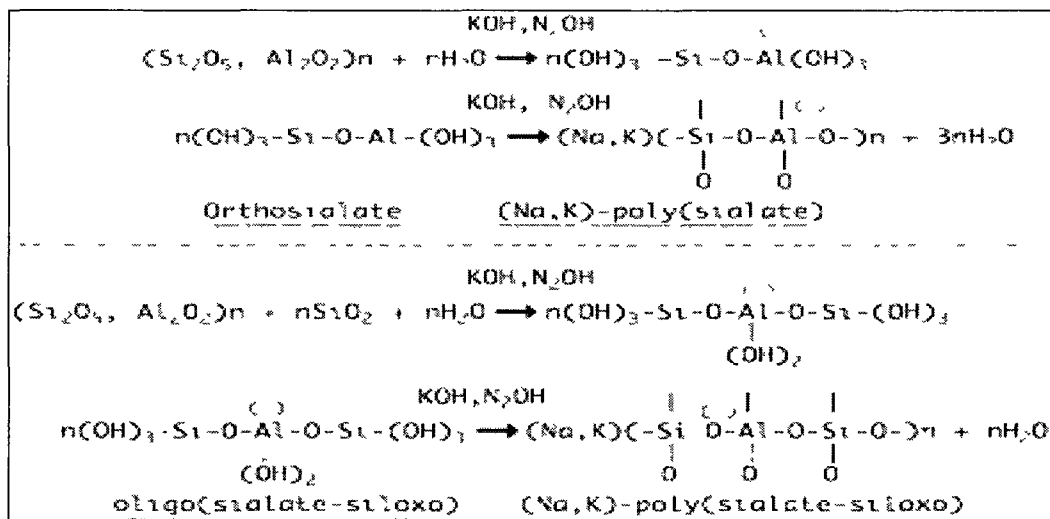


Fig. 2.7 A proposed geopolymerization reaction.

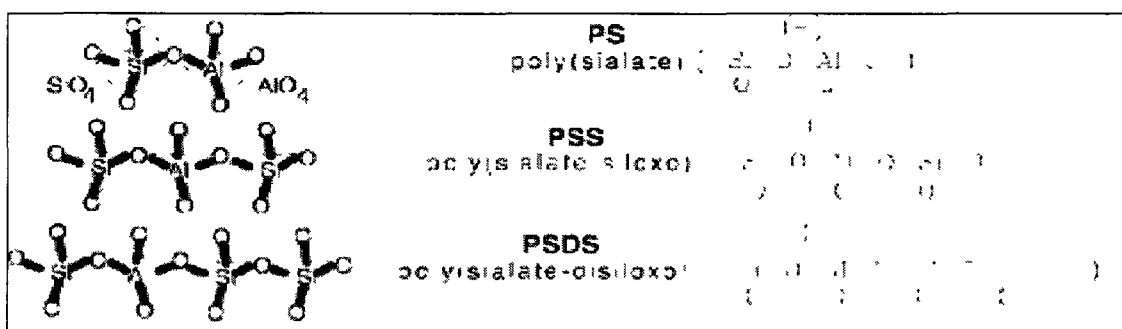


Fig. 2.8 The three types of geopolymer.

Geopolymers morphology ranges from amorphous to nearly crystalline. However, geopolymers used in the construction industry are usually amorphous. Even though the structural model of a geopolymer is still being researched, a hypothetical model proposed by Davidovits is shown in Fig. 2.9 [30].

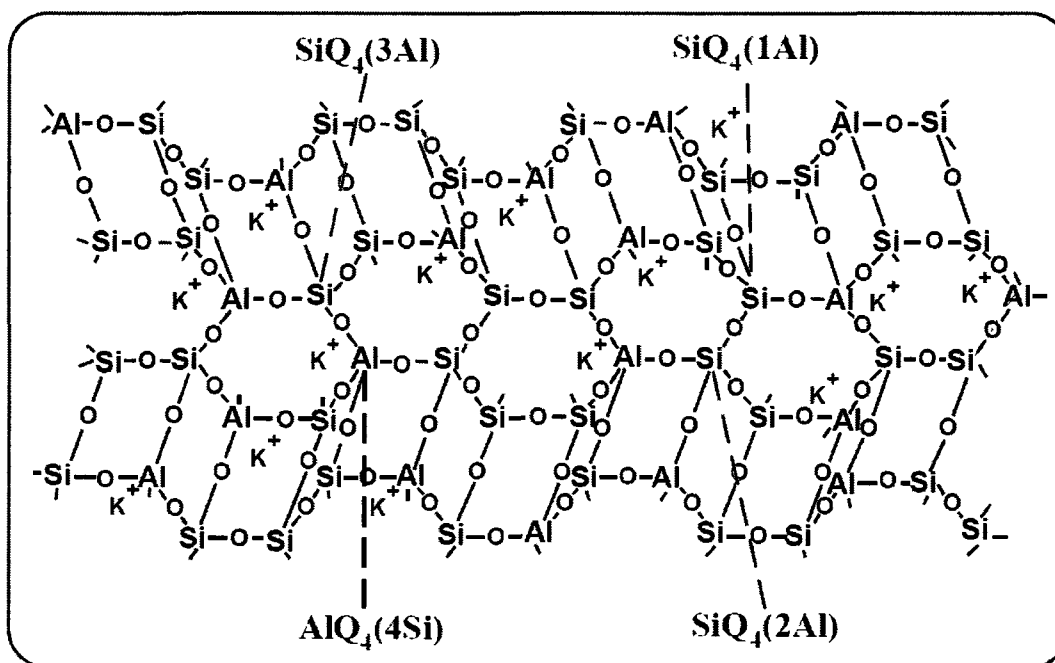


Fig. 2.9 Proposed structural model for K-Polysialate-siloxo geopolymer.

2.3.4 Characterization

The majority of geopolymeric materials of practical interest are non-crystalline. The structure cannot be investigated from X-Ray diffractograms or FTIR alone, NMR-MAS spectroscopy provides better insight to the molecular framework.

X-Ray diffractograms for various (Na-K)-polysialate siloxo reveal that the material has a diffuse peak at about 27-29 2θ . Sometimes, the precursors of geopolymer contain crystalline phases that may remain unreacted after the geopolymerization. FTIR results mainly deal with the behavior of the main (Si-Al-O) band, which is found at about 1000 cm^{-1} . An approximate relationship between the frequency of this band and the ratio of Si:Al in the aluminosilicate framework was observed by Milkey [43]. The higher the Al inclusions, the lower the wavelength.

The IR spectra for poly(sialate) and poly-(sialate-siloxo), as well as the geopolymeric precursors, consist of the strongest vibrations found in aluminosilicates which are assigned to internal vibrations of Si-O-Si, Si-O-Al and are found at 950-1250 cm^{-1} and at 420-500 cm^{-1} . The stretching modes are sensitive to the Si:Al composition of the framework and may shift to a lower frequency with increasing number of tetrahedral aluminum atoms.

^{29}Si and ^{27}Al MAS-NMR studies represent a very powerful tool for the characterization of geopolymers. MAS-NMR can be used to determine if Al is 4-fold coordinated. In ^{29}Si MAS-NMR it was shown that each AlO_4 connected to a SiO_4 connected to SiO_4 group increases $\delta(^{29}\text{Si})$ by approx 5 ppm [38, 44, 45].

2.3.5 Curing

Curing of geopolymers can be done at ambient [46] or with the aid of temperature or steam [47]. Rapid drying during curing should be avoided, due to the large water loss during curing. This procedure is essential to obtain crack free materials [48]. Steam curing is an advantage for the intended application since steam and hot water curing are standard methods already used for long time by the pipe industry [49].

2.3.6 Properties

Since the reaction mechanism of a geopolymer is polymerization and not hydration as for hydraulic cements, this process should mostly be aided by temperature, which may be a constraint for its further applications. Studies have shown [50] that a range of temperatures for the hardening of geopolymers goes from 30 to 90°C, depending on the raw materials used and the molar concentrations of the solutions. However, geopolymers are mostly produced at temperatures not below 60°C.

Setting times are controlled by the temperature of the process, but these cements usually set in a few hours after the beginning of the reaction. The rate of temperature should be carefully controlled to avoid an accelerated loss of moisture which may lead to the propagation of cracks.

Geopolymers are usually more viscous than ordinary cement and harder to handle. The workability of geopolymers depends greatly on the ratio by mass of SiO_2 to NaOH and the concentration of NaOH. [X] Special super plasticizers are recommended as an aid during application. However, in spite of these disadvantages, geopolymers show excellent compressive resistance, superior even to that of rapid-setting cements, and their total strength is achieved in a maximum of three days. The curing period and type of activators are the most significant factors affecting the strength development of geopolymers. Longer curing time and higher curing temperature usually (up to 60°C) result in higher compressive strength, but because of its fast polymerization process, usually its maximum resistance will be attained within the first 3 days of hardening [51]. The compressive strength of geopolymers does not vary with age, and other factors also have influence like rest periods and water content [52].

Corrosion resistance of geopolymers is also a great advantage. Since their chemistry is not based on calcium aluminates which are subject to sulfate attack, these materials are practically inert to sulfate corrosion. The geopolymeric net does not show any affinity for a reaction with sulfate salts. Since it is composed by an alkaline silicate net, these cements are also inert to the alkali-aggregate reaction which commonly happens in Portland cements.

Sulfuric acid attack on geopolymers has been found to be controlled by diffusion mechanisms. There are two basic ways that a geopolymer can be affected by sulfuric acid corrosion: the first way is by the formation of gypsum out of the Ca(OH)_2 present in the paste (usually when the raw material is fly ash, that typically has around 4-5% of CaO) after its reaction with sulfate ions. The second way is the leaching of the alkaline element (sodium or potassium) after the diffusion of the SO^{2-} ions in the geopolymer net. The ionic bond of Na/K to the geopolymer net does not seem to be strong enough to resist sulfuric acid corrosion, although the silicoaluminate net seems to be practically unaffected and the geopolymer can still retain a great percentage of its structural strength after sulfuric acid attack as can be shown under SEM observations [53].

Calcium-low or calcium-free geopolymers are specially recommended for corrosion resistance to sulfuric acid applications because calcium is known to readily react with sulfate ions in order to produce gypsum [54]. Geopolymers are practically immune to attack by nitric and hydrochloric acid, as well as sodium sulfate attack. It is important to select corrosion resistance aggregates in combination with the geopolymer in order to maintain its corrosion resistance properties [55].

Studies show that geopolymers respond to normal impact as brittle solids and their crushing strengths range from 32-57 MPa. Fly ash geopolymers are generally more resistant to erosion than non-fly ash geopolymers [56].

Accelerated chloride diffusion testing shows that the resistance of the geopolymer matrix to chloride penetration is orders of magnitude higher than that of OPC matrices, which provides significant advantages in prevention of rebar corrosion under aggressive salt-laden environments [57].

Further, the geopolymeric net usually has voids where heavy metals and other toxic wastes may be accommodated and, therefore, stabilized preventing them from reaching other surfaces where they may become pollutants [50].

The application of geopolymers as a coating is still a vastly unexplored field. Even though there have been some reports showing that geopolymers may have an excellent adhesion to concrete surfaces [29], other results show the complete opposite results; therefore, the adhesion mechanisms between a geopolymer and a concrete surface need to be sufficiently researched. A geopolymer's behavior as a coating for fire protection has also been researched, showing that a geopolymer coated concrete wall may retain up to 54% of its compressive strength after being fired at 800°C for one hour [58]. Properly designed polyethylene molds were manufactured for the execution of these tests.

2.3.7 Ecological Advantages

There are several ecological advantages of these materials. The first is the reduction of CO₂ emissions by not using Portland cement to make concrete. CO₂ emissions to the atmosphere can be reduced up to 90% by the use of geopolymer cements. One of Portland cements most important component is CaO, which comes from the burning of calcite (CaCO₃) at temperatures of about 1400 C. CO₂ is, therefore, released not only from the raw material combustion, but from the fuels used to reach the required temperature. The rule of thumb establishes that 1 ton of CO₂ is released to the atmosphere by every ton of Portland cement clinker produced. On the other hand, geopolymer cements come from wastes from coal burning processes (fly ash) and, therefore, do not require the manufacture of the raw material (as with Portland cement clinker) [59]. The absence of a high-temperature calcinations step in geopolymer

synthesis from ashes or slags is the main feature that provides this advantage. However, the use of metakaolin would increase the CO₂ emissions coming from geopolymer because of the raw material calcinations step involved, and these emissions hinder their widespread use as raw materials [60]. To assess the CO₂ emissions reduction from geopolymer quantitatively, it is necessary to conduct life-cycle analysis. Results show that when geopolymers are carefully formulated, interesting reductions in their CO₂ footprint can be obtained [61].

The second advantage is that by making use of the waste fly ash, the necessity to landfill this material is greatly reduced, if not eliminated. The danger of landfilling with fly ash was greatly acknowledged after the fly ash spill disaster that occurred in Tennessee in December 2008 which caused great environmental concern and cleaning costs of over \$900 million dollars. This spill was followed a few weeks later by a smaller TVA-plant spill in Alabama which contaminated Widows Creek and the Tennessee River. The danger of these environmental disasters relies predominantly on the amounts of toxic heavy metals in these ashes which can cause water poisoning and, therefore, a great risk for the public health of communities [62].

2.3.8 Uses

Geopolymer cement can be used virtually in any application for which Portland cement is currently used. However, and especially due to the high amounts of heat that are associated with it, geopolymers are starting to be used in pre-cast applications such as railway sleepers, pipes and others [63].

Geopolymers can also be used for cheap construction technologies, like adobe style bricks which use lateritic clay earth as their main raw material, which require much less energy and are less expensive to produce [64].

2.3.9 Metal Encapsulation

A geopolymer's ability to encapsulate heavy metals has been documented by a number of researchers all over the world. Minarikova [65], concluded that fly ash-based geopolymer can encapsulate metals like Zn^{2+} , Cu^{2+} , Cr^{3+} , Cd^{2+} and Pb^{2+} , with minimum losses in compressive strength. Perera [66] reported that geopolymer is able to incorporate Fe_2O in its structure, while TiO_2 and MnO are encapsulated but remained unreacted after the geopolymerization reaction took place. The leaching of many of these metals after geopolymerization was studied by Comrie [67], reporting a great potential for geopolymers to be used as a matrix for waste stabilization. Leaching values of these metals were shown to be much inferior to those in Portland cement concrete. Geopolymer's ability to encapsulate metals, however, is strongly dependant on the pH of the leaching compounds [68], but the level of metals to be encapsulated can be low, and in the order of 0.3-0.5% [69].

This feature is particularly important also for ecological applications. Among the techniques used for toxic waste containment are the construction of barriers and waste encapsulation. A geopolymer's ability to encapsulate heavy metal ions could be a great advantage in this respect. Work has already been conducted in mines in several parts of the world, showing encouraging results to promote geopolymer as an effective means to immobilize these atoms [70].

More particularly and in a more relevant manner to the present research, geopolymers have been shown to be able to encapsulate copper in a stable form. Terzano [71] reported that the mobility of Cu ions can be greatly reduced in the geopolymer matrix and that Cu was present mostly in the uncombined forms of $\text{Cu}(\text{OH})_2$ and CuO . One of the aspects that can favor Cu adsorption is a large pore structure [72]. Among the sources that can be used to obtain copper is $\text{Cu}(\text{NO}_3)_2 \cdot 3\text{H}_2\text{O}$ [73]. However, little is understood still about the mechanism of immobilization of copper in geopolymers and they could be a combined part of the geopolymer structure or simply be embedded interstitially among the pores of the structure [74].

2.3.10 Related Patents

Many geopolymer patents have been filled out; however, the most relevant patent to what this research work accomplishes is an oilwell geopolymer composition [75] to be used in oilwell cementing techniques. The patent comprises a geopolymer admixture modified with a number of set retardants and accelerators and viscosity modifiers. However, many other geopolymer related patents exist.

2.4 Surfactant Theory

2.4.1 Surface Tension

Surface tension is the property of a liquid that causes it to behave as an elastic sheet. It governs the shape that small masses of liquid can assume and the degree of contact a liquid can make with another surface. The units of surface tension are force per unit length or energy per unit area [76].

Surface tension is caused by the attraction between the liquid's molecules by various intermolecular forces. In the bulk of the liquid, each molecule is pulled equally in

all directions by the neighboring liquid molecules resulting in a force of zero. At the surface of the liquid, the molecules are pulled inwards by other molecules deeper inside the liquid and are not attracted so intensely by the molecules in the neighboring medium (air, vacuum, or another liquid). Therefore, all the molecules at the surface are subject to an inward force of molecular attraction which is balanced only by the liquid's resistance to compression, meaning there is no net inward force. However, there is a driving force to diminish the surface area and, in this respect, a liquid surface resembles a stretched elastic membrane. The molecules in the surface are in a higher state of energy than the inside molecules since they have fewer neighbors [77].

The formation of drops occurs when a mass of liquid is stretched. Therefore, liquids with higher surface tensions will form drops of a more circular shape that will take longer to detach from the main liquid.

The surface tension of a liquid is an important factor due to two reasons: sprayability and wetting of a surface. There is a critical surface energy for wetting of a solid body and, thereby, assure adhesion. According to this theory (Zisman) [78], the surface of a solid body is wetted by every fluid whose surface energy is less than the critical surface energy of the solid body.

In the wetting of normal concrete surfaces, the desired contact angle should be around 0 degrees, which means a spontaneous wetting of the concrete and capillary take-up. When the angle becomes larger, a reduction of adhesion can be expected. The presence of low surface energy liquids such as oils, fats and polymers will prevent the adhesion of further layers [23].

2.4.2 Surfactants

Surfactants are wetting agents that lower the surface tension of a liquid, allowing easier spreading. They are usually organic compounds that are amphiphilic, meaning they contain both hydrophobic (“tails”) and hydrophilic groups (“heads”). Therefore they are soluble both in organic solvents and water.

Surfactants reduce the surface tension of water by adsorbing at the liquid-gas interface. Surfactants are often classified into four primary groups: 1) anionic or negatively charged; (e.g., carboxylates formed from the neutralization of carboxylic acids, sulfonates, from sulfonic acids, and sulfate esters); 2) cationic or positively charged; from which the most common example is substituted ammonium ion (RNH^+); 3) non-ionic or uncharged polar portion; (e.g., polyoxyethylenated compounds in which the polarity and solubility are derived from a $(\text{CH}_2\text{CH}_2\text{O})_x$ structure) and 4) zwitterionic or dual charge which are far less common.

The non-polar tail of the molecule is frequently a straight or branched chain hydrocarbon group of perhaps 8 to 20 carbon atoms, alkyl (8-15 carbons) benzene groups, or larger polymer structures. This portion must be comparatively large for there to be a significant surface activity; a short chain will not do.

When a surfactant molecule is adsorbed at an interface, the nature of the molecule allows its two different portions to arrange themselves so as to have the polar head in the liquid phase and the non-polar into the air phase. This phenomena is the cause of the reduction of surface tension. The higher the concentration of a surfactant in solution, the lower the surface tension.

Normally used in the form of sodium salt, the ionized polar group becomes orientated into the aqueous phase, while the hydrocarbon chain orients into the air within the bubble [79].

2.4.3 Air Entraining Agents

Air entraining agents are surfactants which are, as has been stated, materials whose molecules are adsorbed strongly at air-water or solid-water interfaces. That is, molecules that are abstracted from the solution phase and concentrated at the surface. Such molecules are termed “amphipathic”. One portion of the molecule is polar and the other is non-polar.

Air entraining agents are only a subgroup of surfactants. Air-entrainment is essential for the durability of concrete that will become wetted and exposed to freeze-thaw conditions. All concrete should be air-entrained, except where high strength is required. Air entrainment improves the workability and consistency of plastic concrete and reduces bleeding.

It should be noted that many, if not most, surfactants (soaps, detergents, etc.) could probably serve as air-entraining agents for use with concrete. Not all are equally good, and the critically important properties of the entrained air system depend on the nature of the surfactant used.

The following are the most important types of air-entraining agents:

1. Salts of wood resins (vinsol resin). The most widely used resin. Its active ingredient is sodium abietate, the sodium salt of abietic acid.
2. Synthetic detergents (alkyl aryl sulfonates, alkyl sulfates; sodium dodecyl benzene sulfonate, sodium oleyl sulfate, sodium oleate).

3. Salts of sulfonated lignin (poor effect).
4. Salts of petroleum acids.
5. Salts of proteinaceous materials (not common).
6. Fatty and resinous acids and their salts (not very effective).
7. Organic salts of sulfonated hydrocarbons.

Owing to the low cost of all these materials, it is unlikely that more expensive substances will be used in concrete until research proves why others are better.

Vinsol resins, and the resins derived from pinewood and are, in general, are more effective in the presence of alkali metals such as calcium and sodium, and many admixture combinations are derived by prereacting with sodium hydroxide.

Non-ionic surfactants are less efficient than anionic ones, but they are more stable in the presence of calcium ions, when anionic surfactants are precipitated and rely on the sparingly soluble nature of these materials in order to function. Bleed is reduced with the use of air-entrainers.

Air-entraining agents used in concrete should be added as solutions dissolved in the mixing water of the concrete. If other admixtures are also used, the air-entraining agent should be added separately because sometimes there are reactions between materials that could result in a decrease in the effectiveness of the air-entraining agent. The dosage rate is usually between 0.3 to 1 ml/kg of cement, but this rate varies.

Air entraining agents can be used with cements other than Portland cement. When used with blended cements, a larger amount of agent may be required. They have no appreciable effect on the rate of hydration of cement or on the heat evolved by that process. Even if they possess retardant properties, they are used in such small amounts

that such effects are negligible. Apparently they also have no effect on the chemical composition of the hydration products. The pore structure of the hardened cement paste was found to be the same, with or without air-entrainment. The only effect of these agents on cement paste seems to be the inclusion of the air-bubbles [80].

2.4.4 The Effect of Air Entrainment in Concrete

The air bubbles in concrete are generated by the mixing action. All the air-entrainment agent does is stabilize the bubbles that are formed; it does not generate them. Even non-air entrained concrete has some amount of entrapped air, but if the air-entrainer is used, there is more entrapped air and smaller bubble sizes are produced.

The action of the air-entraining agent is to stabilize the smaller bubbles and to ensure they remain in the concrete. To avoid loss of strength, the total volume of the pores should not be larger than necessary; therefore, the pores should be small. The pores should not be readily filled with water if the paste is saturated; small isolated pores are most likely to meet this requirement. Typically, the pores are 10-250 μm in diameter and the average maximum distance from any point in the paste to the nearest void, called the void spacing factor, is about 150 μm .

Without an air-entraining agent, the bubbles incorporated in the concrete by the mixing are lost relatively easily. They coalesce and form larger bubbles when they are brought to each other, then the larger bubbles come to the surface when the mixing action brings them relatively close, and they burst and are lost.

One stabilizing action of the air-entraining agents is the result of its adsorption at the bubble surface. The adsorbed molecules form a film and are oriented with their polar beads in the water phase. If the molecules are charged, the bubble will acquire this

charge, so when two bubbles approach each other during the mixing, they experience an electrostatic repulsion that keeps them separate when they would otherwise coalesce.

Inside the created bubbles, the polar tail is attached to the surface while the non-polar tail is orientated in the inside of the bubble. Therefore, the surface of the air bubble becomes charged, and mutual repulsion between air bubbles occur. This phenomenon prevents the coalescence into larger bubbles.

In cement and mortar, this surface charge causes the stabilized bubbles to adhere to the oppositely charged zones on cement and aggregate particles. The overall net effect is an aggregate-air-cement-air-aggregate type of bridge, improving the cohesion of the mix and further stabilizing the air-void system. This system improves the workability of the mix because of the effect of the bubbles acting like compressible bearings.

Generally, an increased amount of agent dosage will increase the air content. A higher slump will have the same effect. Finely divided (fly ash, carbon black, etc.), material causes a reduction in the air content and an increase in the dosage of air-entraining agent, due to the rapid adsorption of admixture by the amorphous carbon particles in the ash.

Fine fractions tend to “bind” more of the mix water because of the requirement that it coats their larger surface areas, so the water cannot be a part of the bubble stabilizing process. This action is the reason why fly ashes with high LOI cause an especial reduction in air content and require additional air entrainer. The ashes that require more air-entraining agent also cause a greater instability and more rapid loss of the plastic concrete. Excessive sand fines and a richer mix also cause this problem. High temperature decreases bubble formation. Cements with high alkali entrain air more easily

that low-alkali ones; this air entrainment effect could be done due to the increase of the pH of the aqueous phase. Mixing increases air content to a certain value, then further mixing decreases it. Vibration reduces the air of concrete (and that is precisely its purpose).

The air bubbles stabilized in the concrete increase the slump and workability, but they also decrease its strength, however, the improvement is more on workability than on slump. Workability refers to the ease with which concrete can be transported, placed, compacted and finished.

Lean lightweight aggregate concretes are specially benefited by the use of air-entrainment.

The increase in workability brought about by air-entrainment is usually described as some sort of “ball bearing” action of the air bubbles. These bubbles, which are usually several million per in³ of concrete, allow for easier deformation where the concrete is worked, resulting in an increase of workability.

Air-entrainment affects viscosity in a greater way than yield point. Air-entrained concrete is less subject to bleeding and segregation than non-air entrained concrete. Bleeding is the emergence of mix water on the surface of concrete during and after placement. In addition, bleeding sometimes results in the formation of internal channels.

Segregation is the settlement of solids that destroys the homogeneity of the concrete. Entrained air decreases segregation, but cannot correct those who are derived from poor grading of the aggregate, excessively lean or wet mixes and improper handling of concrete.

In terms of finishability, finishers sometimes feel that air-entrained concrete is more difficult to finish owing largely to its lack of bleed water. These are complaints that air entrained concrete is “sticky” and it hangs up on the finishing tools. The solution for this problem is to use magnesium or aluminum floats and a suitable delay before starting the finishing operations. Air entrainment does not affect the setting time of the concrete [81].

2.4.5 Superplasticizers

Superplasticizers or high-range water-reducing admixtures are chemicals known by their dispersing capability that can be used at higher rates than water-reducing admixtures without a gross retardation of set and, therefore, “flowing” concrete can be obtained without excessive addition of water to the mix. All superplasticizers consist of high molecular weight, water soluble polymers with the majority being synthetic chemicals. They generally fall into four different categories: sulfonated melamine-formaldehyde condensates, sulfonated naphthalene-formaldehyde concentrates, modified lignosulfonates and other synthetic polymers such as sulfonated polystyrene, hydroxylated polymers and copolymer dispersions.

Several differences between superplasticizers and surfactants can be pointed out. The first is the size of the molecule. While superplasticizers are usually polymers with n in the order of thousands, surfactants and particularly air entrainers are much smaller molecules only in the size range of carbon chains of n in the order of dozens (Fig. 2.10). The explanation of the figure is the following; surfactants (left): a) Abietic acid, b) Sodium dodecyl benzene sulfonate, c) Sodium oleyl sulfate, d) Sodium oleate; and

superplasticizers (right): top) Sulfonated melamine formaldehyde concentrate, bottom) Sulfonated naphthalene-formaldehyde concentrate.

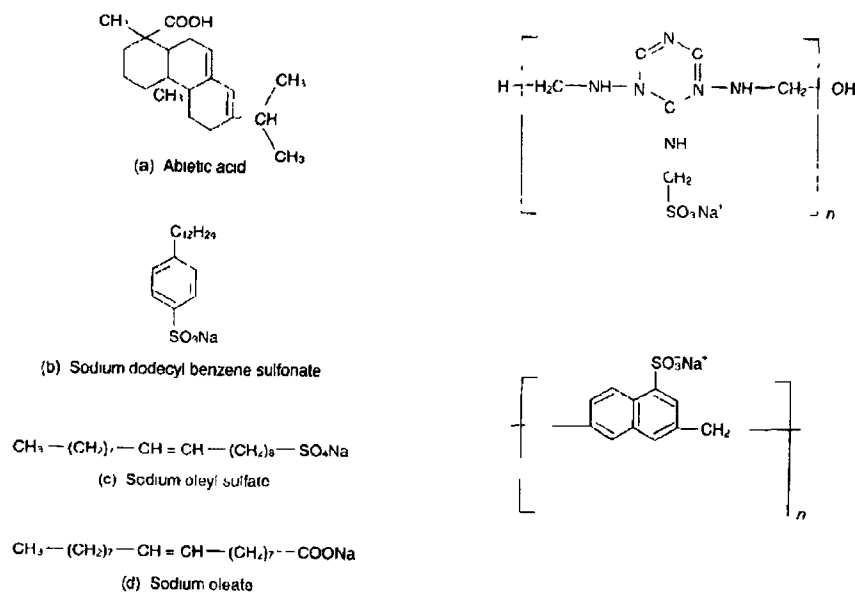


Fig. 2.10 Molecules of surfactants compared to molecules of superplasticizers [81].

The second difference is in terms of the polarity of the molecule. Surfactants have an electrically charged hydrophilic head and a non-charged hydrophobic tail. In the most common surfactants, the head is negatively charged. However, superplasticizers, after being dissolved, will have all of its edges being anionic and, therefore, they will have a negative charge on every end of their molecule (Fig. 2.11).

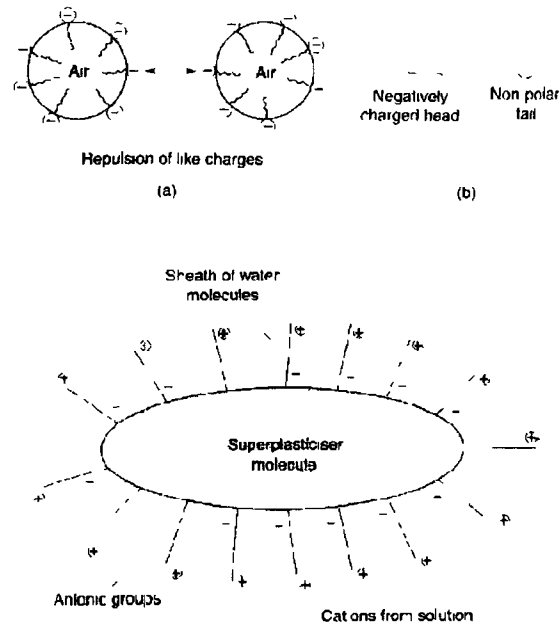


Fig. 2.11 Top: Surfactant molecule and formation of air bubbles (a, b). Bottom: Superplasticizer molecule [81].

The third difference is a result of their structure. As surfactants are polar on the head end and non-polar on the tail, they will adsorb on one end in the aqueous phase and on air in the non-polar end. This is the reason why surfactants are efficient in air-entraining. On the other hand, superplasticizers will pile up around a cement particle and loosely attach to water on the other, producing the charge-repulsing effect that produces a decrease in viscosity (Fig. 2.12). It is fair to say that some modified lignosulfonate superplasticizers also have a weak air entraining effect, but that is not intended to be their primary effect [81, 82, 83].

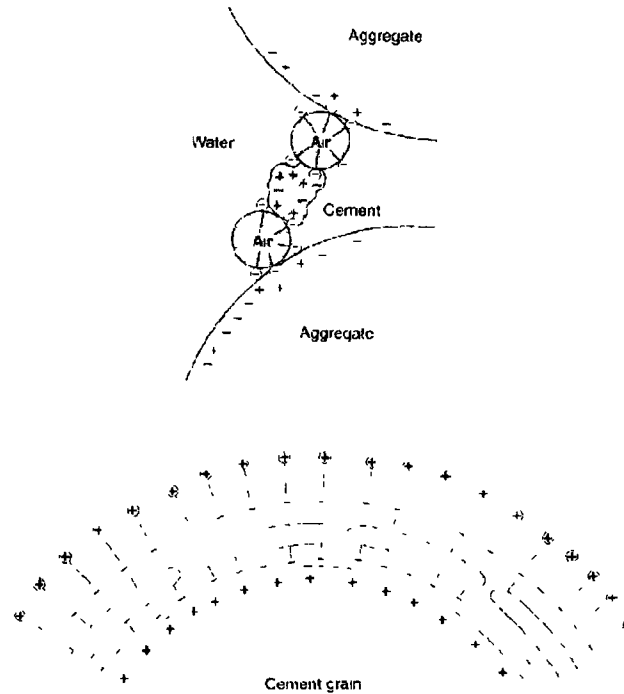


Fig. 2.12. Comparison of the action of surfactant molecules (top) and superplasticizer molecules (bottom) on cement particles.

2.5 Bactericide Coatings

In the past, chemical additions have been tried for the control of hydrogen sulfide in sewerage systems. Some of these additions are metal salts, like iron and zinc salts, which can chemically convert hydrogen sulfide in the wastewater to insoluble metallic sulfides. [84, 85] Various metals also have a toxic effect on sulfate-reducing bacteria (SRB) responsible for generation of sulfide when they are present at high concentrations in the wastewater [86]. However, the use of metal salts in sewage treatment was limited in the last two decades because of its high operational cost, safety concerns and regulations of the Mandated Industrial Pretreatment Program which restricts the levels of certain metals in municipal sewer systems.

Hewayde [14] investigated the effectiveness of a technique to inhibit the growth of *Desulfovibrio Desulfuricans* through coating the pipe's internal wall using either cuprous oxide or silver oxide embedded in epoxy. He found that coating the concrete pipes by either copper or silver oxide effectively reduced the bacteria count in the nutrient solutions. The coatings also helped reducing significantly the internal surface covered by a slime layer. However, mechanical adhesion of the copper oxide coatings was significantly better than for silver coatings, therefore, making it more durable in real life applications.

2.6 General Conclusions

The problem of rehabilitation of sewers in North America is facing a critical phase since many buried infrastructures are in need of repair. Common rehabilitation options include lining with either cementitious or polymeric materials. Portland cement based concrete has limited ability to withstand acidity generated by anaerobic conditions that exist in many sewage conveyance systems over extended periods of time. Over the past 60 years numerous approaches were developed for protecting concrete structures from sulfuric acid attacks with varying degrees of success, but always with significant added cost to either construction and/or operations. It is proposed that a more economic solution might be the development of a novel cementitious material with a different chemical composition that exhibits enhanced resistance to acidic environments by virtue of its own chemical composition.

Geopolymers are cementitious materials of a new generation increasingly gaining reputation for construction applications. Their outstanding final properties like high early compressive strength and high corrosion resistance make them suitable for a large

number of projects worldwide. However, one of the main drawbacks for the generalized use of geopolymers is their poor workability and short setting times.

The raw material for geopolymers is of extreme importance. Fly ash is a great candidate because it is a waste coming from coal burning operations, and it is widely available worldwide. While Class C ash is a more commercial product and can be used as an admixture for Portland cement concrete, Class F ash finds little application and is commonly disposed in landfills.

Therefore, geopolymers seem like a good candidate material for the rehabilitation of sewers and manholes if their workability problems can be resolved.

Surfactants have been commonly used in the concrete industry as air-entrainers. They help the concrete entrap air bubbles of a small and regular size and prevent concrete fatigue under freeze and thaw conditions. However, surfactants also have a significant effect on plastic concrete viscous and surface tension properties. Air entrained concrete is often more workable and easier to pour; however, these characteristics have been poorly researched or taken advantage of in the concrete industry.

These properties of surfactants are of great interest if they can improve geopolymer's workability. Since a geopolymer coating is intended to be developed, it is interesting to investigate if surfactants would be useful to overcome the sprayability problems of geopolymers.

Furthermore, to eliminate the problem of biogenic corrosion from the beginning, attempts have been tried to create biocide coatings by means of incorporating copper oxide in epoxies with successful results. Geopolymers are known to be able to have the capacity to encapsulate heavy metals from wastes. The capability of geopolymer to be

able to encapsulate copper and their posterior use as a biocide could be a tremendous opportunity to create a product with superior properties to those already available in the rehabilitation industry. A complete rehabilitation solution could therefore be available to a wide market of municipalities across North America, and the task of providing a better solution to cope with the growing rehabilitation needs could be achieved.

CHAPTER 3

STUDY OF THE MAIN PARAMETERS OF GEOPOLYMERIZATION

3.1 Introduction

As it was mentioned in the literature review, there are important variables that play a significant role in geopolymerization. When only sodium solutions are used, those variables can be grouped in three sections (Table 3.1).

Table 3.1 Important variables in geopolymerization

RAW MATERIAL	ACTIVATOR SOLUTION	CURING
Type (fly ash, metakaolin, etc)	Silicate type	Type (dry heat, steam, etc, room)
Class (Fly Ash Class C, F, etc)	Hydroxide molarity	Temperature
Chemical composition	Silicate/Hydroxide ratio	Time
Phase distribution	Alkaline solution/Raw material ratio	Rest period
Particle size distribution		
Impurities		

Significant work has been published with respect to all of these variables, however, it was necessary to make preliminary studies at the Trenchless Technology Center at Louisiana Tech University to gain in-house experience with the fabrication of these materials.

The first step was to reproduce a geopolymer formulation from the literature [58] and to evaluate its compressive strength. Next, the effect of the silicate type,

silicate/hydroxide ratio, activator solution/fly ash ratio and different temperature and time regimes was evaluated. The fly ash utilized for this initial test was kept constant. Finally, a more comprehensive study was conducted by means of a Taguchi design of experiments, using three different types of fly ash, the activator solution/fly ash ratios and more temperature/time regimes.

3.2 Production of a Geopolymer Sample at Louisiana Tech Laboratory

3.2.1 Formulation

The formulation for this preliminary test can be seen on Table 3.2 [58].

Table 3.2 Formulation for the first geopolymer experiment at Louisiana Tech.

REAGENT	%
Sodium Hydroxide 15 M	18.3
Sodium Silicate "D"	36.7
Metakaolin	45

3.2.2 Raw Materials

3.2.2.1 Metakaolin

Metakaolin from PowerPozz was used for this first experiment. The chemical composition is shown on Table 3.3.

Table 3.3 Chemical composition of the metakaolin sample used for this test.

OXIDE	WEIGHT %
SiO₂	54,26
Al₂O₃	39,82
Fe₂O₃	2,91
CaO	0,70
MgO	1,51
SO₃	0,01
LOI	0,72
Na₂O	N.A
K₂O	N.A
TOTAL	99,93
Si/Al ratio	1.36

The formulation from the literature [58] is very similar (Table 3.4):

Table 3.4 Chemical composition of the metakaolin used for the literature reference paper.

OXIDE	WEIGHT %
SiO₂	52,1
Al₂O₃	43,0
Fe₂O₃	0,7
CaO	0,0
MgO	0,3
SO₃	N.A.
LOI	0,8
Na₂O	0,1
K₂O	2,5
TOTAL	99,5
Si/Al ratio	1.21

The Si/Al ratio for our metakaolin is slightly superior to the one used by [53], but still suitable for geopolymer cement. Another difference to be taken into account is the 2.91% of ferric oxide in the metakaolin used for our test, which may just cause slight color variations.

The particle size distribution (Fig. 3.1) of the metakaolin used for the experiments was also analyzed. The full results can be seen in Appendix A.1.

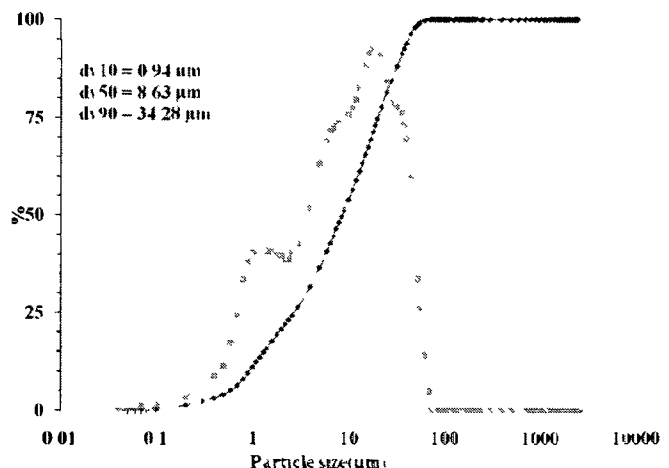


Fig. 3.1 Particle size distribution of the metakaolin used for the test.

The particle size is finer than that of cement, which will make the paste highly reactive, but also highly hygroscopic.

3.2.2.2 Alkaline Solution

A combination of 15 M NaOH solution and a commercial sodium silicate with chemical composition of 14.7 % by weight Na_2O and 29.4 % by weight SiO_2 was utilized as the activator solution for the geopolymer mortar. The silicate was obtained from the PQ company and it is labeled commercially as “D”.

3.2.3 Procedure

The first step was to prepare the alkaline solution. Na(OH) pellets were dissolved in distilled water until a 15 molar solution was obtained. Then, the NaOH solution was mixed with the sodium silicate solution in the proportions indicated in Table 3.2. After a uniform mixture was obtained, metakaolin and activator solution were thoroughly mixed by hand (Fig. 3.2) until they formed a thick slurry.

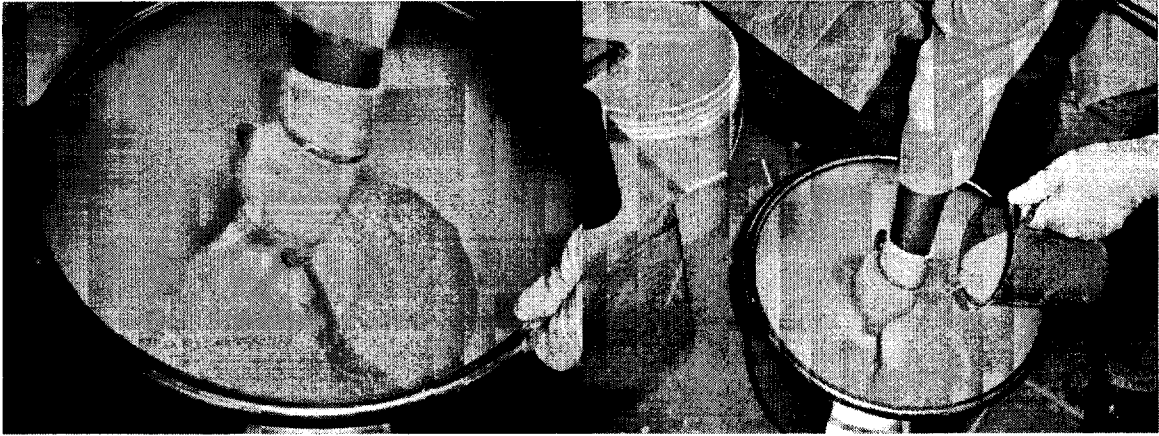


Fig. 3.2 Mixing of activator solution and metakaolin to produce geopolymer cement.

Then, three 3x6" cylinders were casted (Fig. 3.3) and cured for 24 hrs. Two were cured at 75°C and 1 at room temperature.

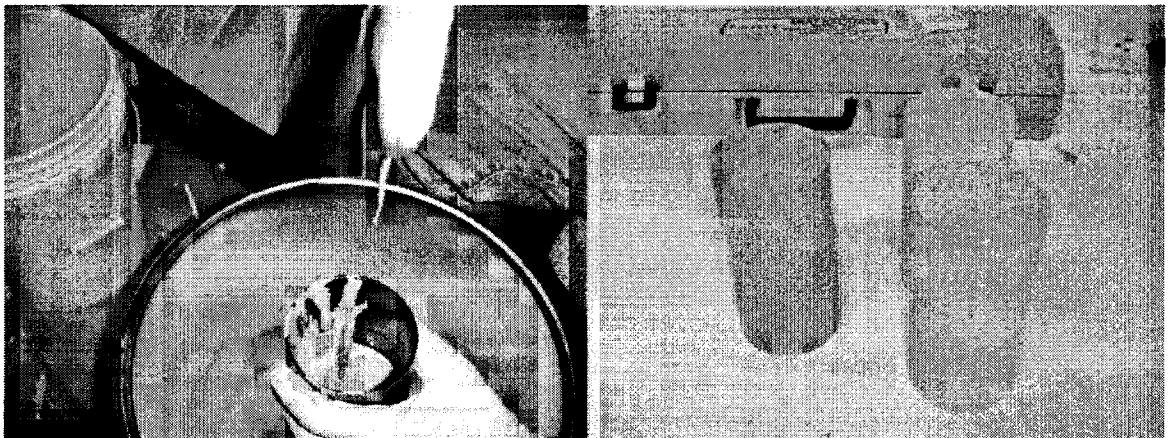


Fig. 3.3 Casting of geopolymer specimen (*left*), Geopolymer specimens obtained at room (*left*) and 75°C (*right*).

3.2.4 Results

The surface of the cylinders was smooth. The specimen cured at room temperature had a slightly darker color, apparently because it did not lose as much water as the other two.

Three day compressive strength was determined for these specimens to establish a comparison with the literature. The results are shown in Table 3.5:

Table 3.5 Compressive strength of sample geopolymer specimens.

SPECIMEN	COMPRESSIVE STRENGTH (psi)
75°C cured (#1)	3895.86
75°C cured (#2)	3574.98
Average of #1 and #2	3735.42
Room temperature cured (#3)	1848.33
Literature (26)	3916.01

3.2.5 Observations

A large difference in compressive strength between the cured and uncured geopolymer specimens could be observed. The paste consistency of these specimens was very thin, so a much lower raw material/activator solution ratio could be utilized. This experiment was the first time that geopolymer cement was produced at Louisiana Tech Laboratories.

3.3 First Preliminary Design of Experiments

3.3.1 Objectives

The evaluation of the effect of five variables (two related to curing and three related to the alkaline solution) in the process of geopolymerization.

3.3.2 Design of Experiments

The Design of Experiments for this stage can be seen in Table 3.6.

Table 3.6 Research variables for the first preliminary design of experiments.

RESEARCH VARIABLE	LEVELS
Silicate type	D and N
Curing time	1, 2 and 3 days
Curing temperature	60 and 90 C
Activator solution/Fly ash ratio (AS/FA)	0.54 and 0.82
NaSiO ₂ /NaOH ratio	1.5 and 2.5
FIXED PARAMETERS	
NaOH concentration	14 M
Fly ash:sand ratio	1:1
RESPONSE VARIABLE	NORM
Compressive strength in cubes	ASTM C-109

Three repetitions were made for each combination for a total of 324 cube specimens. First, the effect of the silicate type was evaluated. Then, the effect of the curing temperature, the activator solution/fly ash ratio and the silicate/hydroxide ratio were evaluated for three curing times.

3.3.3 Materials

Fly ash Class F was obtained from a source in Avon Lake, OH with the chemical composition shown on Table 3.7, the phase composition shown on Table 3.8 and particle size distribution shown on Fig. 3.4. The data for Fig. 3.4 can be seen on Appendix A.2.

Table 3.7 Chemical composition of the fly ash.

<i>Oxide</i>	<i>Ohio Fly Ash, wt%</i>
SiO ₂	50.25
Al ₂ O ₃	22.56
Fe ₂ O ₃	20.0
CaO	2.1
MgO	0.00
SO ₃	0.50
LOI	2.48
Na ₂ O	0.00
K ₂ O	0.00
Total	97.89
SiO ₂ /Al ₂ O ₃	2.23
SiO₂ + Al₂O₃	72.81

Table 3.8 Phase composition of the fly ash.

Minerals	wt%
Quartz	10.33
Mullite	25.27
Amorphous	64.4

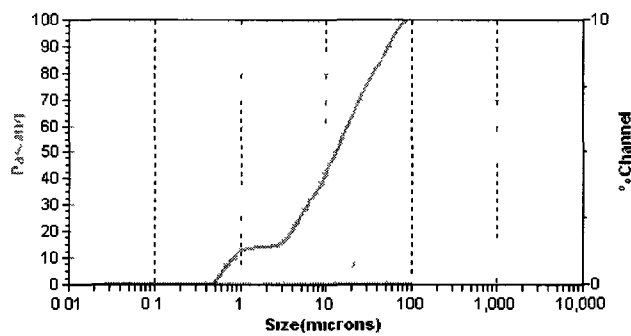


Fig. 3.4 Particle size distribution of the fly ash used in this study.

The composition of the sodium silicate solution used on this set of experiments can be seen in Table 3.9:

Table 3.9 Chemical composition of the sodium silicate utilized.

TYPE	SiO₂/Na₂O	% Na₂O	%SiO₂	VISCOSITY (cPoise)
N	3.22	8.2	26.4	180
D	2	14.7	29.4	400

Sodium hydroxide pellets of 99% purity were used to prepare the molar solutions. ASTM C-778 standard sand was used.

3.3.4 Methodology

A 14 M NaOH solution was prepared by dissolving NaOH pellets in distilled water and allowed to cool one day. An activator solution (AS) was prepared by mixing the hydroxide and silicate in the desired proportions. The weight proportions are shown in Appendix A.3. The activator solution was gradually added and the mixture was stirred manually. The cement was casted on 2” cube molds and oven-cured at 60 or 90 degrees for one, two and three days before testing. Plastic bags were used to cover the samples and prevent the loss of moisture. A universal machine was used to perform the compression tests.

3.3.5 Results and Discussion

The full results of this test are shown on Appendix A.4 and also on Fig. 3.6-3.8.

As it can be seen on Fig. 3.5, silicate “D” (with a larger amount of solids and a NaO/SiO₂ ratio of 2) performs better in terms of compressive strength than silicate “N” (NaO/SiO₂ ratio of 3.5) achieving higher values for all days of curing. Therefore, subsequent analyses were made only for silicate “D”.

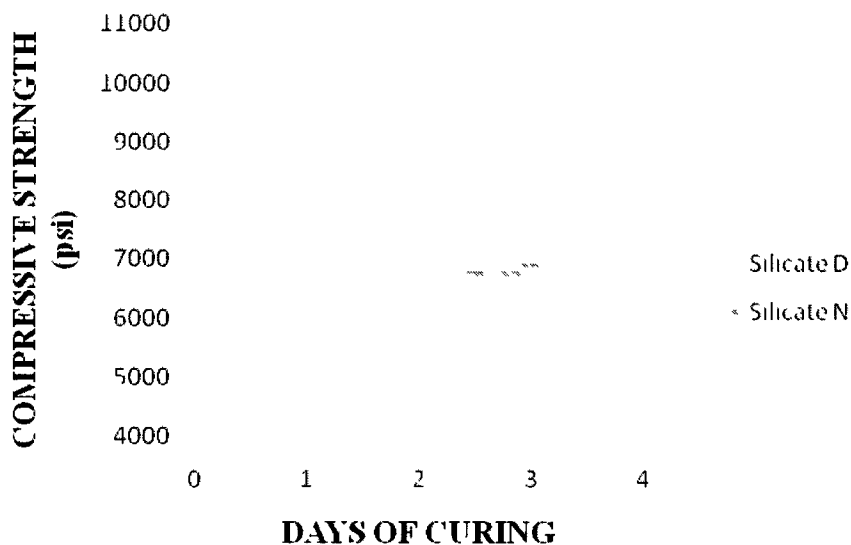


Fig. 3.5 Effect of the type of silicate.

Fig. 3.6 shows that the 0.53 AS/FA ratio gives slightly better results than the 0.82 ratio. Both ratios produced very fluid mortar pastes.

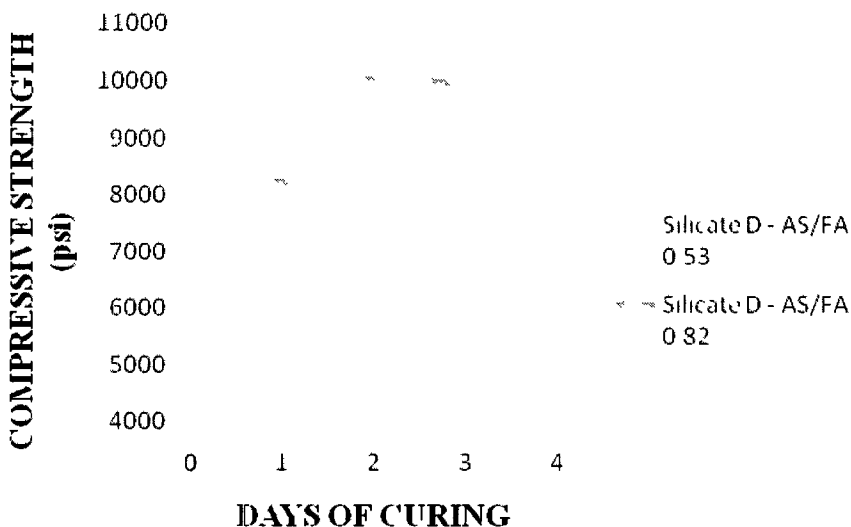


Fig. 3.6 Effect of AS/FA ratio.

Fig. 3.7 shows that there is no significant difference between the two $\text{NaSiO}_2/\text{NaOH}$ ratios chosen. For economical reasons, a ratio of 1.5 was chosen for the

next stage. However, it must be considered the economical convenience might change and that both ratios produce similar results. The temperature effects can be seen in Fig. 3.8. While 90 C shows a slight better performance in 1 day of curing, for longer curing times, there does not seem to be any significant difference with respect to 60 C, so it may be desirable to use 60 C in a certain application if the addition of 30 C implies a higher cost.

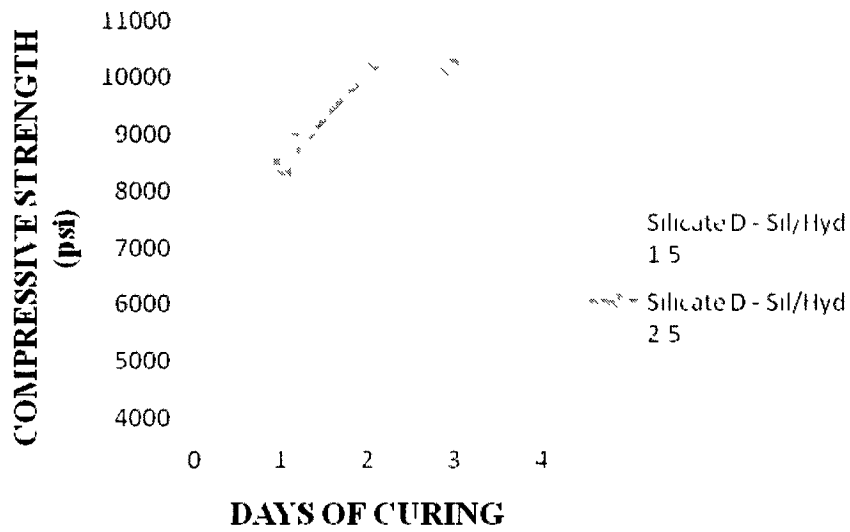


Fig. 3.7 Effect of Sil/Hyd ratio.

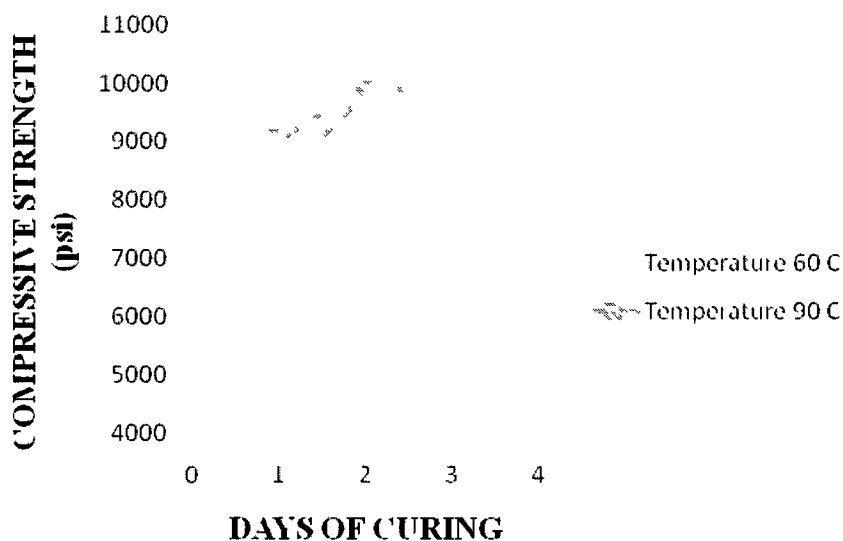


Fig. 3.8 Effect of temperature.

3.3.6 Conclusions

Silicate “D” contains a large amount of solids; therefore, more reactive material will be available to participate in the reaction, that is why silicate “D” provides better compressive strength than silicate “N”.

Similarly, as for Portland cement, a lower w/c ratio down to a certain limit is desirable to obtain better compressive strength, the activator solution/fly ash plays the same role in geopolymer concrete; that may be the reason why a lower ratio produced better compressive strength results for these experiments.

While curing at 90 C provides slightly better results at 1 day, this effect becomes negligible at 2-3 days, this fact is important when cost comes into consideration.

The convenience of using either $\text{NaSiO}_2/\text{NaOH}$ ratio or another will depend on the commercial availability of such products in the market. The fact that these two ratios provided the same results provides flexibility to choose.

3.4 Second Design of Experiments

3.4.1 Objective

To prepare a testing plan for the evaluation of different sources of fly ash as a raw material for geopolymerization and the evaluation of different curing regimes. Lower AS/FA ratios were also tried during this stage.

3.4.2 Design of Experiments

The design of experiments for this stage can be seen on Table 3.10.

Table 3.10 Research variables for the first preliminary design of experiments.

RESEARCH VARIABLE	LEVELS
Fly ash source	Tatum, TX; Ruston, LA and Baton Rouge, LA
Activator solution/Fly ash ratio (AS/FA)	0.35, 0.45 and 0.5
Curing time	0.5, 1, 3, 6, 12 and 24 hrs
Curing temperature	Room, 60 and 90 C
FIXED PARAMETERS	
NaOH concentration	14 M
Fly ash:sand ratio	1:1
Na ₂ SiO ₃ /NaOH ratio	1.5
Na ₂ SiO ₃ type	D
RESPONSE VARIABLE	
Compressive strength in cubes	ASTM C-109

A Taguchi design of experiments for the variables mentioned in Table 3.10 was prepared using MINITAB to reduce the number of experiments, since one of the variables had more levels than the rest. The list of experiments from MINITAB can be seen in Table 3.11. The weights for each experiment can be seen in Appendix A.5.

Table 3.11 Design of experiments obtained using MINITAB.

Time	Temp	SA/FA	Fly ash ¹
0.5	Room	0.35	Tx
0.5	60	0.45	Ti
0.5	90	0.50	Mi
1.0	Room	0.35	Ti
1.0	60	0.45	Mi
1.0	90	0.50	Tx
3.0	Room	0.45	Tx
3.0	60	0.50	Ti
3.0	90	0.35	Mi
6.0	Room	0.50	Mi
6.0	60	0.35	Tx
6.0	90	0.45	Ti
12.0	Room	0.45	Mi
12.0	60	0.50	Tx
12.0	90	0.35	Ti
24.0	Room	0.50	Ti
24.0	60	0.35	Mi
24.0	90	0.45	Tx

3.4.3 Materials

Three different sources of fly ash were used for this study (Tatum, TX; Ruston, LA, Baton Rouge, LA). Their chemical composition can be seen on Table 3.12. Sodium hydroxide in pellets (99% purity) was used to prepare the molar solutions. Type “D” sodium silicate from PQ was also utilized.

¹ Tx = Tatum, Ti = Ruston, Mi = Baton Rouge

Table 3.12 Oxide composition of the fly ashes used in this study.

OXIDE COMPOSITION	BOYCE, LA	MOUNT PLEASANT, TX	TATUM, TX
SiO ₂	37.77	55.61	48.7
Al ₂ O ₃	19.13	19.87	16.6
SiO ₂ /Al ₂ O ₃	1.97	2.80	2.93
SiO ₂ +Al ₂ O ₃	56.90	75.48	65.3
CaO	22.45	12.93	18.72
Fe ₂ O ₃	7.33	4.52	6.93
MgO	4.81	2.49	3.91
SO ₃	1.56	0.49	0.85
Moisture content	0.12	0.02	0.12
LOI	0.17	0.22	0.49
Finess (% passing 325)	80.36	77.30	85.83
Specific Gravity	2.57	2.48	2.48

3.4.4 Methodology

Mortar compressive strength was evaluated under the norm ASTM C-109. 560 g of NaOH powder was dissolved in one liter of tap water and allowed to cool to prepare a 14 M NaOH solution. The NaOH solution was then mixed with the sodium silicate and mixed thoroughly. The fly ash and sand were premixed dry. The activator solution was then added to the admixture of fly ash and sand and mixed until a uniform paste was observed. The fresh geopolymer paste was cast in the 2"x2"x2" in molds and stored in the oven or at room temperature.

3.4.5 Results and Discussion

A summary of the results obtained with the present design of experiments can be seen in Table 3.13 and Fig. 3.8. The full results are in Appendix A.6.

Table 3.13 Results of the TAGUCHI design of experiments obtained with MINITAB.

Time	Temp	AS/FA	Fly ash	Comp strength
0.5	R	0.35	Tx	1091.7
0.5	60	0.45	Ti	1316.7
0.5	90	0.50	Mi	6850.0
1.0	R	0.35	Ti	1700.0
1.0	60	0.45	Mi	12966.7
1.0	90	0.50	Tx	3750.0
3.0	R	0.45	Tx	750.0
3.0	60	0.50	Ti	3950.0
3.0	90	0.35	Mi	12983.3
6.0	R	0.50	Mi	3783.3
6.0	60	0.35	Tx	8441.7
6.0	90	0.45	Ti	10616.7
12.0	R	0.45	Mi	3383.3
12.0	60	0.50	Tx	5766.7
12.0	90	0.35	Ti	16300.0
24.0	R	0.50	Ti	950.0
24.0	60	0.35	Mi	10533.3
24.0	90	0.45	Tx	9325.0

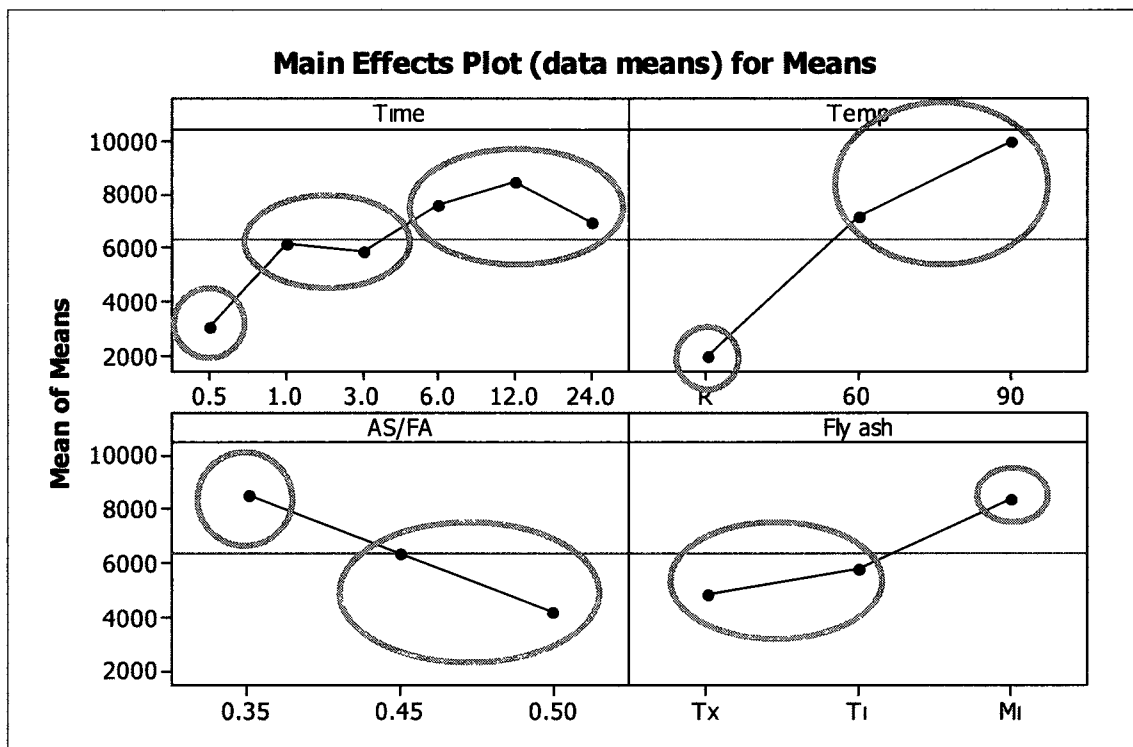


Fig. 3.9 Main Effects Plot from the Taguchi Design of Experiments

It can be seen in the main effects plot that curing times can be divided in three statistical groups. The first group contains only the 0.5 hr curing, for which the effect was similar to curing at room temperature. The second group contains curing times of 1 and 3 hours, with an average near to 6,000 psi of 1-day compressive strength. The third, and most important group, is the one that contains curing times of 6, 12 and 24 hours. The results for this group show that if the right kind of fly ash and mix design is selected, good results in terms of compressive strength may be achieved with times as low as 6 hours of curing. This result is the most important in terms of compressive strength for the evaluation of different curing times. Fig. 3.9 shows an apparent tendency of compressive strength to decay after 24 hrs, but there was no statistical difference compared to the results at 12 hours.

In the curing temperature graph, it is shown the important difference between room and both temperatures of 60 and 90 C. This graph shows the importance of curing temperature in geopolymerization. Curing at room temperature does not “kick start” the geopolymerization reaction and, therefore, the gain in compressive strength and other properties is minimal because of the deficient amount of geopolymer formed. The temperature selected for a given geopolymer application will depend on the final properties desired and the industrial process that will be used for its manufacture (precast etc.)

The descending line in the graph for the activator solution/fly ash ratio shows that there is an inverse relationship between the activator solution/fly ash ratio and the compressive strength of the geopolymer. This relationship means that in this frame, the lower the AS/FA ratio, the higher the compressive strength that will be achieved. There must be an optimal point for this ratio, but the lower limit of workability is more likely to be achieved first.

For the purposes of this study, two fly ashes of the same type (Tatum, TX), but of different source (Tatum, TX and the TXI plant in Ruston) were used; they were assumed to provide similar results and that effect can be seen in the fourth graph of the main effects plot. The fly ash from Louisiana (coded as Mi) provided a significantly higher compressive strength. This result suggests that the type of fly ash used in the admixture is a very important variable. The reason why this variable is put in the fourth place in the ranking is because two of the levels were nearly identical. However, two fly ash types that were initially considered had to be discarded because they did not produce a quality geopolymer. The first one came from Mansfield, LA. The sample seemed to be

contaminated with ammonia, and a caustic smell appeared when it came in contact with the NaOH. The fresh geopolymer contained bubbles and didn't set in 24 hours. The other sample that did not offer a good performance was the one coming from Courtland, LA. The powder was highly hygroscopic; it required 1.8 more activator solution to form a paste with some workability. Further, when cured at 60 C, all the samples expanded and the result was a highly porous rock with little or no compressive strength.

3.4.6 Conclusions

The fly ash source is a very important variable for geopolymerization. It is responsible in a large degree of the mechanical properties of the resulting geopolymer. However, the activator solution also plays a significant role in the final properties, and it seems that a low activator solution/fly ash ratio is desirable, similarly to a low water/cement ratio for Portland cement. The curing temperature is important for low curing times, but if curing times exceed 24 hours a lower temperature can be used with good results.

3.5 General Conclusions

The aforementioned results show the first time that geopolymers were produced in a Louisiana Tech facility. Sodium silicate and hydroxide were selected because of their cheaper price, better performance and local availability. Although several raw materials can be used for geopolymerization, fly ash shows a great potential especially for being a waste and with a more suitable particle size than metakaolin, which is more hygroscopic, for better workability in the practice.

Results conducted at Louisiana Tech also confirmed the thermally-induced nature of geopolymerization and showed that lower activator solution/fly ash ratios are preferred

to achieve high strength. The silicate/hydroxide ratio is also an important variable that can be manipulated to achieve the desired results.

Elevated temperature is only desirable if short curing times are needed, but care must be taken to prevent excessive evaporation and cracking. The optimal curing time is 1 day, and extended curing would only be necessary if low curing temperatures are used.

The fly ash source is additionally a fundamental variable for geopolymerization and critical for the final properties of the hardened material. For some types of fly ash, curing times could be reduced.

CHAPTER 4

CORROSION RESISTANCE OF

GEPOLYMER COMPARED

TO PORTLAND CEMENT

4.1 Introduction

The previous chapter showed the testing conducted to evaluate the effect of several variables relevant to geopolymerization on the compressive strength of the material. The present chapter presents the study of the corrosion resistance of different geopolymer formulations exposed to sulfuric acid corrosion with the intent of selecting the appropriate raw material for the coating design.

ASTM C-261 was selected as the testing procedure to achieve this goal. Geopolymers prepared from three different precursors were used. A corrosion resistant cement developed by [16] was selected as the blank for comparison.

Typical pH from sewers was used for the evaluations.

4.2 Materials

Geopolymer mortar cubes prepared from three precursors were utilized in this study, namely fly ash from Tatum, TX (class C) and Avon Lake, OH (class F) and a commercially available metakaolin powder. A blend comprised of 92 % OPC and 8 % silica fume by weight was utilized for comparison purposes. The chemical composition

of the four precursors was determined by XRF analysis and is given in Table 4.1. The SiO_2 to Al_2O_3 mass ratio and the sum of $\text{SiO}_2 + \text{Al}_2\text{O}_3$ are also listed.

Table 4.1 Chemical composition of metakaolin, fly ash and OPC utilized in study.

<i>Oxide</i>	<i>Metakaolin, wt %</i>	<i>Class C Fly Ash, wt %</i>	<i>Class F Fly Ash, wt%</i>	<i>OPC, wt %</i>
SiO ₂	54.26	48.7	50.25	26.12
Al ₂ O ₃	39.82	16.6	22.56	4.25
Fe ₂ O ₃	2.91	6.93	20.0	3.65
CaO	0.70	18.72	2.1	58.51
MgO	1.51	3.91	0.00	1.59
SO ₃	0.01	0.85	0.50	2.36
LOI	0.72	0.49	2.48	2.67
Na ₂ O	0.00	0.00	0.00	0.14
K ₂ O	0.00	0.00	0.00	0.52
Total	99.93	96.2	97.89	99.8
SiO ₂ /Al ₂ O ₃	1.36	2.93	2.23	6.15
SiO₂ + Al₂O₃	94.08	65.30	72.81	30.37

Chemically resistant fine aggregates were used for all specimens. A combination of 14 M NaOH solution and a commercial sodium silicate with chemical composition of 14.7 % by weight Na₂O and 29.4 % by weight SiO₂ was utilized as the activator solution for the geopolymer mortar.

4.3 Mix Design

The mix designs used for this study are summarized in Table 4.2. The metakaolin formulation was based on a mix design proposed by [32]. Fly ash geopolymer mix designs were based on prior work conducted by the authors [33]. The weight proportions are shown on Appendix B.1.

Table 4.2 Mix designs for fly ash, metakaolin and OPC based mortars.

Raw material	Class C Fly ash	Class F Fly ash	Metakaolin	Portland cement
Raw material/Sand wt ratio	1:1	1:1	1:1	1:1
Na ₂ SiO ₃ /NaOH wt ratio	1.5	1.5	2	-
Activator solution/Raw material wt ratio	0.35	0.45	1.125	0.35*

4.4 Methodology

For the geopolymer mortar, the precursor (fly ash or metakaolin), sand and activator solution were mixed as per ASTM C-305. The mixer used was a Univex SRM20 Planetary Countertop Mixer, 20 Qt. Next, the fresh paste was cast into 50x50x50 mm cubical molds in two layers as per ASTM C-109. Following casting, the specimens were placed in an oven and cured at 60 °C for 24 hours, and then left at room temperature for 6 days before soaked in the corresponding acid solution. The mass of each geopolymer specimen was measured using an ACCULAB scale with an accuracy of ± 0.1 g prior to immersion in the acid bath. The OPC and silica fume blend (8 % by weight as OPC replacement) mortar specimens were also mixed according to ASTM C-305. The fresh paste was cast into 50x50x50 mm molds and was allowed to set under controlled temperature and moisture conditions. The specimens were then removed from the molds and placed in lime saturated water for six days to cure prior to been introduced to the acid baths. The specimens were placed in an oven at 105°C until constant mass was achieved and allowed to cool to room temperature before been immersed in the acid solutions.

Four sulfuric acid solutions were prepared by diluting a 99% laboratory grade sulfuric acid solution with distilled water to form concentrations of approximately 3%, 1%, 0.05% and 0.01% (pH = 0.6, 1, 2 and 3, respectively). Class C fly ash and metakaolin geopolymer, as well as OPC cubes were exposed to all pH levels. Class F ash

geopolymer was exposed only to the lowest pH (0.6) solution. The details of the preparation of the acid solutions can be seen in Appendix B.2. After submerging the specimens, the pH of the solutions was checked daily and adjusted on an as need basis. The ratio of the volume of solution to that of the specimens was 4 to 1 [47]. All solutions were refreshed weekly. Mass loss and remaining compressive strength were selected as the response variables for this study. Specimens were removed from the acid bath for testing at 1, 2, 4, 6 and 8 weeks following immersion. Following removal from the acid bath, specimens were rinsed with tap water to remove leach products and mass that became structurally separated from the matrix. The mass loss value for each precursor/duration/pH combination was taken as the average mass loss of three cubes that were oven dried at 105° C to constant mass. Untreated “blank” specimens were used to determine the 7th day compressive strength. Compressive strength was measured using a universal compressive testing machine. The compressive testing machine was calibrated prior to testing.

The total of cube specimens for the OPC blend, metakaolin and Class C fly ash geopolymer was 75, being 3 cubes for each age in the sulfuric acid test per pH for a total of 60, 3 to obtain the initial compressive strength and 12 to evaluate mass loss at each pH. The total of cube specimens for the Class F fly ash geopolymer was 9, 3 to obtain the initial compressive strength, 3 for the sulfuric acid immersion test and 3 for the mass loss. Results with Class F Fly Ash were evaluated only for a pH of 0.6. All of the specimens for a specific test set were produced out of the same batch.

4.5 Results and Observations

4.5.1 Change in Mass

Mass loss (in percentage of initial weight) was recorded at each measurement period for class C and F fly ash and metakaolin based geopolymer mortars and OPC mortar. The results are shown graphically in Figs. 4.1 through 4.4. and numerically in Appendix B.3.

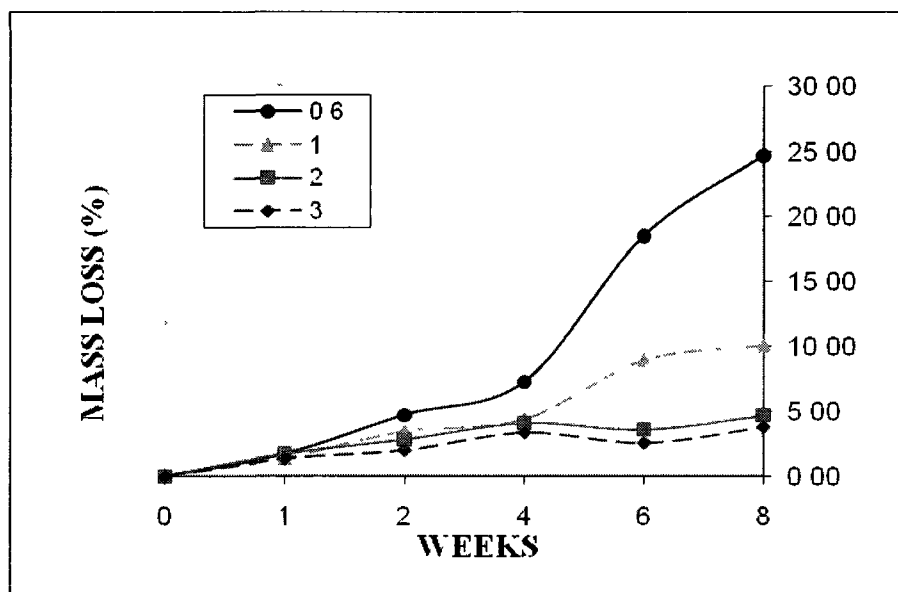


Fig. 4.1 Mass loss vs. immersion time for class C fly ash-based geopolymer mortar.

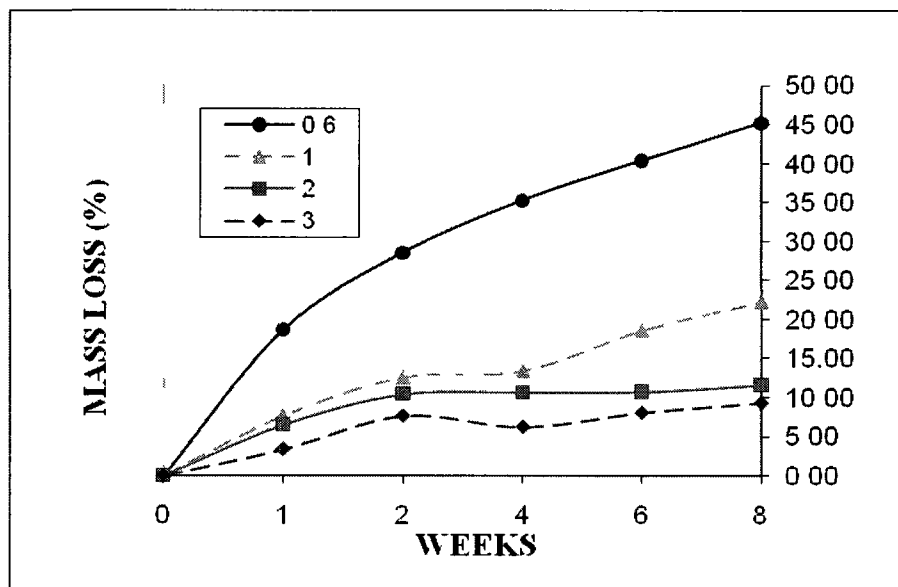


Fig. 4.2 Mass loss vs. immersion time for metakaolin based geopolymer mortar.

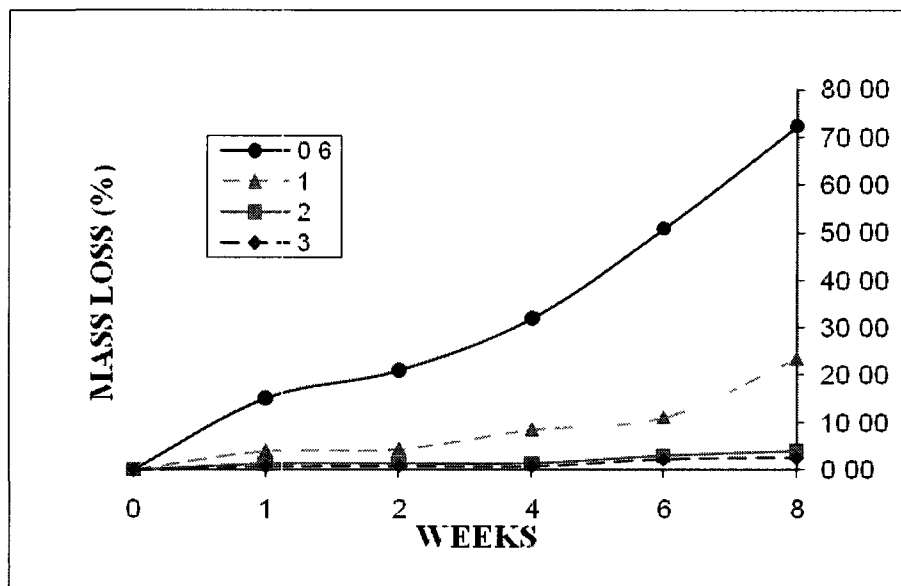


Fig. 4.3 Mass loss vs. immersion time for OPC mortar specimens.

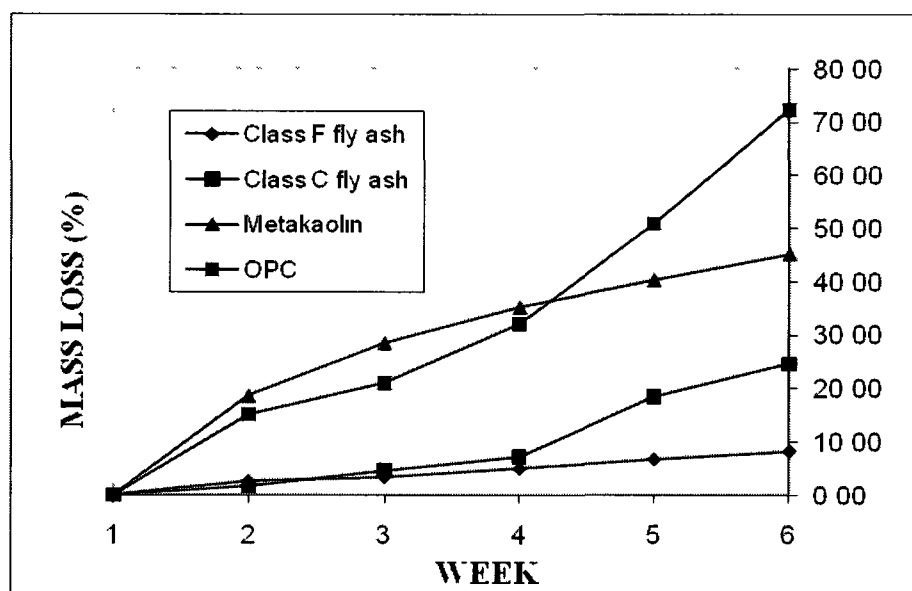


Fig. 4.4 Mass loss vs. immersion time for class F, class C and metakaolin geopolymer and OPC mortar specimens.

From Fig. 4.1, it can be seen that class C fly ash geopolymer specimens immersed in acid baths with pH values of 2 and 3 displayed similar trends in terms of mass loss over the 8-week period, with maximum mass loss of less than 5%. Specimens immersed in a sulfuric acid solution with a pH of 1 exhibited a 10% mass loss at the end of the immersion period, while specimens immersed in a solution with a pH of 0.6 lost 25% of their initial mass. In the case of metakaolin-based geopolymer (Fig. 4.2), the mass loss recorded for specimens immersed in solutions with pH values of 2 and 3 was around 10%. Specimens immersed at an acid bath with a pH of 1.0 lost 20% of their mass, while the mass loss recorded for specimens at the 0.6 pH acid bath was considerably larger, averaging 45%. As for OPC specimens (Fig. 4.3), data revealed mass loss of about 2.5% , 4%, 23% and 72% for specimens immersed in acid baths with pH values of 3, 2, 1 and 0.6, respectively, at the conclusion of the immersion period.

Mass loss values for class C fly ash geopolymer and OPC for pH values of 2 and 3 were similar (< 5%). Mass losses of OPC specimens for pH values of 0.6 and 1 were found to be significantly greater compared with those observed for the class C fly ash geopolymer mortar cubes. Metakaolin geopolymer specimens exhibited mass losses smaller than their OPC counterparts at pH of 0.6, comparable at pH of 1, and greater than the OPC specimens at pH values of 2 and 3.

Fig. 4.4 presents a comparison of the mass loss for classes F and C fly ash and metakaolin geopolymer specimens, and OPC specimens for the case of a pH value of 0.6. The average mass loss of class F geopolymer specimens is less than half that of their class C counterparts, and about eight times smaller than that of the binary OPC blend cubes at the end of the eight week immersion period (9% vs. 72%).

4.5.2 Remaining Compressive Strength

The remaining compressive strength was tested at each measurement period for the fly ash and metakaolin based geopolymer mortar specimens and the OPC mortar specimens. The 7th day compressive strength values for untreated (blank) specimens are listed in Table 4.3. The results for all measurement periods are shown graphically in Figs. 4.5 and 4.6 and numerically on Appendix B.4.

Table 4.3 Seven-day compressive strength of mortar specimens.

Material	7-day compressive strength*
Class C fly ash geopolymer	72.7 MPa
Class F fly ash geopolymer	46.5 MPa
Metakaolin geopolymer	53.5 MPa
Enhanced Portland cement	48.3 MPa

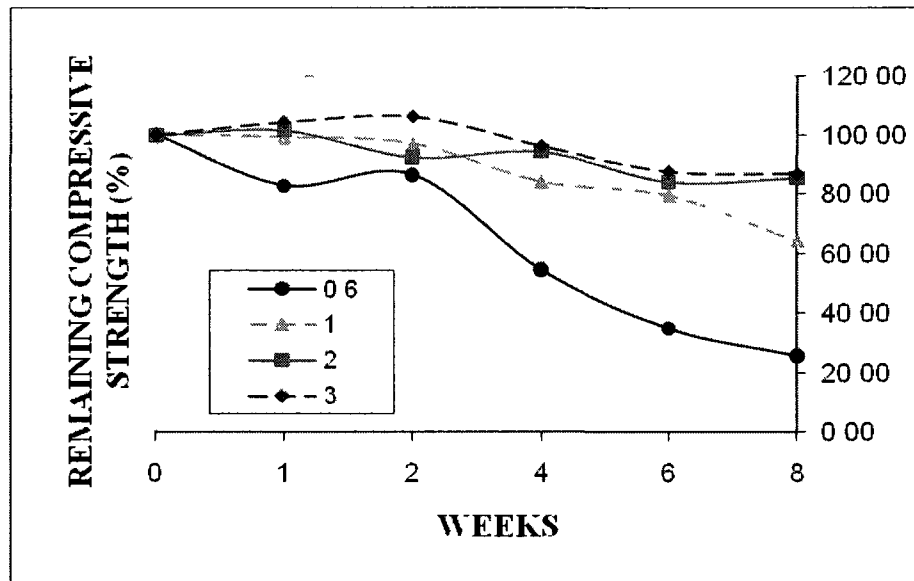


Fig. 4.5 Remaining compressive strength vs. immersion time for class C fly ash-based geopolymer mortar specimens.

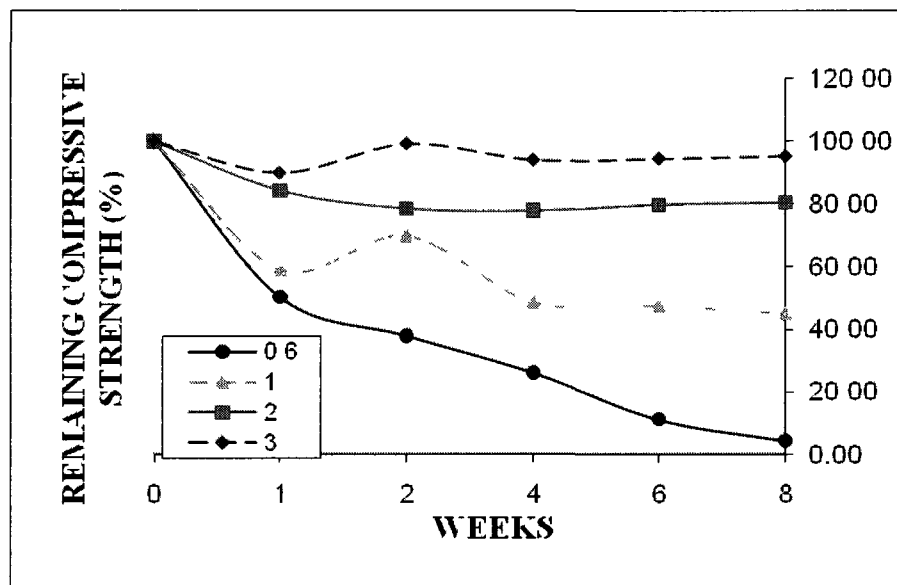


Fig. 4.6 Remaining compressive strength vs. immersion time for metakaolin-based geopolymer mortar specimens.

Fig. 4.5 reveals that class C fly ash geopolymer mortar exhibits high resistance to acids with pH values of 3 and 2, retaining 86% and 85% of its compressive strength respectively, at the end of the immersion period. Specimens immersed in acid baths with

pH values of 1.0 and 0.6 retained 64% and 25% of their original compressive strengths respectively. Metakaolin based specimens immersed in an acid bath with pH of 3 retained 95% of their original strength at the conclusion of the 8-week term. Specimens immersed at pH values of 2, 1 and 0.6 retained 80%, 45% and 4% of their original compressive strengths, respectively, over the same time period (see Fig. 4.6). Fig. 4.7 reveals that the remaining compressive strength of the binary OPC blend specimens was considerably lower than that of the class C fly ash geopolymer cubes for pH values of 0.6, 1 and 2, and similar for a pH of 3.

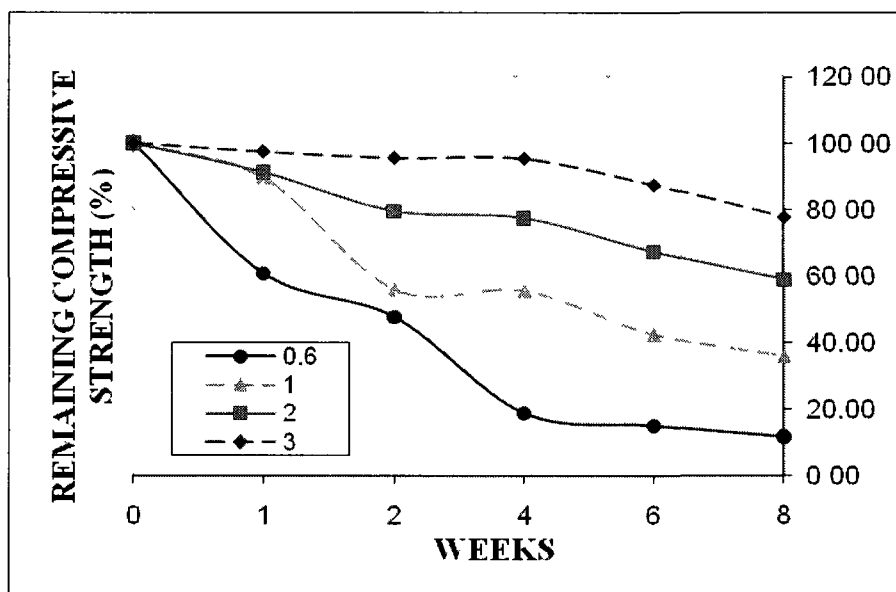


Fig. 4.7 Remaining compressive strength vs. immersion time for OPC mortar specimens versus time.

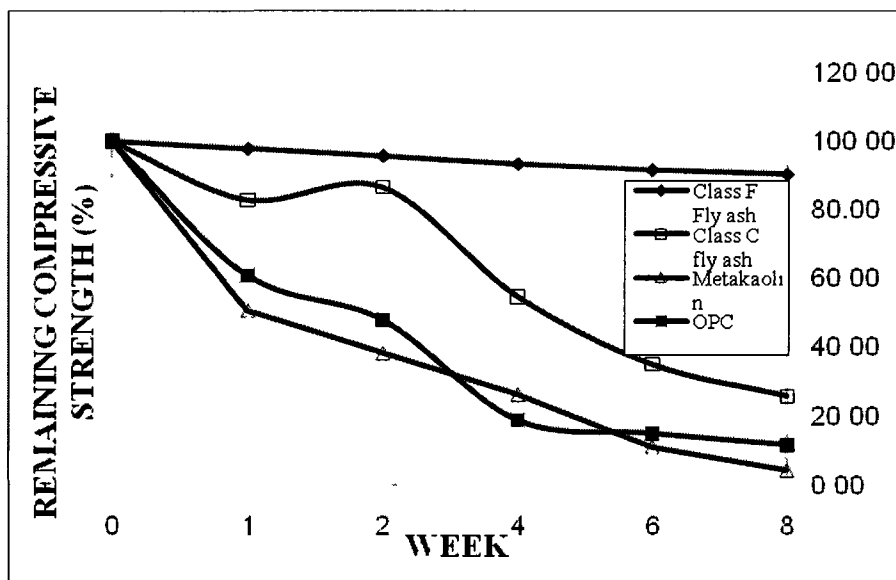


Fig. 4.8 Remaining compressive strength of class F geopolymer after 8 weeks compared to class C fly ash and metakaolin geopolymer and Portland cement (pH=0.6).

Fig. 4.8 shows a comparison of the remaining compressive strengths of class F and C fly ash geopolymer, metakaolin geopolymer and OPC-blend specimens immersed in an acid bath with pH of 0.6. It can be seen that specimens made from class F fly ash geopolymer retains approximately 90% of their original strength at the end of the immersion period, compared with the OPC cubes which retained on average only 12% of their original strength. One possible explanation is the lower amount of CaO in the class F fly ash (2% by weight for class F vs. 18.7% for class C and 58.5% for the OPC). In the case of metakaolin while there is little CaO presence, the poor corrosion resistance could be attributed, at least partially, to the high ratio of activator solution to metakaolin powder needed to achieve adequate workability (1.125:1). Evaporation of the relatively large amount of free water remaining in the matrix following polymerization of the metakaolin is expected to result in large, interconnected pores, which would benefit diffusion of the aggressive species in the acid solution. A graph summarizing the

compressive strengths of fly ash and metakaolin geopolymers and OPC blend specimens for the four acid baths at the end of the 8-week period is shown in Fig. 4.9. The full results of all the corrosion resistance tests can be seen in Appendix B.3-4.

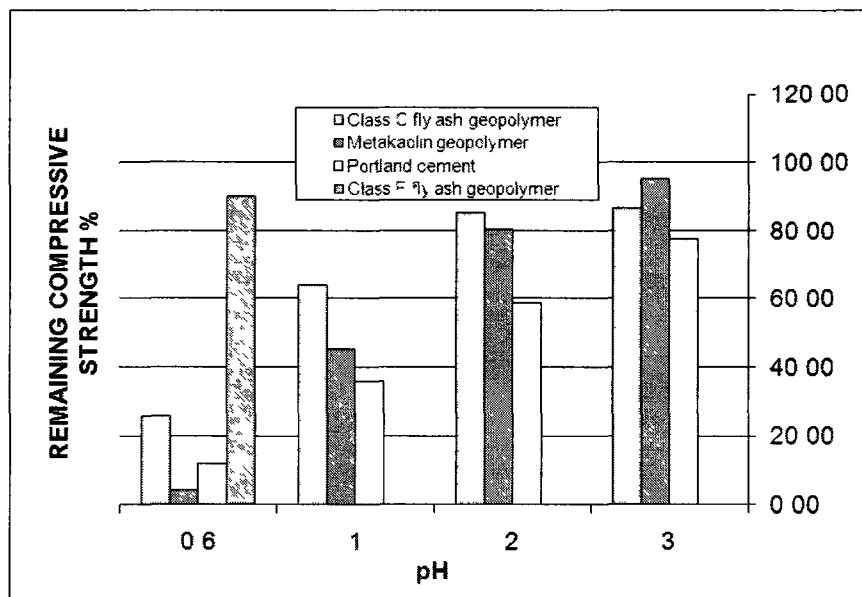


Fig. 4.9 Remaining compressive strengths of fly ash and metakaolin geopolymer and Portland cement.

4.5.3 Visual Appearance

The visual appearance of class C fly ash and metakaolin based geopolymer specimens following an 8-week immersion in the various acid baths is shown in Fig. 4.10. The visual appearance of the OPC specimens after been submerged for 8 weeks in the various acid baths is shown in Fig. 4.11. Fig. 4.12 displays the class F fly ash specimens at the end of the eight week immersion period.

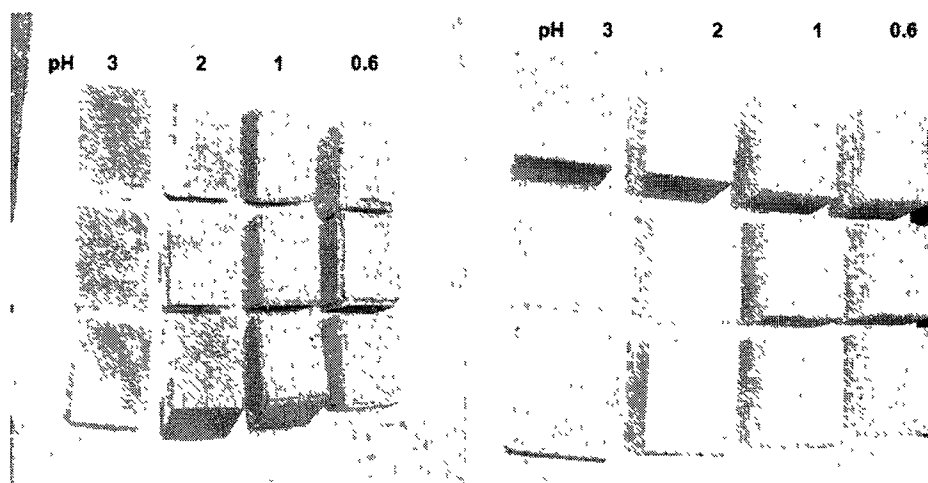


Fig. 4.10 Visual appearance of fly ash geopolymer (left) and metakaolin geopolymer (right) after 8 weeks of exposure.

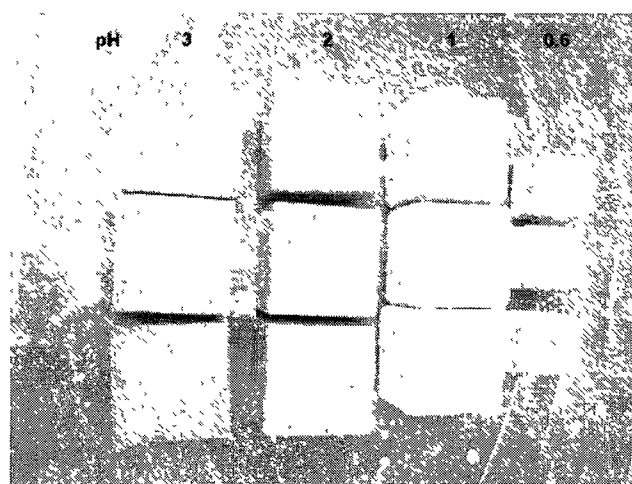


Fig. 4.11 Visual appearance of OPC-silica fume specimens after 8 weeks of exposure.

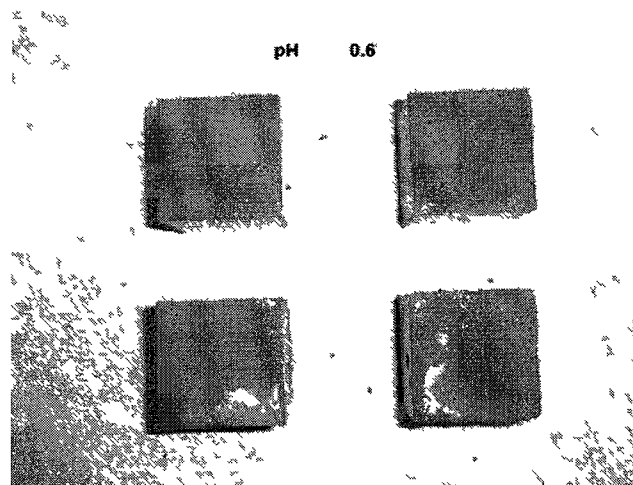


Fig. 4.12 Visual appearance of Class F fly ash geopolymer after 8 weeks of exposure.

Class C fly ash-based geopolymer specimens exposed to an acid with a pH of 0.6 featured eroded surfaces with some cracks at the corners of the specimens. Specimens exposed to sulfuric acid with a pH of 1 exhibited a less severe degree of erosion; however, cracking was noted at the corners of some of the specimens. The specimens' outer surfaces were soft, and free sand particles were present at the surface. Specimens exposed to pH values of 2 and 3 solutions showed little or no visual damage at the end of the 8 week immersion period. Metakaolin based geopolymer specimens placed in the 0.6 and 1.0 pH acid baths exhibited severe erosion and significant dimensional changes in the upper part of the cubes. A white pasty leaching was noted on the surface of the specimens. It is proposed that the precipitate layer was amorphous silica formed by supersaturated silicic acid liberated from the silicates during the depolymerization of the aluminosilicate polymer, as suggested by Iller [87]. In other words, the treatment of a geopolymer matrix with a strong acid might result in a direct attack on the aluminosilicate framework causing breakage of the Si-O-Al bond and leading to mass loss and an increase in the amount of silicic acid in the solution [88]. Specimens placed

in acid baths with pH values of 2 and 3 appeared unaltered. This result was anticipated as silicic acid is most stable at pH of 2 to 3, which can explain observing two different mechanisms of deterioration of the metakaolin geopolymer matrix. Class F fly ash geopolymer specimens exhibited little, if any, alteration in their visual appearance in terms of erosion or change in color following an 8-week immersion in the 0.6 pH sulfuric acid bath. The Portland cement silica fume binary blend specimens exhibited a dramatic visual deterioration at the conclusion of the exposure period compared with the geopolymer-based specimens. This effect is particularly true for the cases of pH values of 0.6 and 1 where a significant reduction in size was noted. OPC specimens immersed in the 2 and 3 pH acid baths exhibited a moderate level of deterioration.

4.6 Discussion

4.6.1 Mass Loss

The large difference observed between the mass loss of class C and F fly ash-based geopolymers and Portland cement can be attributed to the reaction of the calcium silicate hydrate (CSH) present in Portland cement paste with the sulfuric acid. Class C geopolymer contains a small amount of CSH in its structure that contributes to both its lower corrosion resistance (compared to class F fly ash-based geopolymer) and its higher compressive strength (control specimens). The lower compressive strength and higher mass loss of the metakaolin based geopolymer might be attributed to lower reactivity of the metakaolin used in this study due to a high percentage of crystallinity (and thus a lower percentage of amorphous phase), which will result in a lower degree of polymerization [89]. Furthermore, since the particle size of the material was finer than the other raw materials used, it required a significantly higher activator solution to fly ash

ratio to obtain a workable paste. As water serves only as the transport media and does not participate in the reaction, a large number of interconnected pores are left after evaporation, resulting in a reduced mechanical strength.

4.6.2 Remaining Compressive Strength

While the initial strength of class F fly ash geopolymer was lower than that of class C fly ash geopolymer, it retained a higher percentage of its initial strength at the end of the test period in the higher acidity environments. The sharp drop in the compressive strength of the OPC specimens is attributed to the high mass loss and size reduction of the specimens, as can be seen in Fig. 11. The reaction products of CSH + H₂SO₄ are structurally weak and tend to easily leach out of the paste. On the other hand, geopolymer reaction with H₂SO₄ is minimal and does not result in leaching of considerable amounts of reaction products. It is presumed that the metakaolin did not fully react with alkaline solutions due to a high degree of crystallinity and, therefore, did not achieve a satisfactory degree of geopolymerization, resulting in a low corrosion resistance.

4.7 Conclusions

Class C fly ash and metakaolin based geopolymer mortars retained between 80% and 95% of their compressive strengths following an 8-week immersion test in sulfuric acid solutions with pH values of 2 and 3. Visual inspection revealed little wear and no eroded surfaces at these pH levels. Mass loss at eight weeks was 5% and 10% for the fly ash and metakaolin based specimens, respectively. At pH values of 1 and 0.6 a more aggressive corrosion mechanism(s) appears to be at work and performance declined significantly. A comparison with specimens made from enhanced OPC silica fume blend base specimens showed that fly ash-based geopolymer mortar retained a higher

percentage of its initial compressive strength when exposed to sulfuric acid solutions with pH values of 0.6, 1, 2 and 3 at the end of the 8-week test period. Remaining compressive strength values for metakaolin based geopolymer were lower at the pH of 0.6 but higher at pH values of 1, 2 and 3 compared with these of the OPC binary blend specimens. Also, OPC-based specimens exhibited a more severe surface degradation and size reduction compared with specimens made from the geopolymer materials.

The relatively high content of CaO (18.72 %) is believed to be a key reason for the lower corrosion resistance potential (but higher strength) of geopolymer specimens made with class C fly ash precursor compared with specimens made from class F fly ash. On the other hand, class C fly ash geopolymer mortar exhibits superior chemical resistance compared with an enhanced OPC blend, and thus could serve as a viable alternative in applications where both high corrosion resistance and high strength are desired or where class F ash is not locally available. Geopolymer specimens with metakaolin as a precursor yielded an overall residual compressive strength and corrosion resistance comparable to or slightly better than their OPC counterpart but lower than the fly ash-based geopolymers. This result is attributed, at least partially, to the relatively high activator solution to powder ratio needed to achieve adequate workability and, potentially, to a highly crystalline structure that does not easily lend itself to polymerization.

Although the compressive strength results are mostly attributed to the chemical composition of the materials used in this study, it is fair to say that the pore system of the samples surely had also an important effect in the results. Different activator solution/raw material ratios were used in the present work. The reason for that was to achieve the same

workability without using admixtures like superplasticizers. However, the resulting pore system and densities of the samples could be different as a result of this choice. Muntigh [90] conducted a study on the pore systems of geopolymers coming from different formulations. He concluded that an increase in activator solution resulted in longer pores, but these pores were sometimes narrower for some of the fly ashes utilized. He also determined the sulfate diffusion coefficients with the aid of a diffusion cell, and he concluded that these coefficients are significantly lower than those for OPC, mainly because geopolymer is a denser product and because it does not readily react with sulfates. Degradation and opening of the pore space will, therefore, occur in a slower degree. This conclusion is important because it stresses the importance of not having compounds that will readily react with sulfates (such as CaO) present in the geopolymer mix as related to its pore system. It is also mentioned in his work that no generalization can be made in terms of the pore system of a geopolymer produced under particular conditions and that specific studies would need to be performed in every case, until a general model can be approached. He even considered that it could be necessary to use a model alternative to Fick's laws to better describe the diffusion characteristics of geopolymeric materials.

Finally, the most dramatic results were produced under the pH value of 0.6, which is not typical for many sewers. However, these conditions were selected because of the limited time available to obtain results and move to the next stage. It is important to mention that a different mechanism of corrosion may be present for higher pH values and the results of differences in durability may vary. To prove this point, long term corrosion resistance tests at pH values typical of sewers (3-4) should be conducted.

These results also have a relation with the corrosion mechanism involved in geopolymers. Hewayde [2] proposed that at pH values higher than 1, the corrosion mechanism relies mostly on the sulfate ions, and under 1 they rely on both the hydrogen and sulfate ions, therefore, the degree of corrosion resistance increases in a non linear manner for regular OPC concretes. However, due to the high sulfate resistance of geopolymers this change in corrosion rate may not be as dramatic for geopolymers as it is for Portland cement.

CHAPTER 5

OPTIMIZATION OF THE ACTIVATOR SOLUTION

5.1 Introduction

The previous chapters described the test conducted to determine geopolymer's suitability as a rehabilitation material for buried infrastructure. The results showed the promising characteristics of geopolymers to accomplish these goals.

However, in spite of their superior properties, geopolymers' viscous and fresh properties are often a problem that prevents or discourages their use in real life applications. Problems with high viscosity and surface tension often need to be overcome.

It was, therefore, decided to create a design of experiments to optimize the activator solution to be used with the Class F ash selected in the previous chapter. The design would lead to an initial formulation for the sprayable geopolymer mortar.

5.2 Design of Experiments

A 3^3 design of experiments was used for this stage of the research. 3^3 DOEs are useful statistical tools to evaluate the effect of three variables at three levels each. The software MINITAB was used to create the DOE and to evaluate the results. The test variables were three (silicate type; D, N and Star; hydroxide molarity 6, 10 and 14 and

silicate/hydroxide ratio 1, 2 and 3). Three replicates were made for each combination. The result was 27 experiments with three repetitions each. The experiment setup from MINITAB can be seen in Appendix C.1. Four response variables were selected for this study: compressive strength, remaining compressive strength, mass loss and flow. The main effect of all three research variables was evaluated as well as the interaction effect between the research variables. An analysis of contrasts was performed to find out which levels were statistically different for each research variable. The software R was used for this purpose.

5.3 Materials

Class F Fly Ash from the power plant in Miami Fort, FL was used in this study. The three silicates used in this study were obtained from PQ corporation. Sodium Hydroxide 99% pure in flakes was obtained from Baddley Chemicals in Baton Rouge, LA. The sand utilized met standard ASTM C-777. The chemical composition and particle size distribution of the fly ash is shown in Table 5.1 and Fig. 5.1. The chemical composition and other characteristics of the sodium silicate are summarized in Table 5.2.

Table 5.1 Chemical composition of fly ash utilized in this study.

<i>Oxide</i>	<i>Class F Fly Ash, wt%</i>
SiO ₂	50.25
Al ₂ O ₃	22.56
Fe ₂ O ₃	20.0
CaO	2.1
MgO	0.00
SO ₃	0.50
LOI	2.48
Na ₂ O	0.00
Total	97.89
SiO ₂ /Al ₂ O ₃	2.23
SiO₂ + Al₂O₃	72.81

Table 5.2 Mineralogical composition of fly ash utilized in this study.

Minerals	wt%
Quartz	10.33
Mullite	25.27
Amorphous	64.4

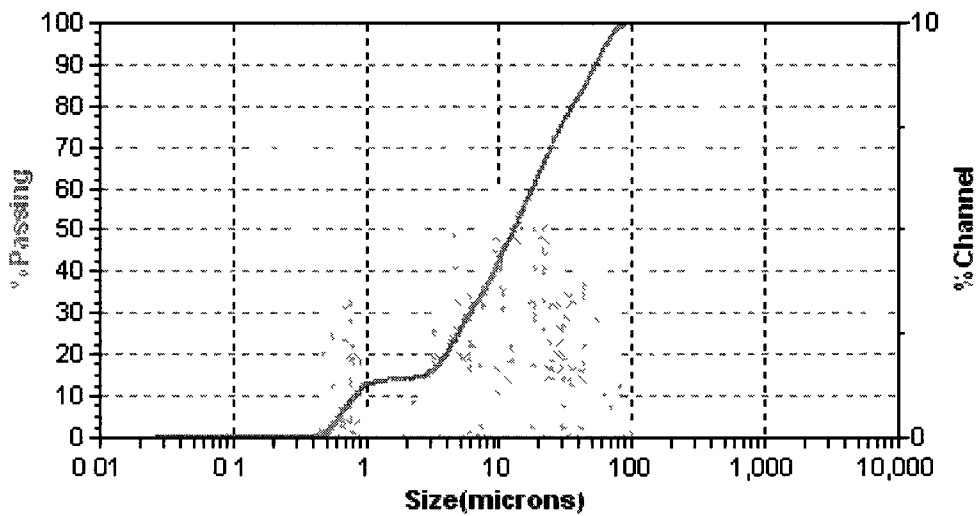


Fig. 5.1 Particle size distribution of fly ash utilized in this study

Table 5.3 refers to the chemical composition and other characteristics of the sodium silicate used for this set of experiments.

Table 5.3 Characteristics of sodium silicates utilized in this study.

SODIUM SILICATE TYPE	Na₂O % wt.	SiO₂ % wt.	SiO₂/Na₂O	Viscosity (cPoise)
D	14.7	29.4	2.00	400
N	8.9	29.7	3.22	180
Star	10.6	26.5	2.5	60

5.4 Methodology

Sodium hydroxide solutions of three different molarities were prepared using tap water. All sodium hydroxide molar solutions were prepared in the lab and allowed to cool off for one day. Then, they were mixed with sodium silicate to prepare the alkaline solution.

Next, the precursor (fly ash) and sand were mixed on a 1:1 ratio. They were mixed with the activator solution as per ASTM C-305. The fresh paste was cast into 50x50x50 mm cubical molds in two layers as per ASTM C-109. Following casting, the specimens were placed in an oven and cured at 60 °C for 24 hours. The specimens that were to be used for the chemical tests were left at room temperature for 6 days before immersion in the corresponding acid solution. The precise weigh proportions are shown on Appendix C.2.

Compressive strength was measured after a 24 hours curing period according to ASTM C-109. To measure corrosion resistance, the remaining compressive strength after soaking the specimens in a 0.6 pH sulfuric acid solution for 8-weeks was evaluated according to ASTM C-267. Mass loss was also evaluated for the same period of time. Flow was evaluated for the fresh paste right after mixing ASTM C-1437.

5.5 Results and Discussion

5.5.1 Compressive Strength

Fig. 5.2 shows the large effect of silicate “D” in compressive strength. An increase in compressive strength as the molarity of the NaOH increases can also be observed. Moreover, a lower Silicate/Hydroxide ratio tends to give higher compressive strengths.

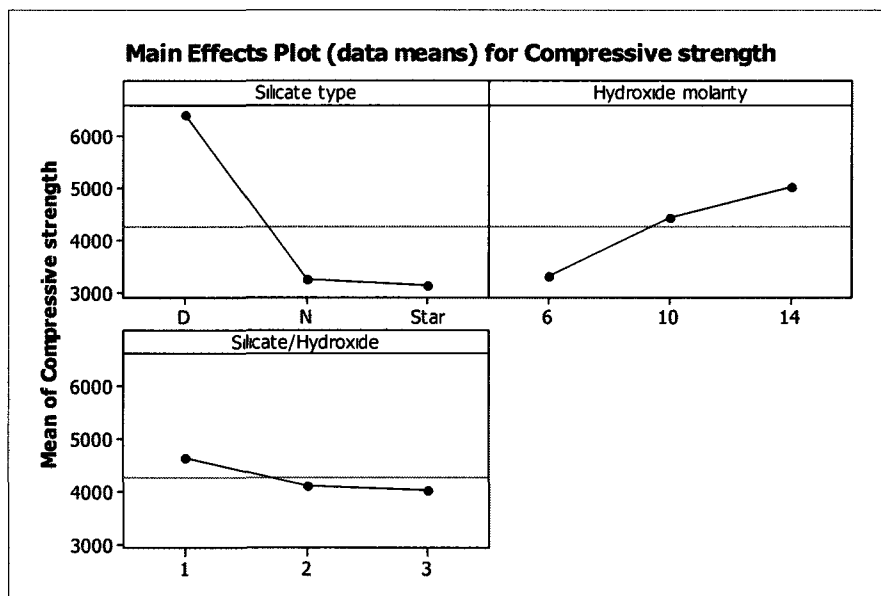


Fig. 5.2 Main effects plot for compressive strength.

In the first box (silicate type vs. hydroxide molarity), of the interaction plot shown in Fig. 5.3 it can be seen that the molarity has the same effect regardless of the silicate type; it always increases the compressive strength as it increases. However, for the “D” silicate, molarities 10 and 14 seem to have the same effect. This fact can be an interesting characteristic for practical applications. In the second plot (Silicate type vs. Silicate/Hydroxide ratio), it can be seen that the ratio affects the silicate N and Star in an opposite way. With the first one it decreases the compressive strength as it increases, and with the Star silicate it increases the compressive strength as it increases. For the silicate D, the ratio of 1 seems to give the best results. No significant interaction can be observed in the last graph, (hydroxide molarity vs. Silicate/Hydroxide ratio); (i.e., the molarity of the hydroxide and the ratio do not seem to have a combined effect).

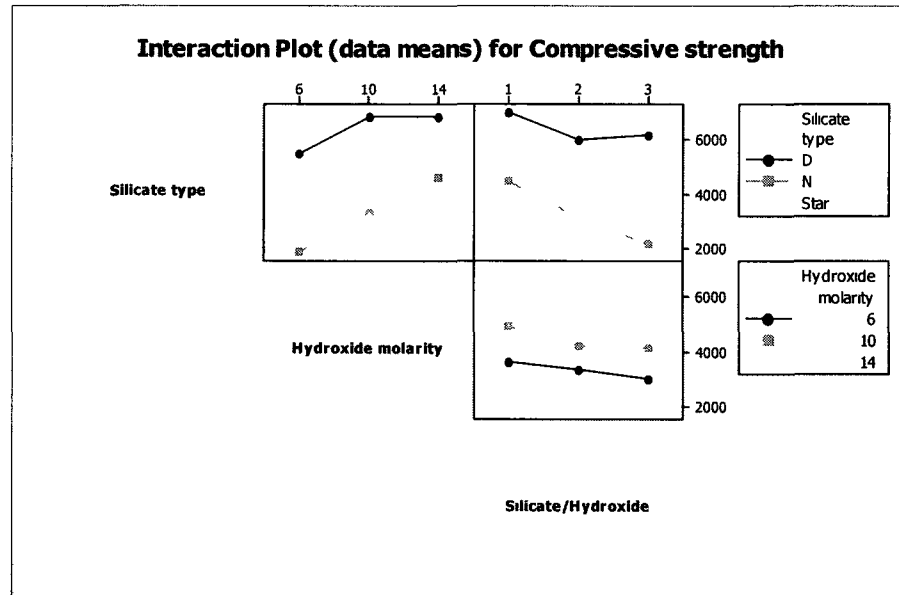


Fig. 5.3 Interaction plot for compressive strength.

Information about the significance of the research variables and interactions is obtained from ANOVA (Appendix C.1). All variables and interactions were significant with the exception of hydroxide molarity-Silicate/hydroxide ratio.

An analysis of contrasts was performed using the software R. The code used to run is shown in Table 5.6.

Table 5.4 Coding for research variables in R.

Silicate Type	Hydroxide type	Silicate/Hydroxide
D = 1	6 = 1	1
N = 2	10 = 2	2
Star = 3	14 = 3	3

These first three contrasts (Appendix C.4) compare the three types of silicate (D vs. N, D vs. Star and N vs. Star). If the p value of the comparison is less than 0.05 (the significance level), the levels are considered statistically equal. The p values from D vs N and D vs. Star are 0.00017 and 3.08299 e-12; therefore, D is considered to give a

statistically different effect, as we clearly saw in the main effects plot. The p value for N vs. Star silicates is 0.93; therefore, they are not different, (e.g., they produce the same compressive strength in average).

The same process was run for the three levels of the hydroxide molarity and since all three p values are less than 0.05, all levels can be assumed to be different.

The same process was run again for the silicate/hydroxide ratio, and it can be concluded that the ratio 1 is different from the ratio of 2 (though slightly since $p = 0.016$, they would be considered equal with a more strict level of significance, like 0.01).

5.5.2 Remaining Compressive Strength

In Fig. 5.4, it can be seen that silicate D and a hydroxide concentration of 14 and a ratio of 3 seem to be the best parameters in terms of corrosion resistance.

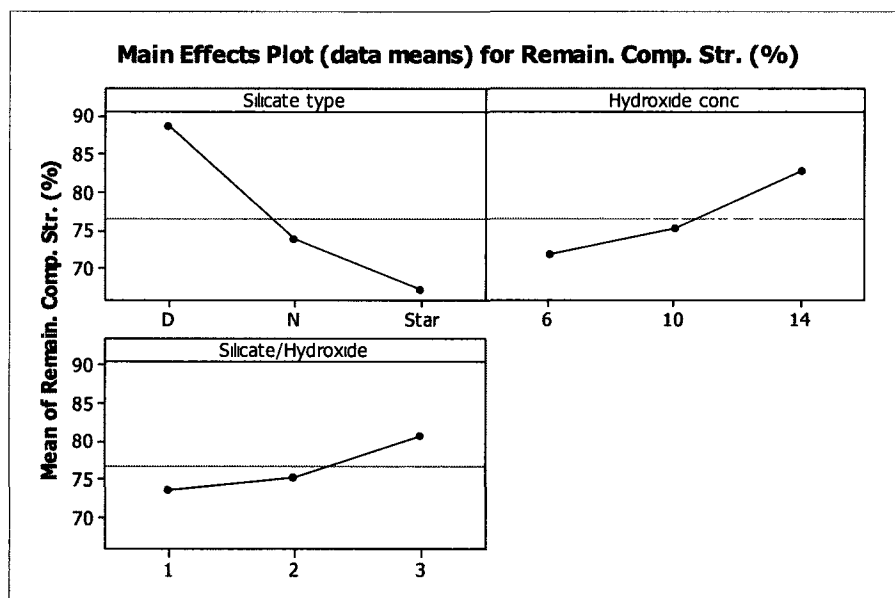


Fig. 5.4 Main effects plot for remaining compressive strength.

From the boxes in Fig. 5.5, it is clear that when using silicate D or Star, the hydroxide concentration becomes more relevant, but when using silicate N, there is not much difference between using a hydroxide concentration of 10 or 14 M. Also, the

silicate/hydroxide ratio affects the three silicates in a different way. For silicate D, there is a slight slope showing the increase in corrosion resistance as the ratio gets higher, but for silicate N, there is a big difference when using a ratio of 2 or 3. The ratio affects silicate Star in an inverse way as the other silicates, (e.g., a ratio of 3 produces the smaller values of remaining compressive strength). In the graph of concentration vs. ratio, it can be seen that when using a concentration of 6, there is not a big effect of the ratio; however, when using a concentration of 10 there seems to be an optimum point using a ratio of 2, and when using a concentration of 14 the best thing is to have a ratio of 3.

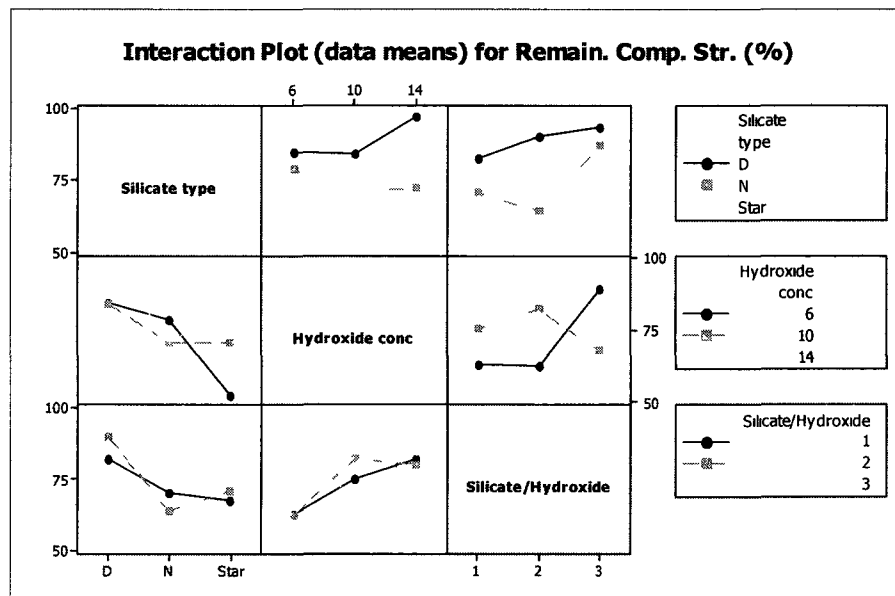


Fig. 5.5 Interaction plot for remaining compressive strength.

The ANOVA Table (Appendix C) shows that all variables and interactions are significant with the exception of the silicate/hydroxide variable. It shows that there is not a significant difference between using silicate D or N, but there is when using silicate Star. Therefore, the results using silicate Star are statistically different (and lower from what we can see in the main results plot).

Even though the ANOVA table showed that the molar concentration was significant, the contrast (Appendix C.5) shows us that there is no significant difference between any of the levels. By doing the LSD (Least significant difference) test, the same conclusion can be reached.

For the silicate/hydroxide ratio contrast it can be seen that the only ones that seem to be significantly different are 1 from 3.

5.5.3 Mass Loss

Both silicate type and hydroxide concentration were significant according to ANOVA. In Fig. 5.6, it can be very clearly seen that the Star silicate produces the highest mass loss, D silicate the least, and the molarity of 14 also the least mass loss. This result could be attributed to the lower density achieved by using the Star silicate and the 6 and 10 M hydroxide solutions, water that leaves voids after evaporating.

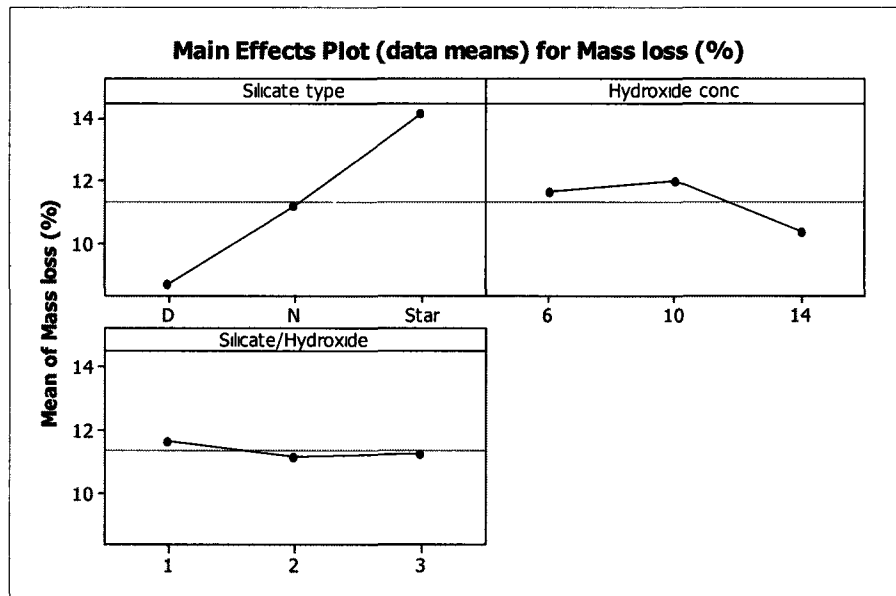


Fig. 5.6 Main effects plot for mass loss.

According to ANOVA (Appendix C.6), the interactions were significant, so from the interaction plot (Fig. 5.7), it can be concluded that if the silicate that produces the least mass loss (silicate D) is chosen a molarity of 14 and a silicate/hydroxide ratio of 3 would have needed to be selected. That makes sense since the amount of silicate “D” is being maximized.

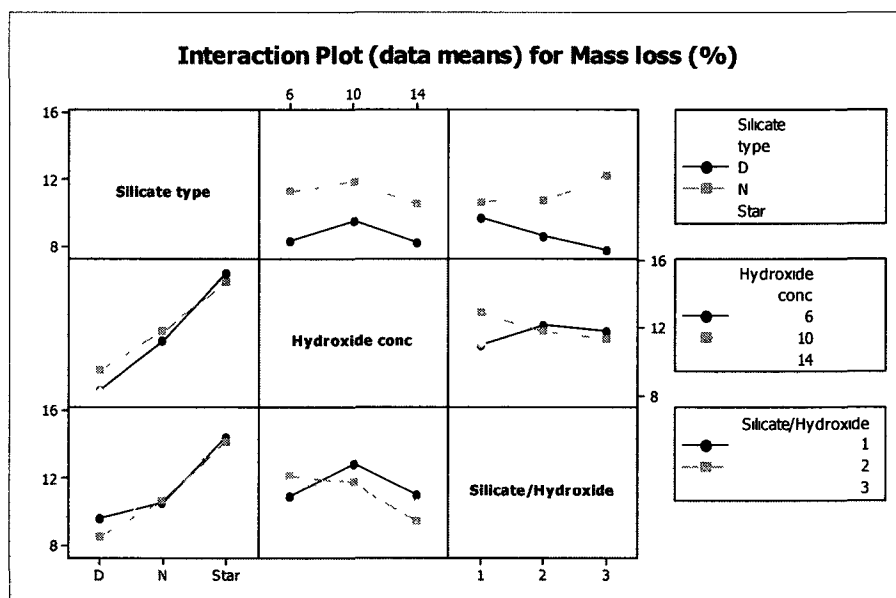


Fig. 5.7 Interaction plot for mass loss.

In the contrasts for the levels of the silicate (Sil), it can be seen that D and N (1 and 2) are not significantly different, but 1 and 3 and 2 and 3 are. This result means that the silicate Star is the one significantly different in terms of mass loss, and it also produces the highest mass loss. In the case of the molarity, it can be seen that the only levels that were significantly different were 10 from 14.

The contrast analysis for the ratios was not calculated since the ratios were not significant in the ANOVA model.

5.5.4 Flow

In Fig. 5.8 it can be seen that the silicate D has the largest effect on flow, while N and Star have similar effects. The hydroxide concentration seems to have a linear effect on the flow, with higher concentrations producing lower values of flow. The silicate/hydroxide ratio has the same linear effect as the hydroxide concentration, but with a smaller slope. The differences between the three levels were evaluated using R.

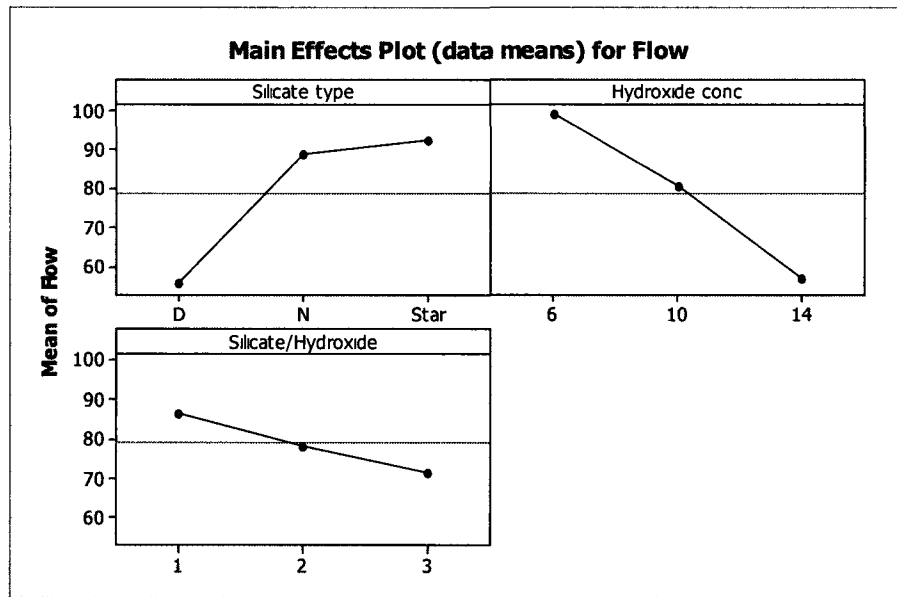


Fig. 5.8 Main effects plot for flow.

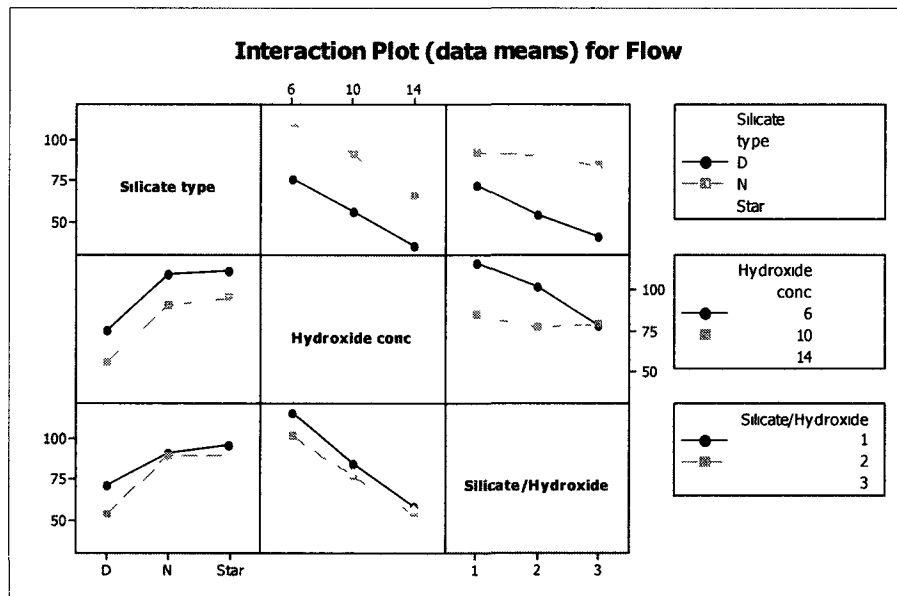


Fig. 5.9 Interaction plot for flow.

ANOVA (Appendix C.8) showed that the silicate*hydroxide interaction had no significance. In Fig. 5.9 it can be seen that the tendency (a higher value of hydroxide concentration produces a higher value of flow) is the same for all types of silicate. With respect to the silicate*silicate/hydroxide interaction, the results show that when using

silicate D, the effect of the ratio (the higher the ratio, the lower the value of the flow) is more significant than when using silicates N or Star. Finally, the effect of the ratio seems to affect more on flow when using a hydroxide concentration of 6.

Appendix C.9 shows the first set of contrasts. It can be observed that the silicate D (1) is the only level that is significantly different from the other two and that the use of silicate N and Star does not make an important difference.

From the analysis of the ratios shown in Appendix C.9 it can also be seen that all levels of the ratio produce different results.

5.6 Decision Support Table

Since it was clear from the previous results that the selected levels of the research variables acted differently for the different response variables, it was decided that a Decision Support Table (Table 5.5) would be created in order to select the best choice of levels for the design of a sprayable coating.

Based on their level of significance, each variable was given a weight to help on the decision making process. Compressive Strength and Flow were the limiting variables since both are important factors but with opposite results; the levels of the variables that produced good results for one did the opposite for the other.

From Table 5.5, it can be extracted that the best combination for compressive strength is D-14-1. However, for the case of flow, the best combination is either N or Star silicate with a hydroxide concentration of 6 and a Sil/Hyd ratio of 1. As it may be noted, both variables produce opposite results in terms of desirability. Fortunately, the analysis for corrosion resistance offers more flexibility; any hydroxide concentration and ratio can be used, as long as silicate N or D is used. Therefore, the combination that gives the best

flow without compromising compressive strength and corrosion resistance was N-10-1 and it was chosen as the initial formulation for tests with the coating.

Table 5.5 Decision Support Table for the Design of Experiments results.

TEST	VARIABLE	LEVEL	MEAN	DESIRABILITY
Compressive strength (psi)	Silicate	D	6413	ok
		N	3250	
		Star	3128	
	Hydrox. Conc.	6	3324.1	
		10	4431.5	
		14	5036.1	ok
	Sil/Hyd	1	4652.8	ok
		2	4100	
		3	4038.9	
Rem. C. Str. (%)	Silicate	D	88.78	ok
		N	73.87	ok
		Star	67.18	ok
	Hydrox. Conc.	6	71.86	ok
		10	75.21	ok
		14	82.76	ok
	Sil/Hyd	1	73.72	ok
		2	75.27	ok
		3	80.84	ok
Mass loss (%)	Silicate	D	8.696	ok
		N	11.203	ok
		Star	14.156	
	Hydrox. Conc.	6	11.666	ok
		10	12.021	ok
		14	10.368	ok
	Sil/Hyd	1	11.642	ok
		2	11.171	ok
		3	11.242	ok
Flow (dim)	Silicate	D	55.53	
		N	88.64	ok
		Star	92.39	ok
	Hydrox. Conc.	6	99.03	ok
		10	80.58	
		14	56.94	
	Sil/Hyd	1	86.81	ok
		2	78.19	
		3	71.56	

5.7 Conclusions

The activator solution is one of the main components of geopolymer. Its correct formulation has a very important effect on geopolymers' final properties; therefore, a careful selection of the levels of each of its variables must be made through a design of experiments.

With regards to the compressive strength, it was concluded that the silicate type had the highest effect and that the higher the alkali concentration of the silicate, the higher the strength achieved. This effect was due to both the higher supply of alkali and the higher density of the obtained geopolymer. The molarity of the hydroxide solutions also played a big role, as the higher the concentration, the higher the achieved strength. Also, a lower silicate/hydroxide ratio tended to produce higher strength. From the interaction plots, it can be seen that the selection of the hydroxide to use should largely depend on the silicate chosen. Hydroxide molarities act differently depending on the silicate type.

All of the three variables studied: silicate type, hydroxide type and the silicate/hydroxide ratio had a significant effect on the remaining compressive strength of the specimens. The Star silicate was the only one to produce significantly different results because of being less concentrated and dense. The molar concentration of 14 is the one that produces the best results; however, if the right silicate is used, a concentration of 10 can also give good results. As for the ratio, the only significant difference was between ratios 1 and 3. It can also be concluded that the molar concentration affects the different silicates differently, affecting more the D and Star silicates. The optimal ratio seemed to be around 2 when using silicates D and Star, but it showed an opposite tendency when

using silicate N. When using a molar concentration of 14, the ratio does not seem to matter much, but when using a concentration of 6, the best ratio is 3 and when using a concentration of 10, the best ratio is 2.

In terms of mass loss, two variables were significant, silicate type and hydroxide concentration. The levels D and 14 were the ones that produced the least mass loss. Further, all interactions were significant and since the levels D and 14 were the best for the silicate and the hydroxide concentration respectively, it can be recommended to use a ratio of 2 and 3 to minimize mass loss. In general, the amount of water of the solutions has an impact on the mass loss of the specimens; however, it was proven by the statistical model that the solutions do not have a significant impact on the remaining compressive strength of the specimens. From this result, we can infer that the corrosion resistance of the geopolymer is not affected by the studied variables, and that the mass loss is mostly due to the loss of water.

For the fourth variable considered in the study, silicate D produces higher values of the flow; meanwhile, there is no significant difference when using silicates N or Star. All hydroxide concentrations produced different results with the higher the concentration, the lower the flow. All ratios produced different results, the lower the ratio, the higher the flow value. From the first interaction plot (silicate vs. hydroxide concentration), we can conclude that all hydroxide molarities affect all silicates the same way, always the higher the concentration, the higher the flow. With respect to the second plot (silicate vs. ratio), there seems to be a more significant effect of the ratio on the silicate D than on the other two. Finally, from the last graph (hydroxide concentration vs. ratio) we can see that

the effect of the ratio is also more significant when using hydroxide concentration of 6 than when using the other two.

Based on all these parameters and on the desirability index chart created, it was decided to use a N-10-1 formulation as an initial trial to achieve sprayability since it could produce the best results for all the variables considered in the design. Further steps were necessary to achieve the final formulation, and they are described in Chapter 6.

CHAPTER 6

DEVELOPMENT OF A SPRAYABLE

GEPOLYMER MORTAR

6.1 Introduction

The previous chapters described the first steps towards the development of a sprayable geopolymer mix to be used as a coating for buried infrastructures. An evaluation of the properties of geopolymers, selection of raw materials and the design of an activator solution had been performed.

In the present chapter, a sprayable geopolymer formulation is designed and tested. The study starts with a study of the effect of the activator solution parameters in the viscosity of fresh geopolymer paste, the evaluation and performance of different surfactants as additives in terms of surface tension reduction, viscosity change, and to enhance sprayability, the properties obtained with the new mix.

The chapter ends with a final sprayable formulation to be used for industrial tests. The results of field tests conducted at the Trenchless Technology Center (TTC) lab are also presented and explained.

6.2 Preliminary Tests of the Mortar as Coating

6.2.1 First Coating Test

Starting from the optimal formulation developed in the previous chapter comprised of silicate N, sodium hydroxide 10 M and a ratio of sodium hydroxide/sodium silicate of 1 (coded N-10-1), a series of preliminary tests were conducted. The activator solution/fly ash ratio used was 0.45. The coating was applied successfully to the inner surface of a 12” concrete pipe using a steel trowel (Fig. 6.1).

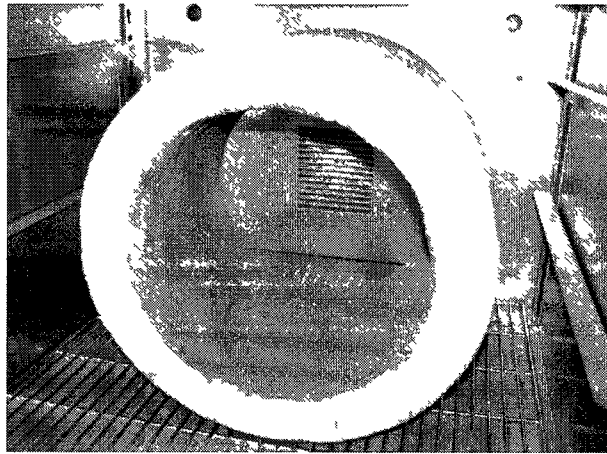


Fig. 6.1 First coating test using a 12” diameter concrete pipe.

The main observations for this test were:

- The paste workability was acceptable, but the paste dried out in about 30 minutes. Layers had to be applied of small, thin sections.
- A few holes had to be covered manually.
- The finishing of the surface was uneven and rough.
- After curing at 60 C, the coating developed some cracks.
- Visually, the adhesion to the parent wall was satisfactory.
- The sample showed some white efflorescence after a few days.

6.2.2 Second Coating Test

A second coating test was performed with the same formulation but now using a 0.5 activator solution/fly ash ratio, to try and improve workability. The same curing temperatures and procedures were used.

Some observations were:

- Workability was significantly improved.
- It could be trowelled successfully, but again, it dried out in less than 30 minutes.
- The paste sagged when heat was applied. No heating curve was used. There was also bubble formation.
- The sample was moisturized during curing and it developed no cracks.
- The sagging could be due to excessive thickness of some of the parts of the layer.

6.2.3 Third Coating Test

After a few setting time tests, it was determined that the low silicate/hydroxide ratio (1:1) was causing short setting times. A new formulation of N-10-1.5 was used for the third coating test (Fig. 6.2). This coating could be applied successfully and the finishing process was a lot easier. This section of the pipe was not cured until after 24 hours rest period at room temperature. It was observed that there was no sagging because the mortar was already dry, and 100 C could be applied directly after this initial time.



Fig. 6.2 Third coating test using the reformulated N-10-1.5 mix design.

6.2.4 Use of Superplasticizer

Several tests using Rheobuild and Glenium superplasticizers were used to improve the workability of the paste. AS/FA ratios of 0.45 and 0.5 and 1% and 2% of superplasticizer were used, but they were found to have no effect on workability.

6.3 Design of Experiments

6.3.1 Effect of NaOH Concentration and Sil/Hyd Ratio on Viscosity

On this occasion, a 2x3 design of experiments was used to further optimize the activator solution. It was desirable to evaluate the effect on viscosity of two parameters, the NaOH and the Sil/Hyd. The setting time of those mixes was also evaluated. (See Table 6.1). The weights used for this design of experiments are on Appendix C.10.

Table 6.1 Design of experiments to evaluate viscosity.

RESEARCH VARIABLE	LEVELS
NaOH concentration	6, 8, 10, 12 and 14 M
NaSiO ₂ /NaOH ratio	1, 1.5 and 2
FIXED PARAMETERS	
Curing time	24 hrs
Curing temperature	100 C
Activator solution/Fly ash ratio (AS/FA)	0.4
Silicate type	N
Fly ash:sand ratio	1:1
RESPONSE VARIABLE	METHOD
Viscosity after 30 minutes	RHEOMETER MANUAL

6.3.2 Materials and Equipment

Hydroxide solutions of 5 different molarities (6, 8, 10, 12 and 14 M) were used. The other parameters remained constant from the previous chapter.

The equipment used was a DV-III Ultra Rheometer from Brookfield, which is a controlled rate rheometer with capabilities to measure, viscosities, yield stress and other rheological characteristics. The equipment includes the necessary spindles and software to perform the measurements.

6.3.3 Procedure

The first step was to plug the rheometer and turn it on. Correct leveling was checked for observing that the bubble on top of the rheometer is centered. On the rheometer screen, “External Mode” was clicked to allow taking the readings from a computer. Ten minutes should be allowed before making any measurement. The rheometer should already be connected to the computer where the software was installed using an USB cable. After the 10 minutes have passed, the Rheocalc software was started. The appropriate USB connection must be selected. The rheometer readings were re-set by clicking on “Re-zero”.

The tutorial was then followed to create a program for the experiment. In this case, it was required to create a curve of viscosity vs. time, so a time of 30 minutes was selected together with a SV-27 spindle and a speed of 5 rpm. The materials were prepared once the program was setup.

Paste samples were prepared according to the weights specified in Appendix D.1. No sand was used to avoid abrasion of the rheometer spindles and also because its presence would not cause an effect on the readings. Fly ash was mixed with the activator solution according to ASTM C-305. The paste was then poured inside the cylindrical mold and the needle was inserted. The cylindrical mold containing the sample was then inserted in the sample holder. The cylindrical spindle was inserted next, making sure not to disturb the sample excessively. After the procedure was started, the rheometer created a viscosity curve with the points selected on the program. The data was then exported to Excel and it then analyzed. The data was be used to construct viscosity vs. time curves and to feed MINITAB for the DOE analysis.

6.3.4 Results

6.3.4.1 Viscosity Curves

Fig. 6.3 shows the viscosity vs. time curves for the five different hydroxide concentrations fo geopolymers pastes with a silicate/hydroxide ratio of 1:1. It can be seen that the geopolymer paste shows a thixotropic behaviour (e.g., its viscosity is reduced when being sheared at a constant rate for a period of time). The viscosity, however, is increased with the increased molarity, but for the concentration of 14 M, setting time occurs around 45 minutes and, therefore, the viscosity grows suddenly. This result shows more clearly why a molar concentration of 14 would be undesirable.

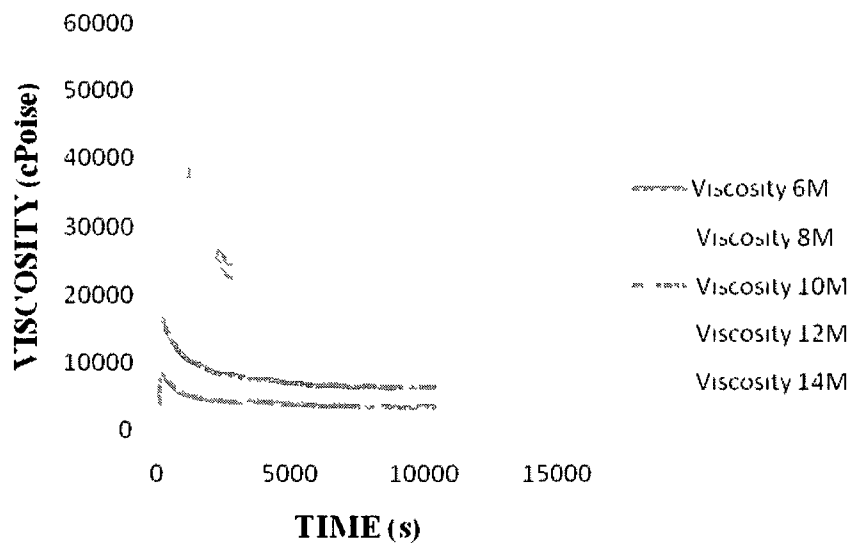


Fig. 6.3 Time vs Viscosity curves for geopolymer pastes made with a sil/hyd ratio of 1.

Fig. 6.4 shows a very similar scenario as Fig. 15. The viscosities of the pastes prepared with hydroxide molarities from 6 to 12 show a normal thixotropic curve, but the paste prepared with a molarity of 14 exhibits shorter setting times and viscosity increase.

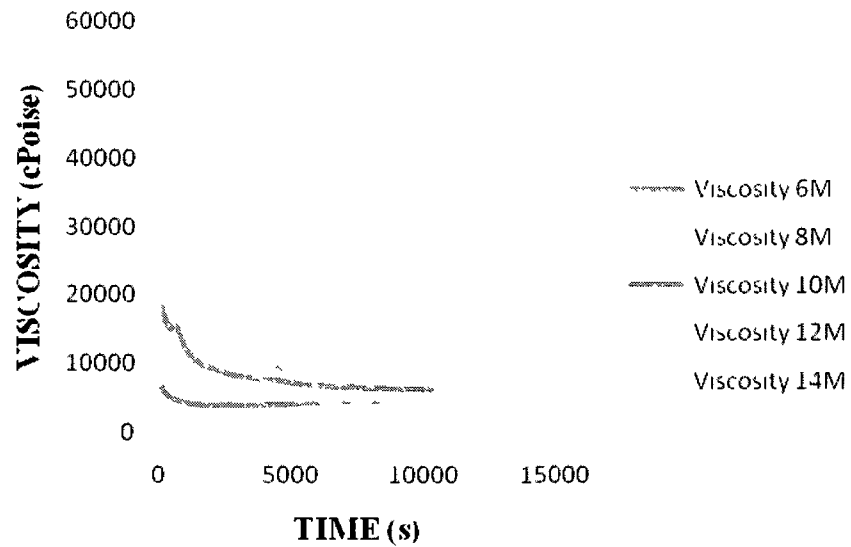


Fig. 6.4 Time vs Viscosity curves for geopolymer pastes made with a silicate/hydroxide ratio of 1.5.

Fig. 6.5 shows that the setting time effect of a hydroxide molarity of 14 can be reduced if the silicate/hydroxide ratio is increased to two. The bump of the curve for a molarity of 14 around 500 s could be attributed to agglomeration of the sample.

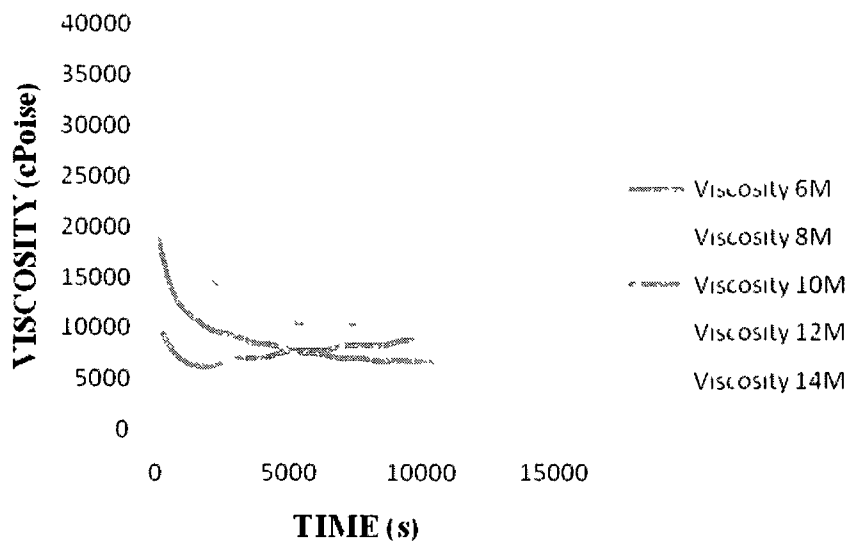


Fig. 6.5 Time vs Viscosity curves for geopolymer pastes made with a silicate/hydroxide ratio of 1.5.

6.3.4.2 DOE MINITAB Results

The main effects curve for viscosity (Fig. 6.6) shows a very clear effect of the hydroxide molarity on the final viscosity after a 3 hours testing period. The silicate/hydroxide ratio of 1 produces a slightly higher viscosity, but a ratio of 1.5 or 2 produce slightly the same effect. The data fed into and the outputs from MINITAB can be seen on Appendix D.2.

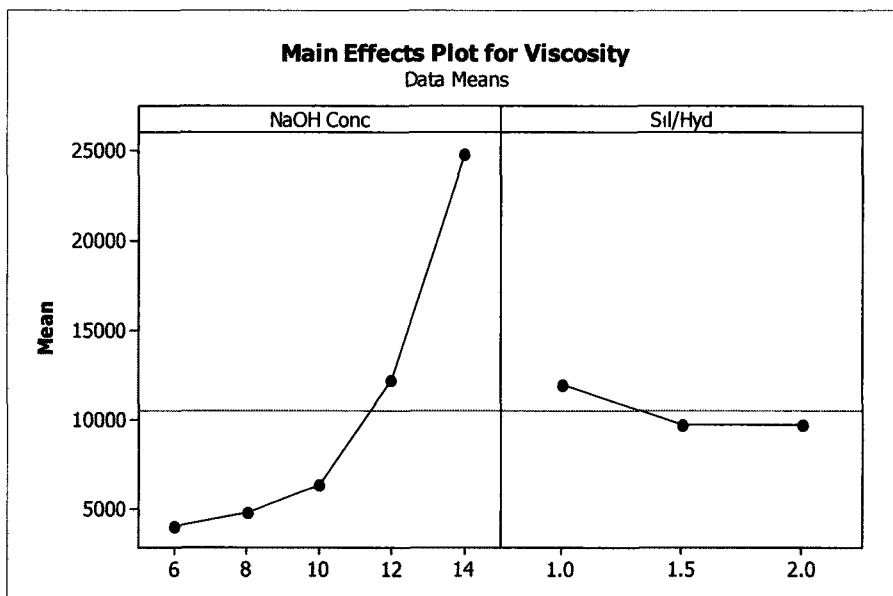


Fig. 6.6 Main effects plot for viscosity.

The interaction plot (Fig. 6.7) shows no significant interaction between these two variables, that means the hydroxide has the same thickening effect without regards to the sil/hyd ratio.

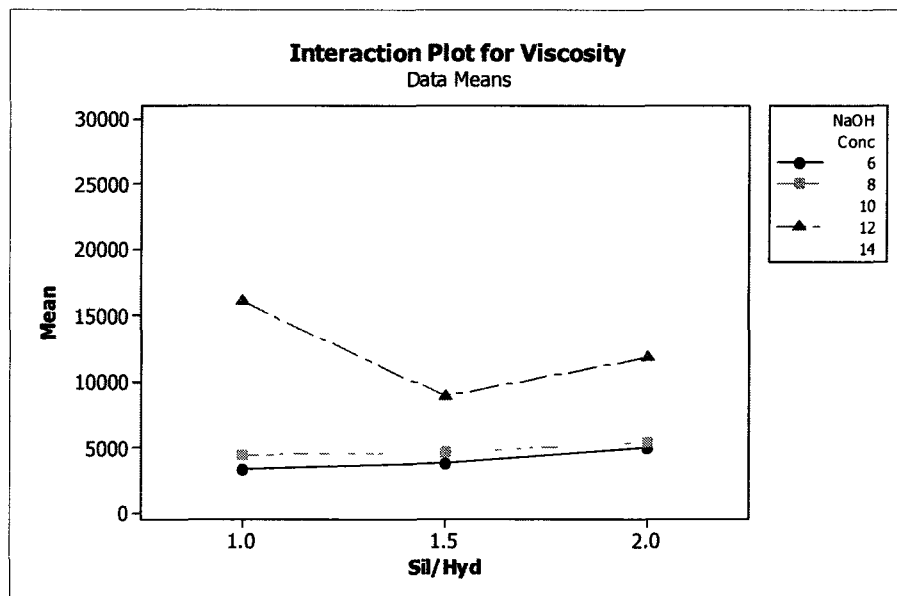


Fig. 6.7 Interaction plot for viscosity.

6.3.5 Conclusions

The hydroxide concentration plays a very significant role increasing the viscosity of geopolymers, while the silicate/hydroxide ratio plays a secondary role. Geopolymers show a thixotropic behavior over a span of 3 hours of testing. A hydroxide molarity of 14 can reduce setting time significantly.

6.4 Preliminary Spraying Tests

6.4.1 Initial Spray Test using Portland Cement

Since a Portland cement mortar of 0.4 w/c ratio commonly used in the cement lining industry, it was decided to make a test with this formulation and evaluate its flow/sprayability. The spraying tests were performed using an air mortar sprayer (Tyrolessa – see Fig. 6.8) with a capacity of 13.2 lb. The pressure needed to operate this sprayer may go from 50 to 120 psi depending on the admixture to be sprayed. To operate the sprayer, it is needed at least a 5 hp compressor for a sprayer 7 acfm @ 90 psi (available at the TTC facilities). The spraying tests were performed over a vertical wood form (Fig. 6.9). The form could be cleaned after each test to avoid build up of mortar. When necessary, the sprayed mortar was finished using a regular square trowel. A successful spraying test was achieved and the paste had a flow larger than 150 (ASTM C-1437).

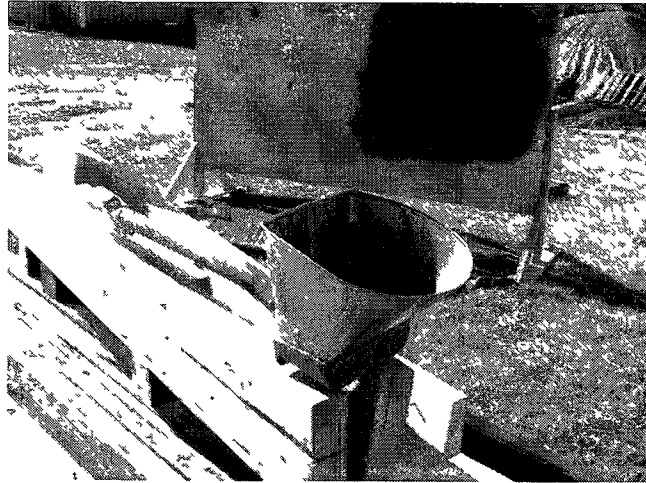


Fig. 6.8 Tyrolessa mortar sprayer.

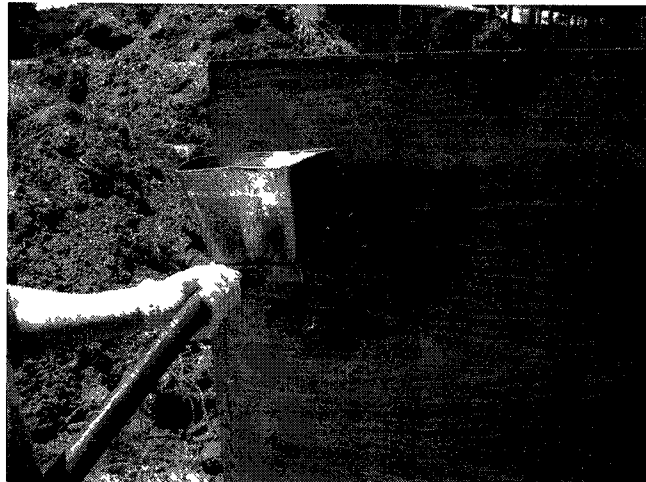


Fig. 6.9 Spraying geopolymer over wood board.

A paste of geopolymer with the successful formulation from the previous test was intended to be sprayed with the same mortar sprayer at the same pressure, but it could not be sprayed. The mortar flew from the holes without being separated into droplets.

From this test, it could be observed that it is not only that the stiffness and weight of the geopolymer paste makes its sprayability difficult, but also that the surface tension of geopolymer is a lot higher. Therefore, the idea of trying a surfactant was conceived.

6.4.2 Achieving Sprayability using Surfactants

6.4.2.1 Initial Tests

The first attempt to use a surfactant as an admixture for geopolymer was using regular hand soap (sodium lauryl sulfate as main ingredient). Fifteen ml of hand soap were diluted in a 300 g of fly ash geopolymer admixture. The result was a fully sprayable admixture, although the paste was a little runny on the surface. These initial results encouraged making of further tests with surfactants. Two types of commercial air-entrainers were ordered (Super Air and Super Air-Plus from Fritz-Pak) and (Daravair 1000 and Daravair 1400 from Grace).

Table 6.2 is a summary of the tests performed with the tyloressa mortar sprayer. The formulation for all the tests was a N-10-1.5 with a 1:1 fly ash:sand ratio and a 0.45 activator solution/fly ash ratio.

Table 6.2 Preliminary spraying tests.

Test number	Surfactant type	Surfactant (%)*	Extra water (%)*	Observations
1	Soap	5	-	Surface tension reduced significantly. Sprayed successfully over vertical surface. Surface difficult to be finished. The paste was runny. The soap was liquid, so it already contained water.
2	Super Air Plus	0.375	-	The spraying was not as efficient as with the soap.
3	Super Air Plus	0.7	3.33	Both the air entrainer and the water amount were increased. Sprayed successfully.
4	Super Air Plus	0.375	3.33	The surfactant amount was reduced to the original 0.375%. Water was added in parts, but it had to be added completely. It could be sprayed successfully.
5	Daravair 1400	0.33	3.33	Spraying was not as efficient as previous tests.

6.4.2.2 Compressive Strength Evaluation/ Curing Regimes/Reformulation

After an initial sprayable paste was obtained, compressive strength under two different curing regimes was also evaluated. The effect of both the air entrainer and extra water were evaluated. The tests performed are summarized in Table 6.3.

Table 6.3 Effect of water, surfactant and curing regime on sprayable geopolymer mortar.

Test number	Surfactant type	Surfactant (%)*	Extra water (%)*	Curing	Compressive strength (psi)
1	None	-	-	60 C after 24 hrs at room temp.	5683.33
2	None	-	3.33	60 C after 24 hrs at room temp.	3933.33
3	Super Air Plus	0.375	-	60 C after 24 hrs at room temp.	3200.00
4	Super Air Plus	0.375	3.33	60 C after 24 hrs at room temp.	2083.3325
5	None	-	-	60 C immediately after casting	4316.67

Several observations could be seen from this test:

- The curing regime has an influence. The sample that was cured immediately (#5) achieved less compressive strength than the one that was cured after 24 hrs.
- The negative effect of the water on the compressive strength of the mortar was found to be less than the effect of the surfactant.
- The combined effect of both the surfactant and the water was found to be a linear combination of both effects.
- The reduction of compressive strength was found to be unacceptable. Therefore, more tests were performed looking to reduce the amount of both surfactant and water and still achieve workability.

These observations led to preparing a new set of tests to achieve this goal.

First of all, the effect of a higher curing temperature was evaluated. Since curing at an industrial stage will be most likely be done using steam, a curing temperature of 100 C was thought to be appropriate.

Test #4 from the previous test was repeated and curing at 100 C for 1 and two days. These were the results (Table 6.4).

Table 6.4 Results from the repetition of the successful mix design under higher temperature conditions.

Test number	Compressive strength (psi) - 1 days of curing at 100 C	Compressive strength (psi) - 2 days of curing at 100 C
4	2425	2700

As it could be seen, the temperature did have an effect on the compressive strength, but curing 2 days does not seem to be necessary because the effect on compressive strength seems to be small. Therefore, 100 C will be set up as the curing temperature for this mortar composition.

Second, the amounts of both air entrainer and water needed to be optimized. It was decided to try to use Super Air regular instead of Super Air Plus (the concentration of Vinsol resin, the active ingredient is half). The following tests were performed (Table 6.5).

Cubes of this last formulation were casted to evaluate compressive strength. A curing regime of 100 C was applied after 24 hours of room temperature curing. Taking into account the linear effects of both air entrainer and water, the estimated compressive strength was 3750 psi. The actual measured compressive strength of the cubes was 3916.67 psi.

Table 6.5 Supplementary spraying tests performed.

Test number	Surfactant type	Surfactant (%)*	Extra water (%)*	Observations
1	None	-	3	Water alone could not help achieve sprayability
2	Super Air	3.75	3	This test worked and proved that sprayability can only be achieved using the air entrainer.
3	Super Air	0.015	3	This amount of air entrainer was the smallest recommended by the supplier. It did not work to achieve sprayability.
4	Super Air	0.05	3	The amount of air entrainer was increased but it was not enough.
5	Super Air	0.1	3	This amount was satisfactory. The mortar could be sprayed in the wall.
6	Super Air	0.1	2.65	A test with reduced extra water was tried. Again, it could be sprayed satisfactorily.
7	Super Air	0.1	1.65	Another test with reduced water was tried. It worked again.
8	Super Air	0.1	0.65	This is the minimum amount of water that could be added.

6.4.2.3 Spraying of a Concrete Wall

Once these results were achieved, a 1' x 1' concrete wall was built. A mortar based on the last successful formulation was prepared and sprayed over the wall. The wall was finished using a roller and a steel trowel (Fig. 6.10).

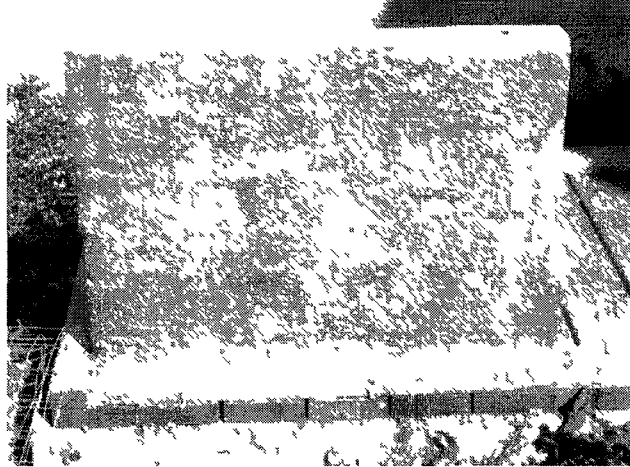


Fig. 6.10 Spraying over a concrete wall.

Among the general observations are that even though the mortar could be sprayed, the efficiency of the spraying was not the best. A lot of material flew through the holes of the sprayer and fell on the floor. Also, some efflorescence appear in the surface once it dried which could be a result of the little extra water that was added on the surface to help on the finishing process.

6.4.2.4 Change of the Order of Mixing the Surfactant

The manufacturer recommended to mix the surfactant on a wet cement paste (the bag dissolves itself), but during our tests, the additive did not seem to be dissolved correctly when added this way. In comparison to using liquid soap, it would seem more logical to have the soap dissolved in advance before adding it to the mix. Moreover, the

component that added the most viscous properties to the geopolymer mix was the sodium silicate.

It was, therefore, decided to try and dissolve the surfactant on the silicate prior to addition to the paste. The results were visibly different. The paste in which the additive was dissolved first looked notably more viscous and workable, and with less surface tension (e.g., the surfactant action was enhanced).

After these results, it was decided to make a DOE to decide which surfactant and the right dosage to produce optimal workability and performance.

6.5 Surfactant Addition Testing Program

6.5.1 Design of Experiments

The design of experiments can be seen in Table 6.6.

Table 6.6 Research variables for the surfactant design of experiments.

RESEARCH VARIABLE	LEVELS
Surfactant type	Vinsól resin and Sodium Lauryl Sulfate
Addition level	0.25, 0.75, 1.25, 1.75%
Concentration	10, 20, 30%
RESPONSE VARIABLE	METHOD
Compressive strength	ASTM C-109
Flow	ASTM C-1437
Viscosity	RHEOMETER

6.5.2 Materials and Formulation

Naturally, the same class F fly ash and formulation from the previous stages was used. The surfactants used were of two different types, the first one being a Vinsol resin by the commercial name of “Air Plus” and the second one Sodium Lauryl Sulfate of 99% purity.

6.5.3 Procedure

First, the desired surfactant amount is mixed in water until a uniform suspension is obtained. It is then immediately added to the sodium silicate to achieve surface tension reduction. The sodium silicate and the hydroxide are then added to the bowl, and fly ash and sand (for compressive strength and flow) comes next. The paste is mixed according the ASTM C-305 procedure for mortar and paste.

Cubes and flow were measured as in the previous chapters. The mix used to determine flow is used to cast the cubes to determine compressive strength. Fresh geopolymer cubes were cured at 100 C for 24 hours. Viscosity in paste was measured after 30 minutes at the same speed and parameters using the procedure detailed on section 6.3.3.

6.5.4 Results and Discussion

6.5.4.1 Compressive Strength

As it can be seen on the main effects plot (Fig. 6.11), the surfactant type has a large effect on the compressive strength. Air Plus (Vinsol resin) produced higher results in average than Sodium Lauryl Sulfate. Furthermore, the addition level decreased the compressive strength, as it could be expected. The reason for Sodium Lauryl Sulfate to affect the compressive strength in a deeper manner is because it is comprised of a longer carbon chain that is more susceptible to thermal expansion. The cubes also showed expansion by the means of a loop on the top of the specimen after curing at 100 C. The input and output values from MINITAB can be seen in Appendix D.3.

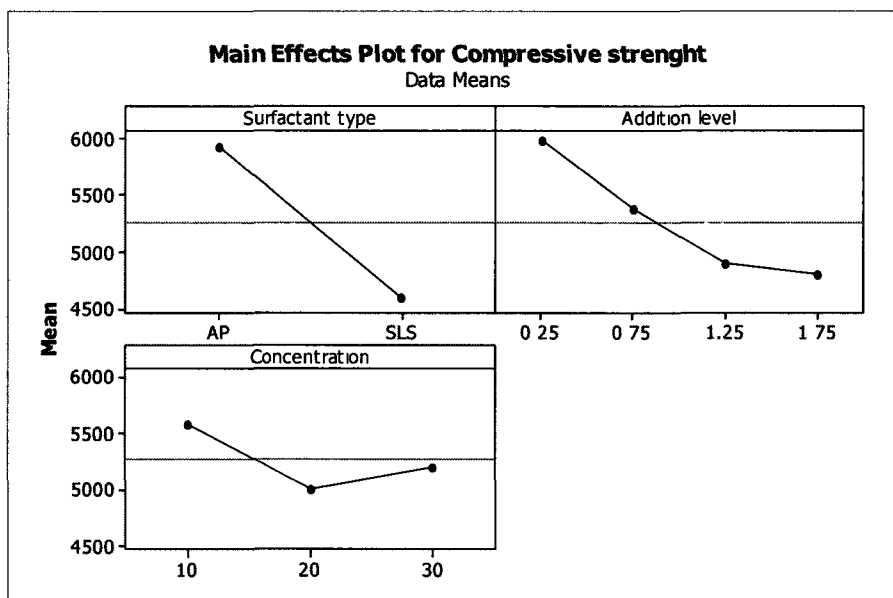


Fig. 6.11 Main effects plot for Compressive Strength.

From the interaction plot (Fig. 6.12), it can be seen now that there is no significant interaction between the silicate type and the addition level, (e.g., for both surfactants the more addition the less the compressive strength). There is also no interaction between the surfactant type and the concentration of the surfactant; they both exhibit the same behavior.

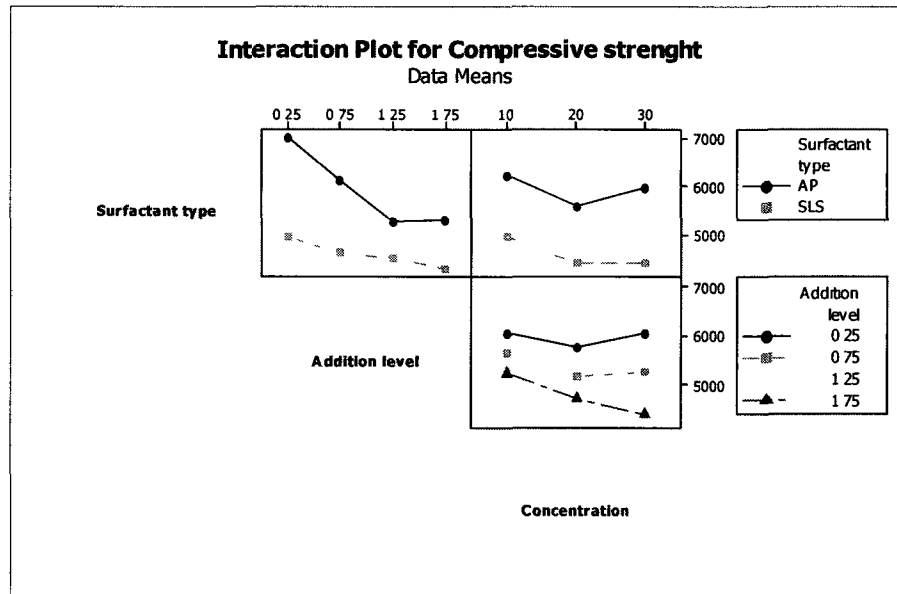


Fig. 6.12 Interaction plot for Compressive Strength.

From the Anova Table (Appendix D.5), it can be seen that all variables and interactions are significant, with the exception of the interaction between surfactant type and concentration.

6.5.4.2 Flow

The main effects plot (Fig. 6.13) for flow shows that again, the surfactant type had a large effect on the flow of the pastes. Sodium Lauryl Sulfate had a greater effect decreasing the flow. The addition level did not seem to have a very important role, as well as the concentration.

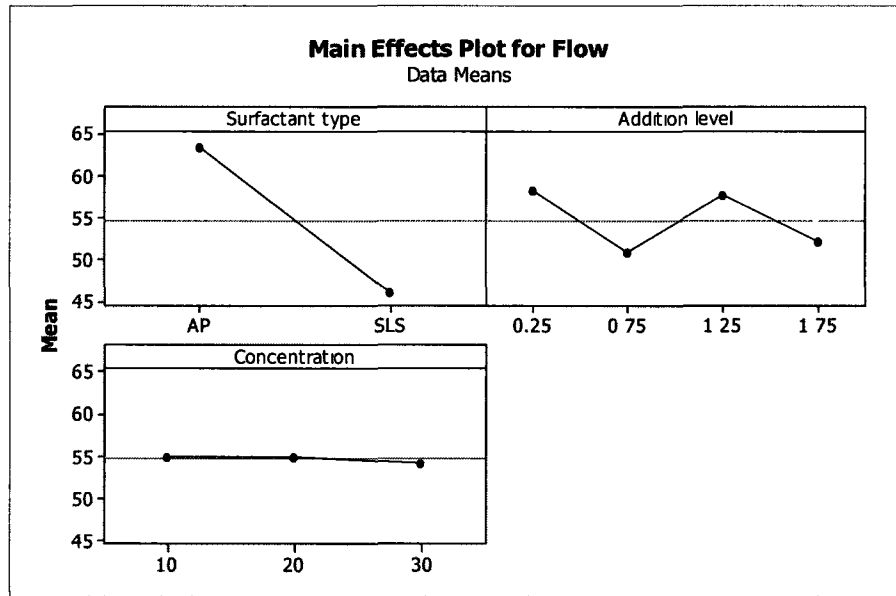


Fig. 6.13 Main effects plot for Flow.

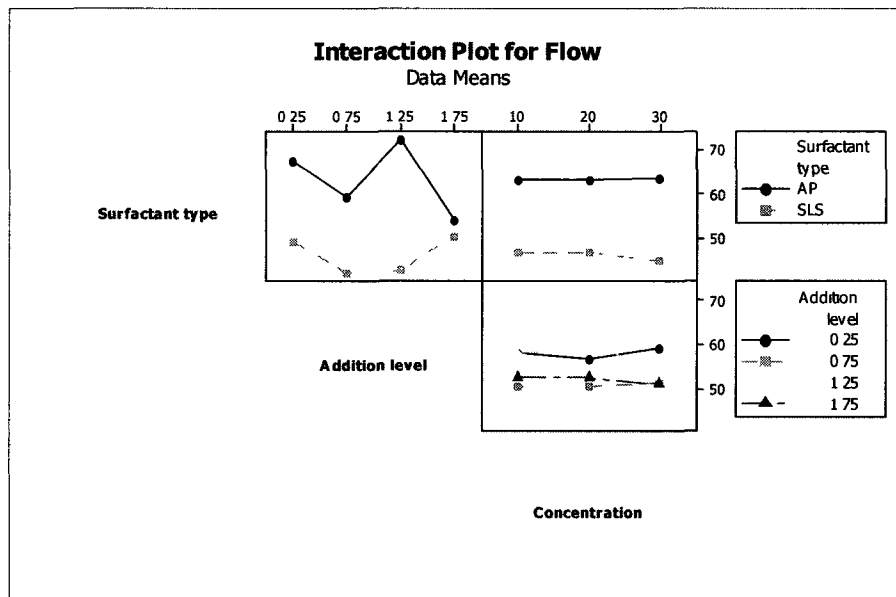


Fig. 6.14 Interaction plot for Flow.

It can be seen in the interaction plot that little or no interaction can be seen for these variables (Fig. 6.14). The ANOVA Table (Appendix D.6) shows that all variables and interactions had an effect with the exception of concentration and surfactant type*concentration. However, The surfactant type has the highest effect with an F of

1262.56, and, therefore, all other variables and interactions can be considered as having little effect.

6.5.4.3 Viscosity

From the main effects (Fig. 6.15) graph for viscosity it can be seen that again the surfactant type played a significant role this time. SLS produced higher viscosities and, therefore, lower workability materials. The addition level had a very clear effect this time, decreasing the viscosity with the addition level; however, as it can be seen, the concentration had an opposite effect, so the reduction on viscosity can be attributed to the increased addition of water and not of surfactant.

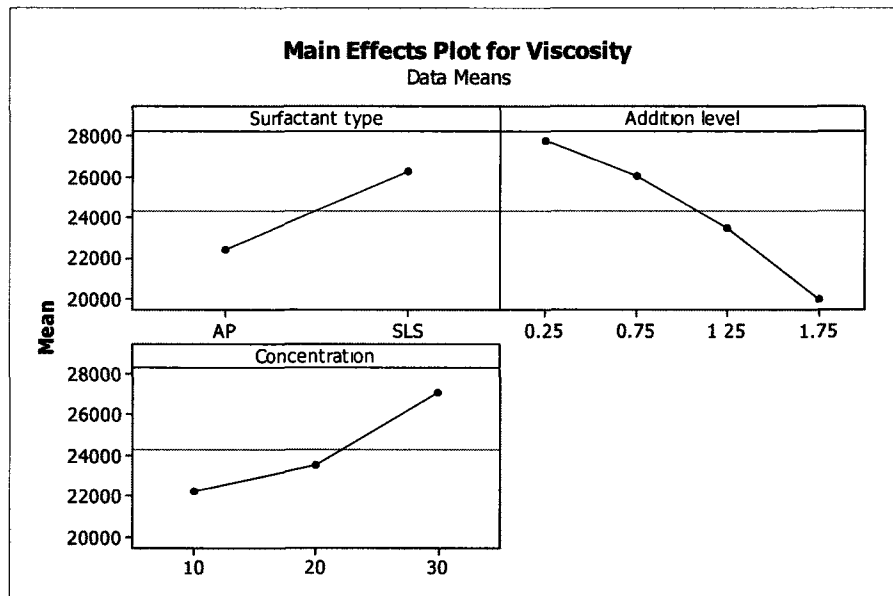


Fig. 6.15 Main effects plot for Viscosity.

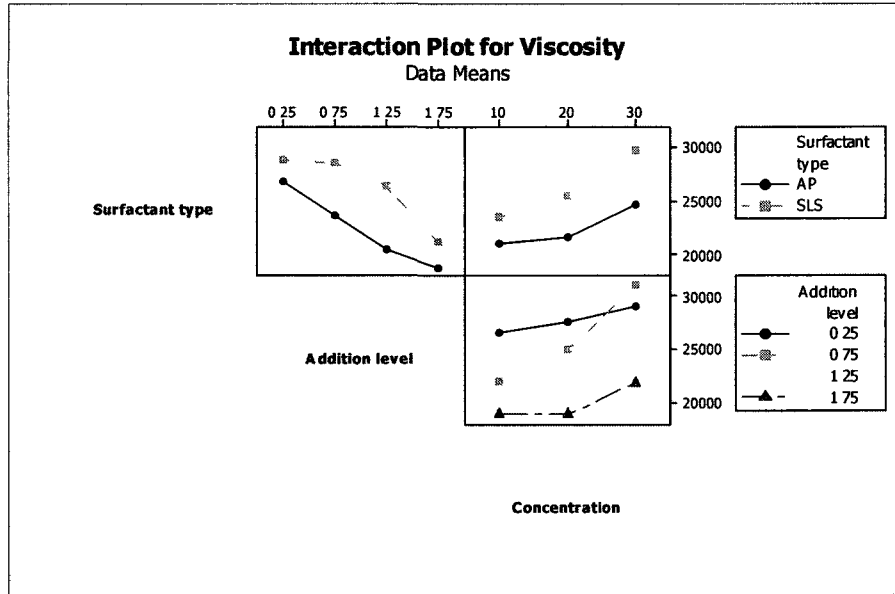


Fig. 6.16 Interaction plots for viscosity.

Again, the MINITAB interaction plots (Fig. 6.16) show little effect of the interactions in this case, which can be confirmed with the use of the ANOVA Table (Appendix D.6).

Moreover, these effects could be seen in the viscosity curves for all these combinations which are summarized in Figs. 6.17 through 6.19.

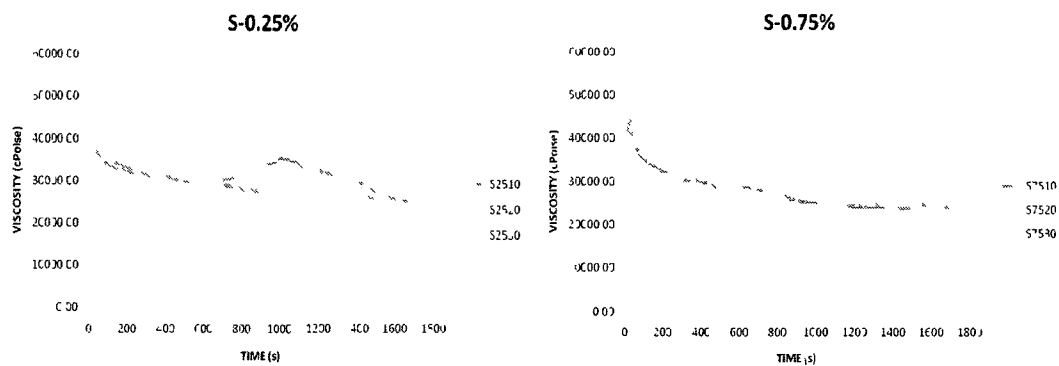


Fig. 6.17 Viscosity Curves for samples with a 0.25% of surfactant (left) and 0.75% of surfactant (right).

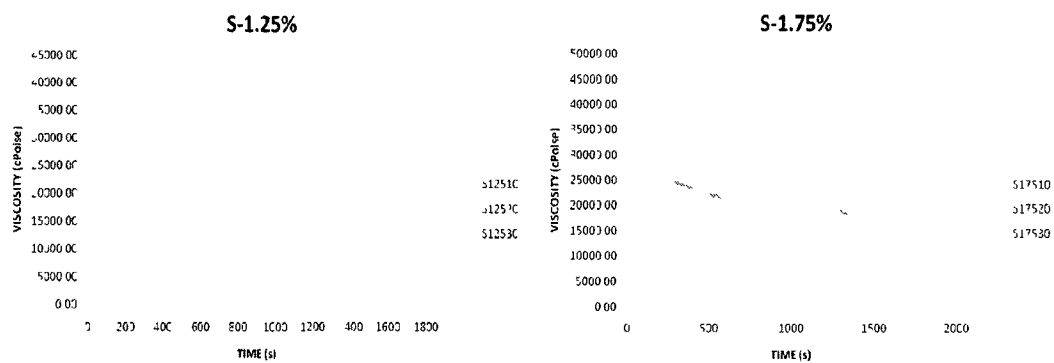


Fig. 6.18 Viscosity Curves for samples with a 1.25% of surfactant (left) and 1.75% of surfactant (right).

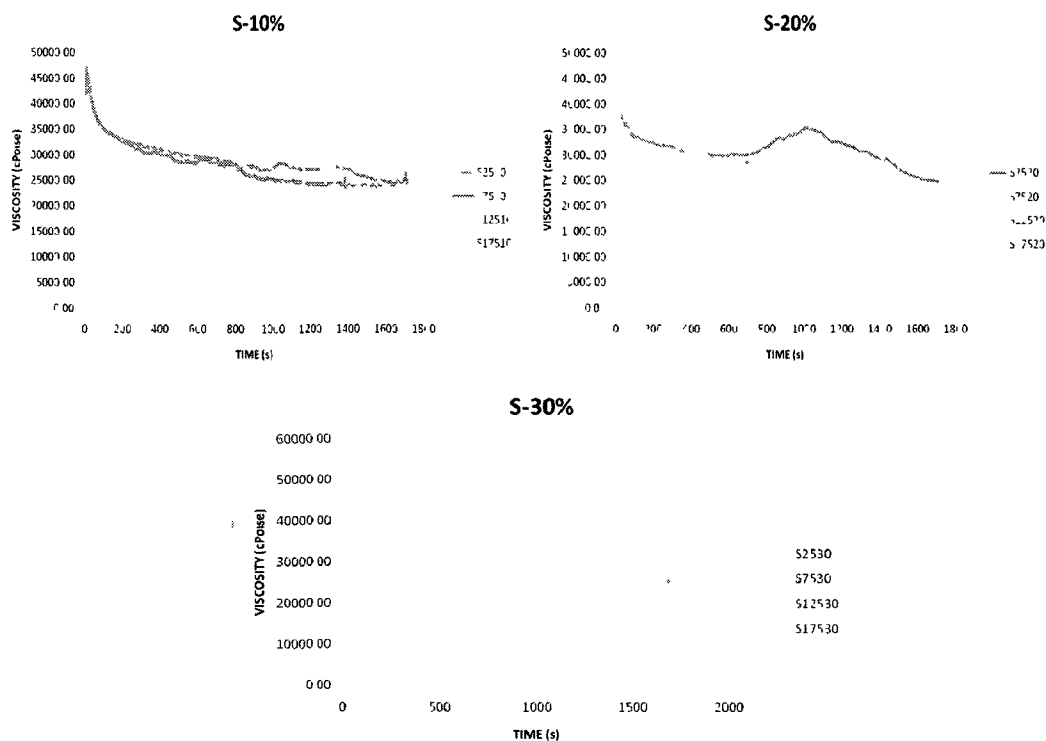


Fig. 6.19 Viscosity Curves for samples with a concentration of 10%, 20% and 30%.

6.5.4.4 Surface Tension

Having observed that SLS had undesirable characteristics, it was decided to drop it out of the design and continue the testing only with Super Air. The same design of experiments for the variables of addition level and concentration was run for this type of surfactant. The results from these tests are displayed in Fig. 6.20. The inputs and outputs from MINITAB can be seen on Appendix D.5.

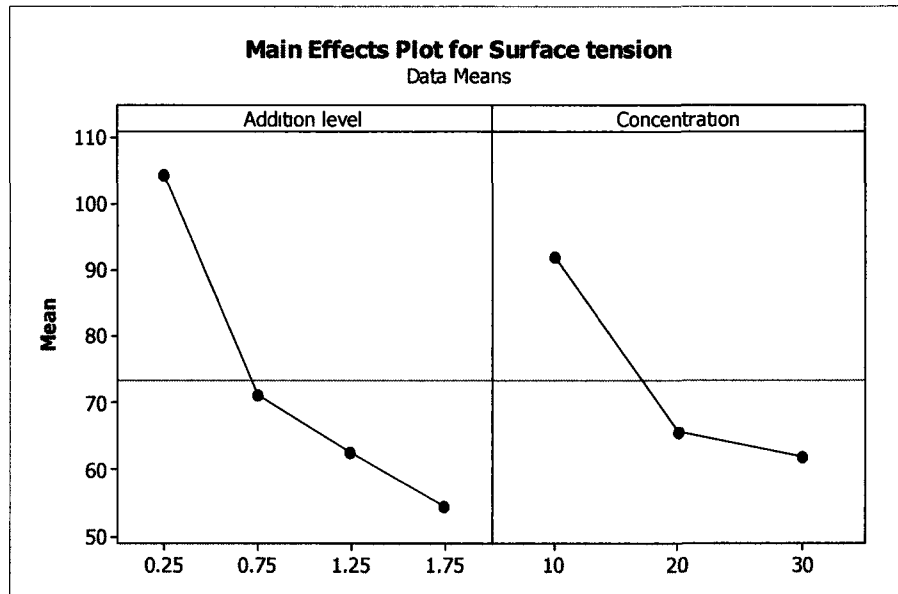


Fig. 6.20 Main Effects Plot for Surface Tension.

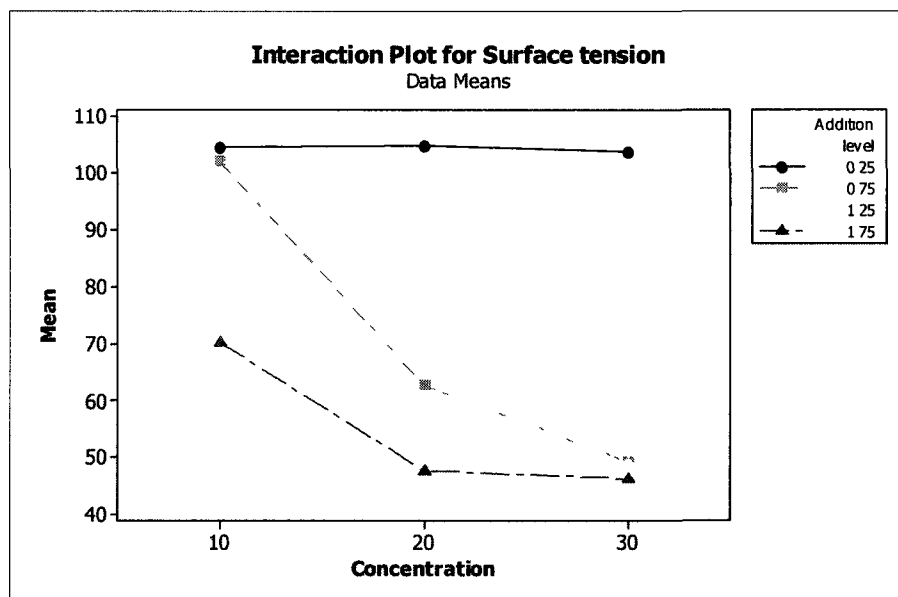


Fig. 6.21 Interaction Plot for Surface Tension.

The interaction plot (Fig. 6.21) and analysis of variance (Appendix D.6) show no interaction between the variables. An example of four drops can be seen in Fig. 6.22.

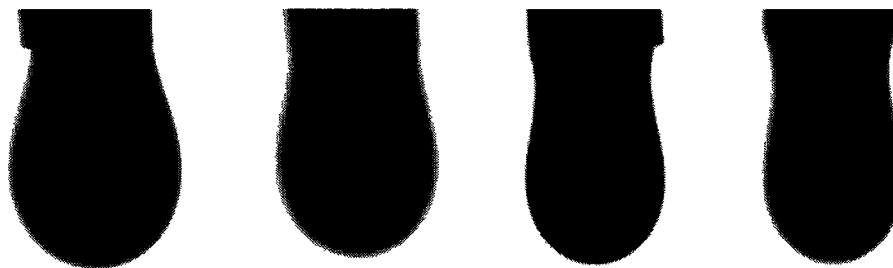


Fig. 6.22 Forms of droplets from the surface tension meter.

6.6 Field Tests

A total of three field tests have been conducted for this geopolymer mix. They have been very useful to more finely tune the parameters obtained from laboratory tests and to provide a more exact formulation to be used in the commercial product. The details of each test are presented as follows.

6.6.1 Field Test with DNA Construction

DNA construction is a large rehabilitating company dedicated to the rehabilitation of concrete manholes. Their staff has over 20 years experience in the field and have worked with a variety of materials including Portland cement, epoxy and hydraulic fast setting cement. Their observations and recommendations were very important in this stage of the project, since they could give an insight view on the product and evaluate if changes needed to be made and if it would be a good product for the industry. The corrosion resistance capabilities of geopolymer were immediately of their interest. They made a few initial observations about the workability of the mix and its fresh adhesion to the concrete wall.

Despite being initially a little reluctant and skeptic about the material, as especially about how would they clean their hoses and equipment, DNA agreed to perform the first industrial test ever with Louisiana Tech University's geopolymer grout.

The resulting mix from a formulation similar to the one in Table 6.7 is shown in Fig. 6.23 through 6.25. The mix showed good consistency and could be sprayed with no problems at all. Some observations were regarding the sagging of the mix, once it started to build. It was recommended to change the sand for a finer and lighter one and also to try and allow the mix to dry a bit quicker.

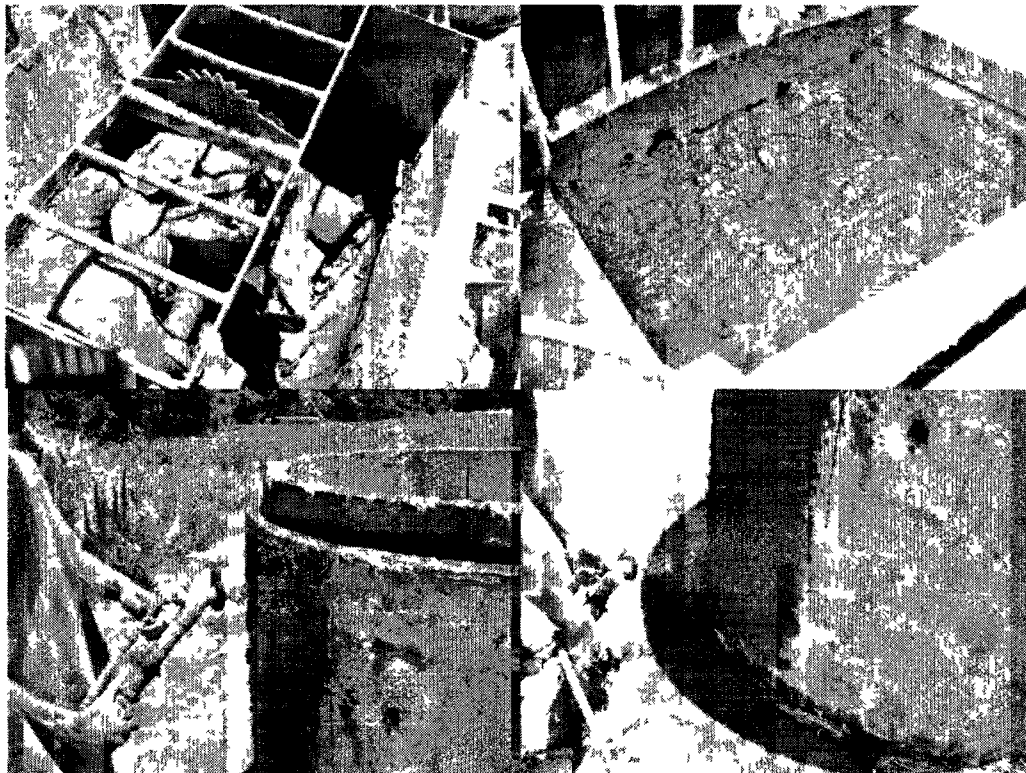


Fig. 6.23 Mixing and spraying with first field test.



Fig. 6.24 Spraying and finishing with DNA.

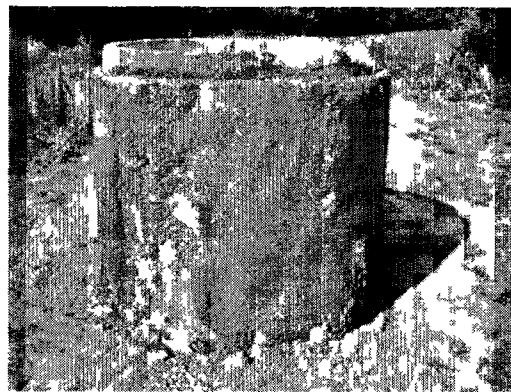


Fig. 6.25 A finished section of the manhole coated with the mix design.

Besides changing the sand, it was decided to change the hydroxide solution molarity to a 12.5 solution not only to allow it to set a little faster, but also to make it more commercially available; 12.5 M hydroxide solutions are known as 50% solutions and are one of the most commercially available hydroxide solutions in the market.

6.6.2 Second Field Test (with Spraybuddy)

After having had positive feedback from DNA Construction, it was decided to make our own test with TTC equipment. A bigger spraying machine was purchased (Spraybuddy) with a capacity of 3 ft³. The machine was a great help to evaluate the mix ourselves without depending from a large company and to make smaller changes to the mix if needed (Fig 6.26).

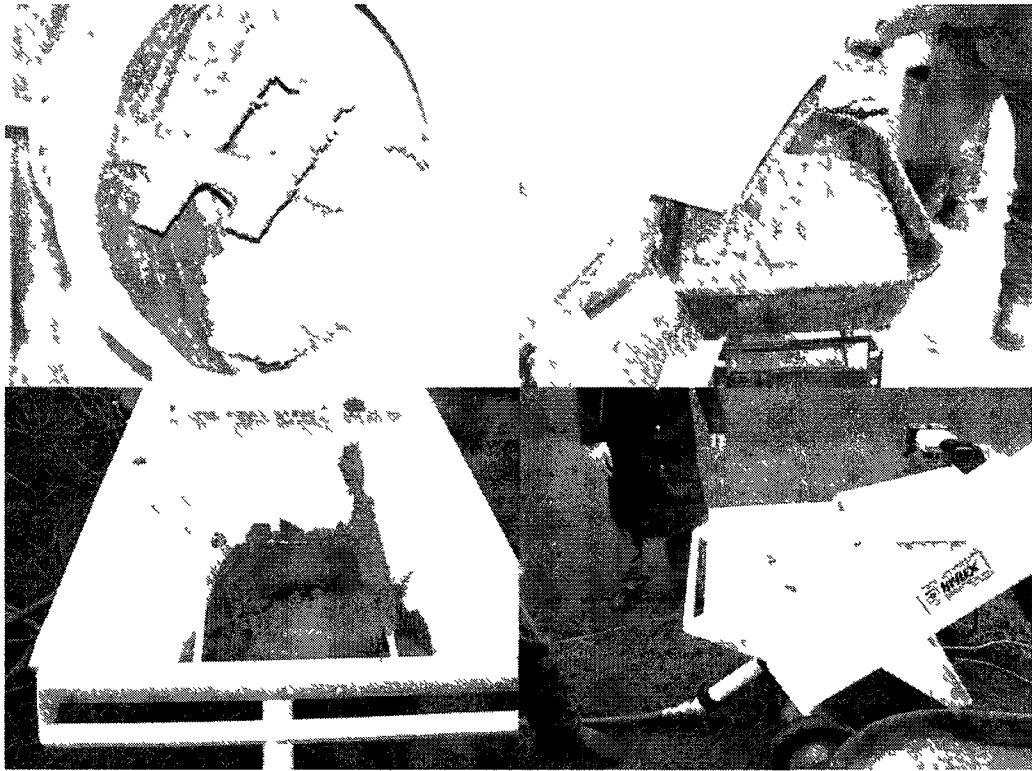


Fig. 6.26 Spraying with Spraybuddy

From this test, it could be concluded that mixing with a rotary mixer is not appropriate for geopolymer grouts. These mixers rely on the ability of the material to fall on a cascade and geopolymer's viscosity makes the mixing process difficult. It is much better and efficient to use a paddle mixer for this purpose. The mix obtained in the drum mixer was drier and more viscous than the previous test and, therefore, difficult to spray.

6.6.3 Third Field Test (Second with Spraybuddy)

For this test, a paddle mixer was used and the workability of the paste was much better. The mix could be sprayed successfully (Fig. 6.27) and finished with a trowel. The final mix design was reported and finalized.

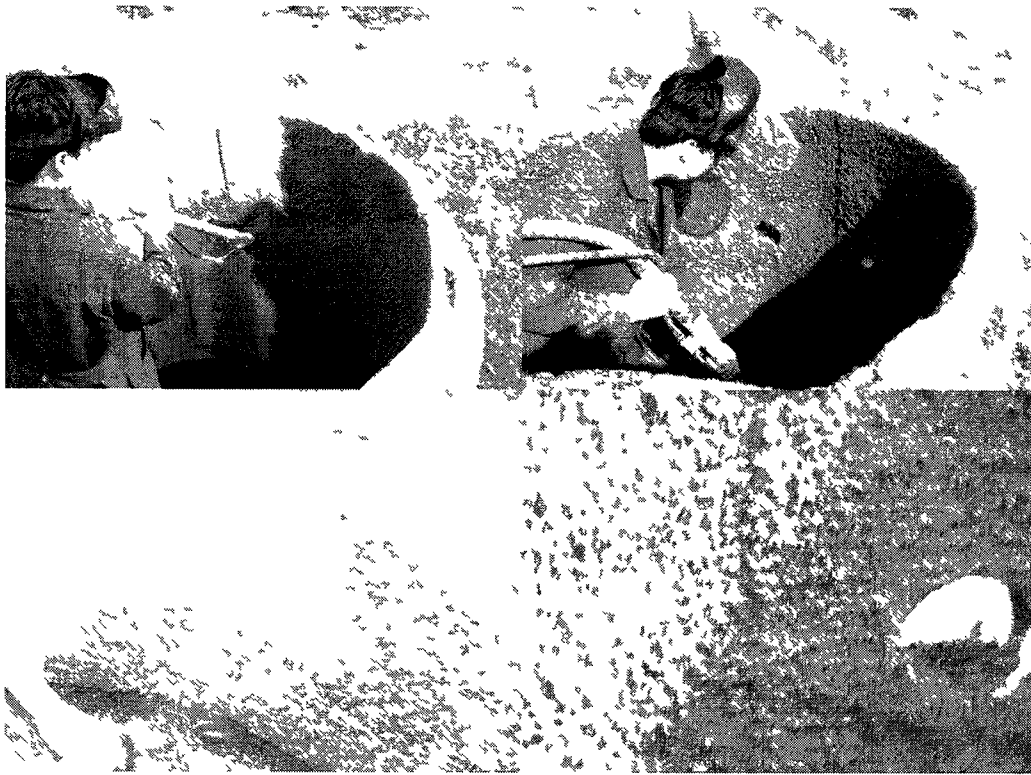


Fig 6.27 Second spraying test with Spraybuddy.

6.6.4 Conclusions

The field tests provided excellent information on the performance of the sprayable geopolymer coating. The results from the lab were close to a satisfactory performance in terms of the field tests. Small changes needed to be done before the final mix design was achieved. Curing would be the next major concern. As it was shown in the previous chapters, a combination of heat and moisture is required for the correct curing of this geopolymer mix. This process could be achieved with the use of a steam generator, but it will be discussed further in Chapter 8.

6.7 Proposed Final Formulation

The proposed final formulation can be seen on Table 6.7.

Table 6.7 Final proposed mix design.

Mix Name	Concrete		Proportions as Designed		Batched Proportions		Yielded Proportions		
Batch Size	1	ft ³	Specific Gravity	Amount (lb/yd ³)	Volume (ft ³)	Amount (lb)	Volume (ft ³)	Amount (lb/yd ³)	Volume (ft ³)
Cementitious Materials									
1 Class F Fly Ash			2.8	1586.047	9.078	58.742	0.336	8.667	0.050
2 CuSO ₄			2.28	12.953	0.091	0.480	0.003	8.64	0.061
Total of Cementitious Materials				1599.160	9.169	59.22	0.340	17.307	0.110
Aggregates									
1 Sand									
Absorption	0.00%								
Batched Moisture Content	0.00%		1.56	799.580	8.214	29.614	0.304	3.726	0.038
Total of all Aggregates				799.580	8.214	29.614	0.304	3.726	0.038
Liquids									
1 Sodium silicate N			1.385	380.651	4.404	14.099	0.163	32.400	0.519
2 Sodium hydroxide 12.5 M solution			1.33	253.767	3.058	9.399	0.113	0.000	0.000
3 Surfactant			1.14	19.826	0.279	0.734	0.010	19.826	0.318
Total Water				654.244	7.741	24.231	0.287	52.226	0.837
Water-Cementitious Materials Ratio				0.4125		0.4125			
Air Content %				7.45%		7.45%			
Density (Unit Weight) pcf				113.09		113.09			
Gravimetric Air Content %				7.00%		7.00%			6.00%
Yield ft ³				27.00		1.00			#REF!

6.8 General Conclusions

A few changes were necessary to adapt the optimal mix design from chapter 5 to a sprayable coating formulation. First of all, a few minor changes were necessary to control setting time and improve flow. The activator solution variables have a deep effect on the flow and viscosity of geopolymers.

Then, the use of surfactants was a key idea to achieve workability. The final addition had to be achieved first by a number of trial tests, then by a full design of experiments to know the exact amounts. The type of surfactants was of great importance for this goal, but the addition level and concentration were as well. The concentration reduces the flow and increases viscosity, and the addition level decreases viscosity but only because of the increased amount of water on the mix.

Controlled viscosity with low surface tension was desirable to achieve the optimal mix. Lab results were confirmed by industrial spraying tests for this product.

CHAPTER 7

QUALITY TESTS, COPPER ADDITION AND COMMERCIAL OPPORTUNITIES

7.1 Background

A successful spraying geopolymer formulation was presented in the previous chapter. However, to have achieved sprayability was not the final stage of this project. The product still needed to undergo a series of testing to assure its quality. The first part of this program refers to the mechanical testing conducted on this material in terms of compressive, flexural and tensile strength. Young's modulus and Poisson ratio were also calculated. The addition of fiber was an important aspect in consideration to improving the flexural strength of this grout. It was carefully considered as well.

Corrosion resistance had already been a useful way to select the raw material and alkaline solution for this coating. It was important to also know the final corrosion resistance of the final mix design, especially after the addition of an air entrainer.

Other important parameters, such as adhesion, wear resistance and expansion were evaluated. In the end, a full specification table for this material, similar to those of commercial products, was created.

In the second part of this chapter, the addition of copper oxide to geopolymer was evaluated. Copper is a known bactericide that has been used since ancient times. Since most of the H₂S in sewers is produced by bacteria, it is a logical idea to try and prevent

their growth by adding a bactericide agent. That prevention would solve the problem from the very beginning. Previous attempts to do this include embedding Cu_2O in epoxy. The results show a significant decrease in bacterial count in the solutions [14].

On the other hand, geopolymers are capable of embedding copper in their structure, although it is not known if it is done in a cation replacement or in an interstitial manner. The main purposes of doing this have been for toxic metal removal out of wastewater [74].

Copper has some impact on the properties of the geopolymer, including the reduction of compressive strength.

It is, therefore, the purpose of this chapter to evaluate the inclusion of a copper agent in three forms (oxide, sulfate salt and nitrate salt) to the geopolymer and evaluate its effect on properties such as compressive strength and flow. XRD analyses were performed. The presence of copper compounds in a crystalline phase is also evaluated by means of a XRD analysis, and conclusions are made on the possible incorporation of copper inside the amorphous structure of geopolymers with the use of TEM/EDS.

At the end of the chapter, important commercial considerations are made for the future and possible commercialization of this product.

7.2 Quality Testing

7.2.1 Mechanical Strength

Mechanical strength was tested in three ways: compressive (cubes and 6 inch diameter cylinders), tensile and flexural. Young's modulus and Poisson ratio of the designed mix were also evaluated. The details of each test are presented on the next subsections.

7.2.1.1 Compressive Strength

Compressive strength was evaluated both in 2 cubic inch cubes and 6 inch diameter cylinders. Standards followed are ASTM C-109 and ASTM C-39. Mortar mix was prepared according to the formulation presented in Table 6.7 and mixed as per ASTM C-305. The mix was then cast into 2 cubic inch and 6 inch diameter cylindrical molds. Three repetitions were made for each case. The samples were left to rest for 24 hours at room temperature then cured at 212 F for another 24 hours period, then they were tested using the Universal Machine. Compressive strength was evaluated for 1, 3, 7 and 28 days in 2 inch cubes and for 24 hrs in 6”x12” cylinders. The results are presented in Table 7.1

Table 7.1 Compressive strength results for the proposed geopolymer mix.

Specimen	COMPRESSIVE STRENGTH (psi)				
	C-109 24 hrs	C-109 3 days	C-109 7 days	C-109 28 days	C-39 24 hrs
1	6028	6544	6960	7022	5825
2	6135	6519	6828	7011	5035
3	6200	6364	6931	6998	5155
Average	6121	6475.67	6960.33	7010.33	5338.33

7.2.1.2 Flexural Strength

Flexural strength was evaluated using 1”x1”x10” bars. The standard used was ASTM C-580. Mortar from the formulation presented in Table 6.7 was mixed according to ASTM C-305 and cured for 24 hours after a rest period of 24 hours. The addition of fibers was considered in this testing program. The fibers used were poly-vinyl alcohol (PVA), fiber glass (FB), poly-propylene (PP), pseudo glass (PG). The details and the results are shown on Table 7.2. The fiber content is expressed in percentage of fly ash. Workability is defined as flow according to ASTM C-1437. It can be seen that the

flexural strength of the mix was about 14% of the compressive strength in cubes and 16% of the compressive strength in cylinders, both values above the typical 10% for most cementitious materials. The table also shows the positive effect of the fiber addition on flexural strength. The best results were achieved with the addition of 1% of fiber glass, increasing the flexural strength to 17.4% of the compressive strength measured in cubes, but good results can also be achieved with as little as 0.25% of Polypropylene fibers (16.9%)

Table 7.2 Flexural strength of geopolymers mix with and without the addition of fibers.

	Without Fiber	PVA			FG		PP		PG	
Fiber Content		0.10%	0.50%	0.75%	0.50%	1.00%	0.10%	0.25%	0.50%	1.00%
Workability	44		48	41	56	52	49	47	52	48
1	976	769	922	1068	715	1004	858	1204	870	850
2	670	956	1048	1147	732	1024	1037	987	926	1000
3	1034	-	978	922	808	1175	982	912	835	906
4	822	853	1007	1003	761	1050	1037	1047	969	899
Average	875.5	859.33	988.8	1035.0	754.0	1063.3	978.5	1037.5	900.0	913.8
% Difference		-1.85	12.94	18.22	-13.88	21.44	11.76	18.50	2.80	4.37

7.2.1.3 Tensile Strength

Tensile strength tests were conducted according to ASTM C-307. Six butterfly specimens were prepared with the mix of Table 6.7 and mixed according to ASTM C-305. They were cured 24 hours at 212 F after a rest period of 24 hrs. They were then tested using the SMS Machine available at the Engineering Lab (Fig. 7.1).

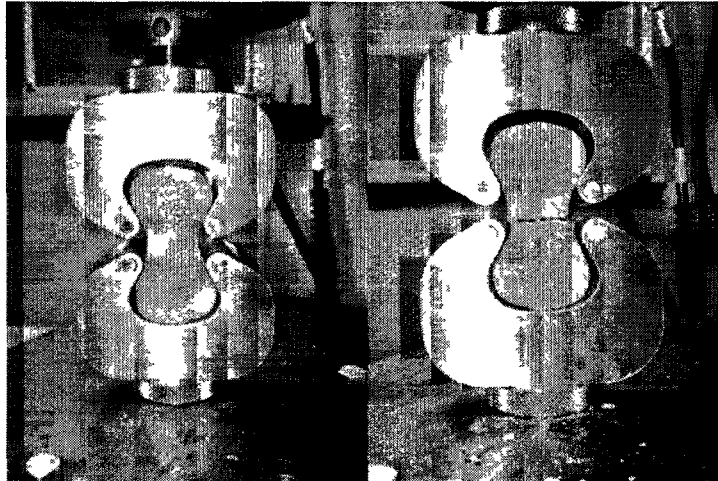


Fig. 7.1 Tensile strength tests on geopolymer mix

The results of this test are summarized on Table 7.3.

Table 7.3 Tensile strength results for geopolymer mix.

SPECIMEN	TENSILE STRENGTH (psi)
1	361.31
2	422.98
3	401.04
4	385.34
5	394.98
6	344.21
AVERAGE	384.97

The tensile strength could also be increased with the addition of fibers, but that will be left for future research.

7.2.1.4 Young's Modulus and Poisson Ratio

Young's modulus and Poisson ratio were calculated according to ASTM C-469. The values are shown on the specification list for this geopolymer grout shown on Table 7.9. The raw data used for this calculation can be seen on Appendix E.1.

7.2.2 Corrosion Resistance

The corrosion resistance of the final mix was evaluated with the same procedure explained in Section 4.4. The results are summarized in Table 7.4. A comparison graph with Portland Cement is shown on Fig. 7.2. It can be seen that eventhough the remaining compressive strength was reduced to the original remaining compressive strength obtained in chapter 4, the addition of surfactant did not have a very strong effect on it if it is compared to the remaining compressive strength of a N-10-2 geopolymer mix (75%).

Table 7.4 Remaining compressive strength and mass loss of final geopolymer mix.

TEST/SPECIMEN	TEST DATE (week)					
	0	1	2	4	6	8
Remaining Compressive Strength (psi)						
1	6028	6058	5725	4952	4504	4356
2	6135	6088	5638	4665	4590	4234
3	6200	6011	5553	4705	4489	4338
AVERAGE	6121	6052.33	5638.67	4774	4527.67	4309.33
MASS LOSS (g)						
1	271.23	265.44	254.95	249.53	244.11	235.97
2	264.54	260.32	251.34	246.02	240.74	235.44
3	268.34	261.99	252.63	245.53	241.55	230.07
AVERAGE	268.03	262.58	250.6	247.02	242.13	233.82

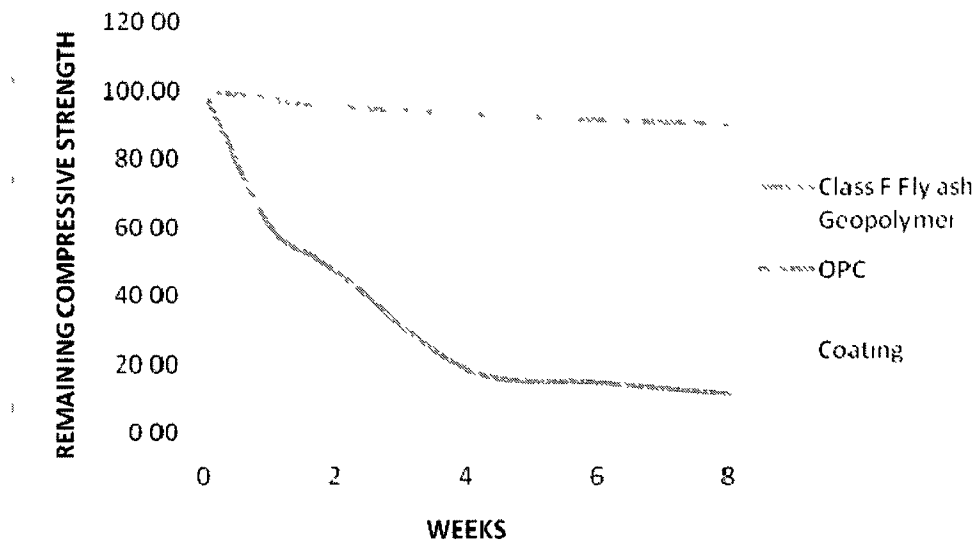


Fig. 7.2 Remaining Compressive Strength from Class F Fly Ash Geopolymer, OPC and the Coating Formulation after 8 weeks of immersion in a H_2SO_4 solution of pH = 0.6.

7.2.3 Absorption, Voids and Air Content

This test was conducted per ASTM C-642. Again, mortar from the formulation shown in Table 6.7 was mixed according to ASTM C-305 and casted on three 3x6" cylindrical molds. The samples were cured as mentioned in the previous sections. ASTM C-642 requires the following weights to be obtained: A) mass of oven dried sample in air, B) mass of surface-dry sample in air after immersion, C) mass of surface-dry sample in air after immersion and boiling and D) apparent mass of sample in water after immersion and boiling. The values for each category for each sample are shown in Table 7.5.

Table 7.5 Mass of specimens required for ASTM C-642.

Required mass (g)	Specimen 1	Specimen 2	Specimen 3
<i>A</i>	1147.73	1214.81	1163.71
<i>B</i>	1222.82	1246.68	1225.71
<i>C</i>	1227.36	1251.23	1232.34
<i>D</i>	707.60	752.96	710.34

The following calculations are required by ASTM C-642:

$$\text{Absorption after immersion, \%} = \left[\frac{B - A}{A} \right] * 100$$

$$\text{Absorption after immersion and boiling, \%} = \left[\frac{C - A}{A} \right] * 100$$

$$\text{Bulk density, dry} = \left[\frac{A}{C - D} \right] \cdot \rho = g_1$$

$$\text{Bulk density after immersion} = \left[\frac{B}{C - D} \right] \cdot \rho$$

$$\text{Bulk density after immersion and boiling} = \left[\frac{C}{C - D} \right] \cdot \rho$$

$$\text{Apparent density} = \left[\frac{A}{A - D} \right] \cdot \rho = g_2$$

$$\text{Volume of permeable voids, \%} = [(g_2 - g_1)/g_2] \times 100$$

Using the above equations, the values calculated for this coating are shown in

Table 7.6.

Table 7.6 Values calculated using standard ASTM C-642.

RESULT	VALUE
Absorption after immersion, %	4.75
Absorption after immersion and boiling, %	5.23
Bulk density, dry, Mg/m ³	2.28
Bulk density after immersion, Mg/m ³	2.40
Bulk density after immersion and boiling, Mg/m ³	2.41
Apparent density, Mg/m ³	2.60
Volume of permeable voids, %	12.30%

The air content of fresh geopolymer coating mix was further evaluated with a pressure meter as required by ASTM C-231. Enough sample for 0.4 ft³ according to the formulation from Table 6.7 was mixed according to ASTM C-305. Then, the sample was poured inside the base of the pressure meter and the paste was spread using a steel bar.

The surface was leveled with a trowel and the cover was wiped off and cleaned. Then the cover is clamped securely with petcocks open. Water was injected in the sample using the supplied syringe until all of the air is displaced and expelled through the opposite petcock. The petcocks were left open until the hand on dial was stabilized at the initial pressure line by pumping up or bleeding off with the air release valve. After the petcocks were closed, the needle valve lever was pressed down to release the air into the base. The needle was held down for a few seconds while lightly tapping on the gauge to stabilize it. Then, the test was done and the percent of entrained air could be read from the dial. The procedure was repeated three times with three different samples and an average was obtained. The result is shown on Table 7.9.

7.2.4 Length Change in a Sulfate Solution

The length change of the coating material in a sulfate solution was evaluated using ASTM C-1012. Enough material from the formulation presented on Table 6.7 was mixed according to ASTM C-305 to produce four 1”x1”x10” bars. The bars were cured with the procedure detailed in previous sections and at the 7th day they were stored in a sulfate solution prepared according to ASTM C-1012. A volume of 4-1 solution to bars was used. The bars were then measured using the length comparator described in the same ASTM. The dates for measuring and the results are shown in Table 7.7. The actual readings can be seen in Appendix E.2.

Table 7.7 Length change (%) of coating formulation bars in a solution of NaSO₄

SPECIMEN	WEEK 1	WEEK 2	WEEK 3	WEEK 4	WEEK 8	WEEK 13	WEEK 15
1	0.034	0.084	0.085	0.088	0.09	0.097	0.105
2	0.089	0.165	0.167	0.171	0.172	0.181	0.187
3	0.012	0.1	0.107	0.11	0.117	0.115	0.12
4	0.05	0.101	0.105	0.108	0.11	0.119	0.124
AVERAGE	0.0462	0.1125	0.1160	0.1192	0.1223	0.1280	0.1340

Therefore, as it can be seen from the table, the maximum length change after immersion in a sulfate solution after 15 weeks is 0.1340%.

7.2.5 Abrasion Resistance

The abrasion resistance test was conducted according to ASTM C-744. This test requires the preparation of samples 4”x 4” square, 15-20mm thick (at the widest section) and a 13mm, drilled hole through the center.. The test set-up and results are the following:

- Instrument: Taber Rotary Abraser – Model 5155
- Abrasive Wheel: CS-17
- Load: 1,000 gram per wheel
- Vacuum Nozzle Gap: 1/8 inch
- Total Cycles: 500

The test Method starts with the recording of the initial weight of the samples. Then each specimen was measured for thickness and an appropriate shim combination was used to achieve a thickness (height) of 40mm. 500 cycles were run, the sample was removed and a final weight was recorded. The wheels were refaced prior to each test.

Per ASTM C744 the Wear Index is to be calculated per ASTM C501 as follows:

$$IW = 88/(WO - WF)$$

Where:

IW =Wear Index

WO = original weight of specimen, g

WF = final weight of specimen, g

The test results are shown on Table 7.8.

Table 7.8 Test results for the geopolymer coating formulation and OPC.

With a full wearpath					
1A	353 58	500	353 46	0 12	733 3
1B	371 23	500	371 11	0 12	733 3
3A	323 81	500	323 64	0 17	517 6
3B	339 86	500	339 70	0 16	550 0
4A	414 70	500	414 48	0 22	400 0
4B	431 64	500	431 43	0 21	419 0

Sample #1 corresponds to the geopolymer formulation with no surfactant. Sample #3 corresponds to the coating formulation presented on this thesis. Sample #4 corresponds to a Portland cement sample. The results show the superior resistance to abrasion of both geopolymer samples compared to Portland cement.

7.2.6 Bond Strength (Adhesion)

This test was conducted using the Positest portable Pull-Off adhesion tester according to ASTM D-4541.

The preparation of the sample consisted on a 6"x12" solid cinder block coated manually with a 1/2" thick layer of geopolymer coating. The sample was cured in the same way as the previous samples.

The first step for this test is the preparation of a 20 mm dolly, which is cleaned and removed of contaminants. The coating is then abraded slightly using an abrasive pad. The adhesive epoxy is then mixed according to instructions and deposited on the dolly with a thickness of approximately 2-4 mils. Then, the dolly is attached to the surface and the adhesive is allowed to cure according to manufacturer's instructions.

After the adhesive has been cured, the provided template must be placed on the coating, surrounding the dolly. With a hand drill (using a 5/32" drill bit), the first positioning hole is drilled. After this, the template was removed, the surface cleaned for

debris and then reinserted again, with a pin inserted in the #1 position. Then hole #2 is drilled. The cleaning procedure and reinserting the template by inserting both pins in the #1 and #2 positions were repeated. Next, the holes corresponding to the 20 mm dolly were drilled. After all these holes have been drilled, the template was placed back onto the surface but rotated so the drilled positioned holes line up with the template repositioning holes labeled 20 mm. A circular hole will be the result of repeating the drilling procedure. After doing this, the sample was ready for the pull-out test.

To perform the pull-out test, the first step was to ensure the relief valve on the pump was completely open. Then the red “drag” indicator on the pressure gauge was turned to zero. The actuator handle was now pushed completely down into the actuator assembly, which is placed over the dolly head. The pressure valve was closed tightly after that. Now, the pumping began with the handle until the black indicator on the pressure gauge started to move. At this stage, pumping must continue at a uniform rate no more than 150 psi per second until the actuator pulls the dolly from the coating. The reading was recorded. Results were repeated on three different samples and they are reported in Table 7.9.

7.2.7 Viscosity and Flow

After following the procedures to measure viscosity indicated on section 6.3.3 and flow as per ASTM C-1437, the following results for the present geopolymer coating were recorded. Fig. 7.3 shows a viscosity vs time graph and Fig. 7.4 shows several shear strain vs. shear stress graphs for different rest periods. It can be seen that the yield stress increases after different times the mix was prepared and the shear stress is increased as well.

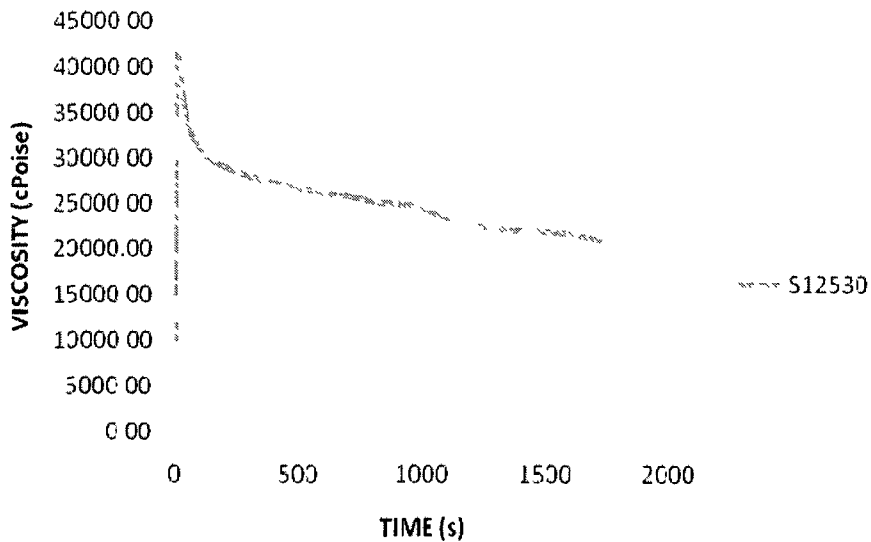


Fig. 7.3 Viscosity vs time graph for 30 minutes.

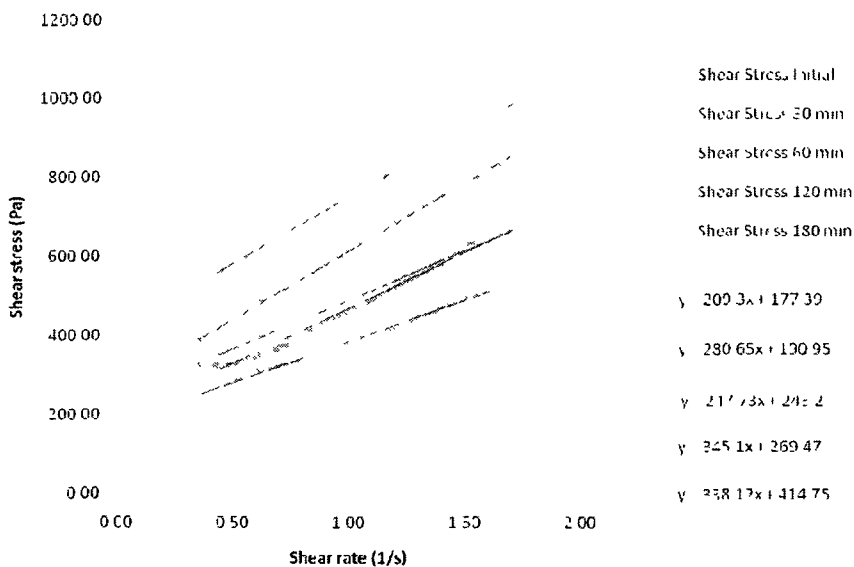


Fig. 7.4 Yield stress after several rest periods.

7.2.8 Pot Life (Setting Time)

A setting time test was conducted according to the ASTM C-403 procedure for mortar. Mortar from the formulation shown in Table 6.7 was prepared and mixed according to ASTM C-305, and then it was cast into a cone mold. Penetration with the

calibrated needle was performed until the penetration was 25 mm and until the sample was completely hardened. Setting time was above 3 hours for all the tests.

7.2.9 XRD Phase Identification Analysis

XRD tests were performed on the final formulation of the coating to identify the amorphous content. As it was explained in the literature review, both the fly ash material and the resulting geopolymer have large amounts of amorphous content. The analysis performed for Class F fly ash and the geopolymer of the coating is presented on Table 7.9, and the spectrums can be seen on F.1.

Table 7.9 XRD Phase analysis of the geopolymer coating and Class F Fly Ash.

Phase	Class F Fly Ash	Class F Fly ash Geopolymer	Geopolymer Coating
Quartz	10.33	5.58	4.6
Mullite	25.27	14.62	10.2
Amorphous	64.4	79.8	84.7

As it can be seen, the amount of amorphous material changes from the Fly ash to the Geopolymer by almost a 15%. This change is a good sign of geopolymerization. Moreover, the height of the lump for the broad part of the spectrum changes from about 23 degrees to about 28 after geopolymerization. It can be seen that the amount of amorphous material for the geopolymer coating is higher, with more of the crystalline minerals reacting. This higher amount could just be a result of the higher temperature of calcinations used to produce the coating. The highest part of the broad section of the spectrum remains around 28 degrees.

7.2.10 Summary (Product Specification Table)

Finally, and after all the testing, a specification sheet was reached and presented on Table 7.10.

Table 7.10 Specification sheet for the geopolymer coating.

TEST	ASTM	VALUE
Compressive Strength Cubes	C-109	
24 hr		6121.00
3 day		6475.67
7 day		6960.33
28 day		7010.33
Compressive Strength Cylinders	C-78	
24 hr		5338.33
Flexural Strength (24 hr)	C-580	875.5
Tensile Strength (24 hr)	C-307	384.97
Young's Modulus	C-469	1717
Poisson Ratio	C-469	0.16
Corrosion Resistance	C-267	
Remaining Comp. Str.		70%
Mass loss		12.7%
Absorption after immersion	C-642	4.75%
Volume of permeable voids	C-642	12.30%
Air content	C-231	14%
Abrasion resistance	C-774	533.5
Bond Strength	D-4541	1400
Initial Viscosity (paste)	-	43,000 cPoise
Viscosity after 30 minutes	-	20,000 cPoise
Pot life	C-403	< 3 hrs

7.3 Copper Addition Testing Program

7.3.1 Design of Experiments

On this occasion, a 2x3 design of experiments was used to evaluate three sources of copper and two addition levels. Response variables were compressive strength, flow and crystalline content. The design of experiments is shown on Table 7.11.

Table 7.11 Design of experiments for copper addition.

RESEARCH VARIABLE	LEVELS
Copper source	Cu ₂ O, CuSO ₄ , Cu(NO ₃ ·3H ₂ O) ₂
Addition level	10 and 50 atomic percent of Na
FIXED PARAMETERS	
Curing time	24 hrs
Curing temperature	100 C
Activator solution/Fly ash ratio (AS/FA)	0.4
Silicate type	N
Fly ash:sand ratio	1:1
RESPONSE VARIABLE	
Compressive Strength	ASTM C-109
Flow	ASTM C-1437
Crystalline content (XRD)	-

7.3.2 Materials

Three sources of copper were studied, copper oxide, copper sulfate and copper nitrate. The decision to use these sources comes from literature, copper oxide was the one embedded in epoxy by Hewayde [14] and copper sulfate and nitrate were used by other authors [67, 68] to encapsulate copper in geopolymer. The results with those three sources would be interesting to be evaluated.

The amounts were decided in terms of Na⁺ cation replacement. Since the main intention was to see if copper would replace Na inside the geopolymer net, it was decided to use a quantity that would replace a certain percentage of Na ions in the geopolymer. The numbers 10% and 50% correspond to 10% and 50% in weight of Cu vs. Na.

7.3.3 Procedure

The usual procedure for mixing was used when testing for compressive strength in cubes and flow. To analyze oxides by XRD, powdered samples with no aggregate were sent to a specialized lab for quantification. The intention was to evaluate the amounts of oxide still present on its crystalline form to evaluate the degree of reaction.

7.3.4 Results

7.3.4.1 Compressive Strength

Fig. 7.5 shows the main effects plot for compressive strength. A strong influence of the copper source can be observed. As expected, the addition level also had a large effect on the compressive strength of the samples. The nitrate source contained a lot of extra bound water that could have helped decreasing the compressive strength.

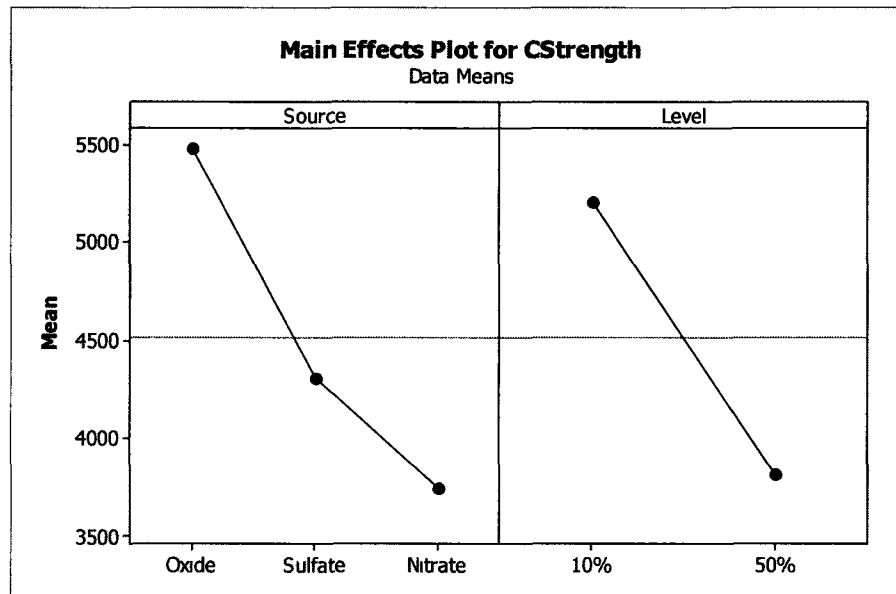


Fig. 7.5 Main effects plot for compressive strength.

It can be seen on the interaction plot (Fig. 7.6) that there is not interaction between the levels of the two variables; in all cases, a higher addition of copper source ended up in lower compressive strength.

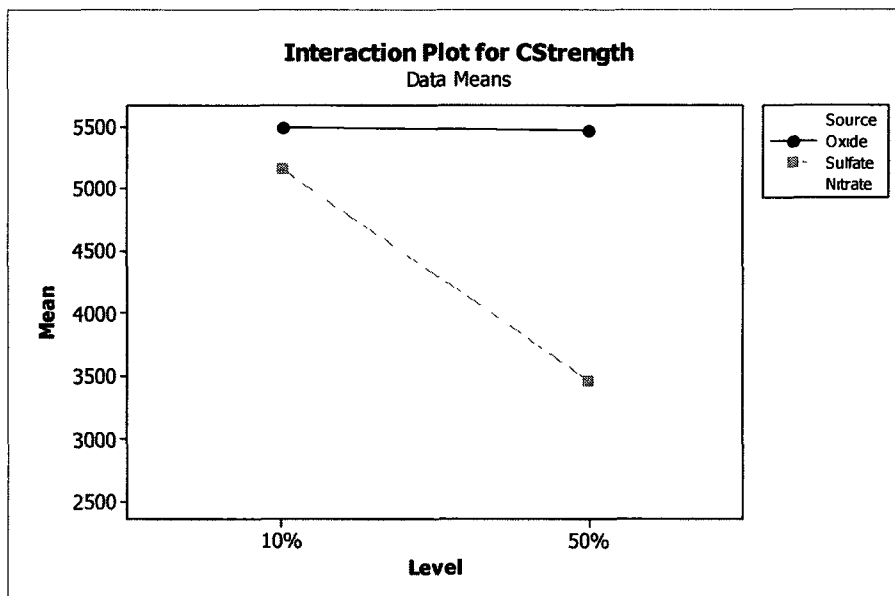


Fig. 7.6 Interaction plot for compressive strength.

7.3.4.2 Flow

Fig. 7.7 shows that the copper source had a large effect on the flow of the paste. Copper nitrate contained 3 molecules of bound water, and its dissolution could have caused the increase of flow. Also, the copper oxide was insoluble in water and made the paste thicker and less workable. The red color of the oxide could be observed while mixing. It can also be seen in the right hand side of the box that the level of addition was not a source of variation for this model. It is the presence of the copper salts and not the amount what makes the flow change significantly.

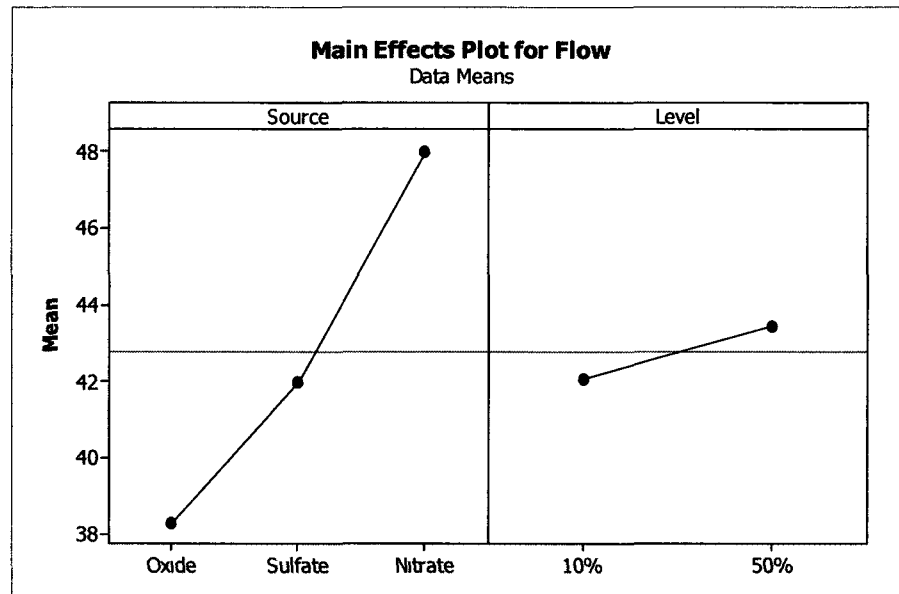


Fig. 7.7 Main effects plot for Flow.

The interaction plot (Fig. 7.8) shows that there is no significant interaction between the variables (i.e., the amount of them used affects all the variables the same way).

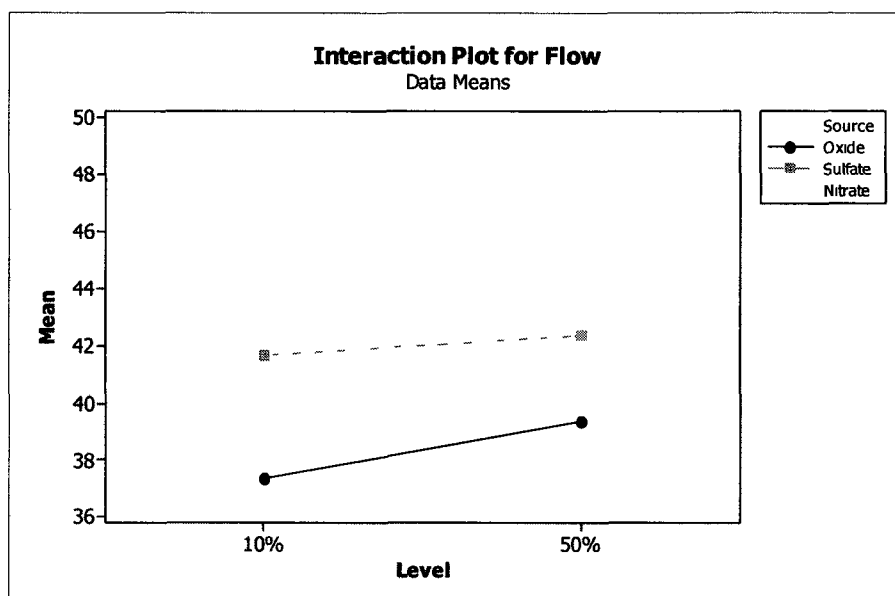


Fig. 7.8 Interaction plot for Flow.

7.3.4.3 XRD

XRD analysis was performed for all the geopolymer samples. Paste samples were prepared, then pulverized and sent to an external lab for analysis. The results are summarized in Table 7.12. The full reports are presented in Appendix G.

Table 7.12 XRD Phase content evaluation.

	10% Cu ₂ O	50% Cu ₂ O	10% CuSO ₄	50% CuSO ₄	10% Cu(NO ₃) ₂ ·3H ₂ O	50% Cu(NO ₃) ₂ ·3H ₂ O
SiO ₂ (Quartz)	4.7	4.7	4.4	5.3	4.8	4.5
(Al ₂ O ₃) _x (SiO ₂) _y (Mullite)	11.3	13.0	10.2	11.8	11.9	10.6
Fe ₂ O ₃ (Hematite)	0.3	1.3	0.1	-	0.2	0.1
Fe ₂ O ₄ (Magnetite)	0.1	0.2	0.2	0.3	0.5	-
Cu ₂ O (Cuprite)	2.7	5.7	-	3.6	-	-
Na ₂ (SO ₄) (Thenardite)	-	-	1.4	3.6	-	-
NaNO ₃ (Nitratine)	-	-	-	-	0.8	2.2
Amorphous	80.9	75.1	83.7	79.0	81.8	82.6

It can be seen on Table 7.12 that the Cu₂O remains unreacted after geopolymerization. The phase amounts presented in Table 7.12 roughly match those that

can be calculated from the amount of oxide that was added. On the other hand, the copper salts did dissolve and release copper ions, which can be proven by the absence of the crystalline phases in the XRD analysis and the presence of replaced sodium salts (sulfate and nitrate) suggesting that copper is indeed replacing sodium. To further explore these suggestions, TEM/EDS evaluations were performed on the material.

7.3.5 TEM/EDS Evaluations

It was proposed that light, scanning electron microscopy (SEM) and transmission electron microscopy (TEM) be used to determine where in the sample the copper ends. In particular, it was valuable to determine the chemical state of the copper, that is, combined with some other element or elements in a crystalline form, or was it part of the abundant amorphous geopolymer material? Electron diffraction is rarely used in these applications, though it seems likely to be extremely useful. A sample of the solid bulk material was thin-sectioned for scanning electron microscopy and energy-dispersive x-ray spectroscopy (EDS). EDS mapping proved to be especially useful.

The results from EDS analysis and TEM imaging and are presented on Figs. 7.9 and 7.10. The first spectrum corresponds to the top picture and so on and so forth. It can be seen that while little or no presence of copper can be found in the unreacted parts of the material (fly ash spheres), the amount of copper increases as the sample section becomes more amorphous, strongly indicating the presence of copper in the geopolymer section of the material. Whether copper is effectively replacing sodium as a modifying cat ion in the geopolymer net remains to be answered by a more specialized technique. However, even if the copper is entrapped interstitially, it could still have practical

applications as a bactericide, since it is not expressly required for copper to be a part of the geopolymer net to have bactericide effects.

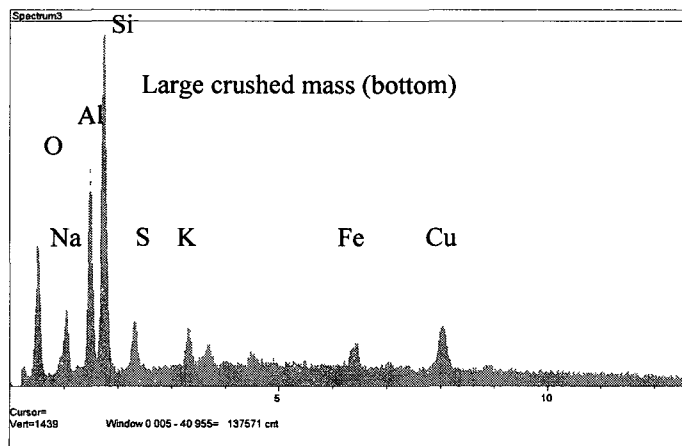
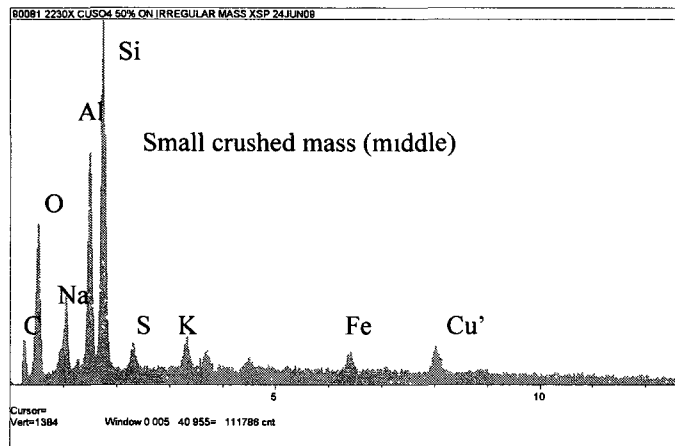
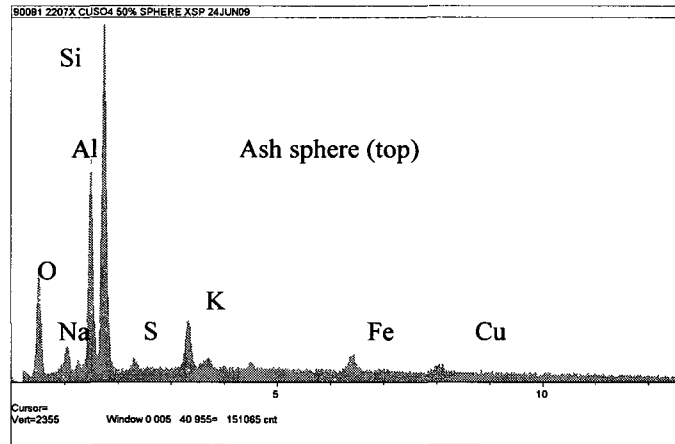


Fig. 7.9 EDS analysis of geopolymer particles.

Top

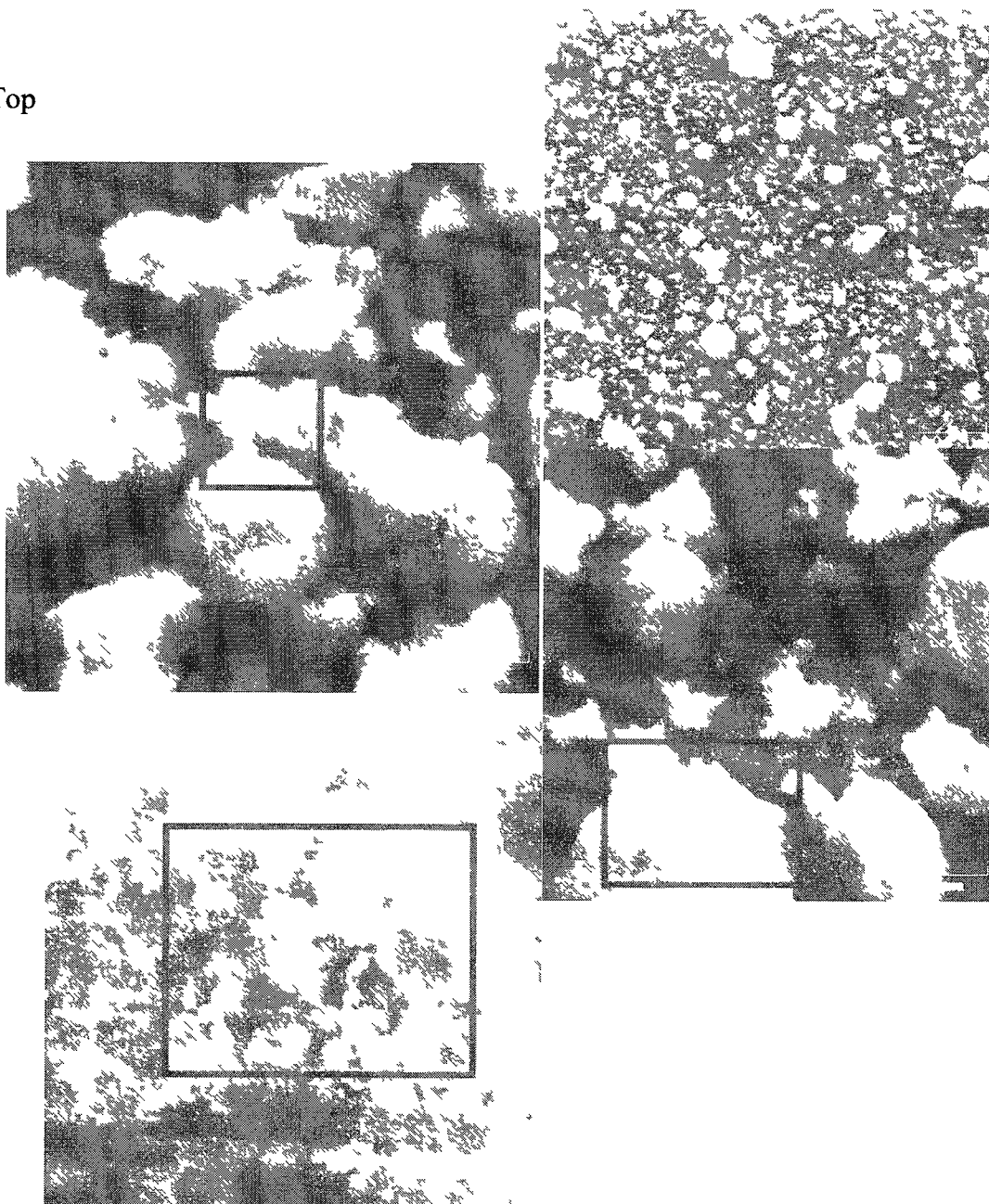


Fig. 7.10 TEM images of the geopolymer coating sample.

7.4 Commercialization Potential

A report by the USA National Innovation Marketplace, a member of Planet Eureka, showed promising commercialization potential for the present invention. With a concept score of 32 while the national average is 29, the invention has odds of selling for \$681.6 million, but could reach up to \$1.1 billion if the marketing concept is improved. The full report is shown in Appendix H.

Further, a study conducted by students from the MGMT 400 class conducted by Dr. Pratts presented a business case scenario for the invention proposed in this thesis work. They assume the USA sewer system to host a 1 million mile sewer system infrastructure. Focusing on the market for large diameter pipe (36" to 240") which size is about \$10.2 billion dollars per year, and assuming that only 3% of those will be rehabilitated per year, they consider that an initial investment of \$3.5 million would provide the investor with an IRR of 65% after year 5 [91].

7.5 General Conclusions

A full testing and characterization program of the formulation from the previous chapter is presented. The properties of the coating are satisfactory for rehabilitation projects for sewers and manholes. The addition of fibers increases the flexural strength of the coating. The Young's modulus for this material is relatively low compared to normal concretes. This characteristic might be beneficial as the coating will be less brittle and resist impact stresses better. Corrosion resistance proved to be significantly higher than that of the OPC-Silica Fume blend. Its value was slightly inferior to that of a Class F Fly ash geopolymer produced with more concentrated solutions, but it was a trade to achieve

better workability. The addition of surfactants did not reduce the coating corrosion resistance to sulfuric acid.

The volume of permeable voids and air content percentage match with the predicted value from the spec sheet of the surfactant manufacturer. The length change of bars under a sulfate solution was only around 0.11% after 15 weeks. The abrasion resistance of the coating also proved to be higher than that of Portland Cement. Bond strength had a satisfactory result of 1400 psi.

The geopolymer coating showed a thixotropic behavior, as most other geopolymeric formulations. The viscosity value can be reduced to half after 30 minutes of mixing. Rest periods of intervals of 30 minutes each showed an increase in the yield stress of the geopolymer paste. The overall value of viscosity was also increased. It is, therefore, recommended to mix and spray as promptly as possible to avoid undesirable thickening of the mix. The low surface tension of the geopolymer coating is achieved by means of the surfactant added. This low surface tension is important to achieve good efficiency while spraying. Once applied, the geopolymer coating will start setting after three hours; however, its full properties will not be achieved until the end of the curing period.

Copper addition to the geopolymer coating was tried with three sources: oxide, sulfate and a hydrated nitrate. The addition of copper is expected to produce a biocide effect on the coating. However, it also has consequences in the properties of the material. All of the sources produced a decrease in compressive strength, with copper nitrate the most significant, mostly because of the extra water included in the molecule. Copper nitrate had slight effects on flow, increasing it slightly.

XRD characterization showed that copper oxide is not dissolved nor incorporated in the geopolymer paste and remained as a crystalline oxide. The copper salts did dissolve and partially substitute sodium ions in the paste. TEM/EDS analysis revealed the presence of copper ions in the amorphous part of the material (geopolymer), but it still needs to be resolved if it is present interstitially or in chemical combination.

Several economic studies have shown a potential for the commercialization of the present invention. The USA National Innovation Marketplace provided an above average score for the invention and showed commercialization potential of \$681.6 million dollars. An internal study conducted by a class at Louisiana Tech showed that when focusing on large diameter pipes, the product could have the potential of returning 65% of revenue after year 5. All of these results are encouraging to pursue a patent request and future licensing of the product by Louisiana Tech.

CHAPTER 8

SUMMARY, CONCLUSIONS AND RECOMMENDATIONS

8.1 Summary

The growing need for rehabilitation solutions of sanitary systems is a serious concern for many municipalities across North America. Common rehabilitation options include lining with either cementitious or polymeric materials. Portland cement based concrete has limited ability to withstand acidity generated by anaerobic conditions that exist in many sewage conveyance systems over extended periods of time, while polymeric coatings are often expensive and out of the budget of cities. Geopolymers are a novel kind of cementitious material with outstanding properties, which makes them promising candidates as a new rehabilitation option. Among geopolymer's excellent properties is their high corrosion resistance to acids like sulfuric acid. However, poor workability and low setting times have shied away many contractors from utilizing them in large scale operations. Surfactants are commonly used in the construction industry in the form of air entrainers. Although the main intention for the use of these materials is to introduce small air bubbles into the concrete with the purpose of increasing freeze-thaw durability, an improvement of the workability of cements is often noticed by many concrete manufacturers. Their use in geopolymers has not been explored yet. Finally, one of the most important efforts made in the field of biogenic corrosion prevention has been

to coat the pipes with bactericide agents embedded in epoxy. Those bactericide agents are in the form of copper and silver oxide. Geopolymer's ability to encapsulate heavy metals and the toxicity of copper could be a great area of opportunity to provide the industry with an enhanced complete solution to eradicate the problem of biogenic corrosion in sewers.

The work conducted at Louisiana Tech was aimed then towards the development of a workable, sprayable geopolymer-based coating to rehabilitate sewers and manholes. The first step was to produce geopolymer in our labs and with locally available materials. Then, the main parameters of geopolymerization were investigated, with the purpose of providing with an idea of the role of the different components of geopolymerization in the final properties of the product. After this first set of tests, corrosion resistance tests were performed on geopolymers prepared from different raw materials and their durability compared to that of an enhanced OPC-Silica Fume blend. When the appropriate raw material was selected, a design of experiments was created to help on the decision making process of the optimization of the activator solution that would complete an initial geopolymer formulation for this project. The next step was to improve the workability of this geopolymer mix to enable it to be applied with currently used techniques (i.e., paddle mixing and spraying). Surfactants were then chosen as the additive to do this task. After a series of lab and field testing an optimum formulation was achieved. Then, quality tests commonly performed on coatings were also performed on this formulation and a specification sheet for the product was created. In the end, the addition of copper was evaluated. Three sources of copper were tried and the final properties evaluated in terms of compressive strength, flow and X-ray diffraction.

Different studies on the economical possibilities of this product in the market were conducted.

8.2 Conclusions

After the initial set of tests, it was concluded that geopolymers are suitable materials to replace Portland cement for spray lining applications. The main parameters that govern geopolymerization are: raw material selection, curing conditions and activator solution formulation. In general, higher curing temperature conditions provide a higher degree of geopolymerization and higher strengths. Curing times longer than 24 hours are not necessary when appropriate temperatures are used. The activator solution to fly ash ratio plays a big role in the geopolymer final properties, and it is recommended to reduce it as much as possible without impeding workability.

The raw material is the most important parameter with respect to the durability properties of geopolymer. Class C fly ash geopolymers generally have higher and earlier development of strength, while Class F fly ash geopolymer, though having lower and slower development of strength, provides better durability in terms of sulfuric acid resistance due to their lower amount of free lime. Both types of geopolymer offer better corrosion resistance than a specially formulated corrosion resistance blend of OPC-Silica Fume.

The most important factor for the design of the activator solution is the silicate type. While a more concentrated silicate (commercially named “D”) provides higher compressive strength, a less concentrated silicate (commercially named “N”) provides better workability and longer setting times. Both silicates provide similar results in terms of corrosion resistance. A secondary advantage of using a lower concentration silicate is

its price. Since this type of silicate comes right out of the primary silicate production process and does not need to be reconcentrated, it is much cheaper and more readily available than the concentrated silicate. The second most important parameter for the formulation of the activator solution is the NaOH concentration. Generally, a higher concentration provides higher strength but at the expense of loss of workability and short setting time. A concentration of 12.5 M or 50% solution was found to be the best for this application. The third parameter involved in the formulation of the activator solution was the silicate/hydroxide ratio. This value proved to be important with respect to the setting time, and a value of 1.5 was found to be optimum since a value of 1 would reduce the setting time. All of these parameters have a great impact on the viscosity of geopolymers, the most important being the sodium silicate, then the hydroxide concentration and, later, the silicate/hydroxide ratio. Geopolymers behave as thixotropic materials.

Surfactants were a great aid to solve the problem of geopolymer viscosity and workability. After a series of lab and field tests, the correct amount and type of surfactant to be used with geopolymers was found. A significant reduction in surface tension helped the material being sprayed more efficiently. A higher amount of surfactant lowered the surface tension of geopolymers while reducing their viscosity. However, a higher concentration of the surfactant used increased the viscosity slightly. This increase happens because when breaking the surface of the liquid, the surfactant impedes the flow and thereby makes it slightly more viscous. However, since the surfactant is added in a suspension form, a higher addition of surfactant also means a higher addition of water and, therefore, a reduction in viscosity.

The quality tests show that the geopolymer coating has better or the same quality than a cementitious coating in most aspects. Copper addition proved to be possible, with partial replacement of the Na ions in the geopolymer paste. The geopolymer coating has important commercial opportunities for Louisiana Tech.

8.3 Recommendations

The most important recommendation is to conduct a full scale testing of the coating under steam curing to prevent cracking. The curing performed in our tests included only temperature and, therefore, a few cracks due to the dry conditions were formed.

Although the biocide properties of copper are widely known, a series of bacterial tests with this coating formulation should be performed, to obtain a quantitative measure of their effect on bacterial growth. Important conclusions are to be drawn from this work, like modifications on the amounts of copper to be used or the benefit of one source over the other. Leaching tests are also necessary to determine geopolymer's ability in the retention of the copper ions inside the matrix.

A complete field test on an actual manhole is recommended to evaluate the behavior of the coating under real life conditions.

Optical and SEM examinations are necessary to evaluate factors like pore size distribution, phase determination, thermally-induced microcracks, etc. An NMR-MAS examination of the coating would also be wise to determine the type of geopolymer that has been produced. The examination of the thermal expansion coefficient for the coating is another important factor to make recommendations for the curing procedure.

Additionally, short curing times will be desirable for many projects. Therefore, the addition of cure-control polymer micro-capsules may be an interesting area of research. These polymer systems have already been used in construction projects with success. The incorporation of these capsules for geopolymer cure-control is definitively an area worth of investigation.

APPENDIX A
EXPERIMENTAL DETAILS FOR CHAPTER 3

A.1 Particle Size Distribution of Metakaolin

Size(μm)	Cumulative	Cumulative(%)	Histogram (%)	Normalized histogram
0.04	0.0009	0.09	0.00	0.00
0.07	0.0032	0.32	0.95	0.04
0.1	0.005	0.5	1.16	0.05
0.2	0.0124	1.24	2.46	0.10
0.3	0.0221	2.21	5.51	0.23
0.4	0.0308	3.08	6.96	0.30
0.5	0.0395	3.95	8.98	0.38
0.6	0.0504	5.04	13.77	0.59
0.7	0.0635	6.35	19.57	0.83
0.8	0.079	7.9	26.73	1.14
0.9	0.0945	9.45	30.30	1.29
1	0.1093	10.93	32.34	1.37
1.1	0.1228	12.28	32.61	1.39
1.2	0.1351	13.51	32.55	1.38
1.3	0.1465	14.65	32.79	1.39
1.4	0.157	15.7	32.62	1.39
1.6	0.1758	17.58	32.42	1.38
1.8	0.1922	19.22	32.06	1.36
2	0.2067	20.67	31.69	1.35
2.2	0.2195	21.95	30.92	1.31
2.4	0.2312	23.12	30.96	1.32
2.6	0.2424	24.24	32.22	1.37
3	0.2636	26.36	34.11	1.45
4	0.3154	31.54	41.46	1.76
5	0.3643	36.43	50.46	2.14
6	0.408	40.8	55.19	2.35
6.5	0.4279	42.79	57.25	2.43
7	0.4465	44.65	57.79	2.46
7.5	0.464	46.4	58.40	2.48
8	0.4805	48.05	58.87	2.50
8.5	0.496	49.6	58.87	2.50
9	0.5109	51.09	60.02	2.55
10	0.5386	53.86	60.54	2.57
11	0.5643	56.43	62.09	2.64
12	0.5884	58.84	63.78	2.71
13	0.6114	61.14	66.16	2.81
14	0.6334	63.34	68.36	2.91
15	0.6546	65.46	70.75	3.01
16	0.6751	67.51	73.14	3.11
17	0.6946	69.46	74.06	3.15
18	0.7132	71.32	74.93	3.18
19	0.7309	73.09	75.38	3.20
20	0.7475	74.75	74.52	3.17
22	0.7776	77.76	72.72	3.09
25	0.8149	81.49	67.19	2.86
28	0.8458	84.58	62.78	2.67
32	0.8818	88.18	62.08	2.64
36	0.913	91.3	60.99	2.59
37	0.9209	91.87	59.24	2.49

Size(μm)	Cumulative	Cumulative(%)	Histogram (%)	Normalized histogram
38	0.9267	92.67	58.34	2.48
40	0.9391	93.91	55.66	2.37
45	0.9638	96.38	48.29	2.05
50	0.9804	98.04	36.28	1.54
53	0.9872	98.72	26.87	1.14
56	0.9922	99.22	20.91	0.89
63	0.998	99.8	11.34	0.48
71	1	100	3.85	0.16
75	1	100	0.00	0.00
80	1	100	0.00	0.00
85	1	100	0.00	0.00
90	1	100	0.00	0.00
95	1	100	0.00	0.00
100	1	100	0.00	0.00
106	1	100	0.00	0.00
112	1	100	0.00	0.00
125	1	100	0.00	0.00
130	1	100	0.00	0.00
140	1	100	0.00	0.00
145	1	100	0.00	0.00
150	1	100	0.00	0.00
160	1	100	0.00	0.00
170	1	100	0.00	0.00
180	1	100	0.00	0.00
190	1	100	0.00	0.00
200	1	100	0.00	0.00
212	1	100	0.00	0.00
242	1	100	0.00	0.00
250	1	100	0.00	0.00
300	1	100	0.00	0.00
400	1	100	0.00	0.00
500	1	100	0.00	0.00
600	1	100	0.00	0.00
700	1	100	0.00	0.00
800	1	100	0.00	0.00
900	1	100	0.00	0.00
1000	1	100	0.00	0.00
1100	1	100	0.00	0.00
1200	1	100	0.00	0.00
1300	1	100	0.00	0.00
1400	1	100	0.00	0.00
1600	1	100	0.00	0.00
1700	1	100	0.00	0.00
1800	1	100	0.00	0.00
1900	1	100	0.00	0.00
2000	1	100	0.00	0.00
2100	1	100	0.00	0.00
2200	1	100	0.00	0.00
2300	1	100	0.00	0.00
2400	1	100	0.00	0.00
2500	1	100	0.00	0.00
			2353.01	100.00

A.2 Particle Size Distribution of Class F Fly Ash

Size(μm)	Cumulative	Cumulative(%)
2000	0.00	100.00
1674	0.00	100.00
1408	0.00	100.00
1184	0.00	100.00
995.5	0.00	100.00
837.1	0.00	100.00
703.9	0.00	100.00
591.9	0.00	100.00
497.8	0.00	100.00
418.6	0.00	100.00
352.0	0.00	100.00
296.0	0.00	100.00
248.9	0.00	100.00
209.3	0.00	100.00
176.0	0.00	100.00
148.0	0.00	100.00
124.4	0.00	100.00
104.6	0.18	100.00
87.99	1.45	99.82
73.99	3.65	98.37
62.22	4.90	94.72
52.32	4.67	89.82
44.00	3.83	85.15
37.00	3.93	81.32
31.11	4.63	77.39
26.16	5.54	72.76
22.00	5.38	67.22
18.50	5.72	61.84
15.55	5.85	56.12
13.08	3.67	50.27
11.00	6.05	46.60
9.25	5.38	40.55
7.78	2.67	35.17
6.54	3.79	32.50
5.50	5.40	28.71
4.62	3.55	23.31
3.89	2.80	19.76
3.27	1.74	16.96
2.750	0.90	15.22
2.312	0.46	14.32

A.3 Weight Proportions for Section 3.3.4

TEST	NAME	Ohio Fly Ash	Sand	Activator Solution	Silicate D	Silicate N	Hydroxide 14 M
1	Silicate D	1500	1500	795	477	0	318
2	Silicate N	1500	1500	795	0	477	318
3	AS/FA 0.53	1500	1500	795	477	0	318
4	AS/FA 0.82	1500	1500	1230	738	0	492
5	Sil/Hyd 1.5	1500	1500	795	477	0	318
6	Sil/Hyd 2.5	1500	1500	795	567.86	0	227.14
7	Temp 60 C	1500	1500	795	477	0	318
8	Temp 90 C	1500	1500	795	477	0	318

Weights are provided in grams.

A.4 Results for Section 3.3.4

TEST	force (lbs)			strength (psi)		
	1	2	3	1	2	3
Silicate D	37200	40200	41400	9300	10050	10350
	36800	41000	42000	9200	10250	10500
	35000	40800	41800	8750	10200	10450
AVERAGE				9083.33	10166.67	10433.33
	1	2	3	1	2	3
Silicate N	24600	25800	26000	6150	6450	6500
	23200	26800	27800	5800	6700	6950
	24800	27400	27200	6200	6850	6800
AVERAGE				6050.00	6666.67	6750.00
	force (lbs)			strength (psi)		
	1	2	3	1	2	3
Silicate D - AS/FA 0.53	38400	41400	42200	9600	10350	10550
	37600	42400	42600	9400	10600	10650
	36600	41800	42800	9150	10450	10700
AVERAGE				9383.33	10466.67	10633.33
	1	2	3	1	2	3
Silicate D - AS/FA 0.82	31800	39800	40400	7950	9950	10100
	33200	38600	39600	8300	9650	9900
	32000	40200	39200	8000	10050	9800
AVERAGE				8083.33	9883.33	9933.33
	force (lbs)			strength (psi)		
	1	2	3	1	2	3
Silicate D - Sil/Hyd 1.5	35000	40200	41000	8750	10050	10250
	35400	41000	40800	8850	10250	10200
	34800	39800	39600	8700	9950	9900
AVERAGE				8766.67	10083.33	10116.67
	1	2	3	1	2	3
Silicate D - Sil/Hyd 2.5	34600	40400	41000	8650	10100	10250
	32200	39600	40200	8050	9900	10050
	33800	40000	40400	8450	10000	10100
AVERAGE				8383.33	10000.00	10133.33

	force (lbs)			strength (psi)		
	1	2	3	1	2	3
Temperature 60 C	32200	38800	39000	8050	9700	9750
	32400	40400	38800	8100	10100	9700
	34000	37600	40200	8500	9400	10050
AVERAGE				8216.67	9733.33	9833.33
	1	2	3	1	2	3
Temperature 90 C	36400	39200	40600	9100	9800	10150
	35800	38600	40400	8950	9650	10100
	36200	40600	41000	9050	10150	10250
AVERAGE				9033.33	9866.67	10166.67

A.5 Compressive Strength Results for Section 3.3.4

TEST	NAME	AS/FA	FLY ASH TX	FLY ASH TI	FLY ASH MI	SAND	ACT SOL	SIL D	HYD 14 M
1	0.5-R-0.35-TX	0.35	500	0	0	500	175	105	70
2	0.5-60-0.45-TI	0.45	0	500	0	500	225	135	90
3	0.5-90-0.5-MI	0.5	0	0	500	500	250	150	100
4	1-R-0.35-TI	0.35	0	500	0	500	175	105	70
5	1-60-0.45-MI	0.45	0	0	500	500	225	135	90
6	1-90-0.5-TX	0.5	500	0	0	500	250	150	100
7	3-R-0.45-TX	0.35	500	0	0	500	175	105	70
8	3-60-0.5-TI	0.45	0	500	0	500	225	135	90
9	3-90-0.35-MI	0.5	0	0	500	500	250	150	100
10	6-R-0.5-MI	0.35	0	0	500	500	175	105	70
11	6-60-0.35-TX	0.45	500	0	0	500	225	135	90
12	6-90-0.45-TI	0.5	0	500	0	500	250	150	100
13	12-R-0.45-MI	0.35	0	0	500	500	175	105	70
14	12-60-0.5-TX	0.45	500	0	0	500	225	135	90
15	12-90-0.35-TI	0.5	0	500	0	500	250	150	100
16	24-R-0.5-TI	0.35	0	500	0	500	175	105	70
17	24-60-0.35-MI	0.45	0	0	500	500	225	135	90
18	24-90-0.45-TX	0.5	500	0	0	500	250	150	100

*Weights in grams.

A.6 Compressive Strength Results for Section 3.4.2

Code	Comp. Str. (24 hrs - psi)	Code	Comp Str. (24 hrs - psi)
5-R-35-TX-1	1050	6-R-50-MI-1	3850
5-R-35-TX-2	1150	6-R-50-MI-2	3850
5-R-35-TX-3	1075	6-R-50-MI-3	3650
Average	1091.67	Average	3783.33
5-60-45-TI-1	1300	6-60-35-TX-1	8000
5-60-45-TI-2	1350	6-60-35-TX-2	9375
5-60-45-TI-3	1300	6-60-35-TX-3	7950
Average	1316.67	Average	8441.67
5-90-50-MI-1	7100	6-90-45-TI-1	10350
5-90-50-MI-2	7150	6-90-45-TI-2	9750
5-90-50-MI-3	6300	6-90-45-TI-3	11750
Average	6850.00	Average	10616.67
1-R-35-TI-1	1750	12-R-45-MI-1	3450
1-R-35-TI-2	1700	12-R-45-MI-2	3150
1-R-35-TI-3	1650	12-R-45-MI-3	3550
Average	1700.00	Average	3383.33
1-60-45-MI-1	13450	12-60-50-TX-1	6250
1-60-45-MI-2	12950	12-60-50-TX-2	5200
1-60-45-MI-3	12500	12-60-50-TX-3	5850
Average	12966.67	Average	5766.67
1-90-50-TX-1	3750	12-90-35-TI-1	16200
1-90-50-TX-2	3600	12-90-35-TI-2	15950
1-90-50-TX-3	3900	12-90-35-TI-3	16750
Average	3750.00	Average	16300.00
3-R-45-TX-1	700	24-R-50-TI-1	1000
3-R-45-TX-2	800	24-R-50-TI-2	950
3-R-45-TX-3	750	24-R-50-TI-3	900
Average	750.00	Average	950.00
3-60-50-TI-1	4200	24-60-35-MI-1	8800
3-60-50-TI-2	3700	24-60-35-MI-2	10800
3-60-50-TI-3	3950	24-60-35-MI-3	12000
Average	3950.00	Average	10533.33
3-90-35-MI-1	12250	24-90-45-TX-1	9325
3-90-35-MI-2	13300	24-90-45-TX-2	9325
3-90-35-MI-3	13400	24-90-45-TX-3	9325
Average	12983.33	Average	9325

APPENDIX B

EXPERIMENTAL DETAILS FOR THE

CORROSION TESTS

B.1 Weight Proportions for Section 4.3

Material	Weight	Sand	AS/FA	Water	S. Silicate	NaOH
Cement blend						
OPC	10,000	12,500	0.35**	4375	0	0
Silica fume	2,500					
Metakaolin	7,500	7,500	1.25	0	6250	3125
Class C ash	12,500	12,500	0.35	0	2625	1750
Class F ash	1,200	1,200	0.45	0	324	216

*Weights are expressed in grams.

** Water/cement ratio

B.2 Preparation of Sulfuric Acid Solutions

		Week				
pH	Volumes (lt)	Initial	1	2	4	6
0.6	Acid (97%)	0 29193	0 24327	0 19462	0 14748	0 09731
	Water	9 14702	7 62252	6 09802	4 57199	3 04901
	Total solution	9 43895	7 86579	6 29263	4 71947	3 14632
1	Acid (97%)	0 09731	0 08109	0 06487	0 04865	0 03244
	Water	9 34164	7 78470	6 22776	4 67082	3 11388
	Total solution	9 43895	7 86579	6 29263	4 71947	3 14632
2	Acid (97%)	0 00482	0 00401	0 00321	0 00241	0 00161
	Water	9 43413	7 86178	6 28942	4 71707	3 14471
	Total solution	9 43895	7 86579	6 29263	4 71947	3 14632
3	Acid (97%)	0 44924	0 00078	0 00062	0 00047	0 00031
	Water	0 44947	7 86501	6 29201	4 71901	3 14600
	Total solution	9 43413	7 86579	6 29263	4 71947	3 14632

B.3 Mass Loss Results

MASS LOSS RESULTS (net weight)

Fly ash C		Weeks					
pH	Original mass	1	2	4	6	8	
0.6	299.93	294.83	285.80	278.07	244.33	225.93	
1	298.93	294.80	288.63	285.83	272.23	268.87	
2	287.40	282.40	279.20	275.50	277.00	273.90	
3	289.87	285.93	284.07	280.07	282.40	278.87	

Metakaolin		Weeks					
pH	Original mass	1	2	4	6	8	
0.6	234.97	191.17	167.93	152.17	140.20	128.80	
1	229.13	211.70	200.40	198.53	186.77	178.37	
2	234.70	219.40	210.17	209.63	209.53	207.40	
3	236.10	228.17	218.07	221.40	217.10	214.13	

OPC		Weeks					
pH	Original mass	1	2	4	6	8	
0.6	289.80	245.77	228.73	196.87	142.27	80.20	
1	286.27	275.00	273.70	261.97	254.57	219.10	
2	283.70	280.10	279.77	279.67	275.20	272.70	
3	284.67	282.67	282.33	282.50	278.40	277.53	

Fly ash F		Weeks					
pH	0	1	2	4	6	8	
0.6	275.50	268.20	266.00	261.70	256.82	252.73	

MASS LOSS RESULTS (%)

Fly ash Class C		Weeks					
pH	0	1	2	4	6	8	
0.6	0.00	1.70	4.71	7.29	18.54	24.67	
1	0.00	1.38	3.45	4.38	8.93	10.06	
2	0.00	1.74	2.85	4.14	3.62	4.70	
3	0.00	1.36	2.00	3.38	2.58	3.79	

Metakaolin		Weeks					
pH	0	1	2	4	6	8	
0.6	0.00	18.64	28.53	35.24	40.33	45.18	
1	0.00	7.61	12.54	13.35	18.49	22.16	
2	0.00	6.52	10.45	10.68	10.72	11.63	
3	0.00	3.36	7.64	6.23	8.05	9.30	

OPC		Weeks					
pH	0	1	2	4	6	8	
0.6	0.00	15.19	21.07	32.07	50.91	72.33	
1	0.00	3.94	4.39	8.49	11.07	23.46	
2	0.00	1.27	1.39	1.42	3.00	3.88	
3	0.00	0.70	0.82	0.76	2.20	2.51	

Fly ash F		Weeks					
pH	0	1	2	4	6	8	
0.6	0.00	2.65	3.45	5.01	6.78	8.27	

B.4 Remaining Compressive Strength Results

COMPRESSIVE STRENGTH RESULTS

Fly ash TX

pH	Initial strength	Weeks				
		1	2	4	6	8
0.6	10550	8733.33	9116.67	5750.00	3683.33	2716.67
1	10550	10466.67	10234.00	8866.67	8383.33	6766.67
2	10550	10716.67	9750.00	9950.00	8866.67	9001.00
3	10550	11000.00	11200.00	10150.00	9233.33	9150.00

Metakaolin

pH	Initial strength	Weeks				
		1	2	4	6	8
0.6	7766.67	3916.67	2950.00	2033.33	866.67	333.33
1	7766.67	4600.00	5433.33	3783.33	3700.00	3500.00
2	7766.67	6550.00	6100.00	6049.00	6200.00	6250.00
3	7766.67	6983.33	7700.00	7300.00	7333.33	7400.00

OPC

pH	Initial strength (7D)	Weeks				
		1	2	4	6	8
0.6	7000	4250.00	3333.33	1316.67	1050.00	816.67
1	7000	6266.67	3916.67	3883.33	2966.67	2516.67
2	7000	6383.33	5566.67	5416.67	4700.00	4116.67
3	7000	6816.67	6683.33	6666.67	6108.33	5433.33

Fly ash OH

pH	0	Weeks				
		1	2	4	6	8
0.6	6750	6600	6450	6293.02	6174.9	6089.85

COMPRESSIVE STRENGTH RESULTS (%)

Fly ash TX

pH	0	Weeks				
		1	2	4	6	8
0.6	100	82.78	86.41	54.50	34.91	25.75
1	100	99.21	97.00	84.04	79.46	64.14
2	100	101.58	92.42	94.31	84.04	85.32
3	100	104.27	106.16	96.21	87.52	86.73

Metakaolin

pH	0	Weeks				
		1	2	4	6	8
0.6	100	50.43	37.98	26.18	11.16	4.29
1	100	59.23	69.96	48.71	47.64	45.06
2	100	84.33	78.54	77.88	79.83	80.47
3	100	89.91	99.14	93.99	94.42	95.28

OPC

pH	0	Weeks				
		1	2	4	6	8
0.6	100	60.71	47.62	18.81	15.00	11.67
1	100	89.52	55.95	55.48	42.38	35.95
2	100	91.19	79.52	77.38	67.14	58.81
3	100	97.38	95.48	95.24	87.26	77.62

Fly ash OH

pH	0	Weeks				
		1	2	4	6	8
0.6	100.00	97.78	95.56	93.23	91.48	90.22

APPENDIX C

**SOFTWARE OUTPUT AND EXPERIMENTAL
RESULTS FOR CHAPTER 5**

C.1 MINITAB Experimental Setup

Multilevel Factorial Design

Factors: 3 Replicates: 3
 Base runs: 27 Total runs: 81
 Base blocks: 1 Total blocks: 1
 Number of levels: 3, 3, 3

General Linear Model: Compressive versus Silicate typ, Hydroxide mo, ...

Factor	Type	Levels	Values
Silicate type	fixed	3	D, N, Star
Hydroxide molarity	fixed	3	6, 10, 14
Silicate/Hydroxide	fixed	3	1, 2, 3

Response variables

Compressive strength
 Remaining compressive strength
 Mass loss
 Flow

C.2 MINITAB Output for Compressive Strength

Analysis of Variance for Compressive strength, using Adjusted SS for Tests

Source	DF	Seq SS	Adj SS	Adj MS	F
Silicate type	2	187248657	187248657	93624329	427.41
Hydroxide molarity	2	40706991	40706991	20353495	92.92
Silicate/Hydroxide	2	6175417	6175417	3087708	14.10
Silicate type*Hydroxide molarity	4	8563519	8563519	2140880	9.77
Silicate type*Silicate/Hydroxide	4	31254259	31254259	7813565	35.67
Hydroxide molarity* Silicate/Hydroxide	4	1024815	1024815	256204	1.17
Silicate type*Hydroxide molarity* Silicate/Hydroxide	8	22585093	22585093	2823137	12.89
Error	54	11828750	11828750	219051	
Total	80	309387500			

Source	P
Silicate type	0.000
Hydroxide molarity	0.000
Silicate/Hydroxide	0.000
Silicate type*Hydroxide molarity	0.000
Silicate type*Silicate/Hydroxide	0.000
Hydroxide molarity* Silicate/Hydroxide	0.334
Silicate type*Hydroxide molarity* Silicate/Hydroxide	0.000
Error	
Total	

C.3 R Output for Compressive Strength

Contrasts for the three levels of silicate type

```
fit.contrast(fact3, Sil, c(1,-1,0))
```

	Estimate	Std. Error	t value	Pr(> t)
Design c=(1 -1 0)	-175.25	21.26976	-8.239396	0.0001726944

```
fit.contrast(fact3, Sil, c(1,0,-1))
```

	Estimate	Std. Error	t value	Pr(> t)
Sil c=(1 0 -1)	3416.667	382.1439	8.940786	3.082991e-12

```
fit.contrast(fact3, Sil, c(0,1,-1))
```

	Estimate	Std. Error	t value	Pr(> t)
Sil c=(0 1 -1)	33.33333	382.1439	0.08722718	0.9308136

Contrasts for the three levels of hydroxide molarity

```
fit.contrast(fact3, Mol, c(1,-1,0))
```

	Estimate	Std. Error	t value	Pr(> t)
Mol c=(1 -1 0)	-866.6667	382.1439	-2.267907	0.02735857

```
fit.contrast(fact3, Mol, c(1,0,-1))
```

	Estimate	Std. Error	t value	Pr(> t)
Mol c=(1 0 -1)	-2433.333	382.1439	-6.367584	4.365507e-08

```
fit.contrast(fact3, Mol, c(0,1,-1))
```

	Estimate	Std. Error	t value	Pr(> t)
Mol c=(0 1 -1)	-1566.667	382.1439	-4.099677	0.0001400809

Contrasts for the three levels of silicate/hydroxide ratio.

```
fit.contrast(fact3, Ratio, c(1,-1,0))
```

	Estimate	Std. Error	t value	Pr(> t)
Ratio c=(1 -1 0)	950	382.1439	2.485975	0.01604577

```
fit.contrast(fact3, Ratio, c(1,0,-1))
```

	Estimate	Std. Error	t value	Pr(> t)
Ratio c=(1 0 -1)	283.3333	382.1439	0.741431	0.4616446

```
fit.contrast(fact3, Ratio, c(0,1,-1))
```

	Estimate	Std. Error	t value	Pr(> t)
Ratio c=(0 1 -1)	-666.6667	382.1439	-1.744544	0.08675387

C.4 MINITAB Output for Remaining Compressive Strength

Analysis of Variance for Residual compressive strength, using Adjusted SS for Tests

Analysis of Variance for Remain. Comp. Str. (%), using Adjusted SS for Tests

Source	DF	Seq SS	Adj SS	Adj MS	F	P
Silicate type	2	4402.39	4402.39	2201.20	29.85	0.000
Hydroxide conc	2	1121.13	1121.13	560.56	7.60	0.002
Silicate/Hydroxide	2	505.24	505.24	252.62	3.43	0.047
Silicate type*Hydroxide conc	4	1952.52	1952.52	488.13	6.62	0.001
Silicate type*Silicate/Hydroxide	4	1685.05	1685.05	421.26	5.71	0.002
Hydroxide conc*Silicate/Hydroxide	4	2997.64	2997.64	749.41	10.16	0.000
Silicate type*Hydroxide conc* Silicate/Hydroxide	8	2248.28	2248.28	281.03	3.81	0.004
Error	27	1991.09	1991.09	73.74		
Total	53	16903.33				

S = 8.58743 R-Sq = 88.22% R-Sq(adj) = 76.88%

C.5 R Output for Remaining Compressive Strength

Contrasts for the three levels of silicate type.

```
fit.contrast(fact3, Sil, c(1,-1,0))
      Estimate Std. Error t value Pr(>|t|)
Sil c=( 1 -1 0 )   11.625   8.587433  1.353722 0.1870493
fit.contrast(fact3, Sil, c(1,0,-1))
      Estimate Std. Error t value Pr(>|t|)
Sil c=( 1 0 -1 )   31.745   8.587433  3.696681 0.000981703
fit.contrast(fact3, Sil, c(0,1,-1))
      Estimate Std. Error t value Pr(>|t|)
Sil c=( 0 1 -1 )    20.12   8.587433  2.342959 0.02674986
```

Contrasts for the three levels of hydroxide concentration.

```
fit.contrast(fact3, Mol, c(1,-1,0))
      Estimate Std. Error t value Pr(>|t|)
Mol c=( 1 -1 0 )   -4.075   8.587433 -0.4745306 0.6389372
fit.contrast(fact3, Mol, c(1,0,-1))
      Estimate Std. Error t value Pr(>|t|)
Mol c=( 1 0 -1 )  -10.88   8.587433 -1.266968 0.2159869
fit.contrast(fact3, Mol, c(0,1,-1))
      Estimate Std. Error t value Pr(>|t|)
Mol c=( 0 1 -1 )   -6.805   8.587433 -0.792437 0.4350138
```

Contrasts for the three levels of silicate/hydroxide ratio.

```
fit.contrast(fact3, Ratio, c(1,-1, 0))
      Estimate Std. Error t value Pr(>|t|)
Ratio c=( 1 -1 0 )  -2.795   8.587433 -0.3254756 0.74733
fit.contrast(fact3, Ratio, c(1,0,-1))
      Estimate Std. Error t value Pr(>|t|)
Ratio c=( 1 0 -1 ) -18.555   8.587433 -2.160716 0.0397543
fit.contrast(fact3, Ratio, c(0,1,-1))
      Estimate Std. Error t value Pr(>|t|)
Ratio c=( 0 1 -1 ) -15.76   8.587433 -1.83524 0.07750954
```

C.6 MINITAB Output for Mass Loss

Analysis of Variance for Mass loss, using Adjusted SS for Tests

Analysis of Variance for Mass loss (%), using Adjusted SS for Tests

Source	DF	Seq SS	Adj SS	Adj MS	F	P
Silicate type	2	268.953	268.953	134.477	306.54	0.000
Hydroxide conc	2	27.245	27.245	13.623	31.05	0.000
Silicate/Hydroxide	2	2.316	2.316	1.158	2.64	0.090
Silicate type*Hydroxide conc	4	13.794	13.794	3.448	7.86	0.000
Silicate type*Silicate/Hydroxide	4	20.847	20.847	5.212	11.88	0.000
Hydroxide conc*Silicate/Hydroxide	4	17.314	17.314	4.329	9.87	0.000
Silicate type*Hydroxide conc* Silicate/Hydroxide	8	32.465	32.465	4.058	9.25	0.000
Error	27	11.845	11.845	0.439		
Total	53	394.779				

S = 0.662343 R-Sq = 97.00% R-Sq(adj) = 94.11%

C.7. R Output for Remaining Mass Loss

Contrasts for the three levels of silicate type.

```
fit.contrast(fact3, Sil, c(1,-1,0))
      Estimate Std. Error  t value Pr(>|t|)
Sil c=( 1 -1 0 )   -0.955  0.6623429 -1.441851 0.1608440
fit.contrast(fact3, Sil, c(1,0,-1))
      Estimate Std. Error  t value Pr(>|t|)
Sil c=( 1 0 -1 )   -7.165  0.6623429 -10.81766 2.561866e-11
fit.contrast(fact3, Sil, c(0,1,-1))
      Estimate Std. Error  t value Pr(>|t|)
Sil c=( 0 1 -1 )    -6.21  0.6623429 -9.375808 5.555252e-10
```

Contrasts for the three levels of hydroxide molarity.

```
fit.contrast(fact3, Mol, c(1,-1,0))
      Estimate Std. Error  t value Pr(>|t|)
Mol c=( 1 -1 0 )    -2.17  0.6623429 -3.276248 0.002888962
fit.contrast(fact3, Mol, c(1,0,-1))
      Estimate Std. Error  t value Pr(>|t|)
Mol c=( 1 0 -1 )    -2.205  0.6623429 -3.329091 0.002527461
fit.contrast(fact3, Mol, c(0,1,-1))
      Estimate Std. Error  t value Pr(>|t|)
Mol c=( 0 1 -1 )   -0.035  0.6623429 -0.05284272 0.9582463
```

C.8 Minitab Output For Flow

Analysis of Variance for Flow, using Adjusted SS for Tests

Analysis of Variance for Mass loss (%), using Adjusted SS for Tests

Source	DF	Seq SS	Adj SS	Adj MS	F	P
Silicate type	2	14814.9	14814.9	7407.4	754.01	0.000
Hydroxide conc	2	16020.0	16020.0	8010.0	815.34	0.000
Silicate/Hydroxide	2	2104.7	2104.7	1052.4	107.12	0.000
Silicate type*Hydroxide conc	4	61.0	61.0	15.2	1.55	0.216
Silicate type*Silicate/Hydroxide	4	1284.3	1284.3	321.1	32.68	0.000
Hydroxide conc*Silicate/Hydroxide	4	2525.6	2525.6	631.4	64.27	0.000
Silicate type*Hydroxide conc* Silicate/Hydroxide	8	614.6	614.6	76.8	7.82	0.000
Error	27	265.3	265.3	9.8		
Total	53	37690.3				

S = 3.13434 R-Sq = 99.30% R-Sq(adj) = 98.62%

C.9 R Output For Flow

Contrasts for the three levels of silicate type.

```
fit.contrast(fact3, Sil, c(1,-1,0))
      Estimate Std. Error  t value    Pr(>|t|)
Sil c=( 1 -1 0 )   -23.75   5.691937 -4.172569 0.0002799551
fit.contrast(fact3, Sil, c(1,0,-1))
      Estimate Std. Error  t value    Pr(>|t|)
Sil c=( 1 0 -1 )   -21.75   5.691937 -3.821195 0.0007089056
fit.contrast(fact3, Sil, c(0,1,-1))
      Estimate Std. Error  t value    Pr(>|t|)
Sil c=( 0 1 -1 )     2     5.691937 0.3513742 0.7280349
```

Contrasts for the three levels of hydroxide molarity.

```
fit.contrast(fact3, Mol, c(1,-1,0))
      Estimate Std. Error  t value    Pr(>|t|)
Mol c=( 1 -1 0 )    34.5   5.691937 6.061205 1.800809e-06
fit.contrast(fact3, Mol, c(1,0,-1))
      Estimate Std. Error  t value    Pr(>|t|)
Mol c=( 1 0 -1 )    53.25   5.691937 9.355339 5.814386e-10
fit.contrast(fact3, Mol, c(0,1,-1))
      Estimate Std. Error  t value    Pr(>|t|)
Mol c=( 0 1 -1 )    18.75   5.691937 3.294133 0.002761360
```

Contrasts for the three levels of silicate/hydroxide ratio.

```
fit.contrast(fact3, Ratio, c(1,-1, 0))
      Estimate Std. Error  t value    Pr(>|t|)
Ratio c=( 1 -1 0 )   20.5   5.691937 3.601586 0.001256791
fit.contrast(fact3, Ratio, c(1,0,-1))
      Estimate Std. Error  t value    Pr(>|t|)
Ratio c=( 1 0 -1 )   56     5.691937 9.838478 2.011232e-10
fit.contrast(fact3, Ratio, c(0,1,-1))
      Estimate Std. Error  t value    Pr(>|t|)
Ratio c=( 0 1 -1 )   35.5   5.691937 6.236893 1.136051e-06
```

C.10 Weights For Section 5.4

Silicate	Hydroxide	Silicate/Hydroxide	Fly ash (g)	Molds	Silicate	Hydroxide
N	10	1	400	3	270	270 00
D	10	1	400	3	270	270 00
N	6	2	400	3	360	180 00
N	14	3	400	3	405	135 00
D	10	3	400	3	405	135.00
D	6	3	400	3	405	135 00
Star	14	3	400	3	405	135.00
N	10	2	400	3	360	180 00
Star	10	3	400	3	405	135 00
N	6	1	400	3	270	270.00
D	14	1	400	3	270	270 00
D	6	1	400	3	270	270 00
Star	14	1	400	3	270	270.00
N	14	2	400	3	360	180 00
Star	10	2	400	3	360	180 00
N	10	3	400	3	405	135 00
Star	6	3	400	3	405	135 00
Star	6	2	400	3	360	180 00
Star	10	1	400	3	270	270 00
D	14	3	400	3	405	135 00
Star	14	2	400	3	360	180 00
D	10	2	400	3	360	180 00
D	6	2	400	3	360	180 00
Star	6	1	400	3	270	270 00
N	6	3	400	3	405	135 00
N	14	1	400	3	270	270 00
D	14	2	400	3	360	180 00

C.11 Compressive Strength Results

FORMULATION	C. Strength (%)	FORMULATION	C. Strength (%)
D-14-2	6750	N-6-3	650
D-14-1	9250	N-14-3	3750
D-6-1	5700	D-14-1	7200
Star-14-3	4950	N-10-2	3150
N-14-3	4200	D-10-3	6750
N-14-2	3050	Star-10-1	3400
Star-6-3	2750	D-6-2	4850
Star-14-1	1750	D-14-3	6100
D-14-2	5300	Star-14-1	1750
D-6-3	5900	D-14-3	4950
Star-6-1	2650	N-6-1	2700
Star-14-2	4450	N-6-1	2450
D-10-2	6900	N-14-1	5750
D-6-3	4900	D-10-3	7200
N-10-1	5000	D-10-1	6150
N-6-3	550	N-6-2	2600
D-10-1	6800	N-10-3	1650
N-6-2	2450	N-14-2	4200
N-10-1	4600	N-14-1	6400
N-10-2	3100	Star-6-2	2500
D-14-3	6600	Star-14-1	1825
D-14-2	7000	N-10-3	2000
D-14-1	8600	D-6-1	5900
D-10-2	5500	Star-6-1	2450
Star-6-2	2750	N-14-1	5950
D-10-1	7150	Star-10-1	3500
Star-10-3	3550	Star-10-2	2550
D-6-2	5050	Star-6-1	2400
Star-14-3	5150	N-14-3	4100
Star-10-2	2700	Star-14-2	3850
Star-10-3	3550	Star-6-3	2650
N-10-3	1750	N-10-1	5000
D-10-3	7350	Star-14-2	4150
D-6-2	5000	D-10-1	6400
Star-10-1	2450	Star-10-2	3050
N-6-3	650	N-14-2	3900
D-6-3	6100	Star-6-3	2700
N-10-2	3250	N-6-2	2450
D-10-2	7800	N-6-1	2450
Star-10-3	3550	Star-14-3	5050
Star-6-2	2400		

C.12 Remaining Compressive Strength, Mass Loss And Flow Results

FORMULATION	Remain. Comp. Str. (%)	Mass loss (%)	Flow
D-10-2	89 85	10 94	52
D-10-2	77 97	10 06	51 5
Star-14-3	81 19	12 56	76 5
Star-6-3	53 7	15 17	101 5
Star-10-2	88 55	13 85	98
D-10-1	84 77	11 02	67
Star-14-1	76 06	11 83	68
N-14-1	61 88	9 47	66 5
D-6-3	94.08	8 12	46
N-14-3	78 42	11 68	71
Star-10-3	67 61	14 51	90
D-14-2	98 43	6.35	28
N-6-2	56	11 68	117 5
Star-14-1	98 59	11 24	65 5
D-14-1	96 88	8 89	26 5
N-6-2	48	11 16	117
D-6-2	74 5	10 14	79 5
D-14-1	85 63	11 09	46 5
D-6-1	80 28	9 18	99 5
N-6-1	65 13	9 25	122
Star-10-2	83 13	12 96	91 5
N-10-2	58 33	12 74	94
Star-10-1	80 21	16 97	96 5
N-10-3	63 89	12 08	102 5
Star-14-3	74 26	11 75	77

FORMULATION	Remain. Comp. Str. (%)	Mass loss (%)	Flow
N-10-2	82 11	11 75	84
D-6-3	98 52	6 94	44 5
N-14-2	65 92	8 96	67
D-14-1	91 62	9 84	49 5
N-10-1	70 89	12 01	91 5
Star-6-1	50	15 46	122
D-10-1	78 87	9 84	66 5
D-6-1	75 21	7 34	103
N-14-1	76 24	11 86	65
N-6-1	67 11	9 18	128
N-10-1	77 05	11 27	83 5
N-14-1	66 3	10 47	60 5
N-6-3	113 51	13 73	84 5
D-14-2	114 17	5 55	32 5
Star-6-3	55 56	14 43	105
Star-6-2	54 9	16 01	108 5
D-6-2	86 58	8 52	82
D-14-3	96.03	7 64	28
Star-14-2	75 9	13 51	69
D-10-3	104 23	7 97	46
D-10-3	70 42	7 09	51
N-12-2	72 63	11 16	89
Star-10-3	42 25	13 85	92
Star-6-1	42	15 39	124
Star-6-2	56 86	15 72	108 5
Star-10-1	60 96	16 31	104
Star-14-2	67 47	13 29	65 5
N-14-3	84 65	10 65	62 5
N-6-3	121 62	12 56	89 5

APPENDIX D

SOFTWARE OUTPUT AND EXPERIMENTAL

RESULTS FOR CHAPTER 6

D.1 Weights for Section 6.3.1

FORMULATION	FLY ASH (g)	S. SILICATE (g)	NA OH (g)
N-6-1	400	80	80.00
N-6-1.5	400	96	64.00
N-6-2	400	106.67	53.33
N-8-1	400	114.29	45.71
N-8-1.5	400	120	40.00
N-8-2	400	124.44	35.56
N-10-1	400	128	32.00
N-10-1.5	400	130.91	29.09
N-10-2	400	133.33	26.67
N-12-1	400	135.38	24.62
N-12-1.5	400	137.14	22.86
N-12-2	400	138.67	21.33
N-12-1	400	140	20.00
N-12-1.5	400	141.18	18.82
N-12-2	400	142.22	17.78

D.2 Viscosity Results for 6.3.4

NaOH Conc	Sil/Hyd	Viscosity after 30 min
12	1	15750
14	1.5	24150
8	2	5600
10	1	6400
12	2	11500
14	2	19550
14	1	30500
10	2	6600
8	1	4400
12	1.5	7800
12	2	12200
6	2	6200
6	1	3500
10	1.5	6150
10	1	6250
10	1.5	6000
14	1	28400
6	1	3250
8	1	4500
8	1.5	4650
6	1.5	3850
14	1.5	26200
12	1.5	10000
8	2	5200
6	2	3900
6	1.5	3700
14	2	20000
10	2	6600
12	1	16280
8	1.5	4650

D.3 ANOVA Table from MINITAB

Multilevel Factorial Design

Factors: 2 Replicates: 2
 Base runs: 15 Total runs: 30
 Base blocks: 1 Total blocks: 1

Number of levels: 5, 3

General Linear Model: Viscosity versus NaOH Conc, Sil/Hyd

Factor	Type	Levels	Values
NaOH Conc	fixed	5	6, 8, 10, 12, 14
Sil/Hyd	fixed	3	1.0, 1.5, 2.0

Analysis of Variance for Viscosity, using Adjusted SS for Tests

Source	DF	Seq SS	Adj SS	Adj MS	F	P
NaOH Conc	4	1790526387	1790526387	447631597	670.91	0.000
Sil/Hyd	2	32210027	32210027	16105013	24.14	0.000
NaOH Conc*Sil/Hyd	8	117272773	117272773	14659097	21.97	0.000
Error	15	10007950	10007950	667197		
Total	29	1950017137				

S = 816.821 R-Sq = 99.49% R-Sq(adj) = 99.01%

D.4 MINITAB Input And Outputs For Section 6.5.4

Surfactant type	Addition level	Conc.	Comp. St.	Flow	Viscosity
SLS	0.25	20	4668	46.5	30650
AP	1.25	20	4283	74	19800
SLS	0.75	10	5313	45	22850
SLS	1.25	10	5166	38.5	22750
AP	1.75	10	5650	56	16750
SLS	0.75	20	3809	41	27300
AP	1.25	20	3795	70	19600
AP	1.75	30	4904	50.5	20600
SLS	0.25	30	4876	48	27700
SLS	1.75	10	4665	47.5	21400
SLS	1.75	30	4002	52	23050
SLS	0.25	10	5151	53	28600
SLS	0.75	20	4317	44	26800
SLS	1.25	10	5040	41	21250
SLS	1.75	20	4222	52	19450
SLS	0.75	30	4600	35	38200
AP	1.25	20	4821	76	20000
SLS	1.75	10	4779	46	20600
AP	0.25	30	6793	69.5	32000
SLS	1.25	10	5026	39	23000
SLS	0.25	30	5270	48	27800
AP	1.25	30	6191	65	21000
AP	0.75	30	6284	66	24900
AP	1.25	10	6016	73.5	19850
AP	0.25	20	6887	68	24650
AP	0.75	10	6439	51	23200
SLS	1.25	30	3975	42.5	31400
SLS	0.75	30	4412	38	35600
AP	0.75	10	6354	55	23800
AP	0.25	10	7118	64	24000
SLS	0.75	30	4721	35	38900
AP	0.25	10	7229	62	23500
SLS	0.25	20	4742	48	31200
AP	1.75	20	5162	53	17350
AP	0.25	20	6835	68	25800
SLS	0.25	20	4635	44	30000

Surfactant type	Addition level	Concentration	Compressive strenght	Flow	Viscosity
SLS	1.25	30	4339	40	30200
AP	0.75	20	6165	58	23200
SLS	0.25	10	5165	53	28800
SLS	1.75	30	3805	50	22050
SLS	1.75	30	3952	56	23550
AP	0.75	20	5699	60	23200
AP	1.25	10	5797	75.5	20200
SLS	1.25	30	4065	46	32650
AP	1.75	30	4834	50	21000
AP	1.75	10	5656	58	15800
SLS	0.75	10	4972	47	21000
AP	1.25	10	4897	80	21000
AP	1.75	30	4960	48.5	21350
AP	1.25	30	5993	70	20800
AP	0.75	30	6104	66	25350
SLS	1.75	10	4721	48	22000
AP	0.75	30	5591	68	23900
AP	0.75	10	6448	55	21000
AP	0.25	20	7006	68	23800
SLS	0.25	10	4845	52	29450
AP	0.25	30	7243	70	31500
SLS	0.75	10	4506	50	20500
AP	0.25	10	6985	66	25400
SLS	1.25	20	4520	47	26000
AP	1.75	10	6061	62	17700
AP	0.25	30	7127	71	30800
AP	1.25	30	5570	68	22350
SLS	0.25	30	5173	50	25000
SLS	1.25	20	4148	48	25600
AP	0.75	20	6162	56	23800
AP	1.75	20	5143	53	18800
AP	1.75	20	5356	55.5	19200
SLS	1.75	20	4301	50	20200
SLS	1.75	20	4201	52	18600
SLS	1.25	20	4478	44	24800
SLS	0.75	20	4973	45	25800

D.5 ANOVA Tables from MINITAB

Multilevel Factorial Design

Factors: 3 Replicates: 3
 Base runs: 24 Total runs: 72
 Base blocks: 1 Total blocks: 1

Number of levels: 2, 4, 3

Analysis of Variance for Compressive strenght, using Adjusted SS for Tests

Source	DF	Seq SS	Adj SS	Adj MS	F
Surfactant type	1	32006667	32006667	32006667	432.32
Addition level	3	15974964	15974964	5324988	71.92
Concentration	2	4050950	4050950	2025475	27.36
Surfactant type*Addition level	3	4729480	4729480	1576493	21.29
Surfactant type*Concentration	2	381575	381575	190788	2.58
Addition level*Concentration	6	2293054	2293054	382176	5.16
Surfactant type*Addition level* Concentration	6	2491448	2491448	415241	5.61
Error	48	3553705	3553705	74036	
Total	71	65481844			

Source	P
Surfactant type	0.000
Addition level	0.000
Concentration	0.000
Surfactant type*Addition level	0.000
Surfactant type*Concentration	0.086
Addition level*Concentration	0.000
Surfactant type*Addition level* Concentration	0.000
Error	
Total	

S = 272.095 R-Sq = 94.57% R-Sq(adj) = 91.97%

Unusual Observations for Compressive strenght

Obs	Compressive strenght	Fit	SE Fit	Residual	St Resid
6	3809.00	4366.33	157.09	-557.33	-2.51 R
7	3795.00	4299.67	157.09	-504.67	-2.27 R
17	4821.00	4299.67	157.09	521.33	2.35 R
24	6016.00	5570.00	157.09	446.00	2.01 R
48	4897.00	5570.00	157.09	-673.00	-3.03 R
72	4973.00	4366.33	157.09	606.67	2.73 R

R denotes an observation with a large standardized residual.

Analysis of Variance for Flow, using Adjusted SS for Tests

Source	DF	Seq SS	Adj SS	Adj MS	F	P
Surfactant type	1	5304.50	5304.50	5304.50	1262.56	0.000
Addition level	3	768.28	768.28	256.09	60.95	0.000
Concentration	2	7.75	7.75	3.87	0.92	0.405
Surfactant type*Addition level	3	1515.83	1515.83	505.28	120.26	0.000
Surfactant type*Concentration	2	16.00	16.00	8.00	1.90	0.160
Addition level*Concentration	6	84.89	84.89	14.15	3.37	0.008
Surfactant type*Addition level* Concentration	6	833.08	833.08	138.85	33.05	0.000
Error	48	201.67	201.67	4.20		
Total	71	8732.00				

S = 2.04973 R-Sq = 97.69% R-Sq(adj) = 96.58%

Unusual Observations for Flow

Obs	Flow	Fit	SE Fit	Residual	St Resid
48	80.0000	76.3333	1.1834	3.6667	2.19 R

R denotes an observation with a large standardized residual.

Analysis of Variance for Viscosity, using Adjusted SS for Tests

Source	DF	Seq SS	Adj SS	Adj MS	F
Surfactant type	1	263542535	263542535	263542535	301.44
Addition level	3	629047049	629047049	209682350	239.84
Concentration	2	307300069	307300069	153650035	175.75
Surfactant type*Addition level	3	48571215	48571215	16190405	18.52
Surfactant type*Concentration	2	19546736	19546736	9773368	11.18
Addition level*Concentration	6	86909931	86909931	14484988	16.57
Surfactant type*Addition level* Concentration	6	293121597	293121597	48853600	55.88
Error	48	41965000	41965000	874271	
Total	71	1690004132			

Source	P
Surfactant type	0.000
Addition level	0.000
Concentration	0.000
Surfactant type*Addition level	0.000
Surfactant type*Concentration	0.000
Addition level*Concentration	0.000
Surfactant type*Addition level* Concentration	0.000
Error	
Total	

S = 935.025 R-Sq = 97.52% R-Sq(adj) = 96.33%

Unusual Observations for Viscosity

Obs	Viscosity	Fit	SE Fit	Residual	St Resid
28	35600.0	37566.7	539.8	-1966.7	-2.58 R
54	21000.0	22666.7	539.8	-1666.7	-2.18 R
64	25000.0	26833.3	539.8	-1833.3	-2.40 R

R denotes an observation with a large standardized residual.

D.6 MINITAB Input and Outputs for Section 6.5.4.4

Addition level	Concentration	Surface tension
1.75	10	62.57
0.25	20	99.65
1.25	20	51.32
0.75	10	101.2
0.25	10	104.08
1.75	30	44.81
0.25	10	104.06
1.25	10	85.43
0.25	30	90.42
0.75	30	49.53
1.75	20	47.43
1.25	30	48.06
0.75	20	56.88
0.75	30	51.88
1.75	20	49.51
0.25	10	106.02
1.75	20	46.03
0.25	30	114.25
1.25	30	50.42
0.25	30	106.53
0.75	20	59.89
0.25	20	101.55
1.25	20	44.06
1.75	10	75.57
0.75	10	107.72
1.75	10	72.49
0.25	20	113.24
0.75	20	71.19
0.75	30	46.22
1.75	30	48.93
0.75	10	97.33
1.25	10	88.73
1.25	20	48.58
1.75	30	44.83
1.25	30	48.16
1.25	10	99.41

D.7 ANOVA Table for Surfactant Addition

Multilevel Factorial Design

Factors: 2 Replicates: 3
 Base runs: 12 Total runs: 36
 Base blocks: 1 Total blocks: 1

Number of levels: 4, 3

General Linear Model: Surface tens versus Addition lev, Concentratio

Factor	Type	Levels	Values
Addition level	fixed	4	0.25, 0.75, 1.25, 1.75
Concentration	fixed	3	10, 20, 30

Analysis of Variance for Surface tension, using Adjusted SS for Tests

Source	DF	Seq SS	Adj SS	Adj MS	F	P
Addition level	3	12885.2	12885.2	4295.1	122.92	0.000
Concentration	2	6429.5	6429.5	3214.8	92.00	0.000
Addition level*Concentration	6	2848.9	2848.9	474.8	13.59	0.000
Error	24	838.6	838.6	34.9		
Total	35	23002.3				

S = 5.91119 R-Sq = 96.35% R-Sq(adj) = 94.68%

Unusual Observations for Surface tension

Obs	Surface tension	Fit	SE Fit	Residual	St Resid
9	90.420	103.733	3.413	-13.313	-2.76 R
18	114.250	103.733	3.413	10.517	2.18 R

R denotes an observation with a large standardized residual.

APPENDIX E

EXPERIMENTAL RESULTS FOR CHAPTER 7

E.1 Young's Modulus and Poisson Ratio

SPECIMEN 1

S1 (psi)	S2 (psi)	e2 (in/in)	e1	E (ksi)
116	2314	0.00130455	4.97E-05	1752

S1 = Stress corresponding to a longitudinal strain (e1) of 0.00005
 S2 = Stress corresponding to 40% of Ultimate load
 e2 = Longitudinal strain produced by stress S2
 Ultimate Stress = 5784 psi

et1	et2	mu
5.54E-06	0.000202	0.16

SPECIMEN 2

S1 (psi)	S2 (psi)	e2 (in/in)	e1	E (ksi)
101	2314	0.001317	4.97E-05	1746

S1 = Stress corresponding to a longitudinal strain (e1) of 0.00005
 S2 = Stress corresponding to 40% of Ultimate Load
 e2 = Longitudinal strain produced by stress S2
 Ultimate Stress = 5784 psi

et1	et2	mu
5.54E-06	0.000219	0.17

SPECIMEN 3

S1 (psi)	S2 (psi)	e2 (in/in)	e1	E (ksi)
97	2315	0.001392	4.97E-05	1653

S1 = Stress corresponding to a longitudinal strain (e1) of 0.00005
 S2 = Stress corresponding to 40% of Ultimate Load
 e2 = Longitudinal strain produced by stress S2
 Ultimate Stress = 5784 psi

et1	et2	mu
8.31E-06	0.000216	0.15

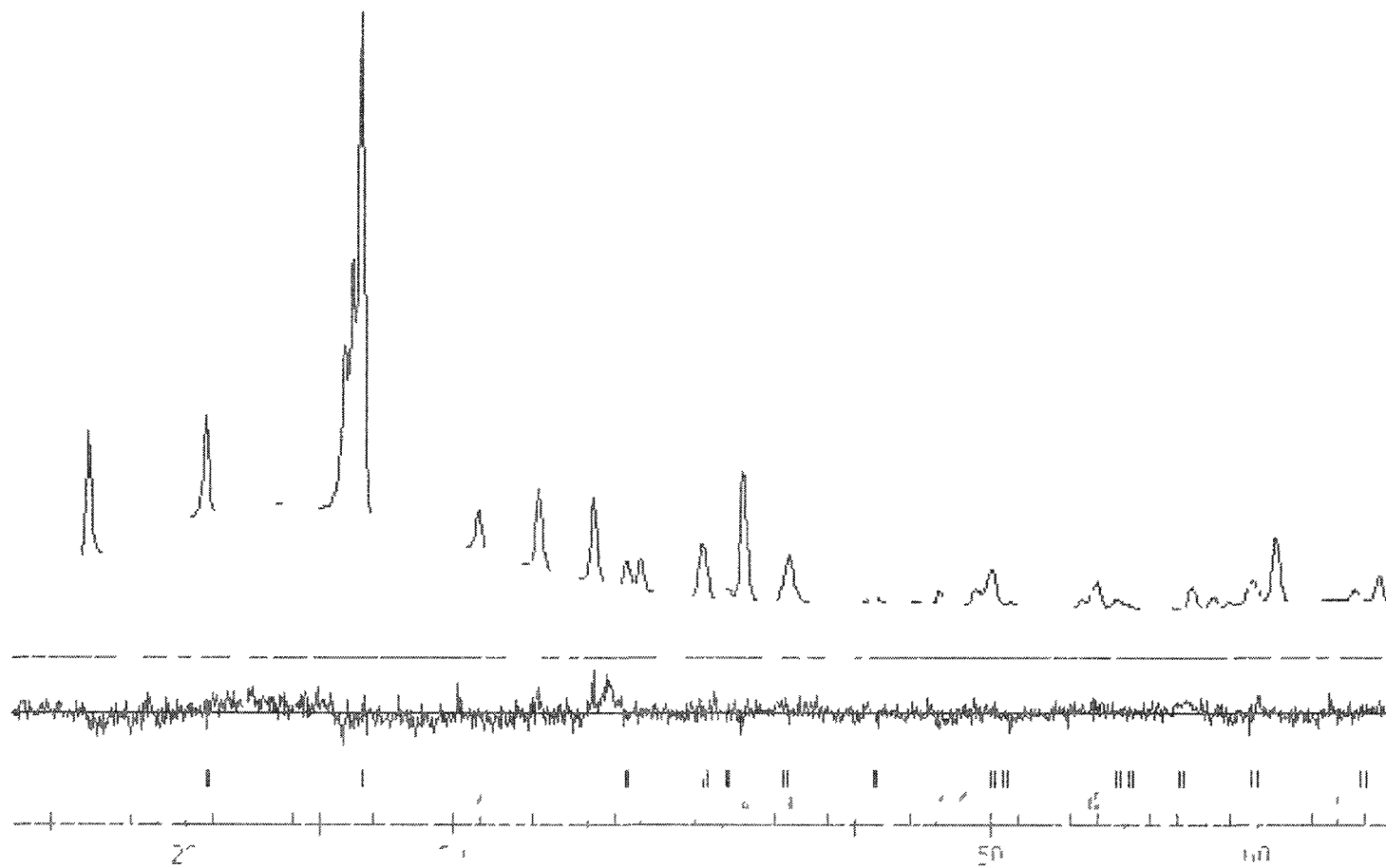
E.2 Data for Length Change in a Sulfate Solution

		READINGS							
		WEEK							
SPECIMEN	0	1	2	3	4	8	13	15	
Reference	0.0817	0.0816	0.0815	0.0815	0.0815	0.082	0.0815	0.0819	
1	0.0952	0.0985	0.1034	0.1035	0.1038	0.1045	0.1047	0.1059	
2	0.1008	0.1096	0.1171	0.1173	0.1177	0.1183	0.1187	0.1197	
3	0.147	0.1481	0.1568	0.1575	0.1578	0.159	0.1583	0.1592	
4	0.1252	0.1301	0.1351	0.1355	0.1358	0.1365	0.1369	0.1378	
		% LENGTH CHANGE							
		WEEK							
SPECIMEN	0	1	2	3	4	8	13	15	
Reference	0.0817	0.0816	0.0815	0.0815	0.0815	0.082	0.0825	0.829	
1	0	0.034	0.084	0.085	0.088	0.09	0.097	0.105	
2	0	0.089	0.165	0.167	0.171	0.172	0.181	0.187	
3	0	0.012	0.1	0.107	0.11	0.117	0.115	0.12	
4	0	0.05	0.101	0.105	0.108	0.11	0.119	0.124	
AVERAGE	0	0.04625	0.1125	0.116	0.11925	0.12225	0.128	0.134	

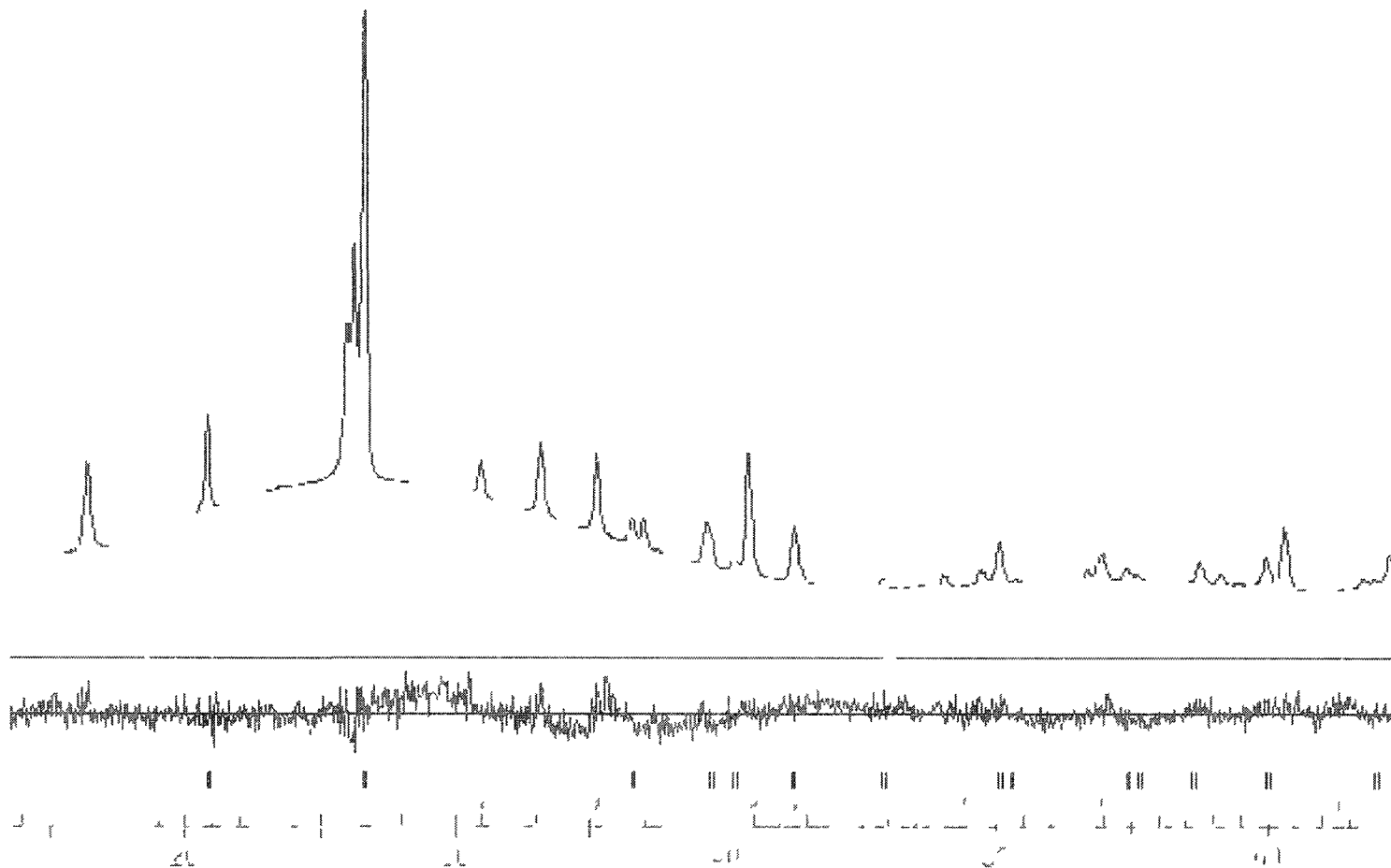
APPENDIX F

XRD CURVES FOR TABLE 7.9

F.1 XRD Pattern for Class F Fly Ash



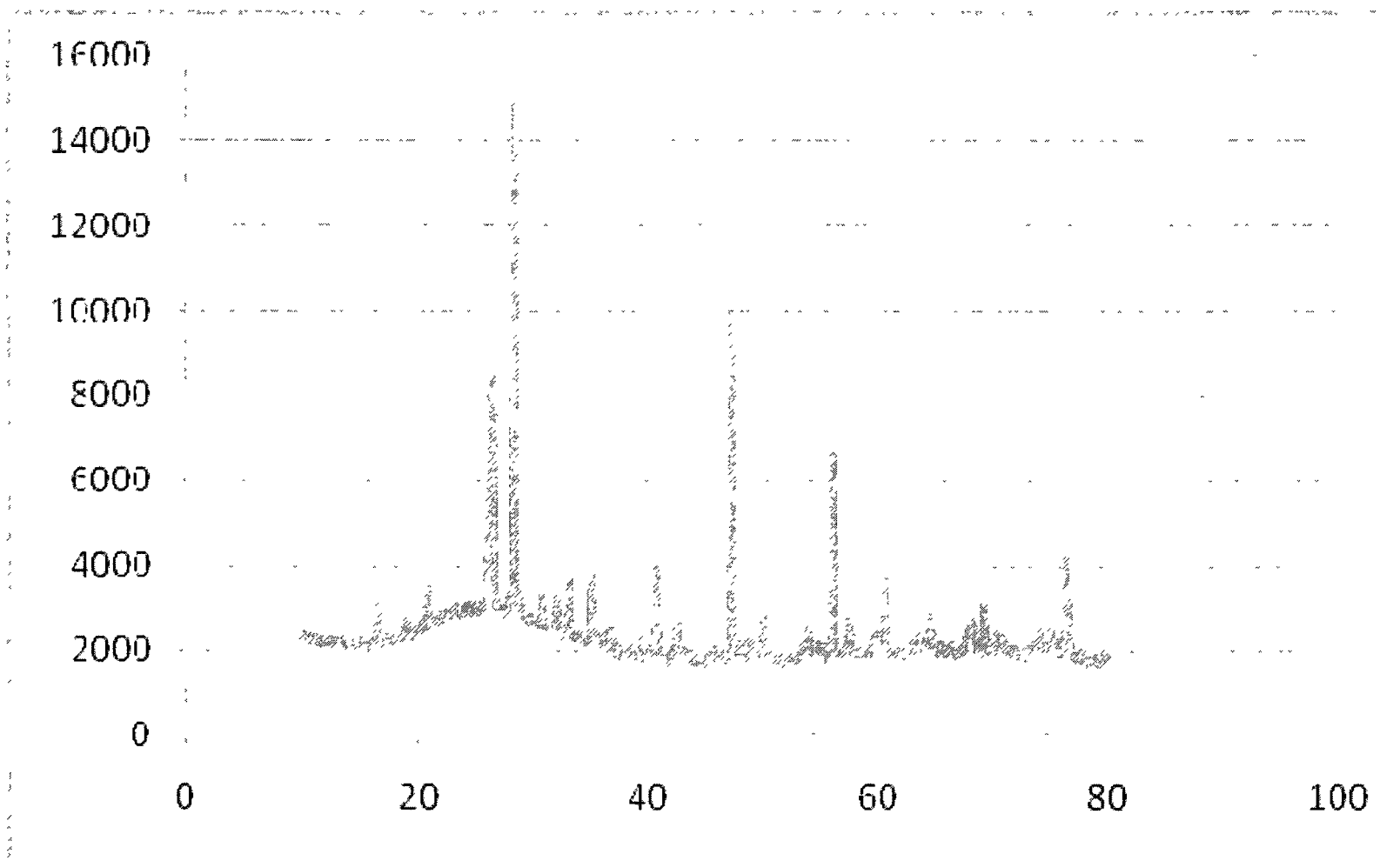
F.2 XRD Pattern for Class F Fly Ash Geopolymer



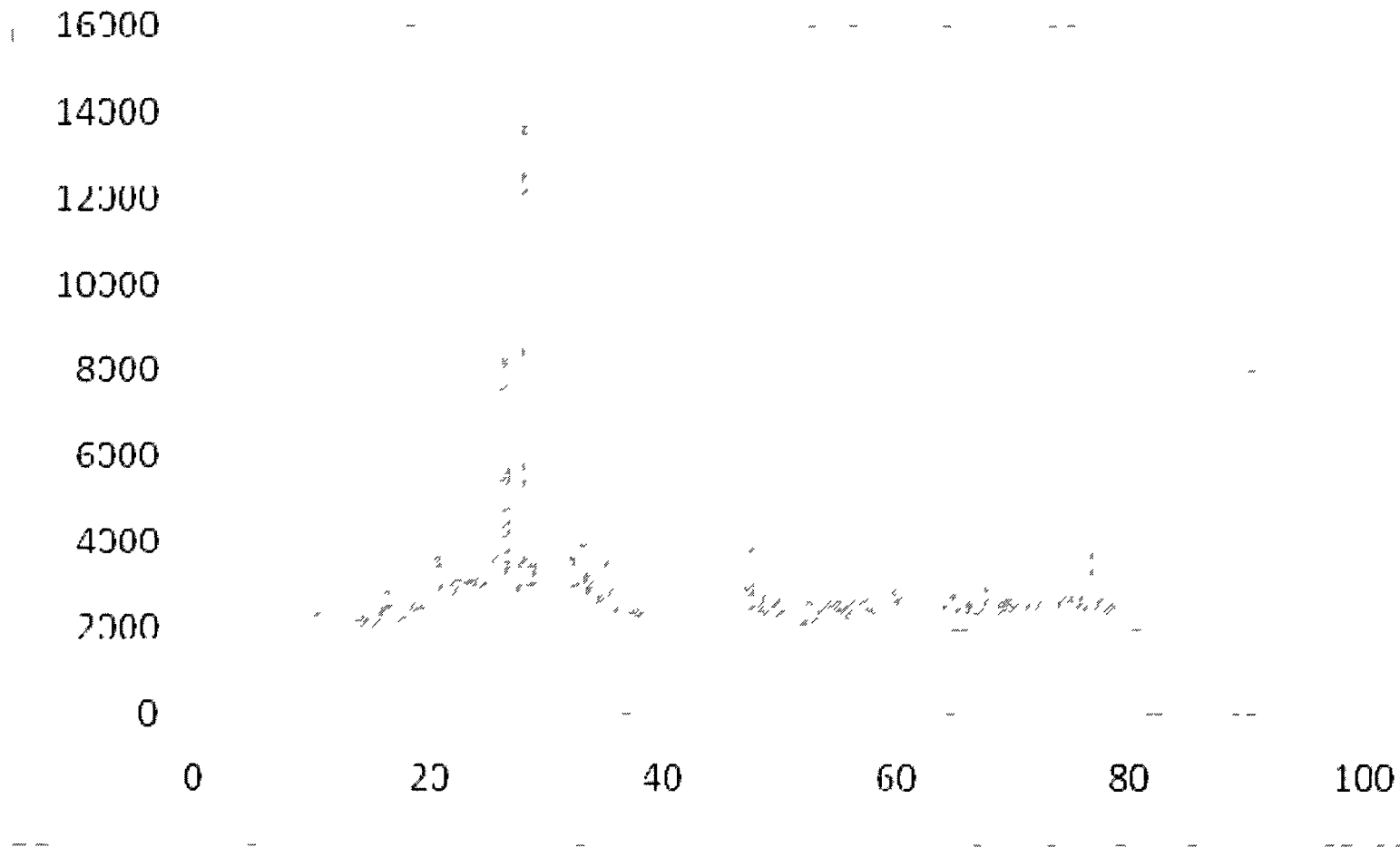
APPENDIX G

**XRD REPORTS FOR GEOPOLYMER WITH
ADDITION OF COPPER**

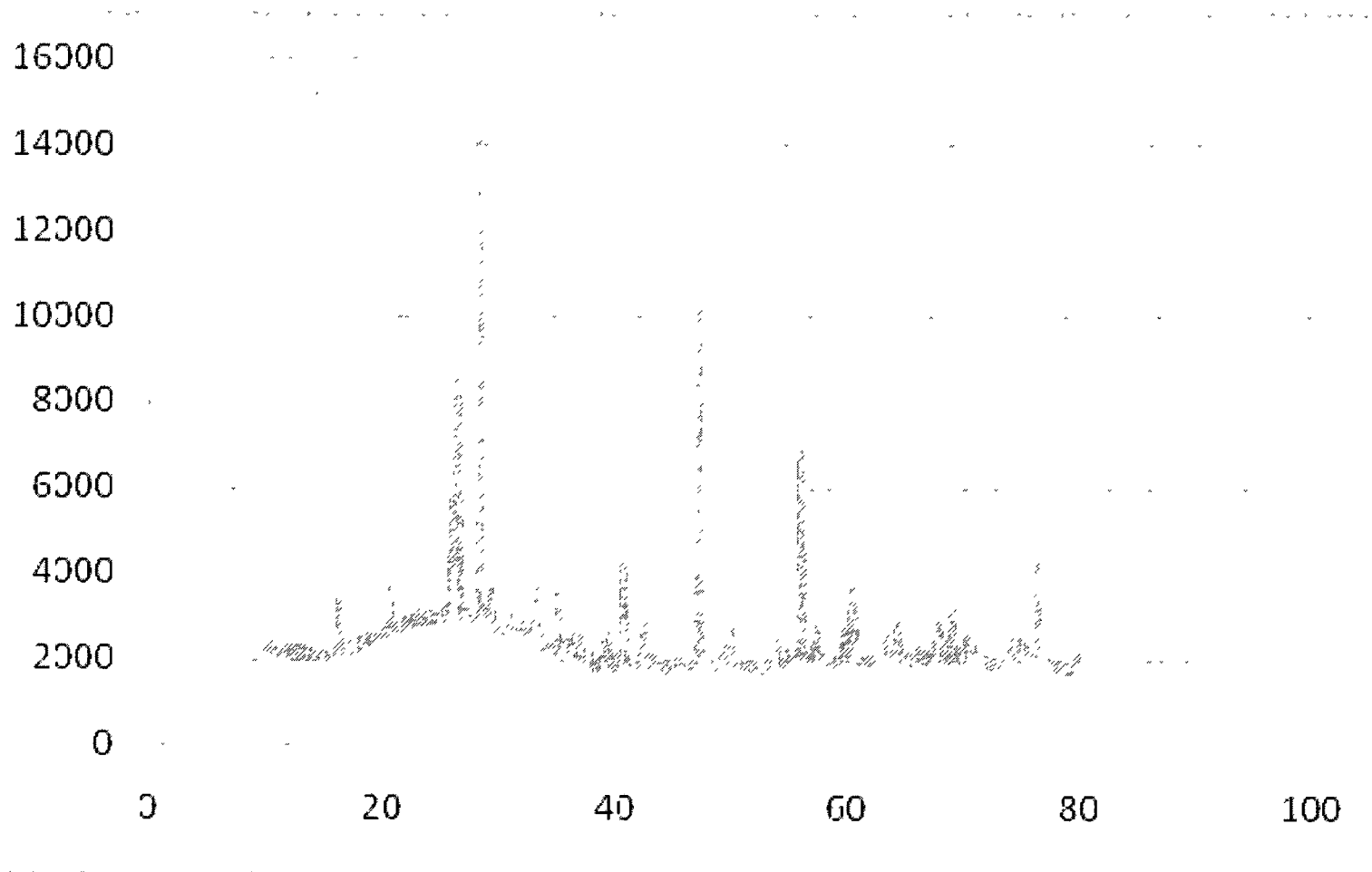
G.1 XRD Pattern for the Sample With 10% Added Cu_2SO_4



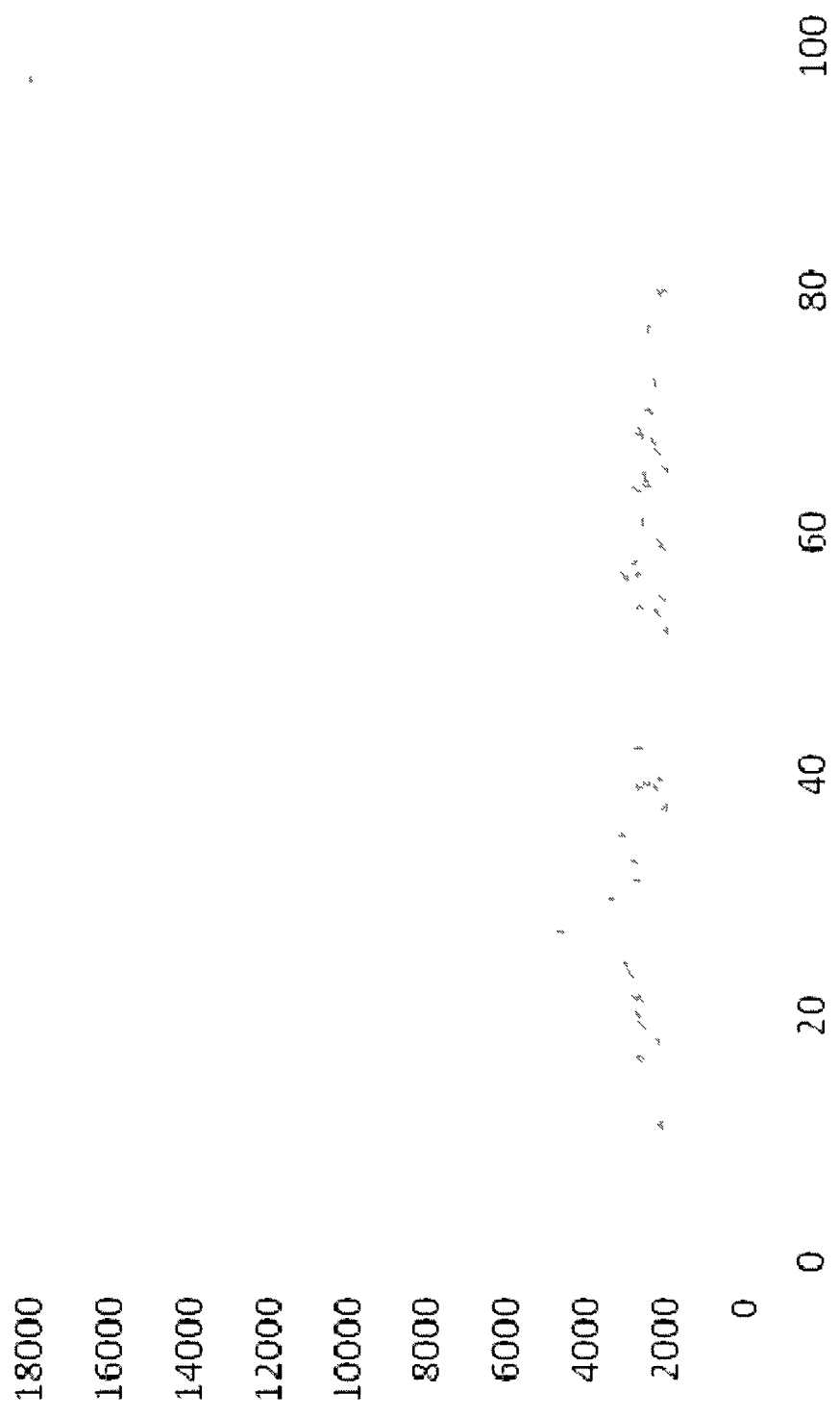
G.2 XRD Pattern for the Sample With 50% Added Cu_2SO_4



G.3 XRD Pattern for the Sample With 10% Added $\text{Cu}_2(\text{NO}_3)_3 \cdot 3\text{H}_2\text{O}$



G.4 XRD Pattern for the Sample With 50% Added $\text{Cu}_2(\text{NO}_3)_2 \cdot 3\text{H}_2\text{O}$



APPENDIX H

PLANET EUREKA REPORT



**USA NATIONAL
INNOVATION MARKETPLACE**
NIST



Planet Eureka!
NATIONAL CENTER



Geopolymer Coating for Concrete

prolongs useful life pipe and storage ponds for municipal water systems

Geopolymer coating restores structural integrity of concrete and prolongs life of existing structures by providing superior mechanical and chemical performance at a lower cost.

Annual Sales Forecast for USA*				Innovation Status		Idea
Need & Marketing Support Level	Conservative 50% odds of selling	Most Likely 60% odds of selling	Aggressive 25% odds of selling	Development Status	Priority Patent Status	Concept Score
Little/Low	\$54	\$15 M	\$22.5 M	2015 Successful Prototypes	1 or 5 Potential for monetization	32
Low Support	\$28.1 M	\$95.5 M	\$327.7 M			
	\$208.1 M	\$681.5 M	\$2.0 B	Remaining Time & Cost to First Sale		
Little/High	\$681.5 M	\$1.3 B	\$6.2 B	3 mo - 1 yr	\$100-\$1M	

Geopolymer Coating for Concrete - prolongs useful life pipe and storage ponds for municipal water systems

Final Decision Maker: Public Water System Admin. (water engineering)

This geopolymer coating provides for rehabilitation of sewers and water pipe storage ponds including tanks, bridges, and other underground or above-ground concrete structures. The coating offers an innovative, sustainable solution for maintaining concrete infrastructure in a manner that enhances public health and safety, and while reducing greenhouse gas emissions.

Application of the coating also reduces the need for existing infrastructure to be engineered and the maintenance costs of infrastructure to be reduced. The product offers superior mechanical, thermal, and chemical performance. The coating adheres well to concrete coated with the geopolymer at depths of 1/8" and abrasion resistance. The geopolymer coating is stronger than C15000, Portland Cement, OPC, and a 24-hour cure. The geopolymer coating also has strength equal to completely cured OPC. Superior strength is sustained for curing additive treatments such as urea solution, sulfuric acid, and hydrofluoric acid. The geopolymer coating resists chemical attack, maintains strength, adheres satisfactorily, and is used as a repair material and end-coat for high temperature. The geopolymer coating outperforms existing specialized products and can be produced at a lower cost.

The coating formulation utilizes products that would otherwise be disposed of in landfills or a burning cost and emit. Use of the product creates the opportunity to capture CO2 to be further enhanced or offset. The geopolymer coating has been used in municipal water systems, industrial applications, transportation projects, petrochemical plants, and defense agencies.

\$1.00 per square yard

Seeking investment, distribution



Report Assumptions and Inventor(s) Commentary

Inventor(s) Assumptions	Value / Likelihood Estimate	Confidence	Inventor(s) Commentary Data Source or Basis for Assumptions
2017 Patent Fee Estimate	25,000	80%	Based on historical data for similar patents and current market rates.
Revenue per Patent	\$250,000.00	60%	Based on industry benchmarks and historical performance of similar patents.
% of Profits	50%	60%	Based on industry standards for patent-related costs.
Number of Patents	4	80%	Based on current patent portfolio and market trends.
Revenue per Patent	\$1,250,000.00	80%	Based on industry benchmarks and historical performance of similar patents.
Revenue per Patent	N/A	N/A	
Revenue per Patent	40%	60%	Based on industry benchmarks and historical performance of similar patents.

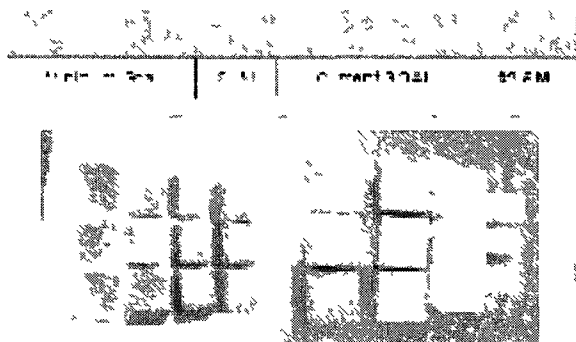
Innovation Metrics			
Development Status	2 of 3 Successful Prototypes	80%	Development progress is on track with successful prototypes.
Cost to First Sale Remaining	\$ 100-150K	60%	Costs are within budget and expected to be completed.
Time to First Sale Remaining	6 mos-1 yr	60%	Timeline is realistic and aligns with development progress.
Confidence in Concept Claims made in description		60%	Confidence is based on technical expertise and market research.
Proprietary Protection Status	1 of 3 Potential for Protection		Proprietary protection is being evaluated for key components.

Concept Score & Diagnostics

Merwyn Concept Score With Confidence Bands			Concept Diagnostic			
			Red	Yellow	Green	
			Bottom 20%	Middle 20%	Top 20%	
Pessimistic 80% odds of at least	Most Likely 60% odds of at least	Optimistic 20% odds of at least	Over Benefit			
			Reason to Believe			
			Dramatic Difference			



Inventor Commentary & Alternative Development Scenarios



Corrosion resistance of geopolymer coating visibly superior following 2 weeks of immersion in sulfuric acid.

Inventor(s) Commentary

Dr. Allouche, technical director of research Technology Center, specializes in advanced cementitious materials. Allouche is fulfilling multiple research contracts on geopolymer concrete products for public and private organizations. He has published over 20 publications on advanced protection systems for concrete structures. Allouche is engaged with 700 industry professionals through forums hosted semi-annually in 11 countries and has presented 150 seminars presentations at industry conferences.

CURRENT SALES FORECAST

Sales & Marketing Support Level	Conservative 20% odds of success	Most Likely 50% odds of success	Aggressive 80% odds of success
Class Low	\$200 M	\$1.3 M	\$22.5 M
Low Support	\$200 M	\$88.3 M	\$31.5 M
Medium Support	\$200 M	\$88.3 M	\$2.0 B
High Support	\$1.0 B	\$3.5 B	\$8.0 B

If MARKETING CONCEPT Improved

(Increase Support & Increase Odds)

Sales & Marketing Support Level	Conservative 20% odds of success	Most Likely 50% odds of success	Aggressive 80% odds of success
Class Low	\$48	\$8.1 M	\$27.5 M
Low Support	\$39.2 M	\$168.3 M	\$48.7 M
Medium Support	\$39.2 M	\$1.1 B	\$2.0 B
High Support	\$1.7 B	\$5.5 B	\$10.0 B

If PRODUCT SERVICE Improved

(Increase Repeat Rate & Number of Repeat Orders and Revenue Per Customer Order)

Sales & Marketing Support Level	Conservative 20% odds of success	Most Likely 50% odds of success	Aggressive 80% odds of success
Class Low	\$21	\$5.2 M	\$4.1 M
Low Support	\$39.8 M	\$171.8 M	\$58.2 M
Medium Support	\$39.8 M	\$1.3 B	\$2.0 B
High Support	\$1.7 B	\$5.5 B	\$10.0 B

If MARKETING CONCEPT and PRODUCT SERVICE Improved

(Increase Repeat Rate & Number of Repeat Orders and Revenue Per Customer Order)

Sales & Marketing Support Level	Conservative 20% odds of success	Most Likely 50% odds of success	Aggressive 80% odds of success
Class Low	\$70	\$6.0 M	\$1.6 M
Low Support	\$85.0 M	\$280.5 M	\$81.3 M
Medium Support	\$85.0 M	\$2.0 B	\$2.0 B
High Support	\$1.5 B	\$5.5 B	\$17.0 B
Very High Support	\$3.0 B	\$11.0 B	\$40.0 B

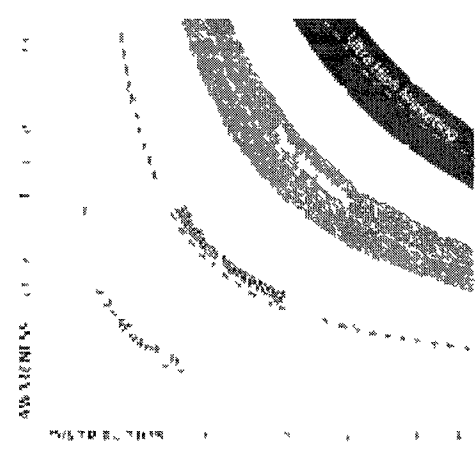


Additional Details

Fair Market Royalty (%)				
	Conservative - 80% Odds Royalty Percentage	Most Likely - 60% Odds Royalty Percentage	Aggressive - 20% Odds Royalty Percentage	
ALCURENT State & Status	1.5%	4.3%	8.1%	
Business Description (Support Level)	Annual Revenue Royalty Revenue			Support Level Royalty Odds
	20% Odds	50% Odds	20% Odds	
Ultra Low Support	\$110,000	\$900,000	\$920,000	\$610,000
Low Support	10.0 M	15.3 M	18.9 M	\$15.5 M
	\$12.0 M	\$72.2 M	\$71.7 M	\$192.5 M
	\$56.0 M	\$52.8 M	1174.8 M	\$277.8 M
Ultra High Support	\$70.1 M	\$174.2 M	\$202.3 M	\$202.0 M

Support Level	Sample Numbers		Support Level	Sample Numbers	Support Level
	%	Count			
Ultra Low Support	2%	1%	7%	40%	
Low Support	20%	10%	2%	70%	
	60%	25%	2%	50%	
	75%	45%	34%	20%	
Ultra High Support	80%	70%	62%	10%	

Graph of FQI/MAI FNT (Awareness x Distribution) Combinations



- 22 3 - Water Supply and Irrigation Systems
- 22 32 - Sewage Treatment/Collection
- 2273 - Highways, Streets and Bridge Construction
- 229 - Petroleum Manufacturing
- 22992 - Explosives Manufacturing

Years EXPERIENCE in related industry	12
GRANTED Patents	6
Learning DEALERSHIPS	0
Innovative that have S-IPPED	~

Planet Eureka! offers a wide range of services to help you grow your business. We provide a comprehensive suite of services including business valuation, financial modeling, and strategic planning. Our team of experts will work with you to identify opportunities for growth and develop a clear path forward. We also offer ongoing support and consulting services to ensure your business remains competitive in a rapidly changing market. Contact us today to learn more about how we can help you achieve your business goals.



Additional Forecasts for Other Countries

Annual Sales - Probability Forecast - for Canada	Conservative 80% odds of selling	Most Likely 60% odds of selling	Aggressive 20% odds of selling
Sales & Marketing Support Level			
Ultra Low	\$0	\$210,500	\$2.2 M
Low Support	\$2.5 M	\$7.0 M	\$33.5 M
	\$22.5 M	\$76.6 M	\$218.1 M
	\$58.8 M	\$204.2 M	\$578.2 M
Ultra High	\$112.1 M	\$386.4 M	\$1.1 B

Annual Sales - Probability Forecast - for United Kingdom	Conservative 80% odds of selling	Most Likely 60% odds of selling	Aggressive 20% odds of selling
Sales & Marketing Support Level			
Ultra Low	£2	£180,000	£2.3 M
Low Support	£2.3 M	£8.6 M	£32.8 M
	£22.4 M	£88.8 M	£198.8 M
	£53.5 M	£186.8 M	£522.1 M
Ultra High	£122.1 M	£398.8 M	£992.4 M

Listing # USA 75 34-409 014

Page 5 of 5

Date Posted 2009-04-13

REFERENCES

- [1] Environmental Protection Agency, "Hydrogen Sulfide Corrosion in Wastewater Collection and Treatment Systems, Technical Report." Source: U.S. Environmental Protection Agency, office of Water, Washington, D.C. 1991.
- [2] Hewayde, E., "Degradation of Concrete Sewer Pipes by Sulfuric Acid." Ph.D. Thesis. University of Western Ontario, Canada. 2005.
- [3] Barton, L., "Sulfate Reducing Bacteria," Plenum Press, New York, USA. 1995.
- [4] Parker, C.D., "The Isolation of Species of Bacterium Associated with the Corrosion of Concrete Exposed to Atmospheres Containing Hydrogen Sulfide," *Australian Journal of Experimental Biology and Medical Science*. Vol. 23, p. 81-90. 1946.
- [5] Islander, R.L., Deviny, J.S., Mansfeld, F., Postyn, A., and Shih, H., "Microbial Ecology of Crown Corrosion in Sewers," *Journal of Environmental Engineering*. Vol. 117, No. 6, p. 751-770. 1991.
- [6] ATV-M 143E: "Inspection, Repair, Rehabilitation and Replacement of Sewers and Drains. Part 1: Principles," Vol. 12. 1989.
- [7] Stein, Dietrich, "Rehabilitation and Maintenance of Drains and Sewers;" Ernst and Sohn, Chapter 2, p. 103-135. 2001.
- [8] Davis, J.R., "Surface Engineering for Corrosion and Wear Resistance;" Davis and Associates, Chapter 3, p. 46-72. 2001.
- [9] Järvenkylä, J. J. Haavisto, K.T.: "The abrasion resistance of sewers." Part 1: Pipes & Pipelines International 9/10; Part 2: Pipes & Pipelines International 11/12. 1993.
- [10] DIN 50900: "Corrosion of Metals – Terminology. Part 1".
- [11] Davis, J.R., "Surface Engineering for Corrosion and Wear Resistance;" Davis and Associates, Chapter 1, p. 4-9. 2001.

- [12] Monteiro, Paulo, J.M., *et al.*, "Accelerated test for Measuring Sulfate Resistance of Hydraulic Cements" for Caltrans *LLPRS Program*, Pavement Research Center, Institute of Transportation Studies, University of California, Berkeley. 2000.
- [13] Davis, J.R., "Surface Engineering for Corrosion and Wear Resistance;" Davis and Associates, Chapter 2, p. 11-42. 2001.
- [14] Hewayde, Esam H., *et al.* "The Impact of Coatings on Biological Generation of Sulfides in Wastewater Concrete Pipes," Department of Chemical and Biochemical Engineering, The University of Western Ontario, London, Ont., Canada. 2005.
- [15] Haile T.G., Nakhla, G. "Protection of Concrete Pipes from Bacterial-induced Corrosion," M.S. Research Project Proposal. University of Western Ontario. 2006.
- [16] Breit, W. "Acid Resistance of Concrete." *Beton* 52 H.10, p. 505-510. 2002.
- [17] Day, R.C. "The effect of secondary ettringite formation on the durability of concrete: a literature analysis." Research and Development Bulletin RD 1089, Portland Cement Association. 1992.
- [18] Hewayde, E., Allouche, E.N. and Nakhla, G.F. "The Use of Metakaolin and Geopolymer Cement to Improve Concrete Resistance to Sulfuric Acid Attack." Proceedings, 7th International Symposium on Utilization of High-Strength/High Performance Concrete, ACI SP-228, p. 1453-1466. 2005.
- [19] Eglinton, M., "Resistance of Concrete to Destructive Agencies." In: Hewlett, P.C. Lea's: Chemistry of Concrete and Cement. Burlington, MA, USA: Butterworth-Heinemann, p. 327-328. 1998.
- [20] Webb, R.E., and Chong, J., "Technologies for the assessment of large diameter lined concrete sewers in the city of Phoenix." Proceedings of the NASTT/ISTT International No-Dig 2003 Show. Las Vegas, Nevada. 2003.
- [21] Koo, D.H., Ariaratnam, S.T., "Innovative method for assessment of underground sewer pipe condition." *Automation in Construction*, Vol. 15, p. 479-488. 2006.
- [22] Stein, Dietrich, "Rehabilitation and Maintenance of Drains and Sewers;" Ernst and Sohn, Chapter 5, p. 395-397. 2001.
- [23] Stein, Dietrich, "Rehabilitation and Maintenance of Drains and Sewers;" Ernst and Sohn, Chapter 5, p. 400-425. 2001.
- [24] ASTM C150 / C150M - 09 Standard Specification for Portland Cement.

- [25] Montes, Carlos; "Utilización de Materias Primas Alternas en la Fabricación de un Cemento de Sulfoaluminato de Calcio," M.S. Thesis, CIMAV. Chihuahua, Mexico. 2003.
- [26] Ohama, Y. "Handbook of Polymer-Modified Concrete and Mortars - Properties and Process Technology," p. 11-21. 1995.
- [27] <http://www.cmit.csiro.au/research/urbanwater/pipes/tech-spray2.cfm>.
- [28] Davis, J.R., "Surface Engineering for Corrosion and Wear Resistance;" Davis and Associates, Chapter 7, p. 183. 2001.
- [29] Balaguru, D.P. "Geopolymer for Protective Coating of Transportation Infrastructures" Center for Advanced Infrastructure and Transportation (CAIT), Civil and Environmental Engineering; Rutgers, The State University, Piscataway, N.J., 1998.
- [30] Davidovits, J. "Properties of Geopolymer Cements," Geopolymer Institute. 1994.
- [31] Davidovits, J., "Soft mineralogy and geopolymers." Paper presented at the Geopolymer '88, First European Conference of Soft Mineralurgy, Compiègne, France. 1988.
- [32] Davidovits, J., "Geopolymer Chemistry and Properties." Paper presented at the Geopolymer '88, First European Conference of Soft Mineralurgy, Compiègne, France. 1988.
- [33] Davidovits, J., "Geopolymers: Inorganic Polymeric New Materials," *Journal of Thermal Analysis*. Vol. 37, p. 1633-1656. 1991.
- [34] Van Jaarsfeld, J.S.J, van Deventer, J.S.J., and Lukey G.C., "The effect of composition and temperature on the properties of fly ash- and kaolinite based-geopolymers." *Chemical Engineering Journal*, Vol. 89 (1-3), p. 63-73. 2002.
- [35] <http://www.metakaolin.com/Operation%20Description.htm>.
- [36] Breck, D., "Zeolite molecular sieves: structure, chemistry, and use" New York, Wiley. 1974.
- [37] <http://www.fhwa.dot.gov/infrastructure/materialsgrp/flyash.htm>.
- [38] Hos J.P., McCormick, P.G., and Byrne L.T., "Investigation of a Synthetic Aluminosilicate Organic Polymer." *Journal of Materials Science*, Vol. 37, p. 2311-2316. 2002.

- [39] Gordon, M., Bell, J.L and Kriven, W.M., "Comparison of Naturally and Synthetically derived, potassium-based geopolymers." *Ceramic transactions*, 165, p. 95-106. 2005.
- [40] Tsuyuki, N., and Koizumi, K., "Granularity and surface structure of ground granulated blast-furnace slags." *Journal of Materials Science*, Vol. 35, p. 249-257. 1999.
- [41] Shi, C., Krivenko, P.V. and Roy, D.M., "Alkali-activated Cements and Concretes." Abingdon, UK, Taylor and Francis. 2006.
- [42] Shimoda, K., Tobu, Y., Kanehashi, K., Nemoto, T. and Saito, K., "Total understanding of the local structures of an amorphous slag: Perspective from multi-nuclear (^{29}Si , ^{27}Al , ^{17}O , ^{25}Mg , and ^{43}Ca) solid state NMR." *Journal of Non-Crystalline Solids*, Vol. 354, p. 1036-1043. 2008.
- [43] Milkey, R. G, "Infrared spectra of some tectosilicates." *Am. Mineral.*, Vol. 45, p. 990-1007. 1960.
- [44] Barbosa V. F. F., Mackenzie K.J.D., Thaumaturgo, C., "Synthesis and characterization of materials based on inorganic polymers of alumina and silica: sodium polysialate polymers," *International Journal of Inorganic Materials*, Vol. 2[4], p. 309-317. 2000.
- [45] Xu H. and van Deventer J.S.J., "The Effect of Alkali Metals on the Formation of Geopolymeric Gels from Alkali-Feldspars," *Colloid. Surf. A*, Vol. 216, p. 27-44. 2003.
- [46] Davidovits, J., "Geopolymer chemistry and sustainable Development. The Poly(sialate) terminology : a very useful and simple model for the promotion and understanding of green-chemistry." *Proceedings World Congress Geopolymer 2005*, Saint-Quentin, France (Ed. J. Davidovits), p. 9-16. 2005.
- [47] Wallah, S.E., and Rangan B.V., "Low calcium fly ash based geopolymer concrete: long-term properties." *Research Report GC2*. Faculty of Engineering, Curtin University of Technology. Perth, Australia. 2003.
- [48] Perera, D.S., Uchida, O., Vance, E.R. "Influence of curing schedule on the integrity of geopolymers." *Journal of Materials Science*, Vol. 42. 2007.
- [49] Gebler, Steven H. "Review of Accelerated Curing in the Concrete Pipe Industry." *Concrete International*, August 1983.
- [50] Hardjito, D., *et al* "Geopolymer Concrete: Turn Waste Into Environmentally Friendly Concrete," *International Conference on Recent Trends in Concrete Technology and Structures*, INCONTEST. 2003.

- [51] Wallah, Steenie E., "Performance of fly-ash based geopolymers concrete under sulfate and acid exposure," Faculty of Engineering and Computing, Curtin University of Technology, Perth, Australia. 2005.
- [52] Hardjito, Djwantoro, Wallah, Steenie E., Sumajouw, Dody M.J., Rangan, B.V. "Factors influencing the compressive strength of fly ash-based geopolymer concrete." *Civil Engineering Dimension*. Vol 6, No.2, p. 88-93. September 2004.
- [53] Song, Xiu-Jiang, "Response of Geopolymer Concrete to Sulfuric Acid Attack," (ACCI, School of Civil and Environmental Engineering, UNSW, Sydney, Australia. Proceedings of the World Congress Geopolymer 2005.
- [54] Allahverdi, Ali, "Sulfuric Attack on Hardened Paste of Geopolymer Cements," College of Chemical Engineering, Iran University of Science and Technology, Tehran, Iran. 2005.
- [55] Song, Xiu-jiang, "Investigation of Cracking Developed in Sulfuric Acid Resistant Concretes," ACCI, School of Civil and Environmental Engineering, UNSW, Sydney, Australia. 2005.
- [56] Goretta, K.C., Gutierrez-Mora, F., Singh, D. "Erosion of geopolymers made from industrial waste." *Journal of Materials Science*, Vol. 4. 2007.
- [57] Provis, John L., Muntingh, Yolandi, Lloyd, Redmond R., Xu Hua, Keyte, Louise M., Lorenzen Leon, Krivenko, Pavel V., Van Deventer Jannie S.J. "Will geopolymers stand the test of time?," *Ceramic Engineering and Science Proceedings*, Vol. 28(9), p. 235-248.
- [58] Varela, Benjamin, "The Use of Geopolymers as Concrete Coatings for Fire Protection." Department of Mechanical Engineering, Rochester Institute of Technology, Rochester, NY. Proceedings of the World Congress Geopolymer 2005.
- [59] Davidovits, J., "Geopolymer Cements to minimize Carbon-dioxide greenhouse-warming." *Ceramic transactions*, Vol. 37, Cement-based materials: present, future, and environmental aspects, m. Moukwa & al. Eds., p. 165-182; American Ceramic Society. 1993.
- [60] Duxson, Peter, Provis, John L., Grant, C. Lukey, van Deventer, Jannie, S.J. "The role of inorganic polymer technology in the development of green concrete." *Cement and Concrete Research*, Vol. 37, p. 1590-1597. 2007.

- [61] Weil, M., Gasafi, E., Buchwald, A., Dombrowski, K. "Sustainable Design of Geopolymers – Integration of Economic and Environmental Aspects in the Early Stages of Material Development." 11th Annual International Sustainable Development Research Conference, Helsinki, Finland 2005.
- [62] <http://www.timesfreepress.com/news/2009/jun/06/tva-ship-spilled-coal-ash/>
- [63] Gourley, J. T., Johnson, G. B., "Developments in Geopolymer Precast Concrete." Proceedings World Congress Geopolymer 2005, Saint-Quentin, France (Ed. J. Davidovits), p. 139-144. 2005.
- [64] http://www.geopolymer.org/fichiers_pdf/ltgs.pdf.
- [65] Minarikova Martina ; Skvara Frantisek; "Fixation of heavy metals in geopolymeric materials based on brown coal fly ash." *Ceramics*. Vol. 50, No. 4, p. 200-207. 2006.
- [66] D S Perera, E R Vance, Y Zhang, Z Zhang, J Davis and P. Yee, "Speciation studies of Fe, Mn, Ca and Ti and dissolution studies in a metakaolinite-based geopolymer with Si/Al ~ 2," Proceedings World Congress Geopolymer 2005, Saint-Quentin, France (Ed. J. Davidovits), p. 57-59.
- [67] Comrie, Douglas, C., Paterson, John H., Ritcey, Douglas J., "Applications of Geopolymer Technology to Waste Stabilization." Available at <http://www.p2pays.org/ref/14/13863.pdf>
- [68] Luna, Y., Querol, X., Antenucci, D., Jdid El-Aid, Fernandez Pereira, C, Vale, J. "Immobilization of a metallurgical waste using fly ash-based geopolymers." World of Coal Ash (WOCA), May 7-10, Covington, Kentucky, USA. 2007.
- [69] Yunsheng Zhang, Wei Sun¹, Wei She¹ and Guowei Sun¹, "Synthesis and heavy metal immobilization behaviors of fly ash based geopolymer," *Journal of Wuhan University of Technology--Materials Science Edition*, Vol. 24, No. 5, October, 2009.
- [70] Davidovits, J., Comrie, D., Paterson, H. and Ritcey, D.J. "Geopolymeric Concretes for Environmental Protection." *Concrete International*, Vol. 12, No. 7, p. 30-39. 1990.
- [71] Terzano, R., Spagnuolo, M., Medici, L., Vekemans, B., Vincze, L., Janssens, K., Ruggiero, P. "Copper Stabilization by Zeolite Synthesis in Polluted Soils Treated with Coal Fly Ash." *Environ. Sci Technology*. 2005.
- [72] Wang, S., Li, L., Zhu, Z.H., "Solid-state conversion of fly ash to effective adsorbents for Cu removal from wastewater." *Journal of Hazardous Materials*. 2007.

- [73] Xu, J.Z., Zhou, Y.L., Chang, Q., Qu, H.Q., "Study on the factors of affecting the immobilization of heavy metals in fly ash-based geopolymers." *Materials Letters*, Vol. 60. 2006.
- [74] Van Jaarsfeld, J.G.S and Van Deventer, J.S.J., "The potential use of geopolymeric materials to immobilize toxic metals: Part 1. Theory and applications." *Minerals Engineering*, Vol 10, No. 7, p. 659-669. 1996.
- [75] Services Pétroliers Schlumberger, "Geopolymer composition and application in oilfield industry." European Patent EP20060291275
<http://www.freepatentsonline.com/EP1887065.pdf>
- [76] <http://www.britannica.com/EBchecked/topic/575080/surface-tension>
- [77] <http://www.answers.com/topic/surface-tension>
- [78] Zisman W A 1964 "Contact Angle, Wettability and Adhesion Advances in Chemistry Series," No. 43. Ed. F M Fowkes. Washington, DC. American Chemical Society.
- [79] Rosen MJ., "Surfactants and Interfacial Phenomena." 3rd Ed. Hoboken, New Jersey: John Wiley & Sons. 2004.
- [80] Dolch, William L., "Air-entraining admixtures." Concrete Admixtures Handbook. Properties, Science, and Technology. 2nd.Ed. Ramachandran, V.S. William Andrew Publishing/Noyes. 1995.
- [81] Edmeades, Rodney M., Hewlett, Peter C., "Cement Admixtures." Lea's Chemistry of Cement and Concrete. Chemistry of Concrete and Cement. Burlington, MA, USA: Butterworth-Heinemann, p. 843-848. 1998.
- [82] Bruere G.M. "Fundamental actions of air-entraining agents." Paper III/I, International Symposium on Admixtures for Cement and Concrete, Brussels, 1967.
- [83] Kreijger, P.C. "Plasticizers and dispensing admixtures." Lancaster: The Construction Press CI80 Admixtures Congress, London, p. 1-16. 1980.
- [84] Pomeroy, R. D., "Prevention of Hydrogen Sulfide in Sewage," Sewage Work Journal, Vol. 18, No. 4, p. 597-640. 1946.
- [85] Pomeroy, R. D., "Control of Hydrogen Sulfide Generation in Sewer," *Water and Sewage World*, Vol. March, p. 133-137. 1956.

- [86] Metcalf and Eddy, "Wastewater Engineering, Treatment and Reuse," 4th edition, McGraw Hill, Inc. 2003.
- [87] Iller, R.K., "The Colloid Chemistry of Silica and Silicates." Cornell Univ. Press, Ithaca, NY, p. 27– 37. 1955.
- [88] Bakharev, T., "Resistance of Geopolymer Materials to Acid Attack." *Cement and Concrete Research*, Vol. 35, p. 658-670. 2005.
- [89] Allouche, E.N., Montes, C., Diaz, I., and Vaidya, S., "Applications of Inorganic Polymer Concrete in Transportation Structures Located in Harsh Environments – Final Report. A technical report prepared for the Louisiana Transportation Research Center under Contract # 736-99-1515," December 2008.
- [90] Muntigh, Y. 2006 "Durability and Diffusive Behaviour Evaluation of Geopolymeric Material." M.S. Thesis. Department of Process Engineering. University of Stellenbosch, S.Africa. 2006.
- [91] Blakely, C., Logan, A., Bozeman, R., Dhanani, A., "Bulldog Concrete Sewer Rehabilitation." Term paper for MGMT Class 400. Supervisor: Dr. J. Pratt. Winter 2010. Louisiana Tech University.